Optimisation et réduction de la dose d'irradiation au scanner : aspects techniques et impact en pratique clinique courante

Alban Gervaise

UNIVERSITÉ DE LORRAINE

Ecole Doctorale BioSE (Biologie-Santé-Environnement)

Thèse

Présentée et soutenue publiquement pour l'obtention du titre de

DOCTEUR DE L'UNIVERSITE DE LORRAINE

Mention : « Sciences de la Vie et de la Santé »

par Alban GERVAISE

« Optimisation et réduction de la dose d'irradiation au scanner : aspects techniques et impact en pratique clinique courante »

03/10/2016

Membres du jury :

Rapporteurs :

Pr DUCOU LE POINTE Hubert	PU-PH, HDR, Université Paris VI, France
Dr BRISSE Hervé	Praticien spécialiste, HDR, Université Paris V, France

Examinateurs :

Pr DRAPE Jean-Luc	PU-PH, HDR, Université Paris V, France
Pr BLUM Alain	PU-PH, HDR, Université de Lorraine, Nancy, France Directeur de thèse
Dr TEIXEIRA Pedro	MCU-PH, Université de Lorraine, Nancy, France
Dr NOEL Alain	Physicien médical, HDR, Université de Lorraine, Nancy, France

Membres invités :

Pr FOEHRENBACH Hervé	Professeur agrégé du Val de Grâce, DCSSA, Paris, France
Dr TACK Denis	Praticien spécialiste, Hôpital RHMS, Baudour, Belgique

---

INSERM U947 Laboratoire « Imagerie Adaptative Diagnostique et Interventionnelle »
CHU de Nancy-Brabois – Bâtiment Recherche – Rez-de-chaussée
rue du Morvan, 54511 Vandœuvre-lès-Nancy

Remerciements

Cette thèse est le fruit de nombreuses années de travail et le résultat de nombreuses collaborations. Je tiens donc à remercier tous ceux qui ont participé de près ou de loin à la réalisation de ces travaux de recherche.

En premier lieu, je remercie le Professeur Jacques Felblinger, directeur du laboratoire d'Imagerie Adaptative Diagnostique et Interventionnelle du CHRU de Nancy, de m'avoir accueilli au sein du laboratoire et de m'avoir toujours poussé à réaliser cette thèse. Même si ma présence au sein du laboratoire a été épisodique, j'en garde un excellent souvenir. Je tiens également à remercier tous les membres du laboratoire qui m'ont aidé dans mon travail. En particulier, je retiendrai ma collaboration fructueuse avec Emilien Micard et Gabriela Hossu. Que ce soit pour l'informatique ou les statistiques, vous avez toujours été disponibles pour m'aider dans mes différents projets.

Je remercie mon directeur de thèse, le Professeur Alain Blum, chef du service d'imagerie Guilloz du CHRU Nancy, de m'avoir donné l'opportunité de réaliser ce travail au sein de son service, de m'avoir accordé sa confiance et de m'avoir permis d'utiliser les équipements modernes dont dispose son service.

Un grand merci au Docteur Pedro Teixeira, mon « presque » co-directeur de thèse pour ses conseils, sa bonne humeur, sa disponibilité et ses compétences scientifiques indéniables. J'espère que nous aurons l'occasion de pouvoir retravailler ensemble !

Je remercie le Professeur Drapé, président du jury de thèse, de l'attention et de l'intérêt portés à mon travail. Ses remarques pertinentes et constructives me permettront d'améliorer mes futurs travaux. Je remercie le Professeur Ducou-Lepointe et le Docteur Brisse d'avoir accepté d'être rapporteurs de mon jury de thèse. Leur expérience en tant que radio-pédiatres et leur expertise en radio-protection ont été d'une grande valeur. Leurs remarques et questions pointues sur mon travail me poussent à encore améliorer mes connaissances sur ce sujet. Je remercie le Professeur Foehrenbach, ancien chef du service de médecine nucléaire de l'Hôpital du Val de Grâce et spécialiste en radioprotection. Son expertise en matière de radioprotection des patients est un modèle pour moi. J'espère pouvoir être à la hauteur des « grands anciens » qui ont fait la réputation du Service de Santé des Armées en matière de radioprotection. Je remercie le Docteur Alain Noël d'avoir accepté d'être examinateur dans mon jury de thèse et de m'avoir fait profiter de ses compétences en radio-physique médicale. Enfin, je remercie le Docteur Denis Tack, tout d'abord pour m'avoir fait l'honneur de faire la route depuis la Belgique, et surtout pour son expertise en radioprotection des patients et en optimisation de la dose au scanner. Son travail de thèse de sciences a été un modèle pour moi depuis de nombreuses années et j'espère que mon travail a pu être à la hauteur du sien.

Je remercie l'équipe médicale et paramédicale du service d'imagerie Guilloz. Cela a toujours été un plaisir pour moi de venir dans ce service. Merci en particulier aux médecins qui ont bien voulu jouer le rôle de relecteur dans mes différentes études : Sophie Lecocq, Benoit Osemont, Mathias Louis, Johny Wassel.

Un grand merci à l'équipe du Service d'Imagerie Médicale de l'HIA Legouest. Ce service restera à jamais mon premier service de radiologie. J'y ai fait mes débuts et je me suis épanoui auprès de vous. Grâce à votre bonne humeur collégiale, j'ai pu progresser et mener mes projets à bien. C'est avec émotion que je vous ai quittés pour de nouvelles aventures parisiennes mais je ne vous oublierai jamais !

Merci aux différents co-auteurs de mes articles ainsi qu'à tous ceux qui ont travaillé dans l'ombre pour permettre leur publication.

Enfin, et surtout, je remercie mon épouse pour son soutien indéfectible et sa compréhension. Tu as toujours cru en moi et tu m'as toujours soutenu. Je te remercie infiniment ma chérie. Je t'aime. Tu m'as aussi donné un superbe fils, Paul, qui est plein de vie ! Mais plus que n'importe quelle thèse, c'est notre famille qui est importante à mes yeux !!! Quant à toi Paul, j'espère que plus tard tu seras fier de ton Papa comme je suis déjà fier de toi.

TABLE DES MATIERES

ABREVIATIONS

AIDR	*Adaptive Iterative Dose Reduction*
ALARA	*As Low As Reasonably Achievable* (Aussi bas que raisonnablement possible)
ASIR	*Adaptive Statistical Iterative Reconstruction*
CHRU	Centre Hospitalier Régional Universitaire
FBP	*Filtered Back Projection* (Rétroprojection Filtrée)
HIA	Hôpital d'Instruction des Armées
IADI	Imagerie Adaptative Diagnostique et Interventionnelle
IMC	Indice de Masse Corporelle
IRM	Imagerie par Résonance Magnétique
IRSN	Institut de Radioprotection et de Sûreté Nucléaire
kV	kilovoltage
mA	milliampérage
mAs	milliampère x secondes
mSv	milliSievert
PDL	Produit Dose Longueur
RLSS	Relation Linéaire Sans Seuil
RCB	Rapport Contraste sur Bruit
RSB	Rapport Signal sur Bruit
T10	Dixième vertèbre thoracique

TABLE DES FIGURES

TABLE DES TABLEAUX

INTRODUCTION GENERALE

Depuis son introduction dans les années 1970, le scanner est devenu une technique d'imagerie médicale incontournable notamment compte-tenu de son excellente performance pour le diagnostic de nombreuses pathologies. Toutefois, le scanner est un examen d'imagerie irradiant, son principe étant basé sur la reconstruction d'image à partir d'un faisceau de rayons X. Même si les doses délivrées en scanographie sont faibles, de l'ordre du milliSievert (mSv), compte-tenu des risques potentiels de cancer radio-induit lié aux faibles doses de rayons X, la réduction de la dose d'irradiation au scanner est primordiale.

Cette thèse s'inscrit dans cette démarche d'optimisation et de réduction de la dose d'irradiation au scanner. Elle est le fruit de plusieurs années de travail au sein du service d'imagerie Guilloz du Centre Hospitalier Régional Universitaire (CHRU) de Nancy et du service d'imagerie de l'Hôpital d'Instruction des Armées (HIA) Legouest de Metz, en collaboration avec le laboratoire d'imagerie IADI (Imagerie Adaptative Diagnostique et Interventionnelle) du CHRU de Nancy.

Le point de départ de ce travail a été l'installation en 2008 dans le service d'imagerie Guilloz d'un nouveau type de scanner à large système de détection : le scanner 320-détecteurs (scanner Aquilion One®, Toshiba Medical Systems, Otawara, Japon). L'originalité de ce scanner était d'être composé d'un large système de détection de 16 cm dans l'axe z grâce à 320 rangées de détecteurs de 0,5 mm. Avec ce nouveau type de scanner, il devenait possible de faire une acquisition d'un volume entier de 16 cm de longueur dans l'axe z en une seule rotation du tube. Cette évolution technologique majeure a permis de pouvoir couvrir en une rotation du tube des organes tels que le cœur, le cerveau ou encore des articulations périphériques comme le poignet ou la cheville. Avec un temps de rotation minimal de 350 ms et des techniques de reconstruction partielle des données, ce scanner bénéficie d'une excellente résolution temporelle permettant une acquisition de 16 cm de données en moins de 175 ms. Grâce à l'introduction de ce nouveau type de scanner à large système de détection, il était devenu possible de réaliser en pratique clinique courante des acquisitions de perfusion ou encore des acquisitions dynamiques des articulations. Toutefois, pour ce type d'examen, de nombreuses phases d'acquisitions doivent être réalisées, ce qui est à l'origine d'une augmentation proportionnelle de la dose. Dans ce contexte, l'optimisation de la dose d'irradiation du patient devient primordiale afin de pouvoir utiliser en pratique clinique courante ce type de protocole.

En 2010, dans l'optique de réduire la dose d'irradiation au scanner, une nouvelle évolution technologique majeure est apparue sur le scanner 320-détecteurs : les reconstructions itératives AIDR (*Adaptive Iterative Dose Reduction*). Ce type de reconstruction a permis de réduire le bruit de l'image par rapport aux reconstructions standard en rétroprojection filtrée (*Filtered Back Projection* - FBP). Ainsi, à qualité d'image équivalente, l'implantation de ces reconstructions itératives était à l'origine d'une réduction significative de la dose d'irradiation au scanner. En 2011, des reconstructions itératives ASIR (*Adaptive Statistical Iterative Reconstruction*) ont également été disponibles sur un nouveau scanner 64-détecteurs (Optima CT660®, GE Healthcare) installé dans le service d'imagerie de l'HIA Legouest. Cette version des reconstructions itératives ASIR nous a notamment permis de mettre au point un protocole de scanner basse dose pour le bilan des coliques néphrétiques.

L'objectif principal de cette thèse est d'étudier les différentes manières d'optimiser et de réduire la dose d'irradiation au scanner, tout en conservant une excellente performance diagnostique. Pour cela, nous avons étudié sur fantôme et sur patient différents facteurs techniques et comportementaux intervenant dans cette démarche d'optimisation et de réduction de la dose au scanner. Nous nous sommes aussi intéressés à l'optimisation de protocoles de scanner dans des applications cliniques particulières comme le scanner basse dose réalisé pour le bilan d'une colique néphrétique et dans de nouvelles applications cliniques avancées comme le scanner dynamique 4D des articulations ou le scanner de perfusion tumorale.

Les objectifs de ce travail sont :

- L'évaluation de l'impact des facteurs comportementaux dans une démarche d'optimisation et de réduction de la dose d'irradiation au scanner.

- L'évaluation sur fantôme et sur patient de plusieurs algorithmes de reconstruction itérative (AIDR et AIDR 3D de Toshiba et ASIR de General Electrics) afin d'évaluer leur performance et d'analyser leur impact en pratique clinique courante sur certains types de pathologies comme la recherche d'une colique néphrétique.

- L'évaluation de la mise en œuvre en pratique clinique courante des techniques de réduction et d'optimisation de la dose d'irradiation à la fois en imagerie abdominopelvienne dans un contexte de recherche de colique néphrétique et en

imagerie ostéo-articulaire, en particulier pour les nouvelles applications cliniques comme le scanner dynamique des articulations, le scanner de perfusion ou encore le scanner double-énergie.

Ce manuscrit est composé de quatre chapitres incluant l'ensemble des articles publiés ou en cours d'évaluation pour publication sur la thématique de la réduction de la dose d'irradiation au scanner. Le premier chapitre abordera des rappels concernant les risques potentiels de cancer radio-induit lié aux faibles doses de rayons X et les différentes modalités de réduction de la dose d'irradiation au scanner. Le deuxième chapitre s'intéressera à l'influence des facteurs comportementaux sur la dose d'irradiation au scanner, le troisième à l'influence des facteurs techniques et le quatrième et dernier chapitre portera sur des exemples d'applications cliniques.

Le deuxième chapitre, portant sur l'influence des facteurs comportementaux, sera composé de trois articles :

- Evaluation de la connaissance des prescripteurs de scanner en matière de radioprotection des patients. Cet article a été publié dans le « Journal de Radiologie » ;

- Evaluation de l'intérêt de l'acquisition abdominopelvienne sans injection lors de la réalisation d'un scanner corps entier chez un patient suspect de polytraumatisme. Cet article a été publié dans le journal « *Diagnostic and Interventional Imaging* » ;

- Optimisation de la longueur d'acquisition des scanners réalisés pour colique néphrétique : proposition d'une nouvelle méthode pour le placement de la limite supérieure de l'acquisition. Cet article est en cours d'évaluation pour publication dans le journal « *British Journal of Radiology* ».

Le troisième chapitre, portant sur l'influence des facteurs techniques, sera composé de quatre articles :

- Réduction de dose dans l'exploration du rachis lombaire grâce au scanner 320-détecteurs : étude initiale. Cet article a été publié dans le « Journal de Radiologie » ;

- Amélioration de la qualité d'image scanographique en utilisant les reconstructions itératives *Adaptive Iterative Dose Reduction* avec une acquisition *wide-volume* sur un scanner 320-détecteurs. Cet article a été publié dans le journal « *European Radiology* » ;

- Réduction de la dose des scanners abdominopelviens grâce aux reconstructions itératives AIDR 3D. Cet article a été publié dans le journal « *Diagnostic and Interventional Imaging* » ;

- Scanner basse dose avec la modulation automatique du milliampérage, les reconstructions *Adaptive Statistical Iterative Reduction* et un faible kilovoltage pour le diagnostic des coliques néphrétiques : impact de l'indice de masse corporelle. Cet article a été publié dans le journal « *American Journal of Roentgenology* ».

Le quatrième et dernier chapitre, portant sur des exemples d'applications cliniques, sera composé de trois articles :

- Scanner basse dose pour la recherche de colique néphrétique : comment faire en pratique clinique ? Cet article a été publié dans le journal « *Diagnostic and Interventional Imaging* » ;

- Optimisation et réduction de la dose en scanner ostéo-articulaire. Cet article a été publié dans le journal « *Diagnostic and Interventional Imaging* » ;

- Scanner ostéo-articulaire à large système de détection : principes, techniques et applications en pratique clinique et en recherche. Cet article a été publié dans le journal « *European Journal of Radiology* ».

LISTE DES PUBLICATIONS ET COMMUNICATIONS

PUBLICATIONS :

- **Articles à comité de lecture international :**

Gervaise A, Osemont B, Lecocq S, Micard E, Noel A, Felblinger J, Blum A. CT image quality improvement using adaptive iterative dose reduction with wide-volume acquisition on 320-detector CT. *Eur Radiol* 2012; 22: 295-301.

Gervaise A, Teixeira P, Villani N, Lecocq S, Louis M, Blum A. Dose optimization and reduction in musculoskeletal CT. *Diagn Interv Imaging* 2013; 94: 371-88.

Naulet P, Wassel J, Gervaise A, Blum A. Evaluation of the value of abdominopelvic acquisition without contrast injection when performing a whole body CT scan in a patient who may have multiple trauma. *Diagn Interv Imaging* 2013; 94: 410-7.

Gervaise A, Osemont B, Louis M, Lecocq S, Teixeira P, Blum A. Standard dose versus low-dose abdominal and pelvic CT: comparison between filtered back projection versus adaptive iterative dose reduction 3D. *Diagn Interv Imaging* 2014; 95: 47-53.

Gervaise A, Naulet P, Beuret F, Henry C, Pernin M, Portron Y, Lapierre-Combes. Low-dose CT with automatic tube current modulation, adaptive statistical iterative reconstruction, and low tube voltage for the diagnosis of renal colic. *Am J Roentgenol* 2014; 202: 553-60.

Teixeira P, Gervaise A, Louis M, Lecocq S, Raymond A, Aptel S, Blum A. Musculoskeletal Wide detector CT : Principles, Techniques and Applications in Clinical Practice and Research. *Eur J Radiol* 2015; 84: 892-900.

Blum A, Gervaise A, Teixeira P. Iterative reconstruction: Why, how and when? *Diagn Interv Imaging* 2015; 96: 421-2.

Gervaise A, Gervaise-Henry C, Pernin M, Naulet P, Junca-Laplace C, Lapierre-Combes M. Low dose CT for renal colic: how to do in clinical practice? *Diagn Interv Imaging* 2016; 97: 393-400.

Gervaise A, Teixeira P, Hossu G, Blum A, Lapierre-Combes C. Optimizing z-axis coverage of abdominal CT scans of the urinary tract: a proposed alternative proximal landmark for acquisition planning. En cours de soumission à *British Journal of Radiology.*

- **Articles à comité de lecture national :**

Gervaise A**,** Louis M, Batch T, Loeuille D, Noel A, Guillemin F, Blum A. Réduction de dose dans l'exploration du rachis lombaire grâce au scanner 320-détecteurs : étude initiale. *J Radiol* 2010; 91: 779-85.

Gervaise A, Esperabe-Vignau F, Naulet P, Pernin M, Portron Y, Lapierre-Combes M. Evaluation des connaissances des prescripteurs de scanner en matière de radioprotection des patients. *J Radiol* 2011; 92: 681-7.

COMMUNICATIONS :

- **Communications affichées :**

Gervaise A, Batch T, Loeuille D, Valckenaere I, Noël A, Guillemin F, Blum A. Comparaison de la dose délivrée par un scanner 320-détecteurs en mode volumique versus hélicoïdal. 57ème Journées Françaises de Radiologie, Paris, Octobre 2009.

Gervaise A, Esperabé-Vignau F, Pernin M, Naulet P, Portron Y, Lapierre-Combes M. Evaluation des connaissances des prescripteurs en matière de radioprotection des patients. 59ème Journées Françaises de Radiologie, Paris, Octobre 2011.

Gervaise A, Micard E, Noel A, Felblinger J, Blum A. Evaluation des reconstructions itératives AIDR sur le scanner 320-détecteurs : étude sur fantôme. 59ème Journées Françaises de Radiologie, Paris, Octobre 2011.

Gervaise A, Osemont B, Lecocq S, Micard E, Noel A, Felblinger J, Blum A. CT image quality improvement using adaptive iterative dose reduction with wide-volume acquisition on 320-detector CT. European Congress of Radiology, Vienna, Austria, 1-5 march 2012.

Villani N, Rovea F, Rossignon B, Gervaise A, Régent D. Comment améliorer le compromis qualité image versus dose en radiologie diagnostique ? 51ème Journées Scientifiques de la Société Française de Physique Médicale, Strasbourg, juin 2012.

Gervaise A, Osemont B, Louis M, Lecocq S, Teixeira P, Blum A. Réduction de la dose des scanners abdominopelviens grâce aux reconstructions itératives AIDR 3D. 60ème Journées Françaises de Radiologie, Paris, Octobre 2012.

Gervaise A, Teixeira P, Villani N, Lecocq S, Louis M, Blum A. Optimisation et réduction de la dose en scanner ostéo-articulaire. 60ème Journées Françaises de Radiologie, Paris, Octobre 2012.

Naulet P, Wassel J, Gervaise A, Blum A. Evaluation de l'intérêt de l'acquisition abdominopelvienne sans injection lors de la réalisation d'un scanner corps entier chez un patient suspect de polytraumatisme. Journée des Assistants et des Internes, Ecole du Val de Grace, Paris, 11 octobre 2012.

Gervaise A, Teixeira P, Villani N, Lecocq S, Louis M, Blum A. Musculoskeletal CT : How to reduce the dose? RSNA 2012, Chicago, USA, 25-30 november 2012. *Certificate of Merit.*

Gervaise A, Osemont B, Louis M, Lecocq S, Teixeira P, Blum A. Full-dose versus low-dose abdominal CT: comparison between Filtered Back Projection versus Adaptive Iterative Dose Reduction 3D. European Congress of Radiology 2013, Vienna, Austria, 1-5 march 2013.

Gervaise A, Naulet P, Beuret F, Pernin M, Porton Y, Lapierre-Combes, Henry C. Evaluation d'un protocole de scanner basse dose pour recherche d'une colique néphrétique. 61ème Journées Françaises de Radiologie, Paris, 10 octobre 2013.

Beuret F, Naulet P, Lapierre-Combes M, Pernin M, Portron P, Gervaise A. Low-dose CT with automatic tube current modulation, adaptive statistical iterative reconstruction, and low tube voltage for the diagnosis of renal colic: impact of body mass index. RSNA 2013, Chicago, USA, 1-6 December 2013.

Gervaise A, Beuret F, Naulet P, Henry C, Pernin M, Portron P, Lapierre-Combes M. Low-dose CT with automatic tube current modulation, adaptive statistical iterative reconstruction, and low tube voltage for the diagnosis of renal colic. European Congress of Radiology 2014, Vienna, Austria, march 2014.

Gervaise A, Gervaise-Henry C, Pernin M, Naulet P, Junca-Laplace C, Lapierre-Combes M. Low dose CT for renal colic: how to do it? European Congress of Radiology 2016, Vienna, Austria, 4-8 march 2016.

Gervaise A, Teixeira P, Hossu G, Blum A, Lapierre-Combes M. Optimizing z-axis coverage of abdominal CT scans of the urinary tract: a proposed alternative proximal landmark for acquisition planning. European Congress of Radiology 2016, Vienna, Austria, 4-8 march 2016.

- **Communications orales :**

Gervaise A, Batch T, Loeuille D, Valckenaere I, Noël A, Guillemin F, Blum A. Comparaison de la dose délivrée par un scanner 320-détecteurs en mode volumique versus hélicoïdal. 57ème Journées Françaises de Radiologie, Paris, 17 octobre 2009.

Gervaise A**,** Pernin M, Naulet P, Junca-Laplace C, Darbois H, Lapierre-Combes M, Esperabe-Vignau F. Evaluation des connaissances des praticiens de l'HIA Legouest en matière de radioprotection des patients. 7ème Journée de Médecine d'Armée de l'Est, Metz, 21 octobre 2010.

Gervaise A. Reconstructions itératives : principes et applications dans la réduction de la dose en scanographie. Séance de l'Association pour la Formation Permanente en Radiologie (AFPR) : les nouveautés en radiologie ostéo-articulaire. Nancy, 24 février 2011.

Gervaise A. Impact des algorithmes itératifs de reconstruction sur l'interprétation des images en scanographie. 50ème Journées Scientifiques de la Société Française de Physique Médicale, Nantes, 9 juin 2011.

Gervaise A, Esperabe-Vignau F, Pernin M, Naulet P, Portron Y, Lapierre-Combes M. Evaluation des connaissances des prescripteurs de scanner en matière de radioprotection des patients. 59ème Journées Françaises de Radiologie, Paris, 21 octobre 2011.

Pernin M, Lapierre-Combes M, Naulet P, Junca-laplace C, Portron Y, Gervaise A. Evaluation des connaissances des prescripteurs de scanner en matière de radioprotection des patients. Journée des Assistants et des Internes, Ecole du Val de Grace, Paris, octobre 2011.

Bisconte S, Manen O, Dubourdieu D, Gervaise A, Hornez AP, Oliviez JF, Deroche J, Brunetti G, Martel V, Perrier E, Généro M. Réflexions sur l'irradiation médicale en expertise aéronautique. Réunion de la SOFRAMAS, Paris, 19 janvier 2012.

Blum A, Gervaise A, Teixeira P. AIDR 3D: a promising dose reduction tool in clinical applications. European Congress of Radiology, Vienna, Austria, 4 march 2012.

Gervaise A, Osemont B, Lecocq S, Micard E, Noel A, Felblinger J, Blum A. CT image quality improvement using adaptive iterative dose reduction with wide-volume acquisition on 320-detector CT. European Congress of Radiology, Vienna, Austria, 5 march 2012.

Gervaise A. Optimisation et réduction de la dose des scanners en pathologie ostéo-articulaire. Séance de l'Association pour la Formation Permanente en Radiologie (AFPR) : les nouveautés en radiologie ostéo-articulaire, Nancy, 6 mars 2012.

Blum A, Teixeira P, Villani N, Lecocq-Teixeira S, Louis M, Gervaise A. How to reduce the CT-scan radiation dose in MSK disorders? 41ème Congrès de radiologie brésilienne, Brasilia, Brésil, 6-8 septembre 2012.

Beuret F, Gervaise A, Naulet P, Pernin M, Portron Y, Lapierre-Combes M. Evaluation d'un scanner basse dose chez des patients adressés pour recherche de colique néphrétique. Journée de printemps de la SFR Lorraine, Metz, 13 avril 2013. *Prix de la meilleure communication libre.*

Naulet P, Junca-Laplace C, Pernin M, Portron Y, Lapierre-Combes M, Gervaise A. Impact du remplacement d'un scanner par un de nouvelle génération sur la qualité d'image et l'exposition des patients aux rayonnements ionisants. Journée de printemps de la SFR Lorraine, Metz, 13 avril 2013.

Gervaise A, Naulet P, Beuret F, Pernin M, Portron Y, Lapierre-Combes M. Intérêt du scanner basse dose dans l'exploration des coliques néphrétiques de l'adulte. 10ème Journée de Médecine d'Armée de l'Est, Metz, 24 octobre 2013.

Gervaise A, Naulet P, Beuret F, Henry C, Pernin M, Portron P, Lapierre-Combes C. Low-dose CT with automatic tube current modulation, adaptive statistical iterative reconstruction, and low tube voltage for the diagnosis of renal colic: impact of body mass index. RSNA, Chicago, USA, 1st December 2013.

Gervaise A. Scanner SubmSv : état des lieux et perspectives. VII Symposium scanner volumique, Nancy, 26 janvier 2016.

CHAPITRE 1 : CONTEXTE ET PROBLEMATIQUE

1- Contexte :

Développé au début des années 1970, le scanner s'est imposé de nos jours comme une technique d'imagerie médicale incontournable. Grâce à des développements technologiques considérables ces dernières années (scanner hélicoïdal en 1989, scanner multi-détecteurs en 1998, scanner bi-tube en 2006, scanner à large système de détection en 2008) et à sa grande disponibilité, le scanner est devenu l'examen de choix pour l'exploration de nombreuses pathologies traumatiques, osseuses, pulmonaires, cardio-vasculaires ou encore néoplasiques. Il permet d'en faire le diagnostic, d'en suivre l'évolution et peut même en permettre le traitement à travers l'émergence de la radiologie interventionnelle.

Compte tenu de ses performances, le nombre de scanners réalisés chaque année est en constante progression. Aux Etats-Unis, ce sont plus de 70 millions de scanners réalisés chaque année [1] (Figure 1). En France, l'Institut de Radioprotection et de Sûreté Nucléaire (IRSN) rapporte une augmentation de 26 % des actes de scanographie entre 2002 et 2007 [2] et une augmentation de 12 % entre 2007 et 2012 [3] avec plus de 8 millions de scanners réalisés chaque année.

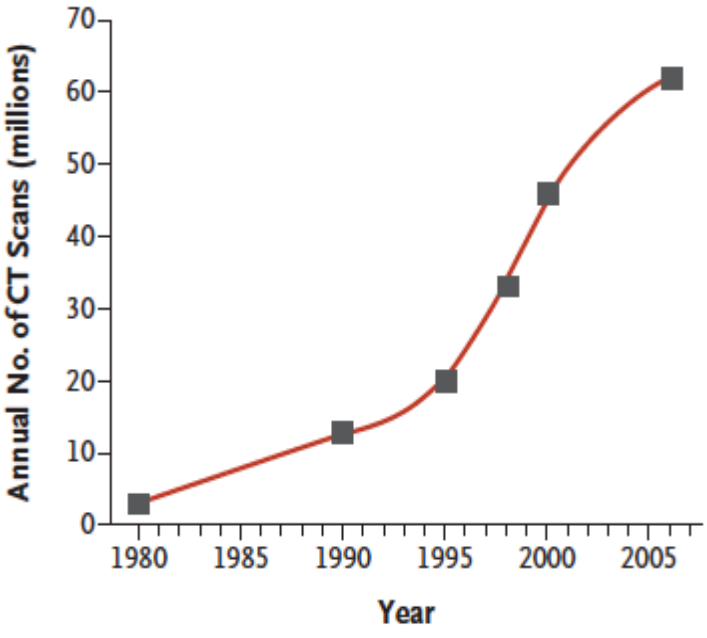

Figure 1: Estimation du nombre de scanners réalisés annuellement aux Etats-Unis (d'après Brenner DJ *et al.* 2007 [1]).

Toutefois, le scanner est une technique d'imagerie irradiante. Son principe est basé sur la reconstruction d'une image à partir du calcul de l'atténuation de multiples projections d'un faisceau de rayons X autour du patient. Même si la dose de rayons X délivrée au décours d'un scanner reste faible, de l'ordre du mSv, le scanner est responsable en France de 71 % de l'irradiation due aux rayonnements ionisants d'origine médicale alors que les actes de scanographie ne représentent que 10,1 % de l'ensemble des actes de radiologie irradiants (Figure 2) [3].

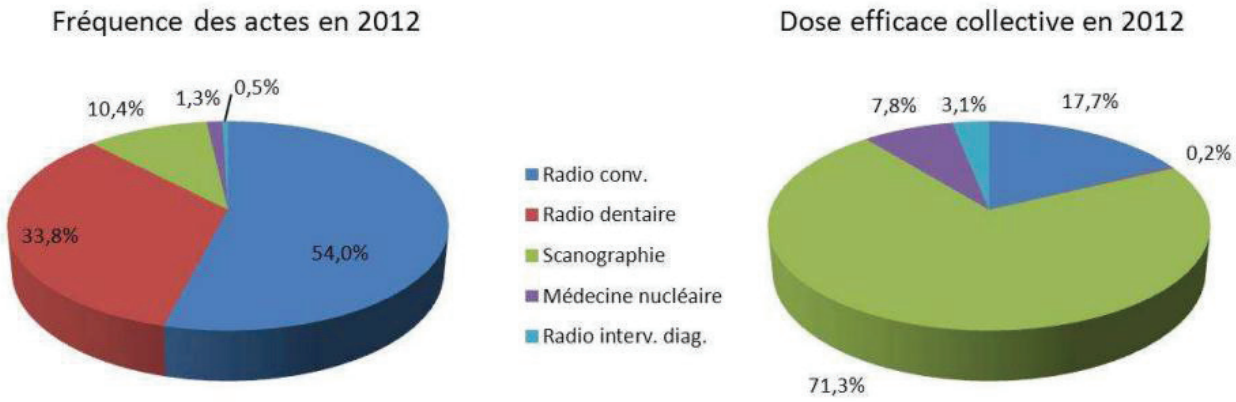

Figure 2 : Fréquence des actes d'imagerie utilisant des rayonnements ionisants et répartition par modalité d'imagerie de la dose efficace collective en 2012 (d'après le rapport IRSN 2014 [3]).

Or, même si le lien entre l'exposition à de faibles doses de rayons X et l'augmentation du risque de cancer radio-induit est fortement controversé, il a été établi par plusieurs grandes institutions et par de nombreux rapports ou publications internationales [4-6]. En particulier, la conférence de consensus BEIR VII (*Biologic Effects of Ionizing Radiation*) qui s'est tenue en 2006 et qui s'appuyait sur les estimations les plus récentes et complètes en matière de risque de cancer suite à l'exposition à de faibles doses de rayonnements ionisants soutient un modèle de relation linéaire sans seuil (RLSS) [4]. Cela signifie que le risque de cancer causé par de faibles doses de rayonnements ionisants augmente de façon linéaire et ne connait pas de seuil (Figure 3). De ce fait, la plus petite dose a le potentiel de provoquer une légère augmentation du risque de cancer radio-induit chez l'homme. En reprenant ce modèle de RLSS des effets des rayons X à faibles doses, des publications ont ainsi estimé le risque de cancer radio-induit lié à la réalisation d'un seul scanner abdominopelvien (avec une dose d'environ 10 mSv) de l'ordre de 1/1000 chez une jeune femme [7].

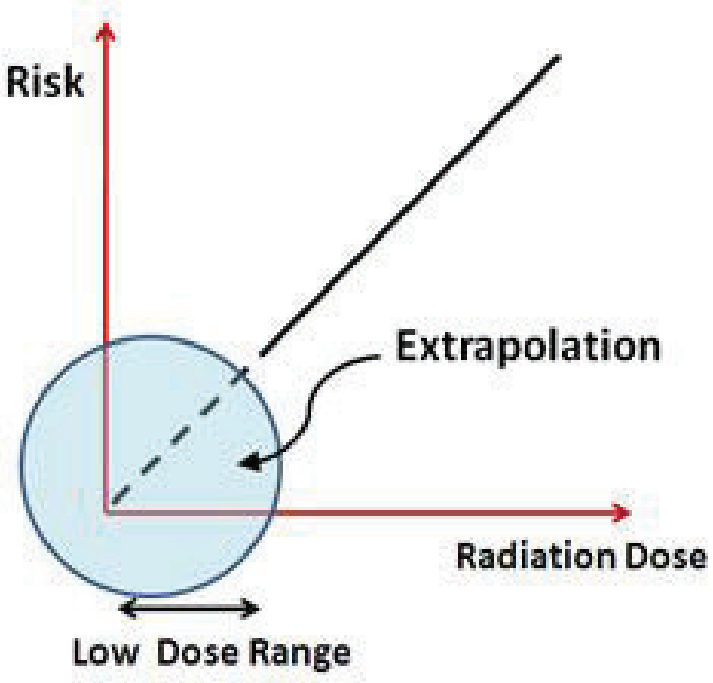

Figure 3 : Graphique représentant la relation entre la dose d'irradiation (Radiation Dose) et les risques de cancer radio-induit (Risk). La ligne continue représente les données connues pour les doses supérieures à 200 mSv, avec une relation linéaire et proportionnelle entre le niveau de dose d'irradiation et le risque de cancer radio-induit. Pour les faibles doses (< 200 mSv), la ligne en pointillé correspond à l'extrapolation des données suivant un modèle de régression linéaire sans seuil (source internet : http://www.gnetrading.com/php/images/lnt.jpg).

Ce risque important reste toutefois un risque maximal théorique. D'autres auteurs estiment pour leur part soit qu'un tel risque n'existe pas, soit qu'il est largement surestimé [8-10]. Enfin, des résultats expérimentaux récents tendent à montrer que suite à une exposition à de faibles doses de rayons X, les effets biologiques ne suivent pas une relation linéaire mais entraineraient des effets positifs selon une réponse adaptative. Cet effet « Hormesis » serait lié à la stimulation des mécanismes de réparation tissulaire secondaire à l'irradiation des cellules par une faible dose de rayons X et apporterait une protection de la cellule vis-à-vis des rayonnements ionisants [10] (Figure 4).

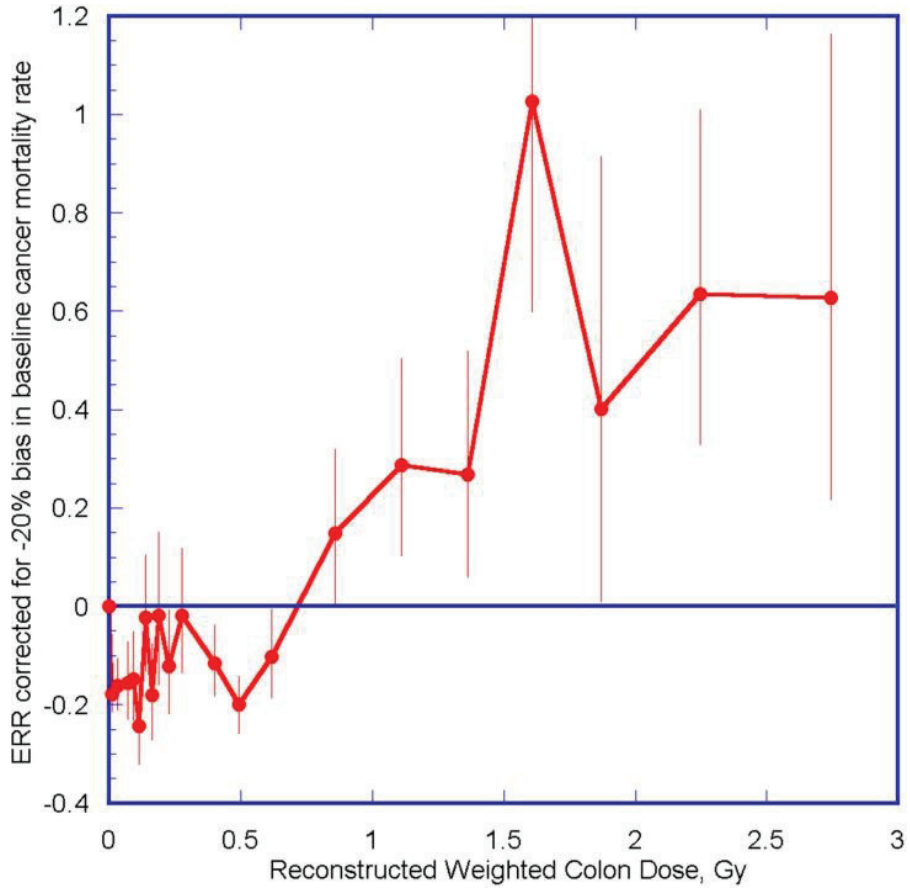

Figure 4 : Excès de risque relatif de la mortalité par cancer solide chez les survivants des bombes atomiques : notez l'inversion du risque relatif pour les doses les plus faibles traduisant l'effet « Hormesis » (d'après Doss M. 2013 [10]).

L'absence de preuves scientifiques formelles allant dans un sens ou dans l'autre impose de suivre le principe de précaution et aboutit à la nécessité de réduire au maximum les doses d'irradiation délivrées aux patients. Ce principe de précaution ALARA (« *As Low As Reasonably Achievable* ») a d'ailleurs été repris par l'Union Européenne dans la directive Euratom 97/43 [11] puis par la directive Euratom 2013/59 [12]. Cette dernière précise que les examens d'imagerie irradiants doivent faire l'objet d'une justification et d'une optimisation constante afin de réduire les doses individuelles et collectives dues aux expositions médicales. Toutefois, même si la réduction des doses délivrées au scanner est devenue primordiale, elle ne doit pas se faire aux dépens de la performance diagnostique des examens, le but étant d'obtenir l'information diagnostique avec la dose de rayons X la plus faible. C'est ainsi que ces dernières années, de nombreux efforts ont été réalisés pour réduire les doses délivrées au cours des scanners.

2- Problématique : comment optimiser et réduire la dose d'irradiation au scanner ?

Les modalités d'optimisation et de réduction de la dose d'irradiation au scanner sont nombreuses. Elles correspondent soit à des facteurs comportementaux, soit à des facteurs techniques.

A- Les facteurs comportementaux :

Les facteurs comportementaux correspondent à l'ensemble des mesures qui permettent de réduire la dose d'irradiation et dont la mise en œuvre est indépendante des facteurs techniques et du matériel scanographique disponible par le radiologue (Tableau I).

Tableau 1 : Principaux facteurs comportementaux à prendre en compte dans une démarche d'optimisation et de réduction de la dose d'irradiation au scanner.

Principaux facteurs comportementaux
- Education et sensibilisation des équipes médicales et paramédicales - Justification de l'indication des scanners - Substitution des scanners par une technique d'imagerie non irradiante - Réduction du nombre de phases d'acquisition - Limitation de la couverture d'acquisition - Positionnement optimal du patient - Utilisation de bouclier de protection en bismuth

L'intérêt principal de ces facteurs comportementaux est qu'ils sont indépendants du type de matériel disponible par le radiologue et donc qu'ils sont utilisables pour n'importe quel type de scanner. Il s'agit aussi de méthodes de réduction de la dose qui sont peu coûteuses, simples et rapides à mettre en œuvre. Nous proposons de faire un bref rappel sur l'intérêt de chacun de ces facteurs comportementaux dans une démarche d'optimisation et de réduction de la dose d'irradiation au scanner.

a- Education et sensibilisation :

L'éducation et la sensibilisation des équipes médicales et paramédicales sont fondamentales [13]. Cette sensibilisation nécessite toutefois la connaissance des doses délivrées par les radiologues et les manipulateurs en radiologie. Dans cette optique, l'affichage du PDL (Produit Dose Longueur) à la console du scanner avant la réalisation de l'acquisition est indispensable et est actuellement systématiquement disponible pour l'ensemble des constructeurs. La sensibilisation des radiologues et des manipulateurs en radiologie est également de plus en plus assurée par le biais de logiciel de recueil et d'analyse des doses délivrées. Outre la connaissance des doses délivrées pour chaque scanner, ces logiciels permettent le suivi dosimétrique par patient et permettent de détecter pour certains des cumuls de dose parfois importants. Ces logiciels comportent également des alertes dosimétriques qui incitent à optimiser les protocoles et apportent une sécurité dosimétrique vis-à-vis des patients. Ils permettent enfin de suivre la réduction globale des doses au cours d'une démarche d'optimisation des protocoles scanographiques [14]. De manière plus globale, des registres de doses nationaux ou internationaux sont également en train de voir le jour, comme par exemple le *CT Dose Index Registry* [15]. Ce registre mis en service par l'initiative de l'*American College of Radiology* a pour but de récupérer les doses scanographiques de nombreux services de radiologie américains et étrangers dans l'optique de comparer les doses et d'harmoniser les pratiques.

Enfin, l'éducation des médecins et des manipulateurs en radiologie permet de mettre en avant les situations pour lesquelles la réduction de dose est particulièrement importante. Notons, par exemple, que l'âge est un facteur primordial puisque le risque potentiel de cancer radio-induit lié aux faibles doses de rayons X décroit avec l'âge [16]. Une vigilance particulière est donc la règle chez les sujets jeunes. De même, la localisation anatomique du scanner est importante à prendre en compte. La dose efficace d'une acquisition à distance des organes radiosensibles, comme c'est le cas pour les articulations périphériques, sera négligeable (avec des doses efficaces parfois inférieures à celle d'une radiographie thoracique !) au contraire d'une acquisition thoraco-abdominopelvienne.

b- Justification et substitution :

La justification et la substitution d'un scanner par une technique d'imagerie non irradiante comme l'échographie ou l'Imagerie par Résonance Magnétique (IRM) sont aussi deux éléments importants dans une démarche de réduction de la dose au scanner : « le scanner qui irradie le moins est celui qui n'est pas réalisé ». Par exemple, Oikarinen H *et al.* [17] ont montré dans leur étude portant sur 30 scanners lombaires réalisés chez des patients de moins de 35 ans, que seulement 7 (23 %) étaient indiqués. Sur les 23 scanners lombaires non indiqués, 20 auraient pu bénéficier d'une IRM tandis que pour 3 patients, il n'y avait aucune indication d'imagerie.

c- Réduction du nombre de phases d'acquisition :

La limitation du nombre de phases d'acquisition d'un scanner permet aussi de réduire la dose. En effet, la dose globale de l'examen est calculée à partir de la somme des doses de chaque acquisition. Par exemple, lors de la réalisation d'un scanner abdominopelvien, la réalisation d'une unique série injectée au temps portal versus deux acquisitions identiques sans et après injection au temps portal permet de réduire la dose de moitié. Tandis que certaines pathologies nécessitent la réalisation d'un examen multiphasique avec une série sans injection et deux ou trois acquisitions après injection de produit de contraste iodé à différents temps (exploration des lésions hépatiques, caractérisation d'une lésion surrénalienne, bilan d'une lésion tumorale rénale) [18-19], pour d'autres pathologies (embolie pulmonaire, poly-traumatisme) des études ont montré l'absence d'amélioration de la performance diagnostique liée à la série sans injection [20].

d- Limitation de la couverture d'acquisition :

La limitation de la couverture d'acquisition est un moyen simple, efficace et rapide pour réduire la dose. En effet, même si la longueur d'acquisition n'affecte pas l'indice de dose scanographique volumique, la dose totale de l'examen est directement liée à la longueur d'acquisition et au risque de cancer radio-induit lié aux faibles doses de rayons X. La couverture d'acquisition doit être centrée sur la zone d'intérêt, préalablement repérée par le ou les topogramme(s) du scanner. Avec les scanners modernes, permettant une acquisition rapide

d'un grand volume, les couvertures d'acquisition des scanners ont tendance à augmenter [21]. Tandis qu'une longueur d'acquisition trop importante est à l'origine d'une augmentation de la dose délivrée, à l'inverse, une réduction trop importante de la couverture d'acquisition peut être à l'origine d'une baisse de la performance diagnostique par la non-visualisation d'une structure pathologique située en dehors de la zone explorée [22]. Par exemple, pour la recherche d'une embolie pulmonaire, une réduction de la couverture d'acquisition jusqu'à 47 % permet de conserver une bonne performance diagnostique pour la recherche d'une embolie pulmonaire [23] mais une réduction trop importante de la longueur d'acquisition peut aussi masquer des diagnostics différentiels [22].

e- Positionnement optimal du patient :

Un centrage précis de la zone anatomique à scanner au centre de l'anneau permet d'obtenir une qualité d'image et une dose délivrée optimales [24]. La résolution spatiale est effectivement meilleure au centre de l'anneau car plus d'interpolations des données y sont réalisées par rapport à la périphérie [25] (Figure 5). Par ailleurs, un bon centrage est particulièrement nécessaire lors de l'utilisation de la modulation automatique du milliampérage car celle-ci considère le patient au centre de l'anneau. En cas de mauvais centrage, la modulation automatique fait augmenter la dose de façon significative [26]. La position du patient influe également sur la dose et la qualité d'image. L'épaisseur du volume scanné doit être la plus fine possible pour limiter les artéfacts de durcissement du faisceau.

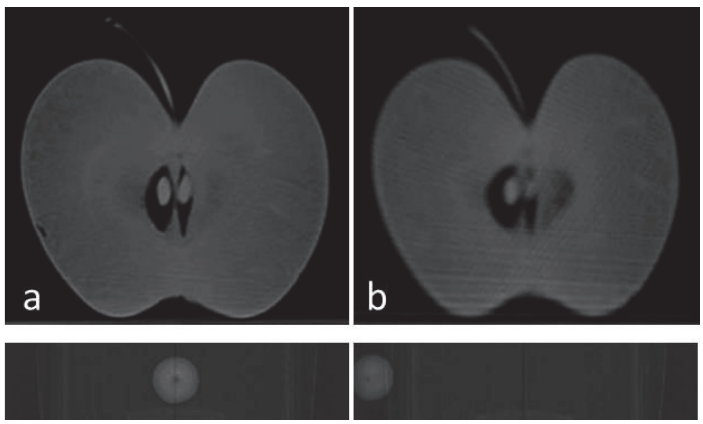

Figure 5 : Exemple montrant la qualité d'image d'une pomme positionnée au centre de l'anneau du scanner (a) et à sa périphérie (b). Notez la dégradation de la qualité d'image et de la résolution spatiale quand la pomme n'est pas centrée (b).

f- Utilisation de bouclier de protection en bismuth

Des boucliers de protection en bismuth sont disponibles pour diminuer la dose d'irradiation aux glandes mammaires lors de l'acquisition d'un scanner thoracique (Figure 6), pour la thyroïde au cours d'un scanner cervical (Figure 7) et pour protéger les yeux lors de l'acquisition d'un scanner cérébral. Par exemple, lors de l'acquisition d'un scanner cérébral avec un bouclier de protection oculaire, Ciarmatori A *et al.* rapportent une réduction de la dose au cristallin de l'ordre de 21 à 28 %, sans modification de la qualité d'image du scanner cérébral [27].

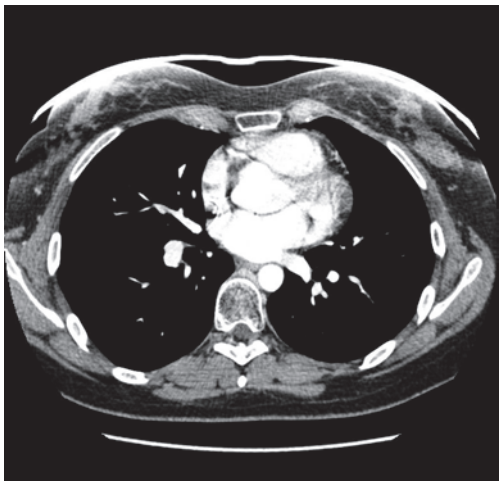

Figure 6 : Bouclier de protection mammaire en bismuth chez une jeune femme. Notez les artéfacts de durcissement du faisceau au niveau des seins et au contact du bouclier de protection traduisant une absorption plus importante des rayons X par le bouclier et permettant ainsi de réduire la dose aux glandes mammaires. Par contre, l'analyse du thorax ne montre pas d'altération de la qualité d'image.

Figure 7 : Bouclier de protection en bismuth pour la thyroïde (source internet : http://www.xraystore.fr/4257-attenurad-protection-thyroide-boite-de-10.html).

B- Facteurs techniques :

Les facteurs techniques sont ceux liés au type et au modèle de scanner utilisé. Ces facteurs sont nombreux. Certains ne sont pas modifiables directement par l'utilisateur comme par exemple la géométrie du couple tube-détecteur, le type de détecteur, la filtration ou encore l'utilisation d'un bouclier anti-hélice. D'autres paramètres sont accessibles et peuvent être modifiés pour optimiser la dose et la qualité d'image, soit au moment de l'acquisition des images, soit a posteriori. Le tableau II reprend les différents paramètres techniques accessibles dans une démarche d'optimisation de la dose.

Tableau 2 : Paramètres techniques permettant d'optimiser la dose et la qualité d'image du scanner au moment de l'acquisition ou a posteriori.

Paramètres accessibles au moment de l'acquisition	Paramètres accessibles après l'acquisition
- Mode d'acquisition : séquentiel ou hélicoïdal - Tension du tube radiogène (kilovoltage) - Charge du tube radiogène (milliampérage) - Nombre de détecteur - Pas de l'hélice (pitch)	- Epaisseur de coupe et l'intervalle inter-coupe - Algorithme de reconstruction - Filtre de reconstruction

a- Mode d'acquisition :

Le mode d'acquisition est l'un des facteurs techniques qui influence la dose et qui est accessible au moment de l'acquisition. Historiquement, les premières acquisitions scanographiques étaient réalisées en mode axial séquentiel (Figure 8a). Avec ce mode d'acquisition, le couple tube-détecteur fait une rotation autour du patient puis la table avance avant de refaire une rotation et ainsi de suite. Dans les années 2000, le développement de l'acquisition hélicoïdale a permis de réduire considérablement le temps d'acquisition. En mode hélicoïdal, l'acquisition est continue et la table avance en même temps que l'acquisition est réalisée, sans marquer d'arrêt (Figure 8b).

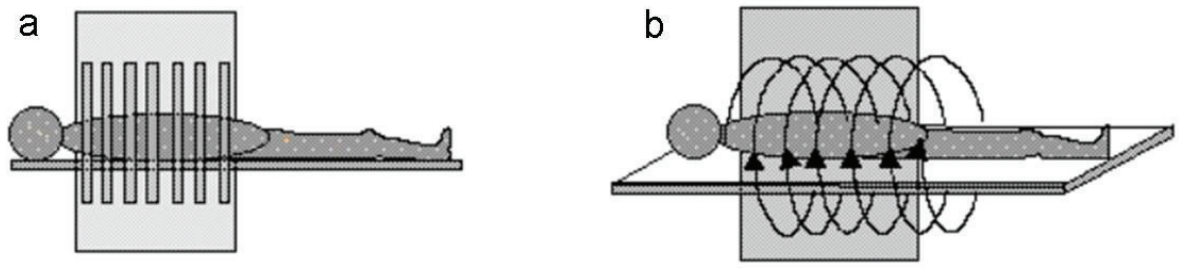

Figure 8 : Comparaison d'un scanner séquentiel (a) et d'un scanner hélicoïdal (b) (source internet : http://runphym.free.fr/NewFiles/scan.html).

Avec le mode hélicoïdal, afin de s'assurer de l'entièreté des premières et dernières coupes de l'acquisition, il est nécessaire de faire un tour supplémentaire à chaque extrémité de la zone explorée. Cette exposition « pré et post-hélice » appelée *overranging* ou *z overscanning* varie proportionnellement en fonction du pitch et du nombre de détecteurs. Le pourcentage de dose liée à l'*overranging* est inversement proportionnel à la longueur d'exploration [28]. De ce fait, avec les scanners modernes comportant fréquemment une rangée de 64-détecteurs, l'*overranging* peut représenter une part non négligeable de l'irradiation totale (de l'ordre de 10 % pour une acquisition abdominopelvienne et jusqu'à 20 ou 30 % pour une acquisition cardiaque) [29]. Plus récemment, les avancées technologiques ont permis de mettre au point des scanners à large système de détection. Par exemple, au CHRU de Nancy, le scanner 320-détecteurs a été installé en 2008 permettant de faire une acquisition de 16 cm en une rotation. Il est donc possible de revenir au mode d'acquisition séquentiel « *wide-volume* » et de réduire la dose par rapport à une acquisition hélicoïdale classique en supprimant l'irradiation inutile liée à l'*overranging* (Figure 9).

Figure 9 : Mise en évidence du phénomène d'*overranging* à partir d'un papier radiochromique (en présence de rayons X, la zone irradiée s'assombrit). Deux acquisitions de même longueur sont réalisées en mode hélicoïdal (papier du haut) et volumique séquentiel (papier du bas). Pour la même longueur d'acquisition, la zone irradiée est plus importante en mode hélicoïdal : cette exposition « pré et post-hélice » correspond à l'*overranging* (doubles flèches).

b- Milliampérage :

Lors de l'acquisition, le principal facteur accessible et modifiable par l'utilisateur est le milliampérage (mA). Le mA correspond à l'intensité du courant du tube radiogène et représente la quantité de photons produite au sein du faisceau de rayons X. Le mA est proportionnel à la dose délivrée et inversement proportionnel au carré du bruit de l'image [30]. Une réduction du milliampérage par 2 permet donc de réduire la dose par 2 mais augmente le bruit de l'image d'un facteur 1,4 (Figure 10).

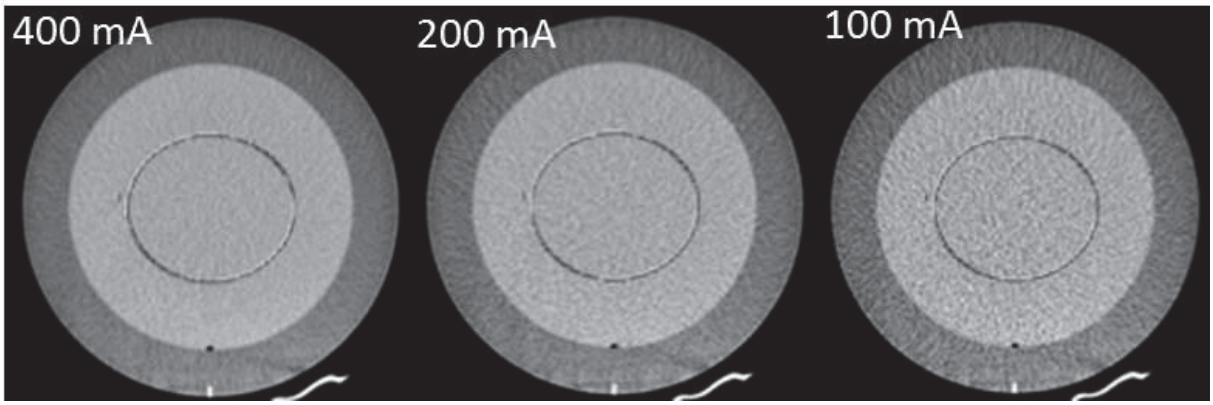

Figure 10 : Exemple de l'influence du milliampérage à partir de trois acquisitions d'un fantôme d'eau avec des valeurs de milliampérage décroissant (400, 200 et 100 mA) et en gardant les autres paramètres d'acquisition constants. Notez la dégradation de la qualité d'image avec une augmentation du bruit quand le milliampérage diminue.

L'optimisation du milliampérage doit aussi prendre en compte le morphotype du patient. En effet, la quantité de photons X nécessaire pour garder une qualité de l'image constante est variable en fonction de l'épaisseur du patient. Pour mieux adapter le mA au morphotype des patients, des techniques de modulation automatique du milliampérage ont été développé au début des années 2000 [31]. Grâce à ces techniques, le mA est automatiquement adapté au morphotype du patient et à la zone anatomique à explorer et le bruit de l'image reste constant sur l'ensemble des images de l'acquisition [32] (Figure 11).

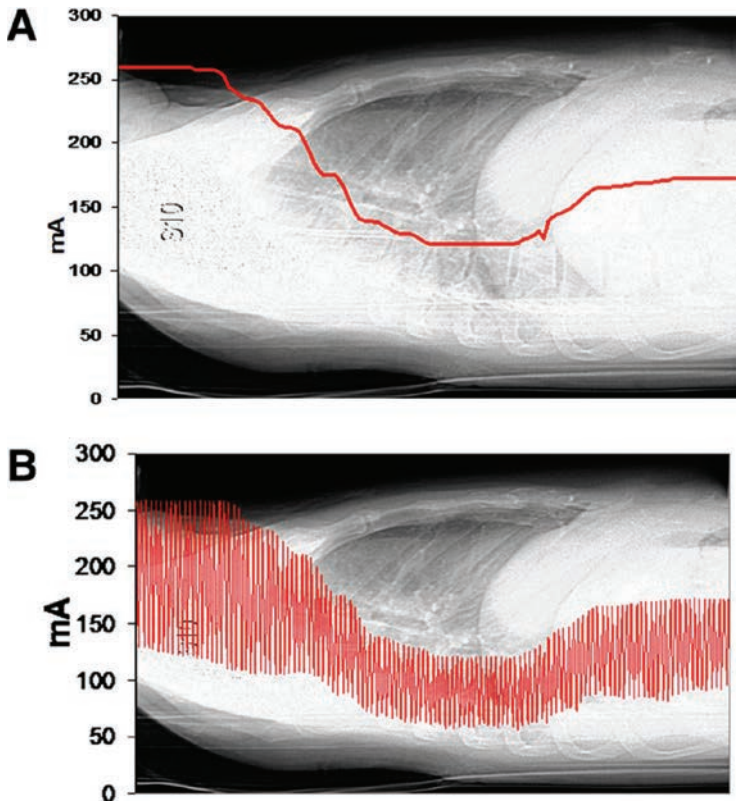

Figure 11 : Représentation graphique de la modulation automatique du milliampérage sur un scanner thoracique. La modulation longitudinale du milliampérage est caractérisée par un changement du milliampérage dans l'axe z en fonction des changements de l'atténuation du patient (A). Une modulation angulaire permet aussi d'adapter le milliampérage au sein d'une même coupe du fait de l'asymétrie de l'atténuation entre les régions antéropostérieures et latérales de la coupe (B) (d'après Singh S *et al.* 2011 [32]).

c- Kilovoltage :

Le kilovoltage (kV) correspond à l'énergie des photons produits au sein du faisceau de rayons X. Il est généralement compris entre 70 et 140 kV. La baisse du kilovoltage est à l'origine d'une réduction importante de la dose (par exemple, en gardant les autres paramètres constants, la baisse du kilovoltage de 120 à 80 kV réduit la dose délivrée d'un facteur 2,2 [26]) mais est aussi à l'origine d'une augmentation du bruit [33] (Figure 12). Une réduction trop importante du kV peut aussi être à l'origine d'artéfact de durcissement du faisceau. Par contre, la réduction du kV améliore le contraste des images réalisées avec injection de produit de contraste iodé car l'abaissement de l'énergie moyenne du faisceau favorise d'absorption des photons X par effet photo-électrique et cela d'autant plus que l'énergie des rayons X est proche du pic de fluorescence de l'iode (Figure 13).

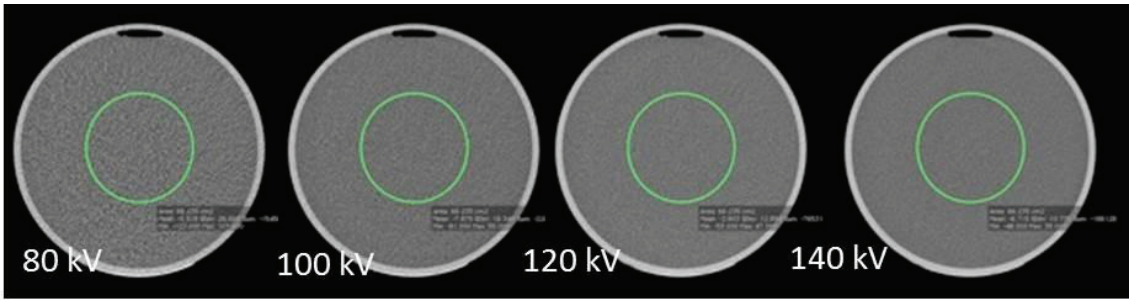

Figure 12 : Exemple de l'influence du kilovoltage à partir de quatre acquisitions d'un fantôme d'eau avec des valeurs de kV croissant (80, 100, 120 et 140 kV) et en gardant les autres paramètres d'acquisition constants. En diminuant le kV de 120 à 80 kV la dose est réduite d'un facteur 2,2 mais le bruit augmente.

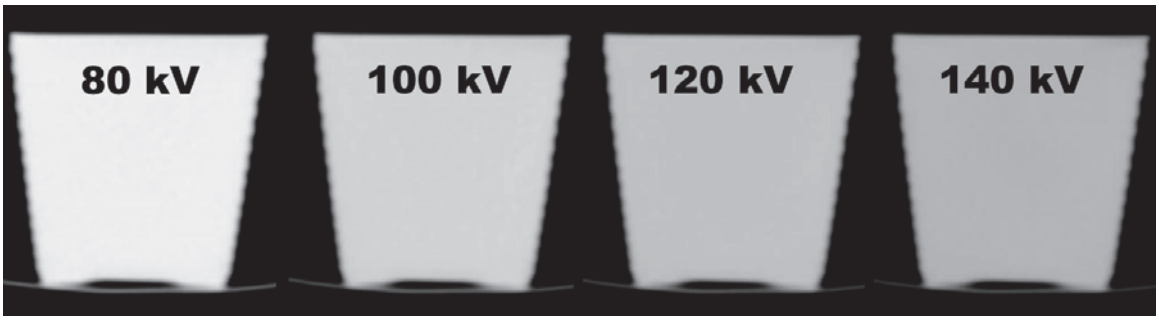

Figure 13 : Exemple de l'influence du kilovoltage en cas de présence de produit de contraste iodé. Acquisitions d'un verre contenant 100 mL d'eau et 5 mL d'IOMERON 400® avec des valeurs de kV croissante (80, 100, 120 et 140 kV) et en gardant les autres paramètres constants. Notez l'augmentation progressive des valeurs d'atténuation quand le kV diminue.

d- Pitch ou pas de l'hélice :

Avec les scanners multi détecteurs actuels comportant les techniques modernes de modulation de la dose, le changement du pitch (pas de l'hélice) ne modifie plus la dose car il s'ensuit une adaptation automatique du milliampérage [34]. Un pitch élevé, de l'ordre de 1,5, sera préféré pour réduire le temps d'acquisition et les artéfacts de mouvement (par exemple, lors de l'exploration d'un patient polytraumatisé). Le pitch doit toutefois rester inférieur à 2 afin de garder une qualité optimale des reformations multi-planaires [34] et d'éviter l'apparition d'artéfacts d'hélice [35]. A l'opposé, un petit pitch sera préféré pour réduire les artéfacts métalliques en rapport avec les matériels d'ostéosynthèse [36].

e- Epaisseur de coupe :

De manière générale, les acquisitions sont réalisées en coupes fines (0,5 à 1 mm) et sont reconstruites en coupes plus épaisses (2 à 5 mm). Les coupes submillimétriques améliorent la résolution spatiale, réduisent les effets de volume partiel et permettent la réalisation de reconstruction dans un volume quasi-isotrope [37]. Par contre, à bruit constant, l'acquisition en coupes fines est à l'origine d'une augmentation de l'irradiation [38]. En cas de réduction excessive du milliampérage, l'acquisition en coupes fines engendre une augmentation importante du bruit de l'image. Ainsi, tandis que l'acquisition se fait en coupes submillimétriques, lors de l'interprétation des images, l'épaississement des coupes permet d'augmenter le rapport signal sur bruit [37] et d'améliorer l'analyse des images [39-40].

f- Reconstructions des images :

La reconstruction des images est un facteur technique important qui est modifiable après l'acquisition et qui influence la qualité des images et donc indirectement la dose. Historiquement, les images des scanners étaient reconstruites à partir d'une rétroprojection filtrée. Cette méthode avait pour avantage d'être simple, robuste et rapide. Par contre, elle était à l'origine d'un bruit important de l'image, notamment en cas de réduction trop importante de la dose [41]. Entre 2008 et 2010, grâce à l'importante augmentation de la puissance informatique, les principaux constructeurs de scanner ont commercialisés des nouveaux algorithmes de reconstruction itérative. Grâce à une meilleure utilisation des données issues des projections, ces algorithmes ont permis de réduire le bruit des images scanographiques [42]. A qualité d'image constante, ces algorithmes ont donc permis de réduire la dose des scanners [43].

g- Filtre de reconstruction :

L'amélioration du rapport contraste sur bruit peut également se faire par l'utilisation de filtres de réduction de bruit à partir de logiciels de post-traitement. L'application de ces filtres se fait sur des images déjà reconstruites ce qui permet de les utiliser à partir de n'importe quelle image scanner, y compris sur des reformations 3D.

3- Environnement de travail :

Au cours de notre travail de thèse, nous avons principalement travaillé dans le service d'imagerie Guilloz du CHRU de Nancy et dans le service d'imagerie médicale de l'HIA Legouest de Metz.

Dans le service d'imagerie Guilloz, nous avons travaillé sur le scanner 320-détecteurs (Figure 14). Ce scanner a été installé en 2008. Il s'agissait à l'époque d'une révolution car il était le premier scanner à large système de détection installé en France.

Grâce à sa rangée de 320 détecteurs de 0,5 mm, ce scanner permet l'acquisition de 16 cm de données dans l'axe z en une seule rotation du tube. Son temps de rotation minimal de 350 ms couplé à des techniques de reconstruction partielle des données permet ainsi d'avoir une excellente résolution temporelle de l'ordre de 175 ms. La répétition de multiples volumes d'acquisition a aussi permis de mettre au point des protocoles de perfusion tumorale ou encore de scanner dynamique des articulations.

Figure 14 : Scanner 320-détecteurs (Aquilion One®, Toshiba). Ce scanner est un scanner à large système de détection (16 cm) comprenant 320 rangées de détecteurs de 0,5 mm. Grâce à ce scanner il est possible de faire l'acquisition en une seule rotation de 16 cm de données.

C'est aussi sur ce scanner qu'a été installé en 2010 pour la première fois au CHRU de Nancy un algorithme de reconstruction itérative : les reconstructions AIDR. Grâce à ces

reconstructions itératives, il était possible de réduire le bruit des images par rapport aux reconstructions standard en FBP (Figure 15).

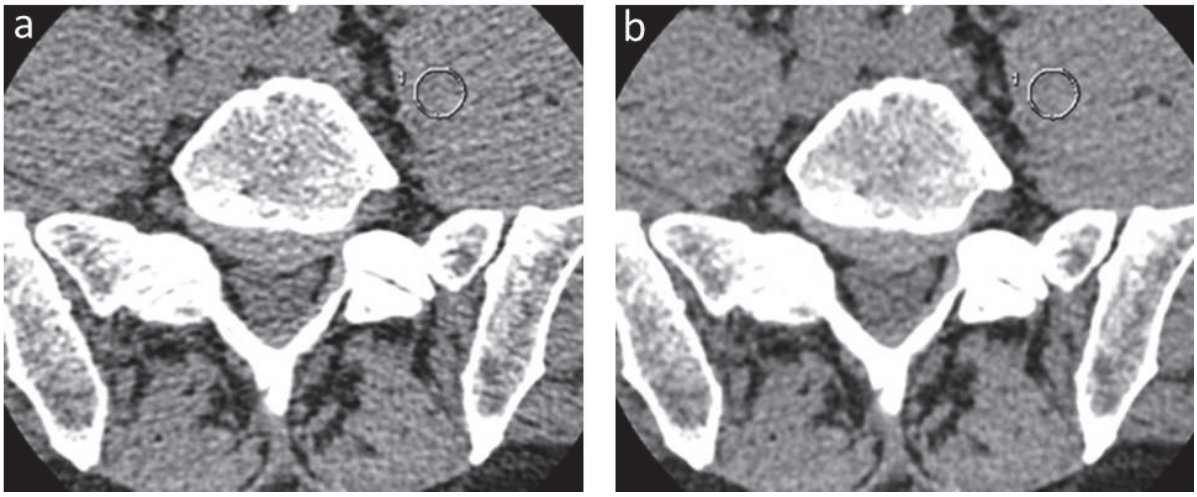

Figure 15 : Scanner lombaire sans (a) et avec les reconstructions itératives AIDR (b). Notez la réduction du bruit de l'image de 34 % grâce aux reconstructions itératives AIDR.

Dans le service d'imagerie de l'HIA Legouest, nous avons eu accès à un scanner 64-détecteurs Optima CT660®. Ce scanner correspond à ce qui se fait classiquement de nos jours dans les services d'imagerie avec un scanner de 64-détecteurs de 0,625 mm et avec un temps de rotation minimal de 500 ms (Figure 16). En même temps que l'installation de ce scanner fin 2011 a été installé les reconstructions itératives ASIR.

Figure 16 : Scanner Optima CT660® installé à l'HIA Legouest.

Au cours de ce travail, nous avons aussi utilisé un fantôme Catphan® 500 (The Phantom Laboratory, Salem, NY, USA) afin de faire des mesures de qualité d'image objective (Figure 17).

Figure 17 : Fantôme Catphan® 500 (The Phantom Laboratory, Salem, NY, USA) (source internet : http://www.jwpacific.com/images/p_catphan3a_lg.jpg).

Ce fantôme est composé de plusieurs modules. Pour calculer le bruit de l'image, le rapport signal sur bruit (RSB) et le rapport contraste sur bruit (RCB) nous avons utilisé le module CTP515. Ce module à faible contraste contient des tiges cylindriques de différents diamètres et trois différents niveaux de contraste (Figure 18).

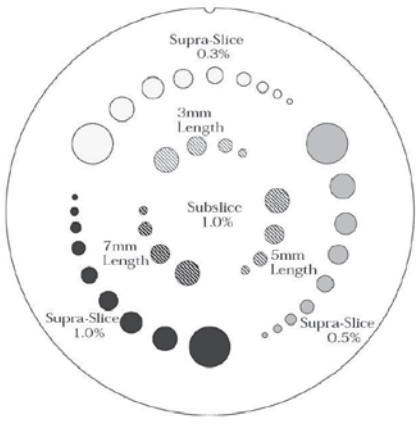

Figure 18 : Dimension et pourcentage de contraste des tiges cylindriques présentes dans le module CTP515 du fantôme Catphan® 500 (d'après Catphan® 500 and 600 Manual, Copyright © 2012).

Pour calculer la résolution spatiale, nous avons utilisé le module 528. Ce module à haute résolution contient deux structures à haute densité pour évaluer la résolution spatiale du scanner (Figure 19). La première structure est un motif circulaire comprenant 21 éléments dont la résolution varie de 1 jusqu'à 21 paires de ligne par cm. La seconde structure comprend deux billes sphériques encastrées dans un matériau uniforme (flèche).

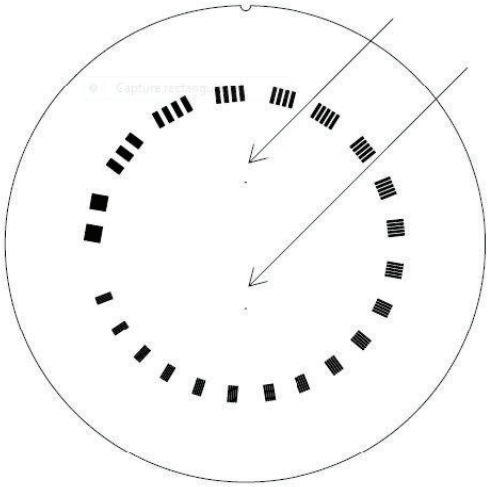

Figure 19 : Coupe axiale du module CTP528 du fantôme Catphan® 500 (d'après Catphan® 500 and 600 Manual, Copyright © 2012).

CHAPITRE 2 : INFLUENCE DES FACTEURS COMPORTEMENTAUX

Ce chapitre est composé de trois articles :

1- Gervaise A, Esperabe-Vignau F, Naulet P, Pernin M, Portron Y, Lapierre-Combes M. Evaluation des connaissances des prescripteurs de scanner en matière de radioprotection des patients. *J Radiol* 2011; 92: 681-87.

2- Naulet P, Wassel J, Gervaise A, Blum A. Evaluation of the value of abdominopelvic acquisition without contrast injection when performing a whole body CT scan in a patient who may have multiple trauma. *Diagn Interv Imaging* 2013; 94: 410-7.

3- Gervaise A, Teixeira P, Hossu G, Blum A, Lapierre-Combes C. Optimizing z-axis coverage of abdominal CT scans of the urinary tract: a proposed alternative proximal landmark for acquisition planning. En cours de soumission à *British Journal of Radiology*.

Les facteurs comportementaux jouent un rôle primordial dans une démarche d'optimisation et de réduction de la dose d'irradiation au scanner. Nous proposons d'illustrer l'intérêt de trois de ces facteurs au cours d'une démarche d'optimisation et de réduction de la dose au scanner : la sensibilisation des médecins prescripteurs par l'évaluation de leurs connaissances en matière de radioprotection des patients, la réduction du nombre de phases d'acquisition et la limitation de la couverture d'acquisition des scanners.

Article 1 : Evaluation des connaissances des prescripteurs de scanner en matière de radioprotection des patients.

La justification des examens d'imagerie irradiants est un des deux grands principes de la radioprotection [12]. Il s'agit d'une responsabilité partagée entre le prescripteur et le radiologue. Son application nécessite toutefois de connaître et de prendre en compte les risques potentiels de cancer radio-induit lié aux faibles doses de rayons X. Pourtant, de nombreuses études ont montré le défaut de connaissance des médecins prescripteurs en matière de radioprotection des patients [44-45].

Le but de cette étude était d'évaluer les connaissances des praticiens prescripteurs de scanner en matière de radioprotection des patients. Il s'agissait de la première étude portant sur ce sujet qui a été conduite en France. Cette étude a été réalisée à partir d'un questionnaire envoyé par courrier à l'ensemble des praticiens hospitaliers de l'HIA Legouest durant le mois d'avril 2010. Le questionnaire était composé d'une première partie analysant les données démographiques des praticiens et d'une deuxième partie comprenant huit questions et abordant plusieurs thèmes testant les connaissances des praticiens en matière de radioprotection des patients.

Les résultats montraient que 70 % des praticiens déclaraient prendre en compte les risques liés aux rayons X lors de la prescription d'un scanner. Par contre, la connaissance des doses délivrées lors de la réalisation d'un scanner abdominopelvien était mal maitrisée et les risques potentiels de cancer radio-induit lié aux faibles doses de rayons X étaient largement sous-estimés. Enfin, seulement 34 % des praticiens avaient bénéficié d'une formation à la radioprotection des patients.

<u>Article 2 :</u> Evaluation de l'intérêt de l'acquisition abdominopelvienne sans injection lors de la réalisation d'un scanner corps entier chez un patient suspect de polytraumatisme.

La limitation du nombre de phases d'acquisition est un moyen simple pour réduire la dose globale d'un scanner. Par exemple, lors de la réalisation d'un scanner abdominopelvien, l'acquisition d'une unique série injectée au temps portal versus deux acquisitions identiques sans et après injection au temps portal permet de réduire la dose de 50 %. La réalisation de plusieurs temps d'acquisition doit donc être justifiée par une amélioration de la performance diagnostique.

Le but de notre étude était d'évaluer la performance diagnostique de la série abdominopelvienne sans injection lors de l'acquisition d'un scanner corps entier chez un patient suspect de polytraumatisme.

Il s'agissait d'une étude monocentrique rétrospective réalisée au sein du service d'imagerie Guilloz du CHRU de Nancy et incluant 84 scanners corps entier de patients suspects de polytraumatisme. Deux lecteurs ont relu de manière indépendante les acquisitions abdominopelviennes sans injection, avec injection et avec les deux séries sans et avec injection. Une deuxième lecture par consensus représentait le gold standard. Lors de la lecture des scanners, les lecteurs devaient dire s'il existait ou non une lésion traumatique abdominopelvienne sur les différentes séries analysées. L'analyse statistique a porté sur la concordance intra- et inter-observateur et sur la sensibilité et la spécificité des différentes acquisitions par rapport à la relecture consensuelle.

Les résultats ne montraient pas de différence significative en terme de sensibilité ou de spécificité pour la recherche d'une lésion traumatique entre l'interprétation de la série injectée versus l'interprétation conjointe des deux séries sans et après injection. La concordance inter-observateur était bonne à excellente. L'acquisition thoraco-abdominopelvienne en contraste spontané représentait 20 % de la dose efficace de l'ensemble de l'examen.

<u>Article 3 :</u> Optimisation de la longueur d'acquisition des scanners réalisés pour colique néphrétique : proposition d'une nouvelle méthode pour le placement de la limite supérieure de l'acquisition.

La réduction de la couverture d'acquisition est aussi un moyen simple, rapide et efficace pour réduire la dose d'irradiation au scanner. Dans le cas des coliques néphrétiques, l'acquisition abdominopelvienne peut être centrée sur les voies urinaires, du pôle supérieur des reins au bord inférieur de la vessie. Tandis que la limite inférieure de l'acquisition est facilement repérée par le milieu de la symphyse pubienne, le placement de la limite supérieure de l'acquisition est plus compliqué. A l'HIA Legouest, nous utilisons la silhouette des reins sur le topogramme de face afin de placer la limite supérieure de l'acquisition. Cette méthode semble toutefois peu fiable avec de nombreux cas où le pôle supérieur d'un rein est coupé lors de l'acquisition. Récemment, Corwin MT *et al.* [46] ont proposé un nouveau repère osseux correspondant au bord inférieur de la dixième vertèbre thoracique (T10). Dans leur étude, cette méthode permettait d'inclure dans tous les cas l'ensemble des reins. Par contre, il semble que la réduction de la dose ne soit pas aussi importante qu'elle pourrait l'être. De ce fait, nous proposons d'introduire un nouveau repère pour le placement de la limite supérieure de l'acquisition qui correspond au point d'intersection entre la coupole diaphragmatique gauche et le bord antérieur des corps vertébraux sur le scout de profil.

Le but de notre étude était de comparer ces trois méthodes de placement de la limite supérieure de l'acquisition d'un scanner abdominopelvien en évaluant la réduction de la couverture d'acquisition et le nombre de reins coupés.

Il s'agissait d'une étude rétrospective monocentrique incluant 365 scanners abdominopelviens. Trois manipulateurs de radiologie ont placés pour chaque scanner la limite supérieure de l'acquisition avec chacune des trois méthodes : méthode 1 utilisant les contours des reins, méthode 2 utilisant le bord inférieur de la vertèbre T10 et méthode 3 utilisant le point d'intersection entre la coupole diaphragmatique gauche et le bord antérieur des corps vertébraux. La réduction de la couverture d'acquisition et le nombre de reins coupés ont été comparés entre les trois méthodes.

Les résultats montraient une réduction moyenne de la longueur d'acquisition de 20,5 %, 15,1 % et 18,2 % avec respectivement les méthodes 1, 2 et 3. La proportion de reins coupés pour les méthodes 1, 2 et 3 était de respectivement 6,7 %, 0,7 % et 1,4 %. Les concordances inter-observateurs et intra-observateurs étaient excellentes pour toutes les méthodes mais les coefficients de corrélation interclasse étaient toujours meilleurs pour la méthode 3.

Chapitre 2

Article 1 : *Evaluation des connaissances des prescripteurs de scanner en matière de radioprotection des patients.*

Gervaise A, Esperabe-Vignau F, Naulet P, Pernin M, Portron Y, Lapierre-Combes M. Evaluation des connaissances des prescripteurs de scanner en matière de radioprotection des patients. *J Radiol* 2011; 92: 681-7.

Journal de radiologie (2011) **92**, 681—687

ARTICLE ORIGINAL / *Pratiques professionnelles*

Évaluation des connaissances des prescripteurs de scanner en matière de radioprotection des patients

Evaluation of the knowledge of physicians prescribing CT examinations on the radiation protection of patients

A. Gervaise[a,*], **F. Esperabe-Vignau**[b], **M. Pernin**[a], **P. Naulet**[a], **Y. Portron**[a], **M. Lapierre-Combes**[a]

[a] *Service d'imagerie médicale, hôpital d'instruction des armées Legouest, 27, avenue de Plantières, BP 90001, 57077 Metz cedex 3, France*
[b] *Service d'imagerie médicale, hôpital d'instruction des armées Robert-Picqué, 351, route de Toulouse, 33140 Villenave-d'Ornon, France*

MOTS CLÉS
Dosimétrie ;
Prescripteur ;
Radiation ionisante ;
Radioprotection ;
Scanner

Résumé
Objectifs. — Évaluer les connaissances des praticiens prescripteurs de scanner en matière de radioprotection des patients.
Matériels et méthodes. — Un questionnaire a été adressé à l'ensemble des praticiens prescripteurs de scanner de notre hôpital. Ce questionnaire comportait plusieurs questions en rapport avec les pratiques et les connaissances des praticiens en matière de radioprotection des patients.
Résultats. — Quarante-quatre questionnaires ont été analysés. Tandis que 70 % des praticiens déclaraient prendre en compte les risques liés aux rayons X lors de la prescription d'un scanner, seulement 25 % de ceux-ci en informaient le patient. La connaissance des doses délivrées au cours d'un scanner abdomino-pelvien était mal maîtrisée et les risques potentiels liés aux faibles doses de rayons X étaient largement sous-estimés. Enfin, seulement un tiers des praticiens avait bénéficié d'une formation à la radioprotection des patients.
Conclusion. — Même si la majorité des praticiens déclare prendre en compte les risques liés aux faibles doses de rayons X, ces risques sont en fait peu ou mal connus. Une diffusion plus large de la formation en radioprotection des patients, notamment au cours du cursus initial des internes, pourrait être une des solutions pour améliorer les connaissances des praticiens hospitaliers en matière de radioprotection des patients.

* Auteur correspondant.
Adresse e-mail : alban.gervaise@hotmail.fr (A. Gervaise).

0221-0363/$ — see front matter
doi:10.1016/j.jradio.2011.03.023

KEYWORDS
Dosimetry;
Ionizing radiation;
Radiation protection;
CT

Abstract
Purpose. — To evaluate the knowledge of physicians prescribing CT examinations on the radiation protection of patients.
Materials and methods. — A questionnaire was distributed to all clinicians on medical staff who prescribe CT examinations. Several questions related to their prescription pattern and their knowledge of radiation protection.
Results. — Forty-four questionnaires were analyzed. While 70% of physicians claimed that they considered the risks from exposure to ionizing radiation when prescribing a CT examination, only 25% informed their patients about those risks. Knowledge of the radiation dose delivered during CT evaluation of the abdomen and pelvis was poorly understood and the risks related to small doses of radiation were grossly underestimated. Finally, only a third of clinicians had received training with regards to radiation protection.
Conclusion. — While most clinicians claim that they consider the risks from exposure to ionizing radiation when prescribing a CT examination, the risks are either not well known or not known at all. Increased formation of clinicians with regards to the radiation protection of patients, maybe through a dedicated clinical rotation while in medical school, could be a solution to improve the knowledge of hospital clinicians with regards to radiation protection.

En France, le recours aux examens d'imagerie médicale, notamment scanographiques, est de plus en plus fréquent au cours de la prise en charge des patients. L'Institut de radioprotection et de sûreté nucléaire (IRSN) rapporte ainsi une augmentation de 26 % des actes de scanographie entre 2002 et 2007 [1]. Cela s'explique par une meilleure disponibilité des scanners, mais surtout par une amélioration constante de la qualité des images, dans un temps toujours plus court et pour une meilleure performance diagnostique.

Pourtant, le scanner est une technique d'imagerie irradiante. Parallèlement à l'augmentation du nombre de scanners réalisés chaque année, il existe également une majoration de l'irradiation individuelle et collective délivrée au cours des actes de scanographie [2]. Ainsi, tandis qu'en 2007 les scanners ne représentaient que 10 % de l'ensemble des actes de radiologie réalisés en France, ils étaient responsables de 58 % de l'irradiation due aux rayons X d'origine médicale [1]. Or, même si le lien entre l'exposition à de faibles doses de rayons X et l'augmentation du risque de cancer radio-induit est fortement controversé, il a été établi par plusieurs grandes institutions (par exemple, le Comité scientifique des Nations-Unies et l'Académie des sciences des États-Unis) et par de nombreux rapports ou publications internationales [3,4]. En prenant en compte le modèle de régression linéaire sans seuil (RLSS) des effets des rayons X à faibles doses, certaines de ces publications n'hésitent d'ailleurs pas à associer à la réalisation d'un seul scanner abdomino-pelvien un risque de cancer radio-induit de l'ordre de 1/1000 [5,6]. Ce risque important reste toutefois un risque maximal théorique. D'autres auteurs estiment pour leur part soit qu'un tel risque n'existe pas, soit qu'il est largement surestimé [7—11]. L'absence de preuves scientifiques formelles allant dans un sens ou dans l'autre impose de suivre le principe de précaution et aboutit donc à la nécessité de réduire au maximum les doses délivrées aux patients. Ce principe de précaution, « As Low As Reasonable Achievable » : aussi bas que raisonnablement possible (ALARA), a d'ailleurs été repris par l'Union européenne dans la directive Euratom 97/43 [12]. Cette dernière précise que les examens d'imagerie irradiants doivent faire l'objet d'une justification et d'une optimisation constante afin de réduire les doses individuelles et collectives dues aux expositions médicales.

C'est dans ce contexte que la communauté radiologique (et plus largement, l'ensemble des professionnels de santé utilisant directement des techniques d'imagerie irradiantes) a été fortement sensibilisée ces dernières années. Sur le plan scientifique par exemple, ce n'est pas moins de 22 articles parus dans la revue *Radiology* en 2009 concernant le thème de la radioprotection ou de la réduction des doses délivrées. C'est également une obligation de formation à la radioprotection des patients à renouveler tous les dix ans pour les professionnels de santé utilisant les rayons X à visée diagnostique (arrêté du 18 mai 2004) [13]. Les radiologues sont aussi soumis à des niveaux de référence diagnostiques (c'est-à-dire des doses « seuil » par examen qu'il est souhaitable de ne pas dépasser) définis par la législation (arrêté du 12 février 2004) [14] avec nécessité d'envoyer annuellement des relevés de dosimétrie à l'IRSN. Enfin, dans l'optique de réduire au maximum les doses délivrées, notamment en scanographie, les radiologues doivent optimiser en permanence les protocoles des examens irradiants.

Tandis que de nombreux efforts ont été réalisés du côté de l'optimisation des examens irradiants, la justification de ces examens ne doit pas être négligée. Cette responsabilité est partagée entre les praticiens prescripteurs et les radiologues. Elle impose le respect des indications, limitant la réalisation des examens entraînant inutilement une exposition. Dans cette optique, le service d'imagerie médicale a mis en ligne sur le réseau de notre hôpital un guide portant sur les indications des examens d'imagerie dans les urgences de l'adulte. Mais qu'en est-il du côté des prescripteurs ? Plusieurs études de la littérature internationale insistent sur le manque d'implication des prescripteurs en matière de radioprotection des patients ainsi que sur leur ignorance en ce qui concerne les niveaux de doses délivrées

et les risques de cancer radio-induit actuellement admis [15]. Aucune étude de ce type n'a jamais été réalisée en France à notre connaissance.

L'objectif principal de notre étude était donc d'évaluer les connaissances en matière de radioprotection des patients des praticiens prescripteurs de scanner au sein de notre hôpital.

Matériels et méthodes

Participants

Un questionnaire (Annexe 1) a été envoyé par courrier à l'ensemble des praticiens prescripteurs de scanner de notre centre hospitalier la première semaine du mois d'avril 2010. Quatre-vingt-trois questionnaires ont ainsi été adressés à 60 seniors (médecins ou dentistes thésés) et 23 internes répartis dans les différents services de l'hôpital.

Questionnaire

Ce questionnaire a été élaboré à partir des données de la littérature, en concertation avec les différents médecins du service d'imagerie médicale et de la personne compétente en radioprotection.

Il comportait une première partie analysant les données démographiques du praticien (interne ou senior, années d'expériences depuis la thèse pour les seniors, service d'appartenance).

Le questionnaire était ensuite composé de huit questions qui abordaient plusieurs thèmes. Le premier thème concernait les habitudes de prescription des praticiens : s'ils prescrivaient des scanners (question 1), s'ils avaient déjà pris en compte le rapport bénéfice/risque lié aux rayons X lors de la prescription d'un scanner (question 2) et s'ils en avaient déjà informé le patient (question 3). Le deuxième évaluait les connaissances des praticiens concernant les doses délivrées au cours d'un scanner abdomino-pelvien (questions 4 et 5) et des risques de cancer radio-induit du fait de la réalisation de ce scanner (question 6). Enfin, la question 7 demandait aux praticiens s'ils avaient déjà suivi une formation à la radioprotection des patients tandis que la question 8 cherchait à savoir si les praticiens savaient qu'il existe un guide portant sur les indications des examens d'imagerie en urgence de l'adulte disponible sur le réseau de l'hôpital.

Récupération et analyse des résultats

Le questionnaire devait être renvoyé au service d'imagerie médicale avant la fin du mois d'avril 2010. Les résultats ont été analysés de manière anonyme.

Estimation des doses délivrées

Afin d'établir la réalité des doses rapportées dans notre questionnaire, nous avons effectué un relevé dosimétrique au sein de notre service d'imagerie médicale concernant les doses délivrées au cours d'un scanner abdomino-pelvien et d'une radiographie thoracique de face.

Concernant la moyenne des doses délivrées au cours d'un scanner abdomino-pelvien, le recueil dosimétrique a porté sur l'ensemble des scanners abdomino-pelviens réalisés au cours du mois d'avril 2010 (avec ou sans injection de produit de contraste, mono- ou multiphasique, scanner standard ou basse dose). Les doses délivrées étaient directement fournies par le rapport d'examen. Elles correspondaient au produit dose longueur (PDL) exprimé en milliGray centimètre (mGy $\times$ cm). La dose efficace (E), exprimée en millisievert (mSv) était ensuite calculée en utilisant le coefficient de conversion tissulaire (k) de l'abdomen à 0,015 [16] selon la formule $E = PDL \times k$ [17].

Pour les radiographies thoraciques de face, l'estimation de la moyenne des doses délivrées a été réalisée à partir du recueil dosimétrique réalisé en 2009 dans le cadre de l'envoi annuel à l'IRSN des niveaux de référence diagnostiques. Ce recueil s'appuie sur les doses équivalentes, correspondant au produit dose surface (PDS) exprimé en Gy $\times$ cm^2, délivrées pour 20 radiographies thoraciques de face. La dose efficace en mSv a été calculée à partir de la dose équivalente en multipliant cette dernière par le coefficient de conversion tissulaire k_{PDS} (avec $k_{PDS} = 0,33$ pour une radiographie thoracique de face) selon la formule $E = PDS \times k_{PDS}$ [18].

Résultats

Estimation des doses délivrées

La moyenne des doses délivrées au cours d'un scanner abdomino-pelvien était de 10,9 mSv et celle d'une radiographie thoracique de face était de 0,07 mSv. Ces résultats étaient en accord avec les niveaux de référence diagnostiques établis par l'IRSN [14] et avec les données de la littérature [5]. Le rapport entre la moyenne des doses d'un scanner abdomino-pelvien et d'une radiographie thoracique de face était donc de 155.

Résultats du questionnaire

Quarante-quatre questionnaires ont été récupérés et analysés, soit un taux de réponse global de 53 % (65 % pour les internes et 48 % pour les seniors). Ce sont donc 15 internes et 29 seniors qui ont répondu à notre questionnaire (soit respectivement 34 et 66 % des effectifs de la population de notre étude).

Tous les praticiens ayant renvoyé le questionnaire étaient prescripteurs de scanner.

Soixante-dix pour cent d'entre eux avaient répondu qu'ils avaient déjà pris en compte le rapport bénéfice/risque lié aux rayons X lors de la prescription d'un scanner, avec un pourcentage équivalent entre internes et seniors. Seulement 25 % des praticiens en avaient déjà informé le patient. C'est ainsi 31 % des seniors qui avaient déjà transmis une telle information au patient, contre seulement 13 % des internes.

Concernant l'évaluation relative de la dose délivrée au cours d'un scanner abdomino-pelvien par rapport à une radiographie thoracique de face, 13 % des praticiens avaient correctement évalué ce rapport entre 100 à 250 fois (Fig. 1). Treize pour cent l'avaient surévalué au-delà de 250 tandis

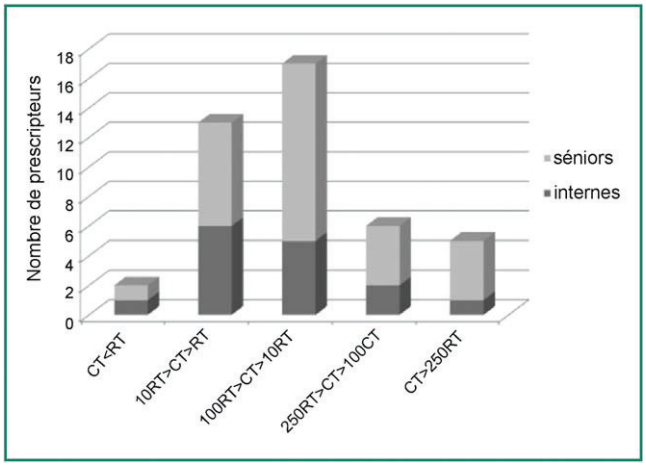

Figure 1. Réponses à la question n° 4 concernant le rapport entre la dose délivrée au cours d'un scanner abdomino-pelvien standard (CT) et une radiographie thoracique de face (RT).

que 74 % des praticiens avaient sous-estimé ce rapport, sans distinction notable entre internes et seniors.

Lors de l'évaluation absolue de la dose délivrée au cours d'un scanner abdomino-pelvien standard, avec pour repère l'irradiation naturelle en France estimée en moyenne à 2,5 mSv par an, 25 % des praticiens avaient correctement évalué cette dose dans une fourchette allant de 5 à 20 mSv (pour une dose moyenne de 10,9 mSv). Vingt-sept pour cent des prescripteurs l'avaient surévaluée tandis que 48 % ne se prononçaient pas ou avaient sous-estimé cette dose (Fig. 2).

Tandis que l'estimation des doses délivrées était mal maîtrisée, les risques de cancer radio-induit étaient également largement sous-estimés puisqu'une grande majorité des praticiens (61 % d'entre eux) avait répondu qu'il n'y avait aucun risque de cancer radio-induit du fait de la réalisation d'un seul scanner abdomino-pelvien.

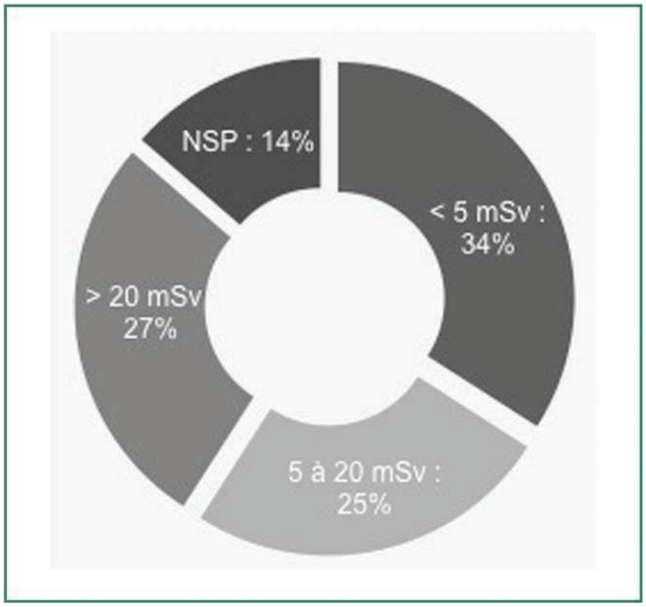

Figure 2. Réponses à la question n° 5 concernant l'évaluation de la dose délivrée au cours d'un scanner abdomino-pelvien (NSP : Ne sais pas).

Par ailleurs, seulement 34 % des praticiens avaient déjà bénéficié d'une formation à la radioprotection des patients. L'analyse plus détaillée montrait qu'aucun interne n'avait suivi de formation de ce type tandis que ce taux était de 52 % chez les seniors.

Enfin, 59 % des praticiens avaient connaissance de l'existence d'un guide portant sur les indications des examens d'imagerie en urgence mis à leur disposition sur le réseau de l'hôpital. Ce taux était plus élevé chez les internes (67 %, contre 55 % chez les seniors).

Discussion

Notre étude confirme la mauvaise connaissance de la part des praticiens des doses délivrées lors de la réalisation d'un scanner abdomino-pelvien et la large sous-estimation du risque de cancer radio-induit qui en découle, compte tenu des données actuelles de la littérature. Il est ainsi logique qu'une part non négligeable d'entre eux ne prenne jamais en compte le rapport bénéfice/risque lors de la prescription d'un scanner et qu'une grande majorité des praticiens n'informe pas le patient de cette balance bénéfice/risque.

Ce constat n'est pas isolé à notre établissement et est au contraire tout à fait concordant avec les données de la littérature. De nombreuses études rapportent des résultats équivalents [15].

Pour Lee et al., qui ont publié une étude comparable en 2004 [19], seulement 9 % des urgentistes pensaient qu'il existait une augmentation du risque de cancer radio-induit du fait de la réalisation d'un seul scanner abdomino-pelvien tandis que seulement 22 % de ceux-ci avaient déjà informé le patient d'un tel risque. Comme dans notre étude, le rapport de dose entre un scanner abdomino-pelvien et une radiographie thoracique de face était largement sous-estimé (seulement 12 % des praticiens avaient correctement évalué ou surévalué ce rapport).

Dans une autre étude publiée en 2004, Jacob et al. [20] retrouvent également, dans une population de médecins hospitaliers, une large sous-estimation du rapport de dose entre un scanner abdomino-pelvien et une radiographie thoracique de face (seulement 30 % des praticiens avaient correctement estimé ce rapport) et une très large sous-estimation du risque de cancer radio-induit du fait de la réalisation d'un seul scanner abdomino-pelvien (12,5 % des praticiens avaient évalué ce risque de manière correcte). Plus surprenant, cette étude a montré que 10 % des prescripteurs pensait que l'imagerie par résonance magnétique (IRM) était aussi un examen d'imagerie irradiant ! Cette étude mettait également en évidence un taux de réponses correctes supérieur au sein du groupe de médecins ayant déjà suivi une formation à la radioprotection des patients comparativement au groupe n'ayant jamais suivi une telle formation.

Enfin, dans une étude publiée en 2007 évaluant les connaissances en matière de risque de cancer radio-induit lié aux faibles doses de rayons X chez des chirurgiens pédiatriques, Rice et al. [21] retrouvent que 31 % des praticiens avaient correctement évalué le risque de cancer radio-induit du fait de la réalisation d'un seul scanner abdomino-pelvien tandis que 32 % estimaient que ce risque n'existait pas. Ces résultats plus favorables étaient, selon l'auteur, dus à deux

facteurs : tout d'abord, le fait qu'il s'agisse d'une étude réalisée chez des chirurgiens pédiatriques, population de médecins traditionnellement plus sensibilisée aux principes de la radioprotection, et deuxièmement, que cette étude était plus récente que les deux précédentes et donc que ces meilleurs résultats pouvaient être expliqués par une meilleure diffusion des connaissances en matière de radioprotection envers les prescripteurs.

La formation des praticiens en matière de radioprotection des patients semble donc jouer un rôle important. Cette importance a été soulignée à la fois par les études de Rice et Jacob mais également par la directive Euratom 97/43 qui notait déjà en 1997 que « l'introduction d'un cours sur la radioprotection dans le programme d'études de base des facultés de médecine et d'art dentaire doit être favorisée » [12]. Plus de dix ans après la diffusion de cette directive, notre étude montre pourtant qu'aucune formation de radioprotection des patients n'est enseignée au cours du cursus initial des médecins.

Deux principales raisons expliquent l'importance d'une telle formation auprès des praticiens prescripteurs d'examens irradiants. Tout d'abord, en accord avec le principe de précaution ALARA et dans l'optique de diminuer au maximum les doses délivrées aux patients, les prescripteurs ont un rôle important quant à la justification des examens d'imagerie irradiants. Cette responsabilité implique que le prescripteur s'interroge sur le bénéfice par rapport au risque d'exposition, l'objectif étant d'obtenir l'information diagnostique recherchée au moyen de la dose d'exposition la plus faible. Toute irradiation, si faible soit-elle, doit être également justifiée par l'absence d'examen alternatif non irradiant (notamment échographie ou IRM) [22].

Deuxièmement, la formation des praticiens à la radioprotection vise à leur permettre de mieux informer les patients par rapport à la balance bénéfice/risque liée à la prescription d'un examen d'imagerie irradiant. Comme dans notre étude et dans les autres articles publiés [19,21], cette information reste très peu communiquée. L'apport systématique au patient d'une telle information nous semble toutefois excessif et discutable. La mention d'un risque de cancer radio-induit ne doit pas dissuader le patient de recourir à un examen qui s'avère souvent nécessaire et dont l'absence peut être plus délétère qu'un risque hypothétique de cancer radio-induit. Toutefois, dans certaines circonstances, cette information semble indispensable. C'est, par exemple, le cas particulier des femmes enceintes ou de jeunes patients présentant une pathologie chronique nécessitant la réalisation répétée de scanner (maladie de Crohn ou mucoviscidose par exemple).

Enfin, les médecins prescripteurs doivent s'attendre à répondre aux interrogations émanant directement des patients. En effet, de nombreuses informations sont dorénavant directement disponibles par le patient lui-même, que ce soit dans la presse grand public ou sur internet [23,24]. Il existe par exemple une application iPhone [25] et un site internet [24] permettant de calculer pour chaque type d'examen d'imagerie irradiant un risque de cancer radio-induit. C'est dans ce contexte que le prescripteur doit être capable de justifier la réalisation d'un examen irradiant comportant un risque éventuel de cancer radio-induit. Le praticien doit notamment insister sur le bénéfice attendu de l'examen et sur le rapport bénéfice/risque qui en découle (alors que les informations directement accessibles par les patients n'abordent souvent que la notion de risque et non pas celle du bénéfice). Les prescripteurs doivent également connaître les modalités de calcul d'un tel risque et le débat actuel concernant sa probable surestimation.

Bien que ce ne soit pas le but de notre étude, plusieurs précisions concernant les risques liés aux faibles doses de rayons X méritent ainsi d'être mentionnées.

Ce risque est effectivement largement débattu au sein des communautés médicales et scientifiques. Malgré la controverse et les divergences de vues entre différentes institutions scientifiques reconnues au plan mondial, le modèle de RLSS est actuellement le modèle le plus largement accepté, y compris pour de faibles doses d'irradiation. Le Comité scientifique des Nations-Unies pour l'étude des effets des rayonnements ionisants (UNSCEAR) a déclaré dans son rapport le plus récent [26] : « Tant que les [...] incertitudes sur les effets des faibles doses ne sont pas résolues, le Comité estime que la théorie selon laquelle l'augmentation du risque de tumeur est proportionnelle à la dose d'irradiation est conforme aux connaissances actuelles, et qu'elle reste donc l'approche la plus valable d'un point de vue scientifique ». De l'autre côté, le rapport commun des experts de l'Académie française de médecine et de l'Académie française des sciences conclut pour sa part que le modèle de RLSS est incompatible avec les dernières données scientifiques portant sur les mécanismes de réparation moléculaire de l'ADN [7]. Les auteurs de ce rapport estiment donc que même si le principe de précaution est valable, il ne doit pas conduire à une surprotection superflue face à une surestimation des risques des faibles doses de rayons X. Ce risque doit plutôt être considéré comme un risque maximal théorique.

Enfin, ce risque éventuel de cancer radio-induit doit être comparé au risque de cancer non radio-induit développé au sein de la population générale. Celui-ci est très élevé, de l'ordre de 42 % [3]. Cela signifie que si la réalisation d'un scanner engendre une augmentation du risque de cancer radio-induit de l'ordre de 1/1000, le risque global de cancer passera donc de 42 à 42,1 %.

L'ensemble de ces données incite donc au principe de précaution sans pour autant surévaluer les risques de cancer radio-induit associés aux faibles doses de rayons X.

Notre étude comporte plusieurs limites qui méritent également d'être mentionnées. Tout d'abord, le faible effectif de notre population d'étude ne nous a pas permis de séparer en différentes catégories les prescripteurs (par exemple, services médicaux contre chirurgicaux, années d'expérience...). De même, les différences entre internes et seniors n'étaient pas statistiquement significatives, sauf en ce qui concerne le taux de formation à la radioprotection. La séparation entre praticien formé et non formé à la radioprotection aurait également été un élément important pour souligner l'efficacité d'une telle formation.

Par ailleurs, la volonté de faire un questionnaire pouvant être rempli facilement et rapidement dans le but d'avoir un taux de réponse le plus élevé possible, ne nous a pas permis d'approfondir certaines questions. Par exemple, il aurait été intéressant de savoir à quelle occasion les praticiens avaient bénéficié d'une formation à la radioprotection. Il aurait aussi été intéressant de demander aux prescripteurs,

comme dans l'étude de Jacob, s'ils pensaient que l'IRM était un examen d'imagerie irradiant.

Enfin, une diffusion plus large du questionnaire aurait été intéressante afin de pouvoir comparer les connaissances en matière de radioprotection au sein de notre population de praticiens hospitaliers vis-à-vis d'une population de médecins généralistes.

Conclusion

Notre étude confirme que, même si la majorité des praticiens déclare prendre en compte les risques liés aux faibles doses de rayons X lors de la prescription d'un scanner, ces risques sont en fait peu ou mal connus. Une diffusion plus large de la formation en radioprotection des patients, notamment au cours du cursus initial des internes, pourrait être une des solutions pour améliorer les connaissances des praticiens hospitaliers en matière de radioprotection des patients.

Déclaration d'intérêts

Les auteurs déclarent ne pas avoir de conflits d'intérêts en relation avec cet article.

Annexe 1. Questionnaire

Question 1 :

Prescrivez-vous des scanners ?

Oui/Non

Question 2 :

Lors de la prescription d'un scanner, avez-vous déjà pris en compte le rapport bénéfice/risque lié aux rayons X ?

Oui/Non

Question 3 :

Lors de la prescription d'un scanner, avez-vous déjà informé le patient des risques liés aux rayons X et du rapport bénéfice/risque qui en découle ?

Oui/Non

Question 4 :

Selon vous, comparativement à la dose délivrée pour une radiographie thoracique (RT) de face, la dose moyenne délivrée au cours d'un scanner abdomino-pelvien standard (CT) équivaut à :

CT < RT

10 RT > CT > RT

100 RT > CT > 10 RT

250 RT > CT > 100 RT

CT > 250 RT

Question 5 :

Sachant que l'irradiation naturelle en France est d'environ 2,5 mSv par an, à combien estimez-vous la dose moyenne délivrée au cours d'un scanner abdomino-pelvien ?

.....

.....

Question 6 :

D'après vous et selon les dernières conférences de consensus, existe-t-il un risque de cancer radio-induit du fait de la dose délivrée au cours d'un seul scanner abdomino-pelvien standard :

Oui/Non

Question 7 :

Avez-vous déjà suivi une formation à la radioprotection des patients ?

Oui/Non

Question 8 :

Savez-vous qu'il existe un guide portant sur les indications des examens d'imagerie en urgence de l'adulte disponible sur le réseau de l'hôpital ?

Oui/Non

Références

[1] Etard C, Sinno-Tellier S, Aubert B. Exposition de la population française aux rayonnements ionisants liée aux actes de diagnostic médical en 2007. Rapport conjoint IRSN/InVS 2010.

[2] National Council on Radiation Protection and Measurements. Ionizing radiation exposure of the population of the United States. NCRP report n° 160, 2009.

[3] Board of Radiation Effects Research Division on Earth and Life Sciences National Research Council of the National Academies. Health Risks From Exposure to Low Levels of Ionizing Radiation: BEIR VII Phase 2. Washington, DC: National Academies Press; 2006.

[4] Brenner DJ, Doll R, Goodhead DT, Hall EJ, Land CE, Little JB, et al. Cancer risks attributable to low doses of ionizing radiation: assessing what we really know. Proc Natl Acad Sci U S A 2003;100:13761—6.

[5] Smith-Bindman R, Lipson J, Marcus R, Kim KP, Mahesh M, Gould R, et al. Radiation dose associated with common computed tomography examinations and the associated lifetime attributable risk of cancer. Arch Intern Med 2009;169:2078—86.

[6] Berrington de González A, Mahesh M, Kim KP, Bhargavan M, Lewis R, Mettler F, et al. Projected cancer risks from computed tomography scans performed in the United States in 2007. Arch Intern Med 2009;169:2071—7.

[7] Tubiana M, Aurengo A, Averbeck A. La relation dose-effet et l'estimation des effets cancérogènes des faibles doses de rayonnements ionisants. Paris: Académie nationale de médecine, institut de France — Académie des sciences; 2005.

[8] Tubiana M, Feinendegen LE, Yang C, Kaminski JM. The linear no-threshold relationship is inconsistent with radiation biologic and experimental data. Radiology 2009;251:13—22.

[9] Land CE. Low-dose extrapolation of radiation health risks: some implications of uncertainly for radiation protection at low doses. Health Phys 2009;97:407—15.

[10] Cordoliani YS. Parlons dose ou « ne dites pas à ma mère que je suis radiologue : elle lit « Le Point ». J Radiol 2007;88:29—30.

[11] Cordoliani YS. La dose efficace individuelle moyenne n'existe pas... et pourtant elle augmente ! J Radiol 2010;91:449—50.

[12] Directive 97/43/Euratom du 30 juin 1997, relative à la protection sanitaire des personnes contre les dangers des rayonnements ionisants lors d'expositions à des fins médicales.

[13] Arrêté du 18 mai 2004 relatif aux programmes de formation portant sur la radioprotection des patients exposés aux rayonnements ionisants. Journal officiel de la République française, version consolidée du 26 septembre 2006.

[14] Arrêté du 12 février 2004 relatif aux niveaux de référence diagnostiques en radiologie et médecine nucléaire. Journal officiel de la République française, 16 mars 2004.

[15] Krille L, Hammer GP, Merzenich H, Zeeb H. Systematic review on physician's knowledge about radiation doses and radiation risks of computed tomography. Eur J Radiol 2010;76:36—41.

[16] Deak PD, Smal Y, Kalender WA. Multisection CT protocols: sex- and age-specific conversion factor used to determine effective dose from Dose-Lengh-Product. Radiology 2010;257:158—66.
[17] International Commission on Radiological Protection. 2007 recommendations of the International Commission on Radiological Protection (ICRP Publication 103). Ann ICRP 2007;37:1—332.
[18] LeHeron J. Estimation of effective dose to the patient during medical X-ray examination from measurements of the dose area product. Phys Med Biol 1992;11:2117—26.
[19] Lee CI, Haims AH, Monico EP, Brink JA, Forman HP. Diagnostic CT scans: assessment of patient, physician, and radiologist awareness of radiation dose and possible risks. Radiology 2004;231:393—8.
[20] Jacob K, Vivian G, Steel JR. X-Ray dose training: are we exposed to enough? Clin Radiol 2004;59:928—34.
[21] Rice HE, Frush DP, Harker MJ, Farmer D, Waldhausen JH. Peer assessment of pediatric surgeons for potential risks of radiation exposure from computed tomography scans. J Pediatr Surg 2007;42:1157—64.
[22] Haute Autorité de santé (HAS). Manuel de certification des établissements de santé. HAS; 2009.
[23] Labbé C, Recasens O. Santé publique : les dangers de la radiologie. Le Point 2006.
[24] http://www.xrayrisk.com.
[25] Radiation Passport. Tidal Pool Softwate. Version 2.0, 2010, http://www.tidalpool.ca/radiationpassport.
[26] UNSCEAR 2000 REPORT Vol. II: sources and effects of ionizing radiation. Annex G : biological effects at low radiation doses. Page 160, paragraph 541.

Chapitre 2

Article 2 : *Evaluation de l'intérêt de l'acquisition abdominopelvienne sans injection lors de la réalisation d'un scanner corps entier chez un patient suspect de polytraumatisme.*

Naulet P, Wassel J, Gervaise A, Blum A. Evaluation of the value of abdominopelvic acquisition without contrast injection when performing a whole body CT scan in a patient who may have multiple trauma. *Diagn Interv Imaging* 2013; 94: 410-7.

Diagnostic and Interventional Imaging (2013) **94**, 410—417

ORIGINAL ARTICLE / *Technical*

Evaluation of the value of abdominopelvic acquisition without contrast injection when performing a whole body CT scan in a patient who may have multiple trauma

P. Naulet[a,*], J. Wassel[b], A. Gervaise[a], A. Blum[b]

[a] *Medical Imaging Department, Hôpital d'Instruction des Armées Legouest, 27, avenue de Plantières, BP 90001, 57077 Metz cedex 3, France*
[b] *Guilloz Imaging Department, CHU Nancy, avenue de Lattre-de-Tassigny, 54000 Nancy, France*

KEYWORDS
Multiple trauma;
Abdominal trauma;
Peritoneal effusion;
Multidetector CT scan;
Iterative reconstruction

Abstract
Purpose: To evaluate the diagnostic value of non-contrast-enhanced abdominopelvic acquisition when performing a whole body CT scan in a patient who may have multiple trauma.
Patients and methods: In a single centre, retrospective study over 1 year, we included 84 patients suspected of having multiple trauma who indeed presented an abdominal or pelvic lesion during the initial CT scan. Two readers independently reread the acquisitions without injection, then those with injection, then all the acquisitions, and scored the presence or absence of abdominopelvic lesions. Statistical analysis focused on intra- and inter-observer agreement, and on the sensitivity and specificity of the different acquisitions in relation to consensus rereading.
Results: This study did not reveal any significant difference, particularly concerning improvement in sensitivity, between interpretation of the acquisitions with contrast injection and interpretation of all the acquisitions with or without injection. Inter-observer agreement was substantial to almost perfect. Non-contrast-enhanced thoraco-abdominopelvic acquisition represented 20% to 25% of the effective dose for the entire examination.
Conclusion: Abdominopelvic acquisition without contrast injection in addition to acquisition with contrast injection in a patient suspected of having multiple trauma does not improve detection of traumatic lesions of the liver, spleen, kidneys or adrenal glands, nor of intra- or retroperitoneal effusion, but increases the dose and should be abandoned.

Abbreviation: DLP, dose-length product.

* Corresponding author.
E-mail address: pierre.naulet@gmail.com (P. Naulet).

2211-5684/$ — see front matter
http://dx.doi.org/10.1016/j.diii.2013.01.018

A whole body CT scan has become the essential element in initial examination of a patient with suspected multiple trauma and for checking stable or stabilised haemodynamics [1,2].

Performed early on, this examination provides an exhaustive report of lesions and reduces mortality in multiple trauma patients [3]. CT scanning protocols vary according to the material available, the team's habits and consideration of the X-ray dose delivered to the patient (although this is secondary where the patient's state is critical). In particular, non-contrast-enhanced abdominopelvic acquisition is debated.

The literature suggests a number of protocols: most teams do not perform non-contrast-enhanced thoracic or abdominal acquisition [1,4—11], while others do undertake thoraco-abdominopelvic [12] or abdominal [13—15] acquisition without contrast injection. This type of acquisition in the abdominal region is thought to be important for looking for spontaneous hyperdensity resulting from the presence of blood [13—15]. In particular, it is considered of assistance in detecting small, particularly mesenteric haematomas, haemoperitoneum and hepatic, splenic or renal haematomas. These lesions are hyperdense before injection but are considered more difficult to detect after injection because of poorer contrast with the organs enhanced (Figs. 1 and 2) [14]. Some teams undertake oral opacification [6,16], while others suggest only making acquisitions centred on the region where trauma is suspected [12] but this attitude is controversial [17].

The recommendations of the Société Française de Radiologie (French Radiology Society) [18] for performing a CT scan in a patient with multiple trauma are: non-contrast-enhanced acquisition of the brain and neck, possibly non-contrast-enhanced thoraco-abdominopelvic acquisition followed by thoraco-abdominopelvic acquisition (possibly extending to the neck and legs) in the arterial phase (20

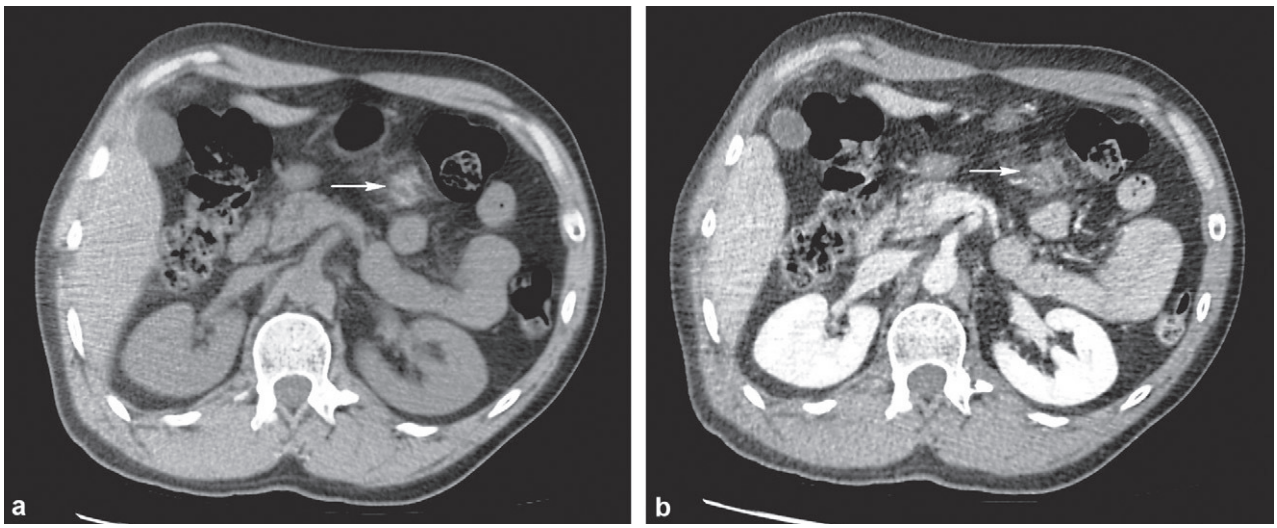

Figure 1. Mesenteric haemorrhagic contusion (white arrow) hyperdense with no contrast agent, showing a lesser degree of contrast with the organs enhanced after injection: a: non-contrast-enhanced acquisition; b: acquisition after contrast injection in the portal phase.

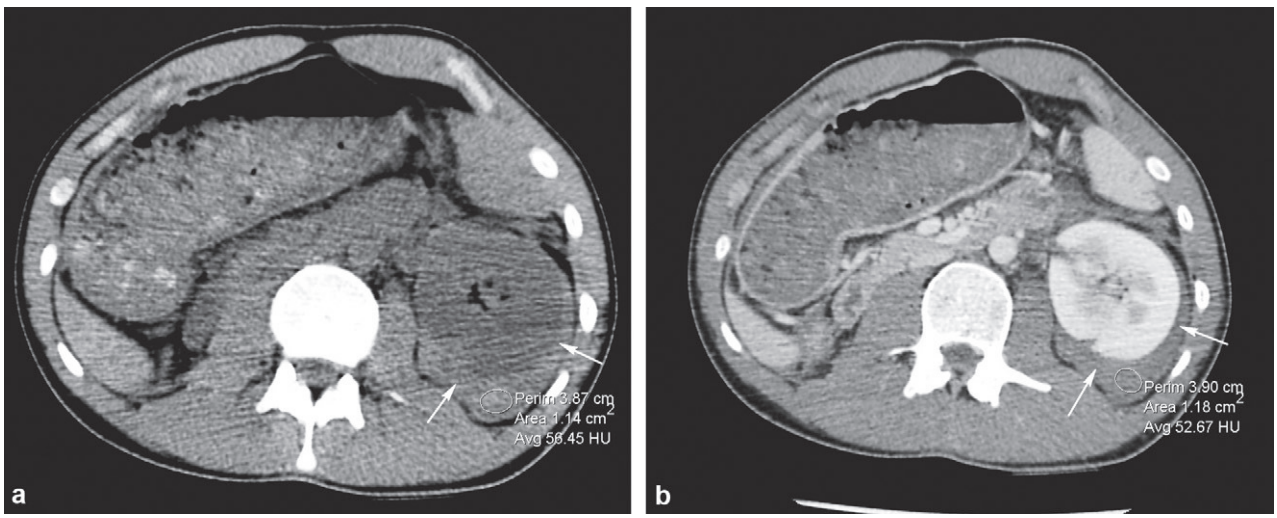

Figure 2. Fracture of the left kidney with perirenal hyperdense haematoma with no injection of contrast agent (white arrows), appearing hypodense after contrast injection but which can be characterised due to its density of 52 HU even with contrast-enhanced acquisition: a: non-contrast-enhanced acquisition; b: acquisition after contrast injection in the portal phase.

to 30 s after starting the injection) then abdominopelvic acquisition in the portal phase (70 to 90 s after the start of the injection) and finally, possibly, where there are renal or perirenal anomalies or if there is any doubt about damage to the bladder, abdominopelvic acquisition in the late phase (5 minutes).

In contrast, in its recommendations of June 2011 [19], the British Royal College of Radiologists considers that non-contrast-enhanced thoraco-abdominopelvic acquisition is of no interest in a traumatic context.

In our establishment, non-contrast-enhanced thoraco-abdominopelvic acquisition is systematically performed in patients suspected of having multiple trauma.

The aim of our study is to evaluate the diagnostic usefulness of this acquisition when performing a whole body CT scan in a potentially multi-trauma patient.

Patients and methods

Population studied

For this single centre, retrospective study, we searched our establishment's PACS for patients who had had an emergency whole body CT scan in the period between 01/01/2010 and 31/12/2010.

This identified 282 patients who had had such a CT scan for suspected multiple trauma. We reread all the reports on these patients and included the 88 patients who had at least one abdominopelvic traumatic lesion. Four patients were excluded because their examination protocol was incomplete: one for whom the non-contrast-enhanced thoraco-abdominopelvic acquisition was missing, three for whom there had been no injection of an iodinated contrast agent (one presenting a compressive acute subdural haematoma had required immediate neurosurgical treatment, one had a history of allergy to iodinated contrast agents and an 84-year-old patient had severe renal impairment).

The only imaging examinations conducted prior to the whole body CT scan were frontal X-rays of the thorax in the resuscitation room, together with an ultrasound examination, in haemodynamically unstable patients, to detect peritoneal, pericardial and pleural effusion.

Technique for performing the CT scan

All the examinations were performed in 64×0.5 mm helical mode, 73 of them using a 320-row detector Aquilion One scanner (Toshiba Medical Systems, Tokyo, Japan) and 11 with a 64-row detector Aquilion 64 scanner (Toshiba Medical Systems, Tokyo, Japan).

The protocol included producing non-contrast-enhanced cervico-encephalic and thoraco-abdominopelvic acquisitions. After injection of 140 ml of contrast agent (iomeprol at 400 mg of iodine/ml, Bracco Altana Pharma, Constance, Germany), acquisition was undertaken in the arterial phase extending from the base of the skull to the toes, followed by abdominopelvic acquisition in the portal phase. Finally, if necessary, the resident or senior doctor present at the console decided whether to undertake a late abdominopelvic acquisition.

The operators produced reformation of the various volumes in the three spatial planes as well as reformation of the spine and aorta, then volume rendering reformation of the thoracic cage, the face and bone lesions.

The resident and senior doctor analysed the results together on the PACS consoles (IMPAX V5, AGFA HealthCare), or this was done first by the resident and then validated by the senior doctor.

Reading the CT scans

In separate sessions at an interval of several days, reader 1 (4th year resident) and reader 2 (senior doctor, registrar in the department) independently reread only the non-contrast injection abdominopelvic acquisitions then only the abdominopelvic acquisitions with injection, and in a third reading, all the abdominopelvic acquisitions with and without contrast agent injection. The two readers then produced a consensus rereading based on the results of all these readings, the examination report recorded in the PACS, the control scans and, for the 12 patients who had abdominal or pelvic surgery, the operation reports.

For each series, they listed the presence or absence of traumatic lesions of the liver, spleen or kidneys, of adrenal haematomas, of haemorrhagic intestinal-mesenteric lesions, of liquid peritoneal and retroperitoneal effusion.

The definitions used were those described in the paper by C. Ridereau-Zins et al. [14].

All lesions were considered as being present whatever their size, severity and clinical significance. In particular, the presence of a traumatic lesion of the liver, spleen and kidneys was noted whenever there was a haematoma, contusion, laceration or fracture. The intestinal-mesenteric lesions noted were oedematous damage, haematomas and mesenteric haemorrhage, as well as digestive ischaemia secondary to these lesions and haematomas of the walls of the digestive tube. Peritoneal and retroperitoneal effusions were listed whatever their spontaneous density and abundance.

Statistical analysis

The study population was subjected to a descriptive analysis. The qualitative variables are shown as percentages and the quantitative variables are means with standard deviation.

Cohen's kappa coefficients, their standard error and the adjusted kappa coefficients (PABAK) were calculated for each lesion, comparing the results of non-contrast-enhanced acquisition, acquisition with injection and all acquisitions with and without injection, in order to estimate intra- and inter-observer agreement. Contingency tables were generated from the analyses performed.

To situate the kappa and PABAK coefficients obtained from our sample, we used the classification proposed by Landis and Koch: no agreement for negative values, slight from 0.0 to 0.20, fair from 0.21 to 0.40, moderate from 0.41 to 0.60, substantial from 0.61 to 0.80, almost perfect from 0.81 to 1 [20—23].

The sensitivity and specificity of each acquisition and the reports recorded in the PACS were calculated relative to the consensus rereading.

Data were entered using the Excel 2010 program from Microsoft Corporation (Redmond, Washington, USA) and the statistical analysis used SAS® 9.2. (SAS Int. Inc., Cary, NC, USA).

The statistical analysis was performed and the results interpreted and presented with the help of an epidemiologist from our establishment's Clinical Epidemiology Department.

Dosimetry

To study the additional dose of radiation delivered to the patient during non-contrast-enhanced thoraco-abdominopelvic acquisition, we analysed the dosimetric reports of the 73 examinations performed with the Aquilion One scanner. With the dosimetric reports of the 11 examinations performed with the Aquilion 64 scanner, the dose-length product (DLP) for non-contrast-enhanced acquisitions could not be separated from the DLP for the acquisitions with injection.

We calculated the mean and standard deviation of the DLPs, expressed in mGy.cm, for the non-contrast-enhanced thoraco-abdominopelvic acquisitions and for the thoraco-abdominopelvic and lower limb acquisitions with contrast injection. (The DLP of lower limb acquisition in the arterial phase could not be separated from that of thoraco-abdominopelvic acquisition performed in the same helix).

The effective dose (E) expressed in millisievert (mSv) was then estimated, with the formula $E = \text{DLP} \times k$, using a tissue conversion coefficient (k) of 18 μSv/mGy cm [24].

Results

The population studied consisted of 65 men (77%) and 19 women (23%) with a mean age of 38.8 years (standard deviation of 17.8).

The prevalence of the various lesions is summarised in Table 1.

Using the adjusted kappa (PABAK), intra-observer agreement between reading the acquisitions with injection and reading all the acquisitions varied depending on the lesions. For reader 1, it was substantial to almost perfect (PABAK varying from 0.67 to 0.91). The agreement for reader 2 was also substantial to almost perfect (PABAK varying from 0.79 to 0.91) (Table 2).

Inter-observer agreement was substantial to almost perfect for all the lesions for reading the acquisitions with and without injection and for reading all the examinations, with the exception of moderate agreement for peritoneal

Table 1 Prevalence of lesions depending on the reader and acquisitions.

Organs	Reader 1			Reader 2			Consensus
	NI	INJ	NI + INJ	NI	INJ	NI + INJ	
Adrenal haematoma	7 (8.3)	12 (14.3)	13 (15.5)	9 (10.7)	13 (15.5)	11 (13.1)	13 (15.5)
Liver lesion	2 (2.4)	22 (26.2)	22 (26.2)	4 (4.8)	26 (31)	25 (29.8)	25 (29.8)
Spleen lesion	5 (6)	24 (28.6)	23 (27.4)	8 (9.5)	23 (27.4)	24 (28.6)	25 (29.8)
Kidney lesion	5 (6)	12 (14.3)	10 (11.9)	6 (7.1)	12 (14.3)	11 (13.1)	13 (15.5)
Intestinal-mesenteric lesion	5 (6)	7 (8.3)	9 (10.7)	15 (17.9)	13 (15.5)	14 (16.7)	11 (13.1)
Peritoneal effusion	34 (40.5)	55 (65.5)	55 (65.5)	46 (54.8)	53 (63.1)	56 (66.7)	57 (67.9)
Retroperitoneal effusion	28 (33.3)	31 (36.9)	41 (48.8)	34 (40.5)	39 (46.4)	32 (38.1)	38 (45.2)

Number of cases (%).
NI: acquisition without contrast injection; INJ: acquisition with contrast injection; NI + INJ: all acquisitions; Consensus: consensus rereading.

Table 2 Intra-observer agreement (acquisitions with contrast injection vs. all acquisitions).

Organs	Reader 1			Reader 2		
	K (SE)	95% CI	PABAK	K (SE)	95% CI	PABAK
Adrenal haematoma	0.67 (0.11)	0.45—0.89	0.83	0.81 (0.09)	0.62—0.99	0.91
Liver lesion	0.88 (0.06)	0.76—0.99	0.91	0.86 (0.06)	0.74—0.98	0.88
Spleen lesion	0.85 (0.06)	0.73—0.98	0.88	0.79 (0.08)	0.65—0.94	0.83
Kidney lesion	0.79 (0.10)	0.59—0.99	0.91	0.75 (0.11)	0.54—0.96	0.88
Intestinal-mesenteric lesion	0.44 (0.16)	0.13—0.77	0.81	0.69 (0.11)	0.48—0.91	0.83
Peritoneal effusion	0.89 (0.05)	0.79—0.99	0.91	0.79 (0.07)	0.62—0.91	0.79
Retroperitoneal effusion	0.67 (0.08)	0.51—0.82	0.67	0.78 (0.07)	0.65—0.92	0.79

K: Kappa; SE: Standard error; CI: confidence interval.

effusion when interpreting non-contrast-enhanced acquisitions (PABAK = 0.48) (Table 3).

There was no improvement in sensitivity between reading acquisitions with injection and reading all the acquisitions with and without injection, except in the case of retroperitoneal effusion by reader 1.

Sensitivity in detecting liver and spleen lesions was significantly improved through interpreting the acquisitions with contrast injection compared with just the non-injection acquisitions. A similar tendency was found for kidney lesions, adrenal haematomas and peritoneal effusions.

Sensitivity in detecting mesenteric lesions and retroperitoneal effusion did not seem to be improved by reading either the acquisitions with or without injection (Table 4).

Specificity was excellent for the two readers and all the acquisitions.

Considering intestinal-mesenteric haemorrhagic lesions more particularly, only two patients had an emergency operation, one for a haematoma of the greater omentum with active haemorrhage, the other for a wound to a branch of the mesenteric artery caused by a penetrating trauma (metal bar transfixing the pelvis, abdomen and thorax, in position when the CT scan was performed). Three other patients underwent surgery for suspected perforation of the digestive tube: the first indeed presented perforation of the small intestine, the second perforation of the bladder (false-positive), while for the third no perforation was found, although he had a pneumoperitoneum. The other intestinal-mesenteric lesions were mesenteric haemorrhagic contusions (5 cases) or small haematomas (2 cases) which did not require surgery and diagnosis of which could not be confirmed.

In our series, the DLP for non-contrast-enhanced thoraco-abdominopelvic acquisition was a mean of 1499 mGy.cm (standard deviation: 482), i.e. 24% of that of all the thoraco-abdominopelvic and lower limb acquisitions, which was 6256 mGy.cm (standard deviation: 1953). The mean of the effective dose for acquisition without contrast injection was approximately 27 mSv.

Discussion

In our study, intra-observer agreement between the acquisitions with injection and all the acquisitions was substantial to almost perfect. In addition, the sensitivity of acquisitions with injection was not improved by interpreting acquisitions without injection at the same time.

There is therefore no advantage to performing non-contrast-enhanced acquisition in addition to acquisition with contrast injection in patients with one or more abdominopelvic traumatic lesions.

This corresponds with the recommendations [19] and the practice of very many teams who do not undertake non-contrast-enhanced abdominopelvic or thoraco-abdominopelvic acquisitions in patients with suspected multiple trauma [1,4—11].

In 1988, Kelly J. et al. [13] showed the usefulness of non-contrast-enhanced abdominal acquisition in addition to contrast-enhanced acquisition for abdominal trauma. In their study, the sensitivity and specificity of all the examinations were improved from 74 to 92% and from 84 to 91% respectively, by acquiring 10 slices of 10 mm spaced at 20 mm without contrast injection on the upper part of the abdomen.

In 1992, a study by Miyakawa K. et al. [25] confirmed these results in 126 patients. Non-contrast-enhanced acquisition helped in particular to diagnose the 12 traumatic intestinal lesions requiring emergency surgical management, whereas with acquisition with contrast injection only 10 were diagnosed.

Since these old studies, however, CT technology and image quality have considerably improved. Volume acquisitions are nowadays interpreted on PACS consoles with multiplanar reformations.

Our study's inter-observer agreement is clearly much higher than in the study by Agostini et al. [11] on the usefulness of dual reading of whole body CT scans in the management of multiple trauma patients, which found an inter-observer kappa of 0.41 (95% confidence interval of 0.35

Table 3 Inter-observer agreement.

Organs	Acquisitions without injection			Acquisitions with injection			Acquisitions with and without injection		
	K (SE)	95% CI	PABAK	K (SE)	95% CI	PABAK	K (SE)	95% CI	PABAK
Adrenal haematoma	0.59 (0.15)	0.29—0.88	0.86	0.77 (0.10)	0.57—0.96	0.88	0.81 (0.09)	0.62—0.99	0.91
Liver lesion	0.66 (0.23)	0.21—1	0.95	0.83 (0.07)	0.69—0.96	0.86	0.79 (0.07)	0.65—0.94	0.83
Spleen lesion	0.75 (0.14)	0.48—1	0.93	0.73 (0.08)	0.57—0.89	0.79	0.73 (0.08)	0.57—0.89	0.79
Kidney lesion	0.90 (0.09)	0.71—1	0.98	0.71 (0.11)	0.49—0.93	0.86	0.62 (0.13)	0.36—0.88	0.83
Intestinal-mesenteric lesion	0.23 (0.13)	−0.03—0.49	0.67	0.33 (0.15)	0.04—0.61	0.71	0.45 (0.14)	0.18—0.72	0.74
Peritoneal effusion	0.49 (0.09)	0.31—0.66	0.48	0.85 (0.06)	0.73—0.96	0.86	0.71 (0.08)	0.55—0.87	0.74
Retroperitoneal effusion	0.75 (0.08)	0.59—0.89	0.76	0.61 (0.09)	0.44—0.78	0.62	0.64 (0.08)	0.48—0.80	0.64

K: Kappa; SE: Standard error; CI: confidence interval.

Table 4 Sensitivity and specificity of lesions depending on the reader and acquisitions.

	Reader 1			Reader 2		
	NI	INJ	NI + INJ	NI	INJ	NI + INJ
Adrenal haematoma						
Sensitivity	0.54 (0.27) [0.27—0.81]	0.85 (0.20) [0.65—1.00]	0.77 (0.23) [0.54—1.00]	0.54 (0.27) [0.27—0.81]	0.85 (0.20) [0.65—1.00]	0.85 (0.20) [0.65—1.00]
Specificity	1.00 (0.00) [1.00—1.00]	0.99 (0.03) [0.96—1.00]	0.96 (0.05) [0.91—1.00]	0.97 (0.04) [0.93—1.00]	0.97 (0.04) [0.93—1.00]	1.00 (0.00) [1.00—1.00]
Liver lesion						
Sensitivity	0.08 (0.11) [0.00—0.19]	0.84 (0.14) [0.70—0.98]	0.88 (0.13) [0.75—1.00]	0.16 (0.14) [0.02—0.30]	0.96 (0.08) [0.88—1.00]	0.92 (0.11) [0.81—1.00]
Specificity	1.00 (0.00) [1.00—1.00]	0.98 (0.03) [0.95—1.00]	1.00 (0.00) [1.00—1.00]	1.00 (0.00) [1.00—1.00]	0.97 (0.05) [0.92—1.00]	0.97 (0.05) [0.92—1.00]
Spleen lesion						
Sensitivity	0.20 (0.16) [0.04—0.36]	0.88 (0.13) [0.75—1.00]	0.88 (0.13) [0.75—1.00]	0.32 (0.18) [0.14—0.50]	0.88 (0.13) [0.75—1.00]	0.88 (0.13) [0.75—1.00]
Specificity	1.00 (0.00) [1.00—1.00]	0.97 (0.05) [0.92—1.00]	0.98 (0.03) [0.95—1.00]	1.00 (0.00) [1.00—1.00]	0.98 (0.03) [0.95—1.00]	0.97 (0.05) [0.92—1.00]
Kidney lesion						
Sensitivity	0.31 (0.25) [0.06—0.56]	0.92 (0.14) [0.78—1.00]	0.77 (0.23) [0.54—1.00]	0.38 (0.26) [0.12—0.65]	0.77 (0.23) [0.54—1.00]	0.77 (0.23) [0.54—1.00]
Specificity	0.99 (0.03) [0.96—1.00]	1.00 (0.00) [1.00—1.00]	1.00 (0.00) [1.00—1.00]	0.99 (0.03) [0.96—1.00]	0.97 (0.04) [0.93—1.00]	0.99 (0.03) [0.96—1.00]
Intestinal-mesenteric lesion						
Sensitivity	0.36 (0.28) [0.08—0.65]	0.55 (0.29) [0.25—0.84]	0.64 (0.28) [0.35—0.92]	0.73 (0.26) [0.46—0.99]	0.64 (0.28) [0.35—0.92]	0.64 (0.28) [0.35—0.92]
Specificity	0.99 (0.03) [0.96—1.00]	0.99 (0.03) [0.96—1.00]	0.97 (0.04) [0.94—1.00]	0.90 (0.07) [0.84—0.97]	0.92 (0.06) [0.85—0.98]	0.90 (0.07) [0.84—0.97]
Peritoneal effusion						
Sensitivity	0.54 (0.13) [0.41—0.67]	0.96 (0.05) [0.92—1.00]	0.96 (0.05) [0.92—1.00]	0.79 (0.11) [0.68—0.90]	0.93 (0.07) [0.86—1.00]	0.91 (0.07) [0.84—0.99]
Specificity	0.89 (0.12) [0.77—1.00]	1.00 (0.00) [1.00—1.00]	1.00 (0.00) [1.00—1.00]	0.96 (0.07) [0.89—1.00]	1.00 (0.00) [1.00—1.00]	0.85 (0.13) [0.72—0.99]
Retroperitoneal effusion						
Sensitivity	0.71 (0.14) [0.57—0.85]	0.76 (0.14) [0.63—0.90]	0.97 (0.05) [0.92—1.00]	0.82 (0.12) [0.69—0.94]	0.89 (0.10) [0.80—0.99]	0.79 (0.13) [0.66—0.92]
Specificity	0.98 (0.04) [0.94—1.00]	0.96 (0.06) [0.90—1.00]	0.91 (0.08) [0.83—1.00]	0.93 (0.07) [0.86—1.00]	0.89 (0.09) [0.80—0.98]	0.96 (0.06) [0.90—1.00]

NI: acquisition without contrast injection; INJ: acquisition with contrast injection; NI + INJ: all acquisitions.
Value (standard error) [95% confidence interval].

to 0.46) for all the lesions of a whole body CT scan. That can be explained by our studying the agreement lesion by lesion, and only being concerned with the abdomen. We also used the PABAK, which sometimes differs from kappa.

On the other hand, in the study by Yu J. et al. [16] on isolated small peritoneal effusions, the kappa coefficient for this single sign between two observers was 0.76, which gives a result close to the inter-observer kappa that we found for free peritoneal effusions (kappa = 0.85 for the acquisitions with injection and 0.74 for all acquisitions).

An important limitation of our study was taking into account all the lesions visible on the CT scan whatever their size and clinical impact. Many of these lesions were of no or little consequence (e.g. simple contusions or small subcapsular haematomas of solid organs, adrenal haematomas and small peritoneal or retroperitoneal effusions) and only required monitoring. A false-positive or false-negative for these lesions had no impact on management of the patient.

Conversely, serious haemorrhagic lesions are life-threatening and require immediate surgery and intensive care. When they concern the liver, spleen or kidneys, their diagnosis poses no problem from just contrast-enhanced acquisitions.

On the other hand, mesenteric and intestinal trauma is rare, particularly serious and more difficult to diagnose. Its early diagnosis depends almost exclusively on the

abdominal CT scan because clinical signs and symptoms are non-specific. A false-negative can result in delayed diagnosis responsible for increased morbidity and mortality due to haemorrhage, sepsis and peritonitis [6,26—29].

A limitation of our study was that it included only very few lesions of this type that had required surgical treatment (one mesenteric haematoma with active bleeding; one haemorrhage due to a penetrating trauma — but detection of this lesion posed no problem since the object causing the injury was still in situ; two bowel perforations, one of which was not found by surgery; and a false-positive for bladder perforation). The seven other lesions only required monitoring.

It could be useful to conduct an additional study focusing solely on traumatic intestinal-mesenteric lesions that have required surgical management. This additional study would help overcome the limitations of our work for these rare but serious lesions that are difficult to diagnose.

There could be two disadvantages to undertaking non-contrast-enhanced thoraco-abdominopelvic or abdominopelvic acquisition during a whole body CT scan in a patient suspected of having multiple trauma: the time taken and the irradiation.

The time for acquisition is less than 10 s, even counting the time for programming it, moving the table, etc. The increase in time for the patient in the CT scan room is 1 to 2 min. Positioning the patient and the topograms are the same as for the contrast-enhanced acquisitions and therefore do not lengthen the protocol. Reconstructions are done during the preparation for and while carrying out the contrast-enhanced acquisitions and do not increase the length of the examination. The time taken to perform this acquisition is therefore negligible compared with the patient's total stay in the CT scan room, which is about 30 min.

Our evaluation of the effective dose is not very precise and has numerous biases: the DLP not taking into account either the length of exploration or the patient's morphotype, the DLP of acquisition in the arterial phase including the legs, and use of a single tissue conversion coefficient (k).

Since performing our study, the protocol has been optimised, while retaining all the acquisitions, with considerable reduction in the exposure parameters and the use of iterative reconstruction algorithms. We therefore studied the dosimetry of the first 20 patients for the month of January 2012 who were scanned using the Aquilion One scanner with a whole body protocol for suspected multiple trauma.

During these examinations, the mean DLP for non-contrast-enhanced thoraco-abdominopelvic acquisition was 449 mGy.cm (standard deviation: 136), i.e. 20% of the DLP of all the thoraco-abdominopelvic and lower limb acquisitions, which was 2282 mGy.cm (standard deviation: 799). On average, the effective dose for non-contrast-enhanced acquisition was about 8 mSv but represented a little more than 20% of the total effective dose. Indeed, the total effective dose is slightly overestimated due to the use of a global tissue conversion factor without separating thoraco-abdominopelvic acquisition in the arterial phase from acquisition of the lower limbs. However, the tissue conversion factor for the lower limbs is much lower than the global tissue conversion factor used.

Since optimisation of the protocol and the use of iterative reconstruction, the DLP and therefore the effective dose, which is proportional to the DLP, have been reduced by about 70% for non-contrast-enhanced thoraco-abdominopelvic acquisition and by about 64% for the entire protocol.

Since these modifications, the additional dose of radiation (8 mSv) due to non-contrast-enhanced thoraco-abdominopelvic acquisition performed at low dose and read in semi-thin slices has been very significantly reduced compared with the former protocol (27 mSv), but it still represents about 20% of the dose of the whole protocol and eliminating it would mean a further dose reduction.

The limitations of our study are due to its retrospective and single centre character and, as we saw earlier, to analysis of all lesions without consideration for either their severity or their therapeutic impact. However, even frequent diagnostic errors on lesions without clinical consequences are less serious than a single error which is life-threatening.

Moreover, even when taking into account operation reports and clinical evolution, consensus rereading is a source for discussion, particularly concerning the presence or absence of minimal lesions which have no therapeutic impact, but may have a statistical impact by modifying the sensitivity and specificity of the different readings. During consensus rereading, a minor lesion was recorded if it had been found by one reader on one acquisition but missed by the other reader or on other acquisitions. This explains a low number of false-positives and thus the excellent specificity of all the acquisitions. To limit these biases, it would have ideally been best to list the severity of the different lesions.

Finally, our study was limited to abdominopelvic lesions to the exclusion of studying thoracic lesions. This choice was made because among the 282 patients suspected of having multiple trauma and who underwent a whole body CT scan, only four presented rupture or dissection of the aortic isthmus necessitating treatment and two presented doubtful untreated lesions which remained stable on the control scans. Moreover, only one presented a haemopericardium. The total number was considered too small to be studied. In addition, the presence of a mediastinal haematoma, detection of which could possibly be improved by non-contrast-enhanced acquisition, shows few specific differences from a large vessel lesion [1].

Conclusion

The disadvantages of performing non-contrast-enhanced abdominopelvic acquisition in addition to acquisition with contrast injection in a patient suspected of having multiple trauma are loss of time, which is minimal, but an increase in dose of about 20 to 25%. It does not improve detection of traumatic lesions of the liver, spleen, kidneys or adrenal glands, nor of intra- or retroperitoneal effusion, and should be abandoned.

Disclosure of interest

The authors declare that they have no conflicts of interest concerning this article.

Acknowledgements

We warmly thank Mrs Irawati Lemonnier, MPH, PhD, of the CIC-CE Inserm, and of the Epidemiology and Clinical Evaluations Department of Nancy University Teaching Hospital for her assistance.

References

[1] Taourel P, Merigeaud S, Millet I, Devaux Hoquet M, Lopez FM, Sebane M. Traumatisme thoraco-abdominal : stratégie en imagerie. J Radiol 2008;89:1833—54.
[2] Miller LA, Shanmuganathan K. Multidetector CT evaluation of abdominal trauma. Radiol Clin N Am 2005;43: 1079—95.
[3] Wagner SH, Lefering R, Qvick L-M, Körner M, Kay MV, Pfeifer K-J, et al. Effect of whole-body CT during trauma resuscitation on survival: a retrospective, multicentre study. Lancet 2009;373:1455—61.
[4] Salim A, Sangthong B, Martin M, Brown C, Plurad D, Demetriades D. Whole body imaging in blunt trauma patient without obvious sign of injury: results of a prospective study. Arch Surg 2006;141:468—73.
[5] Holmes JF, McGahan JP, Wisner D. Rate of intra-abdominal injury after a normal abdominal computed tomographic scan in adults with blunt trauma. Am J Emerg Med 2012;30(4): 574—9.
[6] Brofman N, Atri M, Epid D, Hanson JM, Grinblat L, et al. Evaluation of bowel and mesenteric blunt trauma with multidetector CT. Radiographics 2006;26:1119—31.
[7] Holly BP, Steenburg SD. Multidetector CT of blunt traumatic venous injuries in the chest, abdomen, and pelvis. Radiographics 2011;31:1415—24.
[8] Anderson SW, Varghese JC, Lucey BC, Burke PA, Hirsch EF, Soto JA. Blunt splenic trauma: delayed-phase CT for differentiation of active hemorrhage from contained scular injury in patients. Radiology 2007;243:88—95.
[9] Nguyen D, Platon A, Shanmuganathan K, Mirvis SE, Becker CD, Poletti P-A. Evaluation of a single-pass continuous whole-body 16-MDCT protocol for patients with polytrauma. AJR 2009;192:3—10.
[10] Briggs RH, Rowbotham E, Johnstone AL, Chalmers AG. Provisional reporting of polytrauma CT by on-call radiology registrars. Is it safe? Clin Radiol 2010;65:616—22.
[11] Agostini C, Durieux M, Milot L, Kamaoui I, Floccard B, Allaouchiche B, et al. Intérêt de la double lecture du scanner corps entier dans la prise en charge des polytraumatisés. J Radiol 2008;89:325—30.
[12] Gupta M, Schriger DL, Hiatt JR, Cryer HG, Tillou A, et al. Selective use of computed tomography compared with routine whole body imaging in patients with blunt trauma. Ann Emerg Med 2011;58:407—16.
[13] Kelly J, Raptopoulos V, Davidoff A, Waite R, Norton P. The value of non-contrast-enhanced CT in blunt abdominal trauma. AJR Am J Roentgenol 1989;152:41—8.
[14] Ridereau-Zins C, Lebigot J, Bouhours G, Casa C, Aubé C. Traumatismes abdominaux : les lésions élémentaires. J Radiol 2008;89:1812—32.
[15] Taourel P. Imagerie des urgences. Paris: Masson; 2004, p. 211—34.
[16] Yu J, Fulcher AS, Wang DB, Turner MA, et al. Frequency and importance of small amount of isolated pelvic free fluid detected with multidetector CT in male patients with blunt trauma. Radiology 2010;256(3):799—805.
[17] Tillou A, Gupta M, Baraff LJ, Schriger DL, Hoffman JR, Hiatt JR, et al. Is the use of pan-computed tomography for blunt trauma justified? A prospective evaluation. J Trauma 2009;67(4):779—87.
[18] Guide pratique à l'usage des médecins radiologues pour l'évaluation de leur pratiques professionnelles. Paris: Société Française de Radiologie; 2009. p. 610—2.
[19] The Royal College of Radiologists. Standards of practice and guidance for trauma radiology in severely injured patients. London: The Royal College of Radiologists; 2011.
[20] Landis JR, Koch GG. The measurement of observer agreement for categorical data. Biometrics 1977;33:159—74.
[21] Blum A, Feldmann L, Bresler F, Jouanny P, Briançon S, Régent D. Intérêt du calcul du coefficient kappa dans l'évaluation d'une méthode d'imagerie. J Radiol 1995;76(7):441—3.
[22] Sim J, Wright CC. The Kappa statistic in reliability studies: use, interpretation, and sample size requirements. Phys Ther 2005;85:257—68.
[23] Kundel HL, Polansky M. Measurement of observer agreement. Radiology 2003;228:303—8.
[24] Huda W, Ogden KM, Khorasani MR. Converting dose-length product to effective dose at CT. Radiology 2008;248(3):995—1003.
[25] Miyakawa K, Kaji T, Ashida H, Kuwabara M, et al. Evaluation of non-contrast-enhanced CT in blunt abdominal trauma. Nippon Acta Radiol 1992;52(3):300—7.
[26] Fakhry SM, Brownstein M, Watts DD, Baker CC, Oller D. Relatively short diagnostic delays (8 hours) produce morbidity and mortality in blunt small bowel injury: an analysis of time to operative intervention in 198 patients from a multicenter experience. J Trauma 2000;48(3):408—14 [discussion 414—5].
[27] Le Bedis CA, Anderson SW, Soto JA. CT imaging of blunt traumatic bowel and mesenteric injuries. Radiol Clin North Am 2012;50(1):123—36.
[28] Wu CH, Wang LJ, Wong YC, Fang JF, et al. Contrast-enhanced multiphasic computed tomography for identifying life-threatening mesenteric hemorrhage and transmural bowel injuries. J Trauma 2011;71(3):543—8.
[29] Tan KK, Liu JZ, Go TS, Vijayan A, Chiu MT. Computed tomography has an important role in hollow viscus and mesenteric injuries after blunt abdominal trauma. Injury Int J Care Injured 2010;41:475—8.

Chapitre 2

Article 3 : *Optimisation de la longueur d'acquisition des scanners réalisés pour colique néphrétique : proposition d'une nouvelle méthode pour le placement de la limite supérieure de l'acquisition.*

Gervaise A, Teixeira P, Hossu G, Blum A, Lapierre-Combes C. Optimizing z-axis coverage of abdominal CT scans of the urinary tract: a proposed alternative proximal landmark for acquisition planning. En cours de soumission à *British Journal of Radiology.*

Original Research

Optimizing z-axis coverage of abdominal CT scans of the urinary tract: a proposed alternative proximal landmark for acquisition planning.

Gervaise A, Teixeira P, Hossu G, Blum A, Lapierre-Combes M.

Submitted to British Journal of Radiology on February 2016.

Abstract

Objective: To evaluate an alternative method to reduce the acquisition coverage of urinary tract CT.

Materials and Methods: This retrospective study included 365 abdominopelvic CT studies. Three technologists simulated shortened acquisition coverages using three methods to determine the upper limit of the acquisition: method 1 used the renal contours; method 2 used the inferior margin of the 10th thoracic vertebra; and method 3 used the point of intersection of the left diaphragmatic dome and the anterior margin of the vertebral bodies. Reductions in acquisition coverage and number of cut kidneys were compared between the three methods.

Results: The mean reduction of acquisition coverage for the three readers with methods 1, 2 and 3 were, 20.5%, 15.1% and 18.2%, respectively. The proportions of cut kidneys with methods 1, 2 and 3 and averaged over the three readers were 6.7%, 0.7% and 1.4%, respectively. Inter and intra-reader agreement was excellent with all methods, but inter-class correlation coefficients were higher with method 3.

Conclusion: Using the intersection of the left diaphragmatic dome and the anterior margin of the vertebral bodies for proximal landmark for urinary tract CT is more reproducible than conventional methods and reduces by 18.2% the acquisition coverage without significantly increasing kidneys cuts.

Keywords: Computed Tomography; radiation dosage; anatomical landmark; scan coverage; urinary tract.

A. Gervaise – Corresponding author, M. Lapierre-Combes
Service d'Imagerie Médicale, Hôpital d'Instruction des Armées Legouest, 27 avenue de Plantières, 57070 Metz, CEDEX 3, France.
E-mail: alban.gervaise@hotmail.fr

P. Teixeira, A. Blum
Service d'Imagerie Guilloz, Hôpital Central, CHU-Nancy, 29 Av. Mar De Lattre de Tassigny, 54035 Nancy, France.

G. Hossu
Université de Lorraine, IADI, UMR 947, Tour Drouet, rue du Morvan, 54511 Vandoeuvre-lès-Nancy, France.

Introduction

Since its introduction in the 1990s, unenhanced Computed Tomography (CT) has become the gold standard for urinary tract imaging in patients with renal colic [1, 2]. It offers many advantages: availability, no injection of iodinated contrast medium and excellent diagnostic performance [3]. Its main limitation is related to radiation, especially as urinary stone disease mainly affects young patients with a tendency to relapse [4, 5]. In accordance with the cautionary principle of ALARA (As Low As Reasonably Achievable) and given the potential risk of radiation-induced cancers associated with low X-ray doses [6, 7], reducing the dose urinary tract CT is paramount.

Many studies have shown that it is possible to use low-dose CT to investigate renal colic with excellent diagnostic performance [3]. The researchers primarily evaluated the possibility of reducing the dose by increasing the pitch [8], lowering tube current [9-11], using automatic tube current modulation [12], reducing tube voltage [13, 14] and using iterative reconstruction algorithms [13-19].

Another simple and effective way to reduce the dose is to limit acquisition coverage from the top of the kidneys to the lower edge of the bladder. For the lower acquisition limit, the lower edge of the symphysis pubis bone is an accurate landmark [20, 21]. Identifying the upper limit of the acquisition is more complicated. In our institution, we reduce the acquisition coverage by trying to locate the top of the kidneys on the frontal scout image. However, the renal contours is frequently hard to identify and to our knowledge, the effectiveness of this method has not yet been evaluated.

In order to find a more reliable method of reducing acquisition coverage without cutting the kidneys, two recent studies have evaluated the possibility of using a vertebral bony landmark to define the upper acquisition limit. For de Leon et al. [20] use of the superior margin of 11th thoracic vertebral body (T11) reduced the

acquisition coverage by 18%, compared to standard abdominopelvic acquisition, without cutting the kidneys. For Corwin et al., [21] placing the upper limit of the acquisition at the inferior margin of the 10th thoracic vertebral body (T10) led to a 17.7% coverage reduction without cutting the kidneys. Although these two studies showed that the use of T10 or T11 bony landmark excluded no kidneys during the acquisition, we believe that the reduction of the scan coverage is not so important it could be in many patients. In addition, the relatively high frequency of anatomical variants in the thoraco-lumbar spine and the fact that it is not applicable in patients with scoliosis adds to the difficult in applying these methods in clinical practice.

We propose an alternative method for placement of the upper acquisition limit of urinary tract CT-scans. This method is based on the lateral scout image and uses the point of intersection between the left diaphragmatic dome and the anterior margin of the vertebral bodies. We believe that this may allow optimal coverage reduction while using a simple anatomical landmark, which could represent an advantage over conventional methods. The aim of our study was to compare three coverage-reducing methods with an evaluation of scan coverage reduction percentage and number of cut kidneys.

Materials and Methods

This study was approved by our local ethics committee. Taking into account its retrospective nature, written consent of patients was not necessary.

Study population:

This retrospective single-center study included all patients over 18 years old referred to our imaging department between November 2014 and February 2015 for a standard abdominopelvic CT-scan with injection of iodinated contrast medium. Four patients were excluded because the frontal or lateral scout image did not cover the entire abdomen, one because of severe scoliosis and three because of left pulmonary effusion that precluded visualization of the left diaphragmatic dome on the lateral scout image. Overall, 365 CT-scans involving 343 patients were included in the study.

For all patients, the following parameters were systematically collected at the time of the scan: sex, age (years), weight (kg) and height (m). The Body Mass Index (BMI) was calculated using the formula BMI = weight / height^2 (kg / m^2).

CT acquisition and reconstruction parameters:

All examinations were performed in supine position using a 64-slice multidetector CT scanner (OPTIMA CT660, General Electric Healthcare, USA). Examinations began with a frontal and lateral scout radiograph with 120 kV and 10 mA during a deep in-breath. Acquisition of both frontal and lateral scout radiographs was necessary to enable automatic exposure control. The examinations included at least one abdominopelvic acquisition at the portal phase from the top of diaphragm through the ischial tuberosities. In some cases additional series were performed (unenhanced, arterial or delayed phases). These series were not evaluated in this study. Acquisition parameters included tube voltage from 100-140 kV according to weight, automatic tube current modulation (GE Smart mA) with a noise index of between 18 and 25 and ASIR (Adaptive Statistical Iterative Reconstruction). Images were reconstructed in thin slices of 1.25 mm every 1.25 mm with a soft tissue kernel. All examination images as well as the scout images and the review report with location data for the first and last slices were archived in our PACS database (Picture Archiving and Communication System).

Z-axis scan coverage evaluation:

For each CT-scan, the coverage of the standard abdominopelvic acquisition was calculated as the difference in cm between the location of the first and last slices of the acquisition.

The location of the lower limit of the simulated reduced acquisition was standardized for all three methods and was identical to that used by de Leon et al. and Corwin et al. [20, 21]. It corresponded to the section passing through the inferior aspect of the bony symphysis and was placed on each standard abdominopelvic CT-scan by the study investigator (A.G.), a radiologist with 9 years of clinical experience, using a post-processing workstation ADW 4.6 (GE HealthCare, USA).

The location of the upper limit of the simulated reduced acquisition was different for each of the three methods:

Method 1 corresponded to the placement of the upper limit of the acquisition from the frontal scout image by locating the top of the kidneys. Method 2 was that described by Corwin et al. [21], and corresponded to the placement of the upper limit of the acquisition from the frontal

scout image at the level of the inferior margin of T10. The lowest rib-bearing vertebral body was considered to represent the 12th thoracic vertebral body. Method 3 was the alternative method we propose. With this method, the upper limit of the acquisition was placed on the lateral scout image at the point of intersection between the anterior margin of the vertebral body and the left diaphragmatic dome (Fig 1). The left dome was identified by the lowest position of the right dome. In case of doubt, the frontal scout image was used to confirm the laterality of the dome.

For each scan, the upper limits of the acquisition for all three methods were determined by three CT technologists with at least 4 years of experience in scanning for renal colic in our institution using method 1. With regard to the upper limit selection, technologists had access to frontal and lateral scout images, which had been anonymized and randomized. The upper limit was placed on ADW 4.6 workstation (GE Healthcare, USA) using the "localizer" function, which allowed the determination of the slice location on the z-axis on the scout images. Readers were able to zoom and change the window settings of scout images. A second reading session was conducted by readers 2 and 3, two months after the first reading on 30 CT-scans randomly selected and placed in a different random order to the first session. This second reading was used to calculate intra-observer agreement.

Having determined the upper limits, the lengths of simulated reduced acquisition were calculated for each scan and each method as the difference in cm between the location of the upper and lower limits.

The study investigator (A.G.) noted, for each standard abdominopelvic CT, the z-axis location of the superiormost aspect of the highest kidney. By comparing the location data of the upper limit of the simulated reduced acquisition and the top of the uppermost kidney, it was possible to determine how many kidneys were cut by each method and for each reader and evaluate the length of the kidney portions that were cut out.

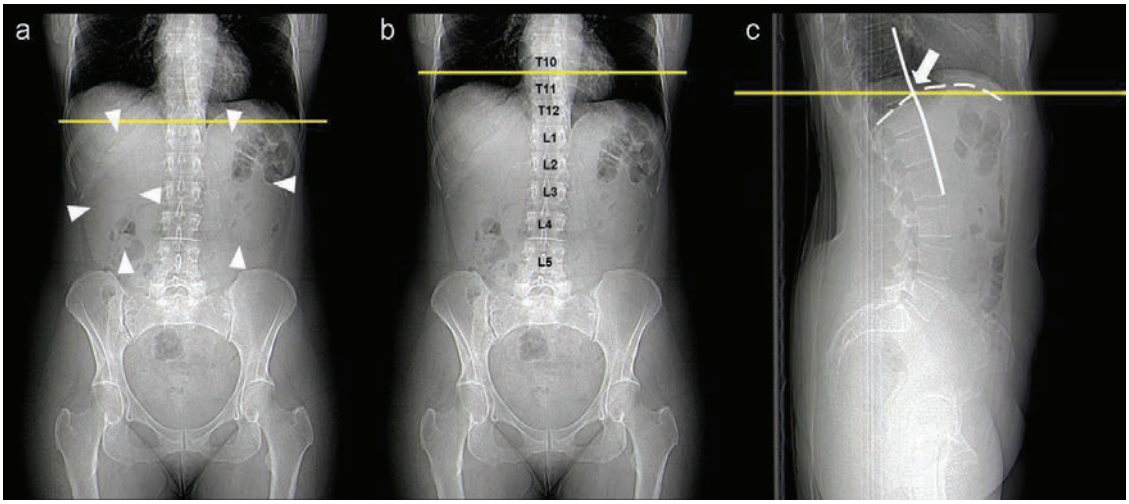

Fig. 1 - Frontal (a, b) and lateral (c) scout images showing how to place the upper limit of the reduced acquisition with the three methods evaluated. For method 1 (a), the upper limit of the acquisition was placed by locating the top of the kidneys using the renal contours as reference (arrowheads). Method 2 (b) used the inferior margin of T10 as reference. Method 3 (c) used the lateral scout image and the point of intersection (arrow) between the anterior margin of the vertebral bodies (solid white line) and the left diaphragmatic dome (dashed white line).

Statistical analysis:

Data were analyzed using R software for Windows Version 3.2.0 (R Foundation for Statistical Computing, Vienna, Austria). The values were given as the mean ± standard deviation with the extreme values in parentheses. For each of the three technologists, the Tukey test and Fisher's exact test were used to compare, respectively, reduced acquisition coverage and proportion of cut kidney among the three methods. An interclass correlation coefficient (ICC) was used to assess the inter-reader agreement and intra-reader agreement for technologists 2 and 3. A p value less than 0.05 was considered to represent a statistically significant difference.

Table 1. Simulated acquisition coverage reduction according to each reader and each of the three methods.

	Simulated acquisition coverage reduction (cm)			p value		
	M1	M2	M3	M2/M1	M3/M1	M3/M2
Reader 1	35.77 ± 2.94	37.25 ± 2.03	36.01 ± 3.10	<0.001	0.483	<0.001
Reader 2	34.10 ± 2.89	37.45 ± 2.08	35.91 ± 3.04	<0.001	<0.001	<0.001
Reader 3	34.96 ± 2.82	37.15 ± 2.12	35.87 ± 3.04	<0.001	<0.001	<0.001

M1 = method 1; M2 = method 2; M3 = method 3.
Results given as mean ± standard deviation

Results

Study population:
Of the 343 patients enrolled, 178 were women and 165 men with an average age of 54.7 years (range 18-92 years), a mean weight of 77.2 kg (35 to 170 kg), an average height of 167.9 cm (143 to 199 cm) and a mean BMI of 27.2 kg / m² (14.9 to 60 kg / m²).

Reduced simulated acquisitions:
The average coverage of standard abdominopelvic acquisition was 43.93 ± 3.81 cm (33.87 to 54.75 cm). The scan coverage of the reduced simulated acquisitions for each of the three methods and all three technologists are shown in Table 1 and Fig 2. For all technologists, method 1 permitted a greater reduction in acquisition coverage over standard abdominopelvic acquisition, and method 2 produced the smallest reduction in acquisition coverage. For readers 2 and 3, the differences between the three methods were statistically significant (p <0.001). For reader 1, only the difference between methods 1 and 3 was not statistically significant (p = 0.483).
Compared to standard abdominopelvic acquisition, the percentage of reduction in acquisition coverage with methods 1, 2 and 3, averaged over the three readers, were, respectively 20.5%, 15.1% and 18.2 %.
The average distance between the lower limit of standard abdominopelvic acquisition and the inferior aspect of the symphysis pubis was 2.3 cm, which corresponded to a 5.2% reduction of the length of acquisition. Reduction of the acquisition coverage linked to the upper limit alone was 15.2%, 9.9% and 13% for methods 1, 2 and 3, respectively.

Number of cut kidneys:
The numbers of CT-scans with a cut kidney for each method coverage optimization are shown in Table 2. The percentage of cut kidneys with methods 1, 2 and 3, averaged over the three readers, were respectively 6.7%, 0.7% and 1.4%. Method 1 resulted in most kidney cuts, with a significant variation between the three readers (from 7 for reader 1 to 46 for reader 2). There was no significant difference between method 2 with respect to method 3, regardless of the reader (P> 0.451). For method 2, three same studies had a cut kidney with reader 1 and 3 and two of these three studies had a cut kidney with reader 2.

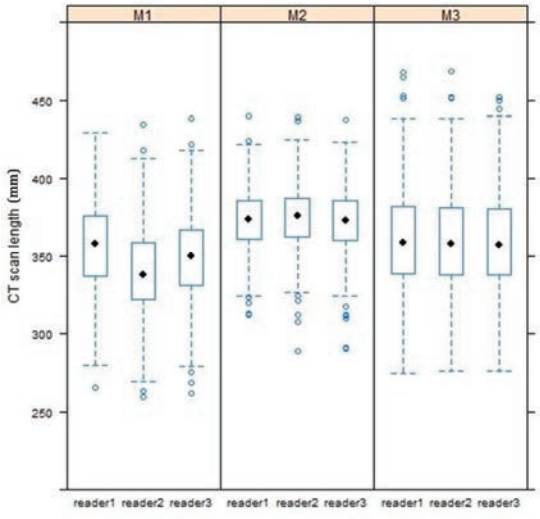

Fig. 2 - Chart showing the distribution of simulated reduced acquisition coverages according to the three methods for each of the three readers. Note that with methods 2 and 3, the acquisition coverages are very consistent between the three readers in comparison with the method 1. Also note the greater reduction in the acquisition coverage with method 3 compared to method 2.

The maximum length of cut out kidney portions with methods 1, 2 and 3 was respectively 4.2 cm, 0.6 cm and 1 cm for the three readers

(respectively 2.1 cm, 0.5 cm and 1 cm for reader 1; 4.2 cm, 0.5 and 1 cm for reader 2; 2.8 cm, 0.6 cm and 0.8 cm for reader 3).

In order not to cut kidneys, the bony landmark should be the middle of the vertebral body of T10.

Table 2. Number of CT-scans with a portion of kidney excluded from the simulated reduced acquisition based on each reader and each of the three methods.

Number of CT-scans with a portion of kidney excluded from the simulated reduced acquisition				**p value**		
	M1	M2	M3	M2/M1	M3/M1	M3/M2
Reader 1	7 (1.9 %)	3 (0.8 %)	5 (1.4 %)	0.772	0.882	0.772
Reader 2	46 (12.6 %)	2 (0.5 %)	5 (1.4 %)	<0.001	<0.001	0.451
Reader 3	20 (5.5 %)	3 (0.8 %)	5 (1.4 %)	0.001	0.005	0.725

M1 = method 1; M2 = method 2; M3 = method 3.
Results given as number and percentage in parentheses.

Intra- and inter-reader agreements:
The inter-reader agreement was excellent regardless of the method (Table 3). There was a progressive increased in ICC values from method 1 to 3, method 3 having the overall best inter-reader agreement. The intra-reader agreements of readers 2 and 3 were excellent, regardless of the method and the reader (Table 4). For reader 3, the intra-reader agreement was significantly better for methods 2 and 3 than for method 1.

Table 3: Inter-reader agreement between the three methods.

Method	**ICC**	**95 % CI**
M1	0.926	0.814 < ICC < 0.962
M2	0.979	0.974 < ICC < 0.983
M3	0.992	0.991 < ICC < 0.994

CI = Confidence Interval; ICC = Interclass Correlation Coefficient;
M1 = method 1; M2 = method 2; M3 = method 3.

Table 4: Intra-reader agreement for readers 2 and 3 based on 30 CT-scans randomly selected.

Readers	**Method**	**ICC**	**95 % CI**
Reader 2	M1	0.937	0.073 < ICC < 0.985
	M2	0.986	0.972 < ICC < 0.994
	M3	0.982	0.962 < ICC < 0.991
Reader 3	M1	0.984	0.962 < ICC < 0.993
	M2	0.999	0.998 < ICC < 1
	M3	1	1 < ICC < 1

CI = Confidence Interval; ICC = Interclass Correlation Coefficient; M1 = method 1; M2 = method 2; M3 = method 3

Discussion

Our study confirms that a 15-20% reduction in the coverage of urinary tract CT-scans can be obtained by optimizing the acquisition protocol. As it has been shown for other CT applications [22, 23], reducing the acquisition coverage is a simple and effective way of limiting the dose in patients and is recommended in clinical practice. Because of the close relation between scan length and effective dose, when the acquisition length is reduced a similar reduction in effective dose can be expected. In a recent study assessing the possibility to reduce the CT scan coverage for acute appendicitis which was also based on T10 anatomical landmark, Corwin et al. found that a reduction of the scan coverage of 24 % corresponded to a dose reduction of 23 % [22]. In addition, by optimizing coverage, it is also possible to reduce the exposure of radiosensitive organs, such as the gonads in men and the breasts in women [24]. In practice, like others dose reduction techniques such as iterative reconstruction algorithms [13-19, 25], optimization of the acquisition coverage could have a significant impact on the dose delivered to patients undergoing a urinary tract CT.

One of the major findings of our study is that the use of the kidney's contours as reference on the frontal scout image is difficult in practice (method 1). Even if it reduces the acquisition coverage by up to 20.5% compared to a standard abdominopelvic acquisition, it was the least reproducible and the most likely method to cut the upper pole of the kidney. For reader 2, in 12% of cases the kidneys were cut with a maximal distance of cut kidney of 4.2 cm, which is not acceptable in clinical practice. This limitation is related to the difficulty of visualizing the kidney on the frontal scout image. These findings underscore the importance of identifying a more suitable anatomical landmark for the determination of the upper limit of urinary tract CT acquisitions [20, 21].

In our study, we used the bony landmark of Corwin et al., which corresponded to the inferior margin of T10 (method 2) [21] and not the superior margin of T11 as de Leon et al. [20]. Although the difference between these two landmarks is minimal, we chose to study the uppermost landmark in order to favor the method that excluded the least kidneys. While for Corwin et al, 100% of kidneys were included in the reduced acquisition, in our study, readers 1 and 3 excluded the upper pole of the left kidney in three patients using method 2. In contrast to de Leon et al. [20] and Corwin et al. [21], our study shows that the superior margin of T10 is not infallible and that in order not to cut kidneys, the bony landmark should be the middle of the vertebral body of T10. However, with such a landmark, reduced acquisition coverage would be increased for roughly 1 cm. In one particular patient with small 12th ribs hardly visible on the scout image, readers 2 did not cut the kidney, because the inferior margin of the 9th thoracic vertebral body was mistakenly used as landmark (Fig 3). This shows that the vertebral bony landmark method can also have pitfalls.

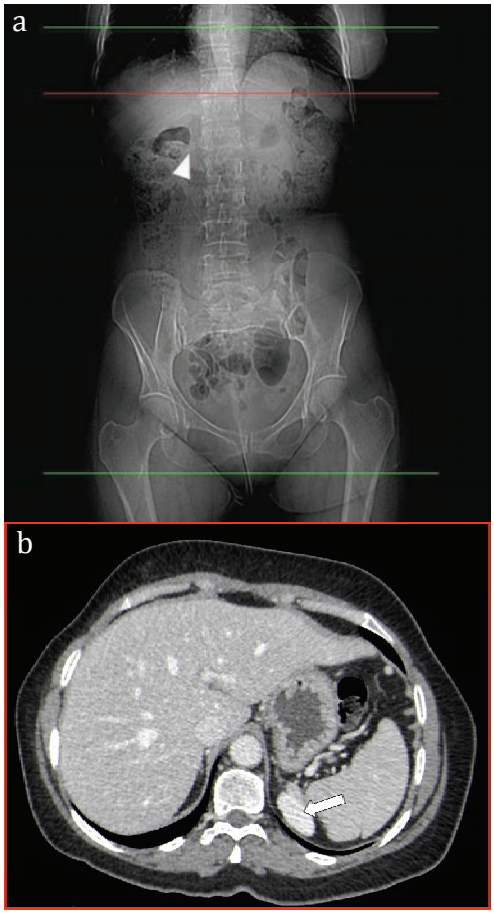

Fig. 3 - Female aged 65 years with a BMI of 26.4 kg / m². Frontal scout image (a) with green lines corresponding to the limits of the standard abdominopelvic acquisition and red line corresponding to the upper limit of the reduced acquisition coverage using method 2. The axial CT slice (b) passing through the lower margin of T10 shows that the top of the left kidney is cut (arrow). Also note the presence of small ribs T12 (arrowhead) that were not seen by reader 2, who mistakenly used the inferior margin of T9 as landmark and didn't cut the left kidney.

The proposed method (3), based on the lateral scout image and taking as a reference point the intersection of the anterior margin of the vertebral bodies and the left diaphragmatic dome may be of interest to optimize the coverage of urinary tract CT-scans and thereby reduce the delivered dose. It was the most reproducible method of the three, both between readers and for an individual reader. It is not hampered by anatomical variants and uses landmarks that are quick and easy to find, which is supported by excellent inter- and intra-reader agreement. In particular, the distinction between the left and right diaphragmatic dome on the lateral scout image poses no problem because the left diaphragmatic dome is often lower than the right. It is also possible to detect its position relative to the right diaphragmatic dome on the frontal scout image. This method allows a significant reduction of the acquisition coverage over method 2 (18.2 against 15.1% p <0.001). Although the proportion of kidneys cut using method 3 was greater than with method 2 (1.4% vs 0.7%), this difference was not statistically significant. In addition, with method 3, in the CT-scans with cut kidneys, less than 1 cm of kidney was out of the field of view, which seems acceptable in patients evaluated for renal colic. This method strikes as a good compromise between method 1 that cuts too many kidneys with a greater reduction in coverage, and method 2, which rarely cuts kidneys but gives a smaller coverage and dose reduction.

Our study has several limitations. First, it is retrospective. A prospective study with a larger patient population would be interesting to confirm our results, especially given the low number of CT-scans with a cut kidney using our new method. Second, we included all patients who had a standard abdominopelvic CT, without selecting those referred for suspected renal colic. This allowed us to include more patients and compare reductions in acquisition length to the length of standard abdominopelvic acquisition in the same patient. However, three patients had to be excluded from our study because they had left pulmonary effusion that masked the left diaphragmatic dome on the scout image and prevented us using the proposed method. In clinical practice, this has little impact since the association of left sided pleural effusion and renal colic is relatively rare. Third, we did not try to assess the frequency of lesions (e.g. pulmonary nodule, adrenal mass) that might be missed on acquisitions with reduced coverage, as it was not among the objectives of this study. Moreover, according to current clinical practice, a patient whose scan was negative would probably undergo an additional standard enhanced CT to search for possible differential diagnoses. Fourth, detail and clarity of scout images may vary across different CT vendors. The results of our study should be confirmed on CT-scanners from others manufacturers. Finally, we used a CT protocol with automatic tube current modulation, which implies that the dose reduction is not strictly proportional to the reduction in acquisition coverage. Therefore, we did not directly estimate the percentage reduction in the dose.

In conclusion, using the intersection of the left diaphragmatic dome and the anterior margin of the vertebral bodies on the lateral scout image to set the upper limit of the acquisitions of CT-scans in patients with suspected renal colic appears to be a good compromise. This method allows for a greater reduction of acquisition coverage in comparison with the inferior margin T10 landmark and excludes fewer kidneys than the method using kidney contours on frontal scout image. It is also the most reproducible method evaluated that we now use in clinical practice.

Acknowledgements:
None.

References

1. Coursey CA, Casalino DD, Remer EM, Arellano RS, Bishoff JT, Dighe M, et al. ACR Appropriateness Criteria® acute onset flank pain: suspicion of stone disease. Ultrasound Q 2012;28:227-233.
2. Kambadakone AR, Eisner BH, Catalano OA, Sahani DV. New and evolving concepts in the imaging and management of urolithiasis: urologists' perspective. Radiographics 2010;30:603-623.
3. Niemann T, Kollmann T, Bongartz G. Diagnostic performance of low-dose CT for detection of urolithiasis: a meta-analysis. AJR Am J Roentgenol 2008;191; 396-401.
4. Broder J; Bowen J, Lohr J Babcock A, Yoon J. Cumulative CT exposures in emergency department patients evaluated for suspected renal colic. J Emerg Med 2007; 33:161-168.
5. Katz SI, Saluja S, Brink JA, Forman HP. Radiation dose associated with unenhanced CT for suspected renal colic: impact of

repetitive studies. AJR Am J Roentgenol 2006;186: 1120-1124.

6. Smith-Bindman R, Lipson J, Marcus R, Lim KP, Mahesh M, gould R, et al. Radiation dose associated with common computed tomography examinations and the associated lifetime attributable risk of cancer. Arch Intern Med 2009;169:2078-2086.

7. Berrington de González A, Mahesh M, Kim KP, Bhargavan M, Lewis R, Mettler F, et al. Projected cancer risks from computed tomography scans performed in the United States in 2007. Arch Intern Med 2009;169:2071-2077.

8. Diel J, Perlmutter S, Venkataramanan N, Mueller R, Lane MJ, Katz DS. Unenhanced helical CT using increased pitch for suspected renal colic: an effective technique for radiation dose reduction? J Comput Assist Tomogr 2000;24:795-801.

9. Tack D, Sourtzis S, Delpierre I, de Maertelaer V, Gevenois PA. Low-dose unenhanced multidetector CT of patients with suspected renal colic. AJR Am J Roentgenol 2003: 180: 305-311.

10. Kluner C, Hein PA, Gralla O, Hein E, Hamm B, Romano V, et al. Does ultra-low-dose CT with a radiation dose equivalent to that of KUB suffice to detect renal and ureteral calculi? J Comput Assist Tomogr 2006; 30:44-50.

11. Poletti PA, Platon A, Rutschmann OT, Schmidlin FR, Iselin CE, Becker CD. Low-dose versus standard-dose CT protocol in patients with clinically suspected renal colic. AJR Am J Roentgenol 2007; 188; 927-933.

12. Mulkens TH, Daineffe S, De Wijngaert R, Bellinck P, Leonard A, Smet G, et al. Urinary stone disease: comparison of standard-dose and low-dose with 4D MDCT tube current modulation. AJR Am J Roentgenol 2007;188:553-562.

13. Kulkarni NM, Uppot RN, Eisner BH, Sahani DV. Radiation dose reduction at multidetector CT with Adaptive Statistical Iterative Reconstruction for evaluation of urolithiasis: how low can we go? Radiology 2012;265:158-166.

14. Gervaise A, Naulet P, Beuret F, Henry C, Pernin M, Portron Y, et al. Low-dose CT with automatic tube current modulation, adaptive statistical iterative reconstruction and low tube voltage for the diagnosis of renal colic: impact of body mass index. AJR Am J Roentgenol 2014;202:553-560.

15. Fontarensky M, Alfidja A, Perignon R, Schoenig A, Perrier C, Mulliez A, et al. Reduced radiation dose with Model-based Iterative Reconstruction versus standard dose with Adaptive Statistical Iterative Reconstruction in abdominal CT for diagnosis of acute renal colic. Radiology 2015;276:156-66.

16. McLaughlin PD, Murphy KP, Hayes SA, Carey K, Sammon J, Crusch L, et al. Non-contrast CT at comparable dose to an abdominal radiograph in patients with acute renal colic; impact of iterative reconstruction on image quality and diagnostic performance. Insights Imaging 2014;5:217-230.

17. Wang J, Kang T, Arepalli C, Barrett S, O'Connell T, Louis L, et al. Half-dose non-contrast CT in the investigation of urolithiasis: image quality improvement with third-generation integrated circuit CT detectors. Abdom Imaging 2015;40:1255-62.

18. Glazer DI, Maturen KE, Cohan RH, Davenport MS, Ellis JH, Knoepp US, et al. Assessment of 1 mSv urinary tract stone CT with Model-Based Iterative Reconstruction. AJR Am J Roentgenol 2014;203:1230-1235.

19. Winklehner A, Blume I, Winklhofer S, Eberli D, Gnannt R, Frauenfelder T, et al. Iterative reconstructions versus filtered back-projection for urinary stone detection in low-dose CT. Acad Radiol 2013;20:1429-1435.

20. de Leon AD, Xi Y, Champine J, Costa DN. Achieving ideal computed tomography scan length in patient with suspected urolithiasis. J Comput Assist Tomogr 2014;38:264-267.

21. Corwin MT, Bekele W, Lamba R. Bony landmarks on computed tomography localizer radiographs to prescribe a reduced scan range in patients undergoing multidetector computed tomography for suspected urolithiasis. J Comput Assist Tomogr 2014;38:404-7.

22. Corwin MT, Chang M, Fananapazir G, Seibert A, Lamba R. Accuracy and radiation dose reduction a limited abdominopelvic CT in the diagnosis of acute appendicitis. Abdom Imaging 2015;40:1177-82.

23. Campbell J, Kalra MK, Rizzo S, Maher MM, Shepard JA. Scanning beyond anatomic limits of the thorax in chest CT: findings, radiation dose and automatic tube current modulation. AJR Am J Roentgenol 2005;185:1525-30.

24. van der Molen AJ, Geleijns J. Overranging in multisection CT: quantification and relative contribution to dose - comparison of four 16-section CT scanners. Radiology 2007;242:208-16.

25. Gervaise A, Osemont B, Lecocq S, Noel A, Micard E, Felblinger J, et al. Image quality improvement using Adaptive Iterative Dose Reduction with wide-volume acquisition on 320-detector CT. Eur radiol 2012;22:295-301.

Discussion et conclusion du chapitre 2 :

Les résultats de nos études mettent en avant l'importance des facteurs comportementaux dans une démarche d'optimisation et de réduction de la dose d'irradiation au scanner.

Article 1 : Evaluation des connaissances des prescripteurs de scanner en matière de radioprotection des patients.

Les résultats de notre étude confirment qu'il existe un défaut de connaissance des praticiens hospitaliers prescripteurs de scanner vis-à-vis des niveaux de dose de rayons X délivrés au cours d'un scanner abdominopelvien et surtout vis-à-vis des risques potentiels de cancer radio-induit lié aux faibles doses de rayons X actuellement admis par la communauté scientifique. Bien que le nombre de réponse soit relativement faible (seulement 44 questionnaires analysés dont 29 séniors et 15 internes), ces résultats sont concordants avec les données de la littérature [44]. Cette étude montre toutefois que 70 % des praticiens prennent en compte les risques liés aux rayons X lors de la prescription d'un scanner. Ce résultat est plutôt positif car cela suggère que plus de la moitié des praticiens est sensibilisée à cette problématique. Or, cette sensibilisation des prescripteurs est un élément important pour pouvoir faire appliquer les principes de justification et de substitution des scanners. Etant donné que seulement un tiers des prescripteurs avait bénéficié d'une formation à la radioprotection des patients, la mise en place de formation pour les médecins au cours des études de médecine et au cours de la formation médicale continue semble être une des solutions pour mieux diffuser ce type de connaissance et pour améliorer la radioprotection des patients. D'ailleurs, suite aux résultats de cette étude, nous avons mis en place une séance de formation de 30 minutes à la radioprotection des patients au profit des nouveaux internes arrivant à l'HIA Legouest.

Article 2 : Evaluation de l'intérêt de l'acquisition abdominopelvienne sans injection lors de la réalisation d'un scanner corps entier chez un patient suspect de polytraumatisme.

La suppression de la série sans injection lors de la réalisation d'un scanner abdominopelvien est un moyen simple pour réduire la dose globale du scanner. Dans notre étude portant sur l'intérêt de la série abdominopelvienne sans injection durant l'acquisition

d'un scanner corps entier pour bilan de polytraumatisme, la série sans injection thoraco-abdominopelvienne était à l'origine de 20 % de la dose totale délivrée au cours du scanner. Pourtant, l'intérêt diagnostique de l'acquisition abdominopelvienne sans injection s'est avéré faible et vraisemblablement sans impact sur la prise en charge du patient. De ce fait, sa suppression permet de réduire la dose globale du patient. Bien que nous n'ayons pas analysé l'intérêt de la série sans injection au niveau du thorax, nous pensons aussi que son impact est limité et qu'il est aussi possible de supprimer cette série. Une autre limite de notre étude était l'absence d'évaluation de l'impact thérapeutique ou du pronostique liée aux lésions traumatiques analysées. Les résultats de notre étude ont toutefois été confirmés par une étude plus récente qui retrouvait aussi l'absence d'amélioration de la performance diagnostique de la série sans injection abdominopelvienne lors de la réalisation d'un scanner corps entier pour bilan de polytraumatisme [20].

Article 3 : Optimisation de la longueur d'acquisition des scanners réalisés pour colique néphrétique : proposition d'une nouvelle méthode pour le placement de la limite supérieure de l'acquisition.

La réduction de la couverture d'acquisition est aussi un moyen simple, rapide et efficace pour réduire la dose. La couverture d'un scanner doit être centrée sur la zone d'intérêt. Dans notre étude, nous avons proposé un nouveau repère pour placer le bord supérieur de l'acquisition d'un scanner réalisé pour suspicion de colique néphrétique. Ce repère est constitué par le point d'intersection entre le bord antérieur des corps vertébraux et la coupole diaphragmatique gauche sur le scout de profil. Avec notre repère, nous avons pu réduire de 18,2 % la longueur d'acquisition contre 15,1 % pour la méthode 2 utilisant le bord inférieur de la vertèbre T10 et 20,5 % pour la méthode 1 utilisant les contours des reins. Parallèlement, la proportion de reins coupés était significativement supérieure pour la méthode 1 avec 6,7 % des reins coupés, ce qui apparaît inacceptable en pratique clinique courante. Par contre, il n'y avait pas de différence significative en termes de proportion de reins coupés entre les méthodes 2 et 3 avec respectivement 0,7 et 1,4 %. Même si notre méthode a montré qu'elle coupe un peu plus de rein que la méthode de Corwin MT *et al.* [46], la distance de rein coupé reste faible, inférieure à 1 cm, ce qui semble acceptable en pratique clinique courante. Nous pensons donc que la nouvelle méthode que nous proposons apparaît comme un bon compromis en permettant une réduction de la longueur d'acquisition plus importante que la

méthode 2 mais en coupant moins de rein qu'avec la méthode 1. Dans notre étude, compte tenu de l'utilisation d'un protocole de scanner avec la modulation automatique du mA, il n'était pas possible de calculer directement le pourcentage de réduction de la dose d'irradiation à partir de la réduction de la longueur d'acquisition. Toutefois, la réduction de la dose est vraisemblablement très proche de la réduction de la longueur d'acquisition. Dans une étude récente portant sur la réduction de la longueur d'acquisition pour des scanners réalisés pour suspicion d'appendicite aiguë, Corwin MT *et al.* ont retrouvé une réduction de la longueur d'acquisition de 24 % pour une réduction de la dose de 23 % [47]. Par ailleurs, outre la réduction de la dose globale du scanner par une réduction de la couverture d'acquisition, ce centrage permet aussi d'éviter au faisceau de rayons X de traverser des organes radiosensibles comme les gonades chez l'homme et les seins chez la femme. De plus, à cause du phénomène d'irradiation pré- et post-hélice, qui peut s'étendre sur 2 à 3 cm de part et d'autre de l'hélice, même si ces organes radiosensibles ne sont pas compris dans les images acquises, ils peuvent être traversés par le faisceau de rayons X s'ils sont situés à proximité des limites du champ d'acquisition.

CHAPITRE 3 : INFLUENCE DES FACTEURS TECHNIQUES

Ce chapitre est composé de quatre articles :

1- Gervaise A**,** Louis M, Batch T, Loeuille D, Noel A, Guillemin F, Blum A. Réduction de dose dans l'exploration du rachis lombaire grâce au scanner 320-détecteurs : étude initiale. *J Radiol* 2010; 91: 779-85.

2- Gervaise A, Osemont B, Lecocq S, Micard E, Noel A, Felblinger J, Blum A. CT image quality improvement using adaptive iterative dose reduction with wide-volume acquisition on 320-detector CT. *Eur Radiol* 2012; 22: 295-301.

3- Gervaise A, Osemont B, Louis M, Lecocq S, Teixeira P, Blum A. Standard dose versus low-dose abdominal and pelvic CT: comparison between filtered back projection versus adaptive iterative dose reduction 3D. *Diagn Interv Imaging* 2014; 95: 47-53.

4- Gervaise A, Naulet P, Beuret F, Henry C, Pernin M, Portron Y, Lapierre-Combes M. Low-dose CT with automatic tube current modulation, adaptive statistical iterative reconstruction, and low tube voltage for the diagnosis of renal colic: impact of body mass index. *Am J Roentgenol* 2014; 202: 553-60.

Les facteurs techniques ont bénéficié de nombreuses innovations technologiques ces dernières années. Nous proposons d'illustrer l'intérêt de plusieurs de ces facteurs techniques dans une démarche d'optimisation et de réduction de la dose d'irradiation au scanner : le mode d'acquisition volumique, les reconstructions itératives et la modulation automatique du milliampérage.

Article 1 : Réduction de dose dans l'exploration du rachis lombaire grâce au scanner 320-détecteurs : étude initiale.

Le mode d'acquisition est l'un des facteurs techniques qui influence la dose et qui est accessible au moment de l'acquisition. L'apparition des scanners à large système de détection, comme le scanner 320-détecteurs, permet d'avoir une couverture d'acquisition allant jusqu'à 16 cm en une seule rotation du tube. Pour des scanners avec une faible couverture d'acquisition, tels que le cœur, le cerveau ou encore les articulations périphériques, il devient possible de faire des acquisitions volumiques en mode séquentiel et non hélicoïdal. De même, en juxtaposant deux volumes d'acquisition (= mode *Wide-volume* ou *Stitching mode*) il est aussi possible de faire une acquisition volumique pour des scanners de plus grande longueur d'acquisition.

Le but de notre étude était de comparer la dose délivrée et la qualité d'image entre un scanner lombaire réalisé en mode hélicoïdal et en mode *Wide-volume* grâce au scanner 320-détecteurs.

Il s'agissait d'une étude monocentrique prospective incluant 20 patients adressés au service d'imagerie Guilloz du CHRU de Nancy pour la réalisation d'un scanner lombaire. Les dix premiers patients ont bénéficiés d'un scanner en mode *Wide-volume* 320-détecteurs et les dix suivants en mode hélicoïdal 64-détecteurs. Les longueurs d'acquisition, les doses délivrées ainsi qu'une évaluation quantitative et qualitative de la qualité d'image ont été comparées entre les deux groupes.

Les résultats montraient une réduction significative de la dose délivrée de 35 % en faveur du mode d'acquisition volumique versus hélicoïdal (produit dose longueur de respectivement 970 mGy.cm versus 1503 mGy.cm). Par contre, il n'y avait pas de différence statistiquement significative de qualité d'image ou de longueur d'acquisition entre les deux groupes.

<u>Article 2 :</u> Amélioration de la qualité d'image scanographique en utilisant les reconstructions itératives Adaptive Iterative Dose Reduction avec une acquisition wide-volume sur un scanner 320-détecteurs.

Malgré le développement de plusieurs innovations technologiques (modulation automatique du milliampérage, collimation active), la réduction de la dose des scanners reste limitée par l'utilisation des reconstructions standard en FBP car celles-ci entraînent une augmentation notable du bruit de l'image en cas de réduction trop importante de la dose [41]. L'apparition récente des reconstructions itératives a permis une réduction significative du bruit de l'image par rapport aux reconstructions standard FBP [42].

Le but de cette étude était d'évaluer l'impact sur fantôme et sur patient des reconstructions itératives AIDR sur la qualité d'image et sur la dose.

L'étude sur fantôme était réalisée à partir d'un fantôme Catphan 500® en faisant des acquisitions volumiques avec le scanner 320-détecteurs avec un milliampérage allant de 25 à 550 mAs (milliampère x secondes). Les images étaient reconstruites en FBP et en AIDR. Le bruit de l'image, le RCB, le RSB et la résolution spatiale des images ont été comparés entre les images FBP et AIDR. Les reconstructions itératives AIDR ont ensuite été testées sur 15 scanners lombaires au cours d'une étude prospective monocentrique sur patient. Les images étaient reconstruites en FBP et AIDR. Le bruit de l'image et le RSB ont été comparés entre les deux séries d'image.

Sur le fantôme, les résultats montraient une réduction significative du bruit de l'image de 40 % en faveur des reconstructions itératives AIDR par rapport aux images FBP. Il existait aussi une amélioration significative du RSB et du RCB avec les reconstructions AIDR. Par contre, il n'y avait pas de différence significative de résolution spatiale entre les deux types d'images. Au niveau des scanners lombaires, il existait une amélioration significative de l'évaluation quantitative et qualitative de la qualité d'image sur les images AIDR versus FBP.

<u>Article 3 :</u> Réduction de la dose des scanners abdominopelviens grâce aux reconstructions itératives AIDR 3D.

Tandis que les reconstructions itératives AIDR n'étaient disponibles que pour une acquisition volumique sur le scanner 320-détecteurs et avec une reconstruction rétrospective

des images, l'introduction des nouvelles reconstructions itératives AIDR 3D a permis leur utilisation en mode d'acquisition hélicoïdal prospectif. Il a ainsi été possible de les utiliser en pratique clinique courante.

Le but de cette étude était de comparer la dose et la qualité d'image d'un scanner abdomino-pelvien en dose normale avec les reconstructions standard FBP versus en basse-dose avec les reconstructions itératives AIDR 3D et les reconstructions FBP.

Il s'agissait d'une étude rétrospective incluant 21 patients ayant eu un scanner abdomino-pelvien au temps portal avant (série FBP dose standard) et après l'implantation des reconstructions itératives AIDR 3D (série AIDR 3D basse-dose et FBP basse-dose). La longueur d'acquisition, la dose délivrée ainsi qu'une évaluation de la qualité d'image ont été comparées entre les trois séries d'images à partir d'un test des rangs signés de Wilcoxon.

Les résultats montraient une réduction significative de la dose des scanners abdomino-pelviens de 49,5 % après l'implantation des reconstructions itératives AIDR 3D (moyenne des PDL de 451 mGy.cm contre 892 mGy.cm, $p < 0,001$). Aucune différence significative n'était observée entre les séries FBP dose standard et AIDR 3D basse-dose concernant l'évaluation de la qualité d'image (score de qualité d'image de respectivement 4,6 ± 0,6 versus 4,4 ± 0,6 avec $p = 0,147$).

Article 4 : Scanner basse dose avec la modulation automatique du milliampérage, les reconstructions Adaptive Statistical Iterative Reduction et un faible kilovoltage pour le diagnostic des coliques néphrétiques : impact de l'indice de masse corporelle.

Le mA correspond à l'intensité du courant du tube radiogène et représente la quantité de photons produite au sein du faisceau de rayons X. Le mA est proportionnel à la dose délivrée et inversement proportionnel au carré du bruit de l'image [30]. L'optimisation du mA doit prendre en compte le morphotype du patient. En effet, la quantité de photons X nécessaire pour garder une qualité de l'image constante est variable en fonction de l'épaisseur du patient. Pour mieux adapter le mA au morphotype des patients, des techniques de modulation automatique du mA ont été développés au début des années 2000 [31]. Grâce à ces techniques, le mA est automatiquement adapté au morphotype du patient et à la zone anatomique à explorer et le bruit de l'image reste constant sur l'ensemble des images de l'acquisition. Par

ailleurs, ces techniques ont permis de réduire les doses délivrées. Leur impact sur la performance diagnostique en fonction du morphotype des patients reste encore à étudier.

L'objectif de notre étude était d'évaluer l'impact du morphotype des patients sur la dose, la qualité d'image et la performance diagnostique de notre protocole de scanner basse dose sans injection réalisé avec un faible kilovoltage, la modulation automatique du mA et ASIR chez des patients avec une suspicion clinique de colique néphrétique.

Il s'agissait d'une étude rétrospective monocentrique incluant l'ensemble des patients adressés dans le service d'imagerie de l'HIA Legouest durant l'année 2012 pour la recherche d'une colique néphrétique et ayant eu un scanner sans injection selon notre protocole basse dose avec les reconstructions itératives ASIR, un faible kilovoltage et la modulation automatique du mA. Les images du scanner basse dose ont été analysées par deux radiologues et une interne en radiologie qui ont évalué la présence d'une colique néphrétique, la confiance dans le diagnostic et la qualité d'image. Ces résultats ainsi que les doses délivrées ont été comparés chez des patients avec des catégories d'Indice de Masse Corporelle (IMC) différents.

Les résultats montraient qu'il n'y avait pas de différence statistiquement significative de performance diagnostique entre le groupe de patients avec un IMC < 25 kg/m² et les patients avec un IMC > 25 kg/m². Par contre, les scores de qualité d'image et de confiance dans le diagnostic étaient significativement meilleurs chez les patients avec un IMC > 25 kg/m² par rapport aux patients avec un IMC < 25 kg/m² (respectivement 3,7 versus 3,4 avec $p < 0,001$ et 2,8 versus 2,5 avec $p < 0,001$). La dose efficace moyenne des scanners était également supérieure pour les patients avec un IMC > 25 kg/m² comparativement aux patients avec un IMC < 25 kg/m² (3,7 mSv versus 2,4 mSv).

Chapitre 3

Article 1 : *Réduction de dose dans l'exploration du rachis lombaire grâce au scanner 320-détecteurs : étude initiale.*

Gervaise A**,** Louis M, Batch T, Loeuille D, Noel A, Guillemin F, Blum A. Réduction de dose dans l'exploration du rachis lombaire grâce au scanner 320-détecteurs : étude initiale. *J Radiol* 2010;91: 779-85.

J Radiol 2010;91:779-85

Réduction de dose dans l'exploration du rachis lombaire grâce au scanner 320-détecteurs : étude initiale

A Gervaise (1), M Louis (1), T Batch (1), D Loeuille (2), A Noel (3), F Guillemin (4) et A Blum (1)

Abstract

Dose reduction at CT of the lumbar spine using a 320-detector row scanner: initial results
J Radiol 2010;91:779-85

Purpose. To compare radiation dose and image quality for CT of the lumbar spine between helical CT and wide volume mode scanning with a 320-detector row CT.
Patients and methods. Monocenter prospective study on 20 consecutive patients divided into two groups. All 20 patients underwent lumbar spine CT on the 320-detector row scanner (Aquilion One, Toshiba). The CT examinations for group 1 were performed using the wide volume mode with 320 detector rows while the CT examinations for group 2 were performed using a 64-detector row helical CT mode. The acquisition length and delivered dose corresponding to the DLPe (extended dose length product) as well as qualitative and quantitative image quality were compared between both groups.
Results. The mean acquisition length was comparable between both groups. There was a significant dose reduction of about 35% for group 1 compared to group 2 (mean DLPe of 970 mGy.cm for group 1 compared to 1503 mGy.cm for group 2, p<0.028) when using the wide volume mode acquisition at 320-detector row CT compared to the 64-detector row helical CT mode. No significant difference was noted for image quality between both groups.
Conclusion. The acquisition of lumbar CT using the wide volume mode at 320-detector row CT allows significant dose reduction to patients compared to the 64-detector row helical CT mode while preserving image quality.

Key words: CT. 320-detector row. Dose. Reduction. Lumbar spine.

Résumé

Objectif. Comparer la dose délivrée et la qualité d'image entre un scanner lombaire réalisé en mode hélicoïdal et en mode Wide volume grâce au scanner 320-détecteurs.
Patients et méthodes. Il s'agit d'une étude monocentrique prospective incluant 20 patients consécutifs répartis en deux groupes. Les 20 patients ont bénéficié d'un scanner lombaire sur le scanner 320-détecteurs (Aquilion One, Toshiba). Les scanners lombaires du groupe 1 ont été réalisés en mode Wide volume 320-détecteurs et ceux du groupe 2 en mode hélicoïdal 64-détecteurs. La longueur d'acquisition, la dose délivrée correspondant au PDL. e (Produit Dose Longueur. étendu) ainsi qu'une évaluation quantitative et qualitative de l'image ont été comparées entre les deux groupes.
Résultats. Les moyennes de longueur d'acquisition étaient comparables entre les deux groupes. Il existait une réduction significative de la dose délivrée d'environ 35 % (moyenne des PDL. e de 970 mGy. cm pour le groupe 1 contre 1 503 mGy. cm pour le groupe 2, p < 0,028) avec le mode Wide volume 320-détecteurs par rapport au mode hélicoïdal 64-détecteurs. Aucune différence significative n'était observée entre les deux techniques concernant l'évaluation de la qualité de l'image.
Conclusion. L'acquisition d'un scanner lombaire en mode Wide volume sur le scanner 320-détecteurs permet de réduire significativement la dose délivrée au patient par rapport à l'acquisition hélicoïdale 64-détecteurs, tout en préservant une qualité d'image équivalente.

Mots-clés : Scanner. 320-détecteurs. Dose. Réduction. Rachis lombaire.

Les lombo-radiculalgies sont un problème majeur de santé publique (1). En France, plus de 70 % des travailleurs ont déjà présenté un épisode de lombalgie et un tiers de ces 70 % a déjà eu un arrêt de travail en rapport à cette symptomatologie (2). De nombreuses explorations radiologiques sont réalisées dans le cadre du bilan de ces douleurs. Tandis que la sensibilité et la spécificité du scanner et de l'imagerie par résonance magnétique sont équivalentes pour la recherche d'un conflit disco-radiculaire (3), cette dernière souffre d'un manque de disponibilité et d'un coût plus élevé. Son utilisation est également limitée par certaines contre-indications (obésité, claustrophobie, pacemaker) et par une reproductibilité interobservateur modérée voire faible, notamment pour l'étude des articulations interapophysaires et des sténoses canalaires ou foraminales (4-7). Cela explique en partie que le scanner lombaire reste l'un des examens scanographiques les plus pratiqués en France (8). Pourtant, le scanner est une technique irradiante. Le lien entre un éventuel risque cancérigène et l'exposition à des faibles doses de rayons X reste très controversé (9-11) et fait l'objet de nombreuses publications (12-17). La réduction de la dose délivrée au patient doit donc être une préoccupation constante du radiologue, en accord avec le principe de précaution ALARA (As Low As Reasonably Achievable). Cela est d'autant plus vrai dans l'exploration scanographique du rachis lombaire qui concerne principalement des patients jeunes (18, 19) et susceptibles de recourir à des examens scanographiques répétés (20).

C'est dans ce contexte que le scanner 320-détecteurs semble pouvoir réduire la dose délivrée au patient par rapport aux scanners hélicoïdaux classiques. Ce nouveau type de scanner bénéficie d'un large système de détection capable d'obtenir en une seule rotation de 0,35 s un volume de 160 mm dans l'axe z. Cette caractéristique technique unique permet de réduire considérablement le temps d'acquisition, donc les artefacts de mouvements, tout en étant capable de couvrir des organes entiers. Ce mode

(1) Service d'Imagerie Guilloz, Hôpital Central, CHU Nancy, 29 avenue du Maréchal de Lattre de Tassigny, 54035 Nancy cedex. (2) Service de Rhumatologie, Hôpital de Brabois, CHU Nancy, allée du Morvan, 54511 Vandœuvre-lès-Nancy. (3) Unité de radiophysique médicale, CRAN UMR 7039 Nancy Université-CNRS, Centre Alexis Vautrin, avenue de Bourgogne, 54511 Vandœuvre-lès-Nancy. (4) Inserm CIC-EC, épidémiologie et évaluation cliniques, CHU de Nancy, 54511 Vandœuvre-lès-Nancy.
Correspondance : A Gervaise
E-mail : alban.gervaise@hotmail.fr

« volumique » est ainsi largement utilisé dans le domaine de l'imagerie cardiaque (21, 22) et vasculaire (23), pour l'étude de la perfusion cérébrale (24) ou d'organes abdominaux (25) et a également trouvé ses indications en imagerie pédiatrique (26). Dans toutes ces applications, il a été montré une réduction significative de la dose délivrée pouvant atteindre 75 % (21). La juxtaposition de plusieurs volumes permet également l'exploration de zones anatomiques plus étendues. Ce nouveau mode d'acquisition, qui est l'équivalent d'un mode « incrémental volumique », est appelé mode Wide volume ou « Stitching mode » et permet de couvrir le rachis lombaire grâce à la juxtaposition de deux volumes. Dans leur protocole de bilan de douleur thoracique, Hein *et al.* (27) ont montré que la triple acquisition thoracique et cardiaque en mode volumique et Wide volume 320-détecteurs était accompagnée d'une réduction de dose d'environ 55 %. À notre connaissance, aucune étude n'a encore évalué cette réduction pour l'acquisition d'un scanner lombaire en mode Wide volume. Le scanner 320-détecteurs possède un autre avantage : grâce à la désactivation d'un certain nombre de détecteurs, il peut fonctionner comme un scanner hélicoïdal (avec 64-canaux de détection et prochainement 160). Il est ainsi possible de comparer sur la même machine la dose délivrée pour l'acquisition d'un scanner lombaire en mode Wide volume 320-détecteurs versus hélicoïdal 64-détecteurs.

L'objectif de cette étude est donc de mesurer la réduction de la dose délivrée au patient lors de la réalisation d'un scanner lombaire entre une acquisition en mode Wide volume 320-détecteurs et hélicoïdal 64-détecteurs tout en comparant la qualité d'image afin de s'assurer qu'une réduction de dose ne s'accompagne pas d'une altération de la qualité d'image.

Patients et méthodes

Population étudiée

Il s'agit d'une étude monocentrique prospective incluant 20 patients consécutifs entre février et mars 2009. Les 10 premiers patients ont bénéficié d'un scanner lombaire en mode Wide volume 320-détecteurs (groupe 1) et les 10 suivants en mode hélicoïdal 64-détecteurs (groupe 2). Seuls les patients de plus de 45 ans ont été inclus. Pour chaque patient, l'âge et l'indice de masse corporelle (IMC) étaient notés.

Technique d'acquisition

Un scanner lombaire sans injection a été réalisé chez tous les patients sur le même scanner 320-détecteurs (Aquilion ONE, Toshiba Medical Systems, Otawara, Japon). Les patients étaient positionnés en décubitus dorsal, pieds les premiers. L'acquisition débutait par la réalisation d'un topogramme de face et de profil. Celui-ci permettait de repérer la zone à explorer et d'utiliser la modulation automatique de la dose dans les 3 plans de l'espace (x, y et z) afin d'adapter les paramètres d'acquisition à la corpulence de chaque patient pour obtenir un niveau de qualité d'image déterminé.

Dans le groupe 1, le scanner était réalisé en mode Wide volume 320-détecteurs grâce à 2 volumes couvrant T12 à S2 dont la séparation se faisait à hauteur des crêtes iliaques (135 kV, modulation automatique des milliAmpère (mA) dans les 3 plans (maximum 500 mA et minimum 100 mA) avec pour référence un indice de bruit (IB) à 7,5 pour une coupe de 5 mm avec un filtre standard mou, temps de rotation (TR) à 0,75 s, 320 × 0,5 mm avec reconstruction en coupe axiale de 1 mm tout les 1 mm, filtre de reconstruction FC 08).

Dans le groupe 2, le scanner était réalisé de T12 à S2 en mode hélicoïdal 64-détecteurs (135 kV, modulation automatique des mA dans les 3 plans (maximum 500 mA et minimum 100 mA) avec pour référence un IB à 6 pour une coupe de 5 mm avec un filtre standard mou, pitch à 0,641, TR à 0,75 s, 64 × 0,5 mm avec reconstruction en coupe axiale de 1 mm tout les 1 mm, filtre de reconstruction FC 08).

Après avoir été automatiquement envoyés dans le PACS, les images et le rapport de dose du scanner étaient accessibles à partir d'une station de travail IMPAX V5 (Agfa, Ridgefield Park, NJ, USA).

Évaluation de la longueur d'acquisition

La longueur d'acquisition était exprimée en cm et correspondait à la différence de position entre la première et la dernière image de l'acquisition.

Évaluation de la dose délivrée

La dose délivrée était directement fournie par le rapport d'examen. Elle correspondait au PDL.e (Produit Dose Longueur. étendu) exprimé en mGy.cm (le terme « étendu » est lié à la nécessité d'extrapoler les valeurs de PDL à partir des relevés de dosimétrie classique compte tenu de la largeur importante du système de détection du scanner 320-détecteurs). Les valeurs de PDL.e relevées dans le groupe Wide volume étaient en accord avec la formule décrite pour les scanners volumiques dynamiques (28) : $PDL.e = CTDI_{vol}.e \times BW_{nom}$ avec $CTDI_{vol}.e = CTDI_{w}.e \times R$ où le $CTDI_{vol}.e$ est l'index de dose scanographique volumique étendu (Computed Tomographic Dose Index volume. extended), BW_{nom} est la largeur de faisceau nominal (Beam Width), le $CTDI_{w}.e$ est le CTDI pondéré étendu et R est le nombre de rotations.

Évaluation de la qualité d'image

La qualité d'image a été évaluée de manière quantitative par la mesure du bruit de l'image. Celui-ci était estimé à partir de la déviation standard (en Unité Hounsfield) d'une région d'intérêt (ROI) de 1 cm^2 placée dans le muscle psoas droit, sur une coupe axiale de 1 mm en fenêtre parenchymateuse, à hauteur des pédicules de L5. Les ROI ont été placées chez les 20 patients sur une console IMPAX par le même radiologue.

L'évaluation qualitative a été réalisée sur les coupes axiales natives de 1 mm en fenêtre parenchymateuse à partir d'une échelle de score allant de 0 à 4 (0 = qualité d'image médiocre ne permettant pas une interprétation ; 1 = mauvaise qualité de l'image interférant avec la qualité diagnostique de l'examen ; 2 = image de qualité moyenne ; 3 = bonne qualité de l'image ; 4 = excellente qualité de l'image). Cette évaluation a été réalisée indépendamment par 3 radiologues, après une séance de lecture commune, sur des consoles IMPAX, après anonymisation et en l'absence d'affichage des paramètres d'acquisition.

Analyse statistique

Compte tenu du faible effectif de patients inclus, un test des rangs signés de Wilcoxon était utilisé pour comparer les valeurs de longueur d'acquisition, de PDL.e et de qualité d'image entre les deux groupes. Une valeur de p inférieure à 0,05 était considérée comme significative.

Résultats

La moyenne d'âge et l'IMC moyen du groupe 1 étaient de respectivement 65,1 ans (de 53 à 88 ans) et 28,3 kg/m^2 (de

19,1 à 46,5 kg/m^2) contre 61,4 ans (de 46 à 74 ans) et 27,8 kg/m^2 (de 20,2 à 33,8 kg/m^2) pour le groupe 2.

Les longueurs d'acquisition étaient comparables entre les 2 groupes. Il existait une différence significative entre les PDL.e du groupe 1 et du groupe 2 *(tableau I)* avec une réduction de 35 % de la dose délivrée en mode Wide volume par rapport au mode hélicoïdal. Aucune différence significative n'était mise en évidence concernant l'évaluation qualitative ou quantitative de la qualité d'image *(tableau II)*.

Discussion

Notre étude confirme que la réalisation d'un scanner lombaire grâce au mode Wide volume 320-détecteurs permet de réduire de façon significative la dose délivrée au patient sans altérer la qualité d'image. Cette réduction peut s'expliquer par trois principales caractéristiques techniques.

Tout d'abord, en mode hélicoïdal, pour s'assurer de l'entièreté des premières et dernières images de l'acquisition, il est nécessaire de faire un tour supplémentaire à chaque extrémité de la zone explorée. Cette exposition « pré et post-hélice », également appelée overranging ou z overscanning, varie proportionnellement en fonction du pitch et du nombre de détecteurs et est inversement proportionnelle à la longueur d'exploration (29, 30). Ce phénomène est visualisé sur la *figure 1*. L'utilisation d'un film radiochromique permet de mettre en évidence une longueur supplémentaire irradiée de 15 mm en début et fin d'hélice pour une même longueur d'acquisition de 160 mm. Dans notre étude, l'overranging en mode hélicoïdal a été estimé à environ 15 % de la dose totale. L'abandon de l'hélice grâce au mode Wide volume supprime ce phénomène d'overranging et permet de réduire d'autant la dose délivrée au patient. Chez les jeunes femmes, cette suppression est bénéfique puisque l'exposition post-hélice d'un scanner lombaire concerne des organes radiosensibles que sont les ovaires. L'installation prochaine sur l'Aquilion One d'une collimation active par bouclier permettra toutefois de réduire de manière importante la part de l'overranging en mode hélicoïdal (sans toutefois pouvoir égaler la réduction induite par la suppression de l'hélice).

Deuxièmement, la réduction de dose s'explique par une moindre importance de l'effet d'overbeaming. Ce dernier correspond au phénomène de pénombre : afin de couvrir l'ensemble des détecteurs avec un rayonnement d'intensité égale, le faisceau de rayons X doit déborder du champ des détecteurs *(fig. 2)*. Cela entraîne une exposition supplémentaire qui ne contribue pas à la formation de l'image mais participe à la dose délivrée au patient (31). L'importance de l'overbeaming diminue proportionnellement avec la largeur du système de détection (32) et est donc proportionnellement moins importante pour un scanner à large système de détection (33). L'efficience de dose (encore appelée z efficiency) informe l'utilisateur sur la proportion de rayonnement qui ne contribue pas à la formation de l'image. Cette valeur dépend principalement de l'épaisseur de coupe, et dans une moindre mesure, de l'effet d'overbeaming. Cependant, l'épaisseur de coupe étant constante entre nos deux modes d'acquisition, l'efficience de dose permet d'évaluer l'effet d'overbeaming. Sa valeur est donc d'autant plus faible que l'effet d'overbeaming, et donc l'exposition non contributive à l'image, augmente. Ainsi, tandis que pour la réalisation d'un volume de 160 mm, l'efficience de dose est d'environ 93 % en mode volumique 320-détecteurs, elle ne dépasse pas 85 % pour le mode hélicoïdal 64-détecteurs. Par ailleurs, l'effet d'overbeaming se répète à chaque rotation du tube. La diminution du nombre de rotations en mode Wide volume (seulement 2 en mode Wide volume contre environ 13 tours d'hélice pour couvrir le

Tableau I
Comparaison des longueurs d'acquisition et des doses délivrées entre les modes Wide volume et hélicoïdal.

	Mode Wide volume	Mode hélicoïdal	Valeur de p
Longueur d'acquisition (cm)	26,23 ± 1,75	26,99 ± 1,33	p > 0,578
PDL. e (mGy. cm)	970,9 ± 359,8	1 503,2 ± 324,1	p < 0,028

Les données correspondent aux moyennes des mesures ± la déviation standard.

Tableau II
Évaluation quantitative et qualitative de la qualité de l'image des scanners lombaires en mode Wide volume et hélicoïdal.

	Mode Wide volume	Mode hélicoïdal	Valeur de p
Évaluation quantitative			
Déviation standard de la ROI (UH)	24,00 ± 6,84	20,90 ± 4,77	p > 0.359
Evaluation qualitative			
Lecteur 1	3,4 ± 0,52	3,6 ± 0,52	p > 0,375
Lecteur 2	3,3 ± 0,67	3,6 ± 0,52	p > 0,437
Lecteur 3	3,4 ± 0,52	3,7 ± 0,48	p > 0,312

Les données correspondent aux moyennes des mesures ± la déviation standard.

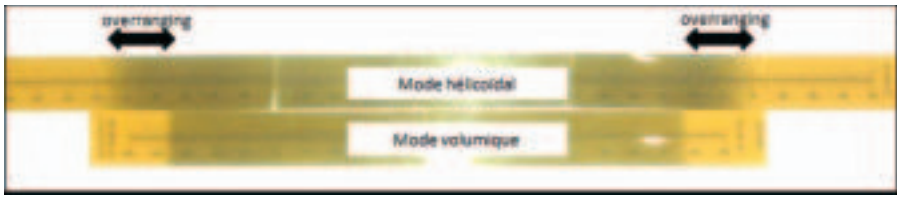

Fig. 1 : **Mise en évidence du phénomène d'overranging à partir d'un papier radiochromique** (en présence de rayons X, la zone irradiée s'assombrit). Deux acquisitions de même longueur sont réalisées en mode hélicoïdal (papier du haut) et volumique (papier du bas). Pour la même longueur d'acquisition, la zone irradiée est plus importante en mode hélicoïdal : cette exposition « pré et post-hélice » correspond à l'overranging (doubles flèches).

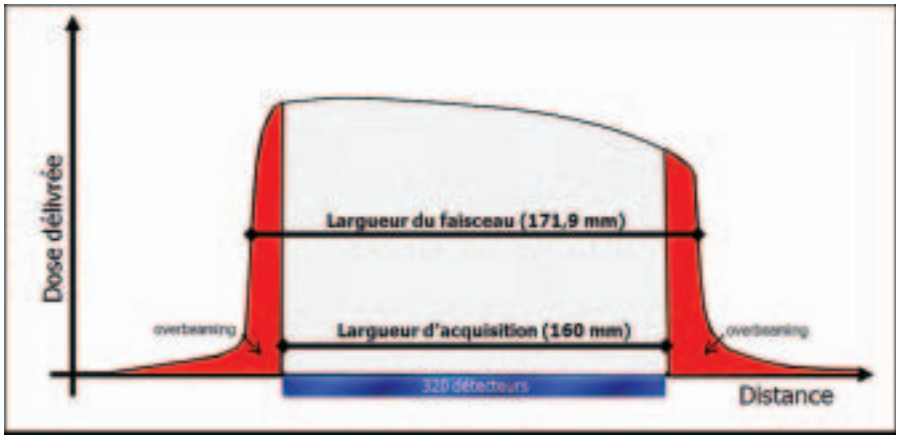

Fig. 2 : **Profil de dose d'un volume de 160 mm : le faisceau déborde du champ des détecteurs.** Ce phénomène correspond à l'overbeaming. Le rapport entre la largeur de la zone explorée (160 mm) et la largeur de la zone irradiée (171,9 mm) correspond à l'efficience de dose (93 % dans cet exemple). Noter également la forme asymétrique du profil de dose due à l'effet talon de l'anode.

rachis lombaire) contribue aussi à réduire l'importance de l'exposition due à l'overbeaming en mode Wide volume.

Enfin, en mode hélicoïdal, le déplacement de la table lors de l'acquisition de l'hélice nécessite une interpolation des données à l'origine d'une dégradation du rapport signal à bruit (RSB) et du profil de coupe (34). En mode Wide volume, comme en mode incrémental conventionnel, il n'y a pas d'interpolation des données qui sont cohérentes puisque les projections sont toutes acquises au même niveau anatomique pour reconstruire une coupe. Cela procure une amélioration du RSB permettant une réduction des paramètres d'exposition. Par contre, la géométrie particulière du faisceau, secondaire à la largeur importante du système de détection en mode Wide volume 320-détecteurs (angle d'ouverture du faisceau de 15,2° contre 3,05° pour le mode hélicoïdal 64-détecteurs), engendre des effets de cône qui nécessite l'utilisation d'un algorithme de reconstruction adapté (ConeXact pour l'Aquilion One) permettant d'éliminer ces artefacts. Cet algorithme de reconstruction est toutefois très performant puisqu'il est possible de reconstruire 640 coupes à partir des 320 coupes natives d'un volume de 160 mm. Cet algorithme de reconstruction « double-coupe » permet donc de disposer de reconstructions chevauchées de 0,5 mm tout les 0,25 mm à l'origine d'une diminution des effets de cône et des artefacts de volume partiel.

Par contre, l'utilisation du mode Wide volume nécessite un chevauchement partiel des volumes afin de s'assurer qu'il n'y a pas de données manquantes. Ce chevauchement entraîne une exposition plus importante à la jonction des deux volumes. Le raccourcissement de cette zone de chevauchement par l'amélioration de l'algorithme de reconstruction est une des solutions pour permettre de réduire cette surexposition.

Le principe de la modulation automatique de la dose est également différent entre les deux modes d'acquisition. Tandis qu'en mode hélicoïdal l'adaptation du milliampérage se fait tout au long de l'hélice et permet de réduire la dose délivrée jusqu'à 33 % (35), une seule valeur de milliampérage est disponible par volume. La modulation automatique de dose pour le scanner lombaire en mode Wide volume ne bénéficie donc que de deux valeurs de milliampérage (une pour chacun des deux volumes). Pour adapter cette modulation binaire à l'acquisition d'un scanner lombaire, nous avons placé les 2 volumes de part et d'autre des crêtes iliaques *(fig. 3)*. Ce placement suit effectivement l'évolution anatomique puisque l'épaisseur du bassin entraîne une atténuation plus importante du faisceau de rayons X nécessitant une augmentation du milliampérage pour garder une qualité d'image optimale. Malgré cette adaptation, on peut supposer que la modulation automatique de la dose est moins efficace en mode Wide volume par rapport au mode hélicoïdal. La comparaison des coefficients de corrélation entre IMC et dose délivrée dans chaque groupe serait intéressante pour estimer l'efficacité de celle-ci. Malheureusement, compte tenu du faible effectif de notre étude, nous n'avons pas réalisé ce calcul.

De plus, cette modulation est à l'origine d'une discrète différence de densité à l'interface des deux volumes due à la différence de milliampérage *(fig. 4)*. A celle-ci

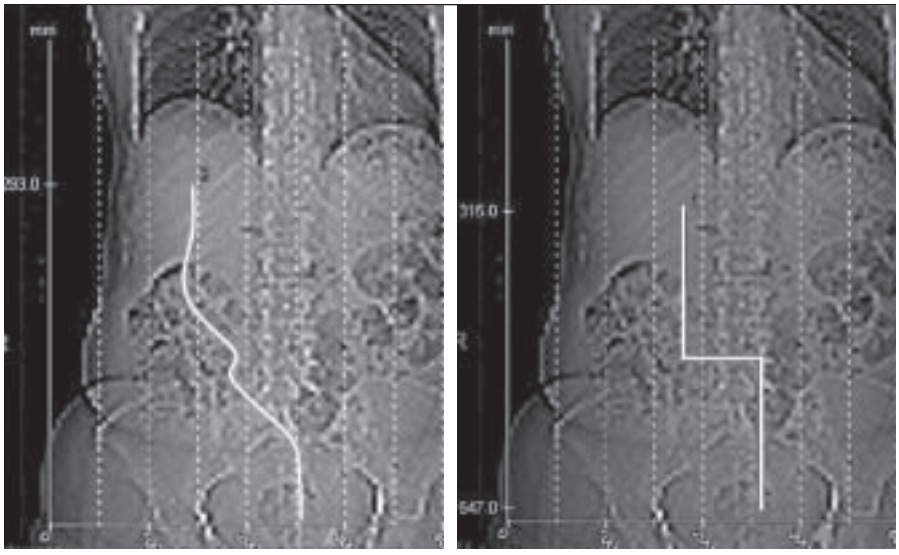

a | b

Fig. 3 : **Modulation du milliampérage en mode hélicoïdal et Wide volume.**

a **En mode hélicoïdal, le milliampérage varie tout au long de l'hélice.** Compte tenu de l'épaisseur du bassin, on note que le milliampérage augmente à partir des crêtes iliaques.

b **En mode Wide volume, chaque volume possède sa propre valeur de milliampérage.** La position des 2 volumes dont la jonction se fait à hauteur des crêtes iliaques permet de rapprocher la courbe de milliampérage du mode Wide volume avec celle du mode hélicoïdal.

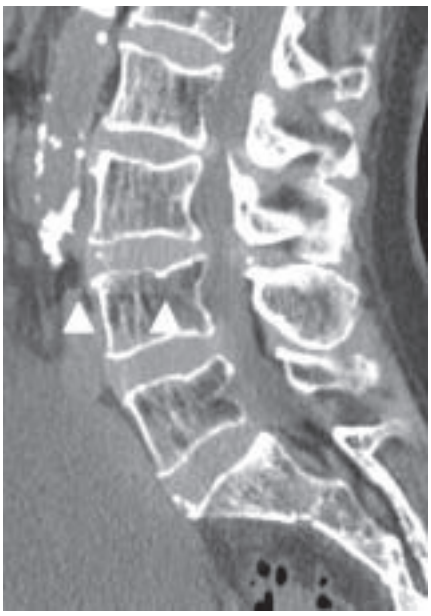

Fig. 4 : **Reconstruction sagittale d'un scanner lombaire en mode Wide volume :** discrète différence de densité entre les deux volumes, due à la différence de milliampérage, à l'origine d'une ligne de démarcation (têtes de flèches).

peut également se rajouter un artefact de décalage entre les deux volumes contigus. Ce décalage est engendré par les mouvements du patient ou les minimes mouvements de table entre les deux acquisitions. Bien que cet artefact soit quelque fois visible sur les reconstructions sagittales ou frontales, il est en fait très peu marqué pour le scanner lombaire compte tenu de la courte durée séparant l'acquisition des deux volumes (1,4 s) et de sa correction lors de la reconstruction des images.

Une autre particularité du scanner 320-détecteurs réside dans le calcul des données de dosimétrie. Classiquement, les paramètres de dosimétrie sont automatiquement transmis par le scanner sous la forme du $CTDI_{vol}$ et du PDL. Le $CTDI_{vol}$ correspond à la dose moyenne pour une coupe en prenant en compte le pas de l'hélice ($CTDI_{vol}$ = $CTDI_w$/Pitch) (30). Le $CTDI_{vol}$ est donc une mesure adaptée à l'acquisition hélicoïdale mais perd sa signification lors de l'utilisation d'un scanner volumique (33). Par ailleurs, les chambres d'ionisation, actuellement utilisées et définies par la législation pour faire les relevés de dosimétrie (36, 37), ont une longueur active de 100 mm. Elles ne sont donc pas adaptées pour mesurer le $CTDI_{vol}$ du scanner 320-détecteurs car il est impossible d'enregistrer l'intégralité du profil de coupe d'un volume de 160 mm à partir de ces chambres d'ionisation. Cela est d'autant plus vrai qu'il faut que la largeur de la chambre d'ionisation prenne également en compte l'overbeaming ainsi que le rayonnement diffusé. Pour Mori *et al.* (38), il faut donc une chambre d'ionisation d'au moins 300 mm pour permettre de mesurer le $CTDI_{vol}$ lors de l'acquisition d'un volume de 160 mm. Toutefois, plusieurs études ont montré qu'il était possible d'extrapoler, grâce à une simulation de Monte Carlo, la valeur du $CTDI_{vol}$ d'un volume de 160 mm à partir des mesures de dosimétrie d'une chambre d'ionisation standard de 100 mm (33, 39). La mesure du $CTDI_{vol}$ peut donc se faire avec le matériel standard mais la nécessité d'utiliser une formule d'extrapolation explique que les données de dosimétrie du scanner 320-détecteurs correspondent au $CTDI_{vol}$. e et au PDL. e (« e » pour « extended » ou étendu). Enfin, le PDL rend compte de la dose délivrée au cours d'une procédure complète (40) et permet d'estimer la dose efficace (41). Le PDL est donc directement en rapport avec le risque stochastique pour le patient et c'est pourquoi nous avons choisi d'utiliser cette valeur pour comparer les doses délivrées entre les deux groupes.

Bien qu'il ne s'agisse pas de l'objectif principal de notre étude, ces relevés de dosimétrie sont l'occasion d'évaluer les doses délivrées pour un scanner lombaire dans notre service. On peut tout de suite remarquer que le scanner lombaire ne fait pas partie des examens soumis aux niveaux de référence diagnostiques (NRD) (42) bien qu'il représente un nombre important d'examens réalisés chaque année. Le rapport 2008 de l'IRSN (8), portant sur la mise à jour des NRD, propose d'ailleurs que le scanner lombaire figure parmi les régions anatomiques concernées par ce recueil des données dosimétriques. Par rapport aux données de la littérature, on peut également observer que les doses délivrées pour la réalisation d'un scanner lombaire sont très variables, allant de 3 à 19 mSv (16, 43-48). Ces valeurs correspondent aux doses efficaces exprimées en milliSievert (mSv). Dans notre étude, les doses efficaces étaient de 14 mSv pour le groupe 1 et 22,5 mSv pour le groupe 2 (la dose efficace (E) est calculée en utilisant le coefficient de conversion tissulaire (k) de l'abdomen à 0,015 selon la formule E = PDL. e × k (49)). Cette disparité tient d'abord au fait que certaines études prennent en compte les doses délivrées sur des fantômes (43). Ces doses ne sont donc pas comparables à celles de population dont le morphotype n'est pas « standard ». Ainsi, dans notre étude, seulement 4 patients du groupe 1 et 3 du groupe 2 avaient un IMC compris entre 18 et 25, or l'augmentation de la corpulence nécessite une majoration des doses délivrées afin de garantir une qualité d'image équivalente. De plus, les longueurs d'acquisition sont souvent différentes. Tandis que la longueur d'exploration du rachis lombaire n'excède pas 7 cm dans certaines études (44), notre longueur d'acquisition moyenne était de 26 cm. Notre choix est critiquable mais est lié à la volonté de couvrir systématiquement la jonction dorso-lombaire afin de permettre la recherche d'éventuels signes de spondylarthropathie ou de faire le bilan d'un canal lombaire étroit. On peut d'ailleurs remarquer l'intérêt de l'utilisation du mode Wide volume : tandis que les doses en mode hélicoïdal sont supérieures à la dose moyenne de 19 mSv de l'étude de Biswas et al (46), l'utilisation du mode Wide volume permet de réduire ces doses sous cette moyenne tout en gardant une longueur d'exploration importante.

Notre étude comporte plusieurs limites. La première réside dans le faible effectif de patients inclus et dans l'absence de randomisation des patients entre les deux groupes. Ainsi, même si la différence de dose est significative, une étude randomisée avec un effectif plus grand est nécessaire pour confirmer l'absence de différence significative en terme de qualité d'image. Deuxièmement, nos critères d'évaluation de la qualité d'image sont également discutables. Pour l'évaluation quantitative, nous avons opté pour la mesure du bruit de l'image à partir de la déviation standard d'une ROI, comme cela a déjà été décrit par plusieurs auteurs (50, 51). Toutefois, le bruit de l'image n'est pas un critère suffisant et d'autres critères, plus difficilement analysables, participent également à appréhender la qualité d'image (comme le contraste par exemple ou encore la différence de signal rapportée au bruit) (52). L'évaluation qualitative d'une image n'est pas non plus une méthode très robuste d'autant plus que notre évaluation n'a pu se faire qu'à partir des coupes axiales. En effet, sur les reconstructions sagittales ou frontales, les possibles artefacts à la jonction des deux volumes risquaient d'informer le lecteur du groupe auquel appartenait le patient. Pourtant,

la qualité des reconstructions, notamment sagittales, serait également un élément de comparaison intéressant à prendre en compte pour l'évaluation de la qualité d'image entre les deux groupes. Troisièmement, notre étude a été réalisée sur le même scanner. Il serait intéressant d'évaluer la dose délivrée pour un scanner lombaire sur des scanners hélicoïdaux comportant un nombre différent de détecteurs (par exemple, un scanner 16-détecteurs) ou sur des machines de constructeurs différents. Enfin, il existe quelques différences de paramétrage entre les deux modes d'acquisition. Ainsi, l'absence de pitch en mode Wide volume (en l'absence de mouvement de la table lors de l'acquisition des données, il n'y a pas de pitch) peut faire discuter l'influence de sa valeur en mode hélicoïdal. On peut également noter que l'on a utilisé des indices de bruit légèrement différents entre le groupe 1 (IB à 7,5) et le groupe 2 (IB à 6). Cette différence, liée au réglage « empirique » de la qualité d'image, est toutefois faible et ne semble pas pouvoir expliquer l'écart significatif de dose entre les deux groupes. Par contre, notre protocole ne comporte pas d'adaptation du kilo-Voltage en fonction du poids du patient. Ce paramètre était constant dans notre étude afin de rendre les deux protocoles d'examens comparables (cela explique le faible effectif de notre étude et l'inclusion de patients âgés de plus de 45 ans). Toutefois, en pratique courante, pour optimiser la réduction de la dose délivrée au patient, le kilo-Voltage devrait être adapté en fonction du morphotype du patient, en accord avec le principe ALARA (53).

Conclusion

En conclusion, notre étude confirme que l'acquisition d'un scanner lombaire en mode Wide volume 320-détecteurs permet de réduire significativement la dose délivrée au patient par rapport à l'acquisition hélicoïdale 64-détecteurs. Le mode Wide volume 320-détecteurs a donc remplacé dans notre service le protocole hélicoïdal standard des scanners lombaires. D'autres études doivent être menées pour évaluer l'intérêt de ce nouveau mode d'acquisition dans la réduction de la dose délivrée au patient, notamment dans le cadre des explorations thoraciques ou abdomino-pelviennes.

Conflits d'intérêt

Aucun.

Références

1. Valat JP. Epidémiologie des lombalgies. Rev Rhum 1998;65:172-4.
2. Gepner P. Lombalgies, aspects socio-économiques, épidémiologiques et médicolégaux. Rev Rhum 1994;61:5-7.
3. Boos N, Lander PH. Clinical efficacy of imaging modalities in the diagnosis of low-back pain disorders. Eur Spine J 1996;5:2-22.
4. Stieber J, Quirno M, Cunningham M, Errico TJ, Bendo JA. The reliability of computed tomography and magnetic resonance imaging grading of lumbar facet arthropathy in total disc replacement patients. Spine 2009;34:833-40.
5. Lurie JD, Tosteson AN, Tosteson TD et al. Reliability of readings of magnetic resonance imaging features of lumbar spinal stenosis. Spine 2008;33:1605-10.
6. Carrino JA, Lurie JD, Tosteson AN et al. Lumbar spine: reliability of MR imaging findings. Radiology 2009;250:161-70.
7. Arana E, Royuela A, Kovacs FM et al. Lumbar spine: agreement in the interpretation of 1.5-T MR images by using the Nordic Modic Consensus Group Classification Form. Radiology 2010;254:809-17.
8. Talbot A. Analyse des données relatives à la mise à jour des niveaux de référence diagnostiques en radiologie et en médecine nucléaire. Rapport DRPH n°2008-02, Institut de Radioprotection et de Sûreté Nucléaire. 2008, 126 p.
9. Tubiana, M, Aurengo A, Averbeck A. La relation dose-effet et l'estimation des effets cancérogènes des faibles doses de rayonnements ionisants. Académie Nationale de Médicine, Institut de France–Académie des Sciences, Paris, 2005.
10. Tubiana M, Feinendegen LE, Yang C, Kaminski JM. The linear no-threshold relationship is inconsistent with radiation biologic and experimental data. Radiology 2009;251:13-22.
11. Land CE. Low-dose extrapolation of radiation health risks : some implications of uncertainty for radiation protection at low doses. Health Phys 2009:97:407-15.
12. Brenner DJ, Doll R, Goodhead DT et al. Cancer risks attributable to low doses of ionizing radiation: assessing what we really know. Proc Natl Acad Sci USA 2003;100:13761-6.
13. Board of Radiation Effects Research Division on Earth and Life Sciences National Research Council of the National Academies. Health Risks From Exposure to Low Levels of Ionizing Radiation: BEIR VII Phase 2. Washington, DC: National Academies Press; 2006.
14. Smith-Bindman R, Lipson J, Marcus R et al. Radiation dose associated with common computed tomography examinations and the associated lifetime attributable risk of cancer. Arch Intern Med 2009;169:2078-86.
15. Berrington de González A, Mahesh M, Kim KP et al. Projected cancer risks from computed tomography scans performed in the United States in 2007. Arch Intern Med 2009;169:2071-7.
16. Richards PJ, George J, Metelko M, Brown M. Spine Computed Tomography Doses and Cancer Induction. Spine 2010;35:430-3.
17. Little MP, Wakeford R, Tawn EJ, Bouffler SD, Berrington de Gonzalez A. Risks associated with low doses and low dose rates of ionizing radiation: why linearity may be (almost) the best we can do. Radiology 2009;251:6-12.
18. Spangfort EV. The lumbar disc herniation: a computer-aided analysis of 2,504 operations. Acta Orthop Scand Suppl 1972;142:1-95.
19. Hourcade S, Treves R. Etude rétrospective concernant le scanner lombaire dans les lombalgies et lombosciatiques dans le département de le Haute-Vienne, à propos de 132 cas. Rev Rhum 2002;69:589-96.
20. Sodickson A, Baeyens PF, Andriole KP et al. Recurrent CT, cumulative radiation exposure, and associated radiation-induced cancer risks from CT of adults. Radiology 2009;251:175-84.
21. Pasricha SS, Nandurkar D, Seneviratne SK et al. Image quality of coronary 320-MDCT in patients with atrial fibrillation: initial experience. Am J Roentgenol 2009;193:1514-21.
22. Torres FS, Crean AM, Nguyen ET et al. Abolition of respiratory-motion artifact in computed tomography coronary angiography with ultrafast examinations: a comparison between 64-row and 320-row multidetector scanners. Can Assoc Radiol J 2010;61:5-12.
23. Brouwer PA, Bosman T, van Walderveen MA, Krings T, Leroux AA, Willems PW. Dynamic 320-section CT angiography in cranial arteriovenous shunting lesions. AJNR Am J Neuroradiol 2010;31:767-70.
24. Page M, Nandurkar D, Crossett MP et al. Comparison of 4 cm Z-axis and 16 cm Z-axis multidetector CT perfusion. Eur Radiol 2010;20:1508-14.
25. Kandel S, Kloeters C, Meyer H, Hein P, Hilbig A, Rogalla P. Whole-organ perfusion of the pancreas using dynamic volume CT in patients with primary pancreas carcinoma: acquisition technique, post-processing and initial results. Eur Radiol 2009;19:2641-6.

26. Kroft LJ, Roelofs JJ, Geleijns J. Scan time and patient dose for thoracic imaging in neonates and small children using axial volumetric 320-detector row CT compared to helical 64-, 32-, and 16- detector row CT acquisitions. Pediatr Radiol 2009;40:294-300.
27. Hein PA, Romano VC, Lembcke A, May J, Rogalla P. Initial experience with a chest pain protocol using 320-slice volume MDCT. Eur Radiol 2009;19:1148-55.
28. International Electrotechnical Commission (IEC). Medical electrical equipment – Part 2-44: Particular requirements for the basic safety and essential performance of X-ray equipment for computed tomography, International Standard. Genève, Suisse : IEC 60601-2-44, 2009.
29. Tsedakis A, Damilakis J, Perisinakis K, Stratakis J, Gourtsoyiannis N. The effect of z overscanning on patient effective dose from multidectector helical computed tomography examinations. Med Phys 2005;32:1621-9.
30. van der Molen AJ, Geleijns J. Overranging in multisection CT : quantification and relative contribution to dose - comparison of four 16-section CT scanners. Radiology 2007;242:208-16.
31. Cordoliani YS, Boyer B, Le Marec E, Jouan E, Hélie O, Beauvais H. Vademecum du scanner hélicoïdal : estimation des doses, choix des paramètres. J Radiol 2002;83:685-92.
32. Perisinakis K, Papadakis AE, Damilakis J. The effect of x-ray beam quality and geometry on radiation utilization efficiency in multidetector CT imaging. Med Phys 2009;36:1258-66.
33. Mori S, Nishizawa K, Kondo C, Ohno M, Akahane K, Endo M. Effective doses in subjects undergoing computed tomography cardiac imaging with the 256-multislice CT scanner. Eur J Radiol 2008; 65:442-8.
34. Blum A. Scanographie volumique multicoupe. Paris : Masson, 2002. pp 39-62.
35. Kalra KM, Maher MM, Toth TL, Kamath RS, Halpern EF, Saini S. Comparison of Z-axis automatic tube current modulation technique with fixed tube current CT scanning of abdomen and pelvis. Radiology 2004;232:347-53.
36. Décision du 22 novembre 2007 fixant les modalités du contrôle de qualité des scanographes. Journal Officiel de la République Française, 7 décembre 2007.
37. Commission européenne. European guidelines on quality criteria for computed tomography. Publication EUR 16262 EN. Bruxelles, Belgique : Commission européenne, 2000.
38. Mori S, Endo M, Nishizawa K et al. Enlarged longitudinal dose profiles in cone-beam CT and the need for modified dosimetry. Med Phys 2005;32:1061-9.
39. Geleijns J, Salvadó Artells M, de Bruin PW, Matter R, Muramatsu Y, McNitt-Gray MF. Computed tomography dose assessment for a 160 mm wide, 320 detector row, cone beam CT scanner. Phys Med Biol 2009;54:3141-59.
40. Task Group on Control of Radiation Dose in Computed Tomography. Managing patient dose in computed tomography: a report of the International Commission on Radiological Protection. Ann ICRP 2000;30:7-45.
41. Huda W, Ogden KM, Khorasani MR. Converting dose-length product to effective dose at CT. Radiology 2008;248:995-1003.
42. Arrêté du 12 février 2004 relatif aux niveaux de référence diagnostiques en radiologie et médecine nucléaire. Journal Officiel de la République Française, 16 mars 2004.
43. Blum A, Noel A, Winninger D et al. Dose optimization and reduction in CT of the musculoskeletal system including the spine. In: Tack D, Genevois PA, Radiation Dose from Pediatric and Adult Multidetector Computed Tomography. Springer-Verlag eds 2007. pp 185-194.
44. Calzado A, Rodríguez R, Muñoz A. Quality criteria implementation for brain and lumbar spine CT examinations. Br J Radiol 2000;73:384-95.
45. Ngaile JE, Msaki P, Kazema R. Towards establishment of the national reference dose levels from computed tomography examinations in Tanzania. J Radiol Prot 2006;26:213-25.
46. Biswas D, Bible JE, Bohan M, Simpson AK, Whang PG, Grauer JN. Radiation exposure from musculoskeletal computerized tomographic scans. J Bone Joint Surg Am 2009;91:1882-9.
47. Fazel R, Krumholz HM, Wang Y et al. Exposure to low-dose ionizing radiation from medical imaging procedures. N Engl J Med 2009;361:849-57.
48. Heggie JC. Patient doses in multi-slice CT and the importance of optimisation. Australas Phys Eng Sci Med 2005;28:86-96.
49. International Commission on Radiological Protection. 2007 recommendations of the International Commission on Radiological Protection (ICRP Publication 103). Ann ICRP 2007;37:1-332.
50. Wintermark M, Maeder P, Verdun FR et al. Using 80 kVp versus 120 kVp in perfusion CT measurement of regional cerebral blood flow. AJNR Am J Neuroradiol 2000;21:1881-4.
51. Smith AB, Dillon WP, Lau BC et al. Radiation dose reduction strategy for CT protocols: successful implementation in neuroradiology section. Radiology 2008; 247:499-506.
52. Zarb F, Rainford L, McEntee MF. Image quality assessment tools for optimization of CT images. Radiography 2010;16:91-168.
53. McCollough C, Primak AN, Braun N, Kofler J, Yu L, Christner J. Strategies for reducing radiation dose in CT. Radiol Clin North Am 2009;47:27-40.

Chapitre 3

Article 2 : *Amélioration de la qualité d'image scanographique en utilisant les reconstructions itératives Adaptive Iterative Dose Reduction avec une acquisition wide-volume sur un scanner 320-détecteurs.*

Gervaise A, Osemont B, Lecocq S, Micard E, Noel A, Felblinger J, Blum A. CT image quality improvement using adaptive iterative dose reduction with wide-volume acquisition on 320-detector CT. *Eur Radiol* 2012; 22: 295-301.

Eur Radiol
DOI 10.1007/s00330-011-2271-7

COMPUTED TOMOGRAPHY

CT image quality improvement using adaptive iterative dose reduction with wide-volume acquisition on 320-detector CT

Alban Gervaise · Benoît Osemont · Sophie Lecocq · Alain Noel · Emilien Micard · Jacques Felblinger · Alain Blum

Received: 14 July 2011 / Revised: 25 August 2011 / Accepted: 31 August 2011

Abstract
Objectives To evaluate the impact of Adaptive Iterative Dose Reduction (AIDR) on image quality and radiation dose in phantom and patient studies.
Methods A phantom was examined in volumetric mode on a 320-detector CT at different tube currents from 25 to 550 mAs. CT images were reconstructed with AIDR and with Filtered Back Projection (FBP) reconstruction algorithm. Image noise, Contrast-to-Noise Ratio (CNR), Signal-to-Noise Ratio (SNR) and spatial resolution were compared between FBP and AIDR images. AIDR was then tested on 15 CT examinations of the lumbar spine in a prospective study. Again, FBP and AIDR images were compared. Image noise and SNR were analysed using a Wilcoxon signed-rank test.
Results In the phantom, spatial resolution assessment showed no significant difference between FBP and AIDR reconstructions. Image noise was lower with AIDR than with FBP images with a mean reduction of 40%. CNR and SNR were also improved with AIDR. In patients, quantitative and subjective evaluation showed that image noise was significantly lower with AIDR than with FBP. SNR was also greater with AIDR than with FBP.
Conclusion Compared to traditional FBP reconstruction techniques, AIDR significantly improves image quality and has the potential to decrease radiation dose.
Key Points
- *This study showed that Adaptive Iterative Dose Reduction (AIDR) reduces image noise.*
- *In a phantom image noise was reduced without altering spatial resolution.*
- *In patients AIDR reduced the image noise in lumbar spine CT.*
- *AIDR can potentially reduce the dose for lumbar spine CT by 52%.*

Keywords Computed tomography · Multidetector CT · Dose reduction · Image quality · Iterative reconstruction · Lumbar spine

A. Gervaise (✉)
Service d'Imagerie Médicale,
Hôpital d'Instruction des Armées Legouest,
27 Avenue de Plantières,
57070 Metz, France
e-mail: alban.gervaise@hotmail.fr

A. Gervaise · B. Osemont · S. Lecocq · A. Blum
Service d'Imagerie Guilloz, CHU NANCY,
29 avenue de Lattre de Tassigny,
54035 Nancy, France

A. Noel
CRAN UMR CNRS 7039, Centre Alexis Vautrin,
avenue de Bourgogne,
54511 Vandoeuvre-lès-Nancy, France

E. Micard · J. Felblinger
CIT 801, INSERM, CHU Nancy,
allée du Morvan,
54511 Vandoeuvre-lès-Nancy, France

E. Micard · J. Felblinger
IADI, U947, INSERM, CHU Nancy,
allée du Morvan,
54511 Vandoeuvre-lès-Nancy, France

Introduction

In the last decade, the number of CT examinations performed has continually increased, reaching more than 68.7 million per year in the United States in 2007 [1, 2]. While this increase is associated with significant improve-

Published online: 17 September 2011

ments in diagnostic performance, it has also caused an increase in individual and collective radiation [3] and the potential associated risk of radiation-induced cancer [4, 5]. Thus, reducing the dose of radiation has become a major concern. Despite the development of several technological innovations, such as automatic tube current modulation [6–8], the development of dynamically adjustable *z*-axis X-ray beam collimation and the use of volumetric acquisition mode to reduce over-ranging phenomenon [9, 10], dose reduction remains limited by the use of Filtered Back Projection (FBP) reconstructions. Indeed, these reconstructions create a significant increase of image noise in the case of excessive reduction of the dose [11]. Thanks to an important reduction in image noise, the recent development of iterative reconstruction enables health practitioners to solve this problem, thus allowing a significant reduction in dose compared with FBP reconstructions [12].

In our institution, these iterative reconstructions have been available since summer 2010 under Adaptive Iterative Dose Reduction (AIDR) and can be applied to volumetric and wide-volume modes. AIDR constitutes a new reconstruction algorithm based on statistical iterative reconstruction techniques [13] and can be adapted for large cone-beam CT examinations and for the particular three-dimensional (3D) FBP used to reconstruct volumetric and wide-volume acquisitions. The AIDR algorithm reduces image noise through iteration loops in the reconstruction domain. Noise reduction is based on the comparison of images reconstructed with a pre-established noise model. The final iterative image and the original image are weighed and combined to create the AIDR image. The summation of the two images ensures that the spatial resolution is preserved whilst the overall image noise is reduced. To our knowledge, there is no study on the possible use of this algorithm on non-helical acquisitions.

The purpose of our study was to evaluate the impact of AIDR reconstructions on image quality and radiation dose in phantom and patient studies.

Materials and methods

Phantom study

Phantom

A phantom (Catphan 500; The Phantom Laboratory, Salem, NY, USA) was examined in volumetric mode with a 320-detector volume CT system (Aquilion ONE, Toshiba, Japan). Using a low-contrast module CTP515 and a high-resolution module CTP528, we respectively evaluated low-contrast resolution [image noise, Signal-to-Noise Ratio (SNR) and Contrast-to-Noise Ratio (CNR)] and high-contrast resolution (spatial resolution). The phantom was positioned at the isocentre of the gantry.

Acquisition protocol

The protocol consisted in the acquisition of a volume covering the entire phantom (16 cm in the *z*-axis), with 13 different tube current values (25, 50, 80 mA, followed by 100 to 550 mA in increments of 50 mA). Because of the small diameter of the phantom (20 cm), the kilovolt peak (kVp) was set at 100 kVp. Other acquisition parameters for the 13 acquisitions were: 1 s of rotation time, beam width of 320 detectors with 0.5 mm slice collimation, 512×512 matrix, and 240 mm Field Of View (FOV).

CT image reconstructions

The 13 image sets were reconstructed using traditional 3D FBP reconstruction and AIDR iterative reconstruction with the same parameters (transverse 0.5 mm slice thickness with 0.5 reconstruction interval, soft-tissue kernel FC 07). Then, the 26 reconstructed volumes were sent and archived in the Picture Archiving and Communication System (PACS) of our institution (Impax V5, ES; AGFA Technical Imaging Systems, Ridgefield, NJ, USA).

Evaluation of image quality

The image quality was evaluated from the measurement of image noise, SNR, CNR and spatial resolution. To assess reproducible placement of a Region Of Interest (ROI) for all acquisitions, a software based on Matlab™ (The MathWorks Inc.; Natick, Massachusetts, USA) was developed. Two ROIs (ROI #1 and #2) of 60 mm^2 were placed in a synchronised manner on the 26 volumes inside the phantom by a computer engineer (E. M.). ROI #1 was positioned in a 1% low-contrast target of 15 mm in diameter, and ROI #2 was located in the background area, adjacent to the measured target (Fig. 1). Noise corresponded to the measurement of the standard deviation of the measured Hounsfield Units (HU) of ROI #2. The ratio between the difference of mean attenuation values of these two ROIs (ROI #1 and ROI #2) and the standard deviation of ROI #2 corresponded to the CNR [14], while the ratio between the mean attenuation value of ROI #2 and the standard deviation of ROI #2 corresponded to the SNR [15].

The spatial resolution of the image was assessed in a qualitative manner by a visual side-by-side comparison of the patterns of pairs of lines with the high-contrast resolution module, between FBP and AIDR sets. Two radiologists (B.O. and S.L.) with six and eight respective years of experience in reading CT examinations, performed the reading on sections with identical FOV and visualiza-

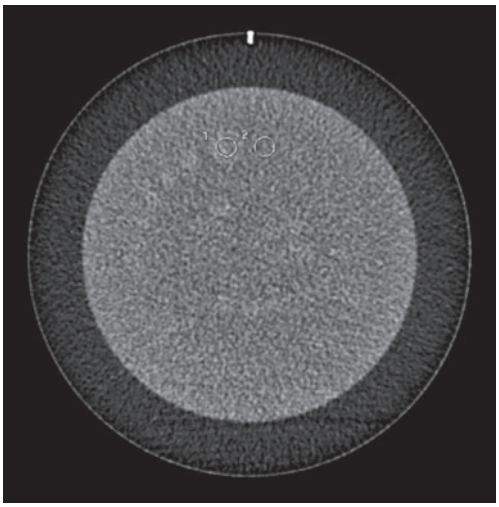

Fig. 1 Transverse CT slice of the phantom's low-contrast module. ROIs #1 and #2 were placed in the phantom to evaluate image noise, CNR and SNR. ROI #1 was positioned in a 1% low-contrast target of 15 mm in diameter, and ROI #2 was placed in the background area, adjacent to the measured target

tion window (Window/level setting: 400/50 HU). A calculation of the modulation transfer function was also carried out at 50% and 5% between the FBP and AIDR sets, respectively. This modulation transfer function was computed as the angular mean of the two-dimensional Fourier transform of the point-spread function, measured from CT images of a 0.28 mm tungsten wire centred in the phantom.

Patient study

Our institutional review board approved the study and informed consent was obtained from all patients participating in the study

Population studied

This prospective monocentric study included 15 consecutive patients (6 men and 9 women, mean age of 53.6 years old) between December 2010 and February 2011 referred to us for lumbar CT without injection of any contrast agent, in search of a disco-radicular conflict. Exclusion criteria were patients under 18 years old, pregnant women, trauma and patients with prior lumbar surgery.

Acquisition protocol

The lumbar spine examinations were performed on a 320-row detector CT (Aquilion ONE, Toshiba, Japan), in wide-volume mode, with an acquisition in two volumes covering the lumbar spine from T12 to S2, with identical acquisition parameters (135 kVp, *x,y,z*-axis tube current modulation (^{SURE}Exposure 3D, Toshiba) with noise index set at 7.5 for a 5-mm slice with soft filter and with minimum/maximum mA set at 100/500, rotation time: 1 s, beam width: 320×0.5 mm).

Image reconstruction

The images were reconstructed using traditional 3D FBP reconstructions and AIDR iterative reconstructions, with the same reconstruction parameters (transverse slices of 0.5 mm every 0.5 mm, reconstruction filter FC07, identical FOV between the two series). Once the reconstructions completed, both sets of FBP and AIDR images were sent and archived in our PACS.

Image quality evaluation

The image noise was evaluated in a quantitative manner by measuring the standard deviation of a ROI rounded by 100 mm^2 and placed in a standardised manner by the same radiologist (A.G.) in a homogeneous region of the left psoas muscle at the level of the L5 pedicles, on an transverse section of 0.5 mm in a soft-tissue window [6]. This step was performed with an Aquilion ONE CT Workstation (Display console version 4.62, Toshiba, Japan) with synchronisation of the FBP and AIDR sets of each patient (identical ROIs placed on a cut at the same level and same place for each patient).

The SNR was calculated for each ROI by dividing the mean attenuation value by the standard deviation [15].

Two board-certified radiologists (B.O. and S.L.), with six and eight respective years' of experience in reading musculoskeletal CT, then performed independent qualitative image noise analysis. They were neither involved in selecting patients nor in conducting CT examinations. They were blind to all patient identifiers. The visual perception of noise, defined by the grainy appearance of the CT images, was evaluated on 0.5 mm soft tissue transverse CT slices viewed with a standard window setting (window/level: 400/50 HU). The image noise was graded in three categories, according to the degree of image noise (1 = minimal, 2 = moderate and 3 = significant). This grading was done on PACS workstations (AGFA Impax ES review station, AGFA Technical Imaging Systems) after a common training session. During the reading session, the FBP and AIDR datasets were presented randomly to the readers.

Statistical analysis

All data were analysed with R for Windows (R Foundation for Statistical Computing, Vienna, Austria). The image quality scores for qualitative image noise were recorded for each radiologist, resulting in a total score for the assessment of image noise for each reconstruction technique. A

Wilcoxon signed-rank test was used to compare SNR, CNR, quantitative and qualitative image noise evaluations between both reconstruction modes. An interobserver agreement for the two radiologists was estimated using the Kappa test. A *P* value less than 0.05 was considered to represent a statistically significant difference.

Results

Phantom study

There was a mean noise reduction of 40% (range 35–44%), comparing AIDR and FBP reconstructions (Fig. 2). This noise reduction was accompanied by an improvement of the SNR (mean improvement of 61%, range 56–67%) and the CNR (mean improvement of 54%, range 33–67%). The percentage of noise reduction, SNR and CNR improvement was constant, regardless of the initial level of image noise, including low-dose acquisitions.

However, there was no significant difference between AIDR and FBP images, whether for the qualitative evaluation of spatial resolution (Fig. 3), or for the quantitative evaluation based on MTF measurements (Fig. 4).

Patient study (Table 1)

The quantitative measurement of image noise showed a significant reduction of noise on AIDR images (mean 15.6 ±4 HU, range 11.1–26.6 HU) compared to FBP reconstructions (mean 22.5±5 HU; range 16.6–36.2 HU), with a $p<0.001$. This corresponds to a mean reduction of 31% of image noise with the AIDR (range 24–37%).

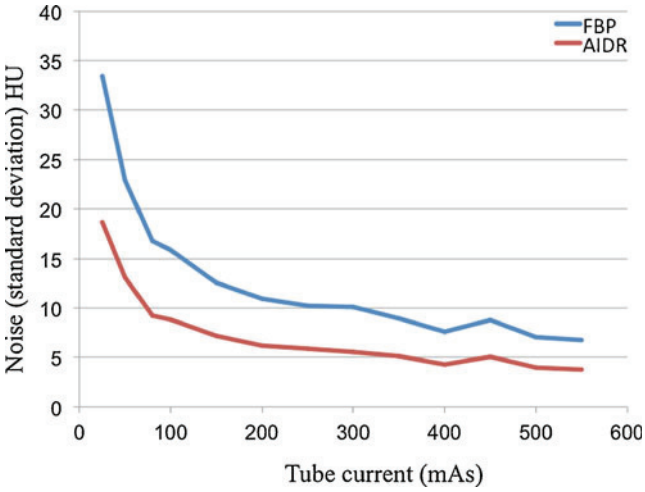

Fig. 2 Graph showing image noise reduction with adaptive iterative dose reduction (AIDR: *red line*) compared with the 3D-filtered back projection technique (FBP: *blue line*), at different tube currents in the phantom study

The scoring of qualitative image noise was also significantly better for the AIDR set (1.33±0.7) compared to the FBP set (2.1±0.6) with a $p<0.005$. The calculation of the Kappa coefficient showed a good interobserver concordance ($\kappa=0.74$).

The SNR was significantly improved with the AIDR reconstructions compared to FBP reconstructions (2.36±0.6 vs. 3.50±0.9 respectively, with a P=0.003), which was equivalent to a mean improvement of 47% (range 33–63%).

Discussion

Our phantom study confirms that at an equivalent dose and compared to the traditional 3D-FBP algorithm used for volumetric reconstruction, AIDR iterative reconstruction generates a significant reduction of image noise. Interestingly, the reduction level is equivalent, regardless of the initial quality of the original images. This means that AIDR reconstruction shows similar performances in terms of noise reduction for images acquired at normal dose than for noisy images acquired at low dose.

This noise reduction can be considered to either improve the image quality by keeping the dose constant, or to reduce the delivered dose while maintaining an equivalent image quality. Given that there is a direct relationship between the delivered dose (or milliamperage, in our study), and the image noise (when the radiation dose decreases by 1/*c*, the image noise increases by the square root of *c* [16]), it is possible to estimate the potential dose reduction based on our noise reduction measurements. Indeed, in our phantom study, we calculated that a mean reduction of image noise by 40% was associated with a potential dose reduction of about 64%. This estimate done with the phantom dose reduction is comparable to phantom measurements provided by the manufacturer.

Our phantom study also highlighted a significant improvement of SNR and CNR values, thanks to AIDR iterative reconstructions and compared to 3D-FBP reconstructions. Indeed, in the absence of changes in attenuation values during the process of reconstruction, noise reduction is automatically accompanied by an improvement of these parameters. At the same time, our study shows that the significant noise reduction does not alter spatial resolution. This point is critical because in regular clinical practice, several other methods already enable the reduction of image noise. However, these different techniques cause either a degradation in spatial resolution (use of a “soft” reconstruction filter, thickening of the slices [17]), or an increase of the delivered dose (increase of kVp or mAs). On the other hand, AIDR iterative reconstruction reduces noise without altering spatial resolution and without increasing the dose. When considering other types of iterative

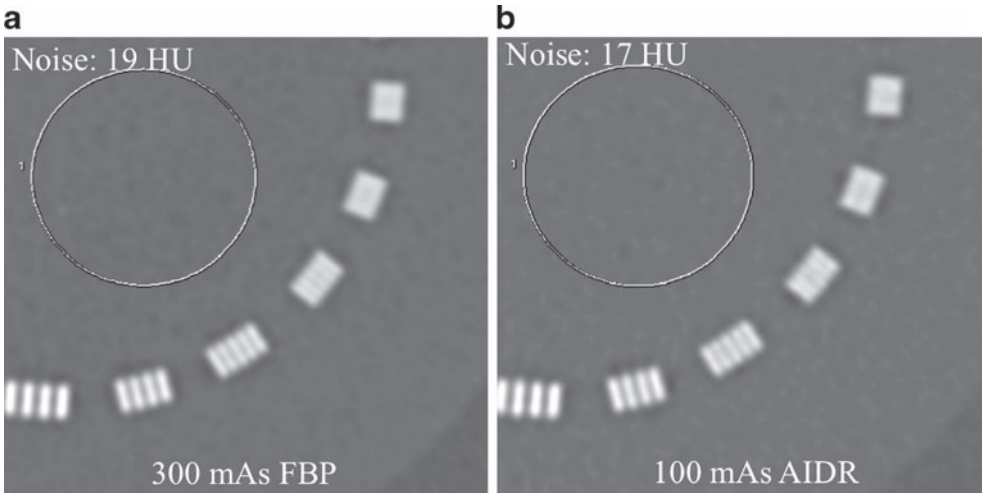

Fig. 3 Transverse CT image of the high-contrast module with 3D-filtered back projection (FBP) at 300 mAs (**a**) and adaptive iterative dose reduction (AIDR) at 100 mAs (**b**). Note the same spatial resolution assessed by high-contrast objects and the nearly same image noise

reconstruction, the data regarding spatial resolution alteration during reconstruction are variable. The phantom study of Hara et al. [12] revealed a slight deterioration of the high-contrast image of an object using half-dose iterative ASIR (Adaptive Statistical Iterative Reconstruction) reconstruction, compared to FBP reconstruction. The qualitative evaluation of spatial resolution on images of patients was also the only parameter worse with ASIR, in comparison with FBP reconstruction, without affecting the diagnostic value of the image [12]. In their study, Prakash et al. showed that ASIR-high definition reconstruction led to a slight improvement in spatial resolution on phantom studies [18]. Finally, for Ghetti et al., IRIS (Image Reconstruction in Image Space) iterative reconstruction preserved spatial resolution during the reconstruction process in the course of a phantom study [19]. These differences can probably be explained by the conceptual differences of these algorithms, which operate either in the image domain, in the raw-data domain, or in both.

Our patient-based study shows that AIDR allows a mean reduction of image noise by 31% for lumbar spine CT compared to 3D-FBP reconstruction. This noise reduction was significant both during quantitative ($p<0.001$) and qualitative assessment by the two radiologists ($p<0.005$), despite the small number of patients included. An extrapolation based on noise reduction allows an estimate of the potential dose reduction to about 52%. This major dose reduction potential at equivalent image quality is even more valuable since lumbar spine CT performed in a context of discoradicular conflict detection, mainly concerns young patients [20] who are likely to undergo repeated examinations [3].

To our knowledge, this is the first study to evaluate the performance of AIDR iterative reconstruction on patients using 320 multidetector CT. Comparing our results with other types of iterative reconstruction is difficult because

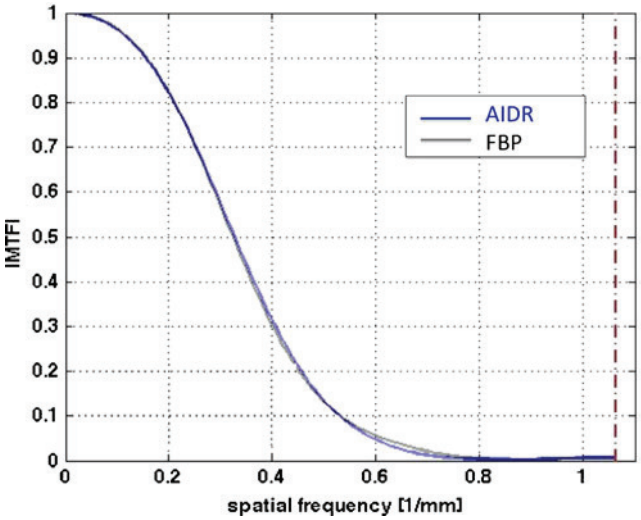

Fig. 4 Graph showing no significant difference in spatial resolution at 50% modulation transfer function (MTF) with adaptive iterative dose reduction (AIDR) compared with the 3D-filtered back projection (FBP) technique

Table 1 Quantitative and qualitative image quality comparison in lumbar spine CT with adaptive iterative dose reduction (AIDR) vs. 3D filtered back projection (FBP)

	FBP	AIDR	*p* value[a]
Quantitative image quality evaluation			
Noise (HU)	22.5±5	15.6±4	0.001
Signal to noise ratio	2.36±0.6	3.50±0.9	0.003
Qualitative image noise quality score[b]			
Reader 1	2.07±0.5	1.33±0.5	0.005
Reader 2	2.13±0.3	1.33±0.5	0.001
Average	2.1±0.6	1.33±0.7	0.005

Except for *p* value, data are mean ± standard deviation

[a] Statistically significant for all parameters

[b] Grading scale for noise: 1 = minimal, 2 = moderate and 3 = important

their implementation is different for each manufacturer. Indeed, with wide-volume acquisitions, enlarged cone angles for volume scanning require reconstruction algorithms based on a 3D FBP. Then, ASIR and IRIS iterative reconstructions respectively require the choice of a percentage of mixture between FBP and ASIR images and the selection of a number of iterations during the IRIS reconstruction process. The level of dose reduction and the final image quality, depend on these parameters [15, 18, 21–23]. Choosing a too-large percentage of ASIR, or a too-high number of IRIS iterations, can cause an alteration of the usual aspects of images with the emergence of the phenomenon of "oversmoothing", due to changes in the image noise spectra [11, 13]. This was particularly shown during the use of ASIR at 100%, which enables a dose reduction of more than 75%, but at the expense of the deleterious occurrence of this "oversmoothing" [21]. The use of ASIR at 40% helps to maintain a correct aspect of the image, while allowing only a 50% dose reduction [12].

As far as AIDR iterative reconstructions are concerned, they automatically choose the number of iterations and perform a mix between original and AIDR reconstructed images, allowing for a compromise between dose reduction and maintenance of a typical image quality. This technical specificity has the advantage of avoiding the choice of parameters. However, it becomes impossible to study these effects on dose reduction and image quality. In practice, despite an important reduction in image noise, we have not experienced a significant change in their appearance (Fig. 5).

Our study has several limitations. First, it is a preliminary study involving a small number of patients, which indirectly evaluates the benefit of AIDR iterative reconstruction on dose reduction based on an extrapolation of measurements of image noise reduction. A study comparing image quality between a scan at half-dose with the AIDR and at normal dose with the FBP reconstruction is necessary to confirm our encouraging results. Moreover, the choice to study AIDR iterative reconstruction using lumbar spine CT examinations does not allow comparison with other types of iterative reconstruction, which have been mainly studied using anatomic areas associated with higher-delivered doses or requiring follow-up studies, such as abdomen and chest CT [24]. This limitation is due to the fact that at the time of our study, AIDR iterative reconstruction was only available in the volumetric and wide-volume modes, which is the acquisition mode at which we performed our lumbar spine CT. The upcoming installation of a new version, which will allow the reconstruction of acquired images in helical mode, will thus enable us to evaluate AIDR performance on thorax or abdomen CT.

Second, in our patient study, we evaluated the improvement of image quality and not the impact of AIDR iterative reconstruction on the diagnostic performance of the exam. Moreover, we did not evaluate the influence of AIDR on bone structure. However, CT is preferred for the assessment of the bony structures of the spine [25]; hence numerous lumbar examinations are still performed in our institution. Nevertheless, the analysis of bone structures is less sensitive to noise variations than that of soft tissue and alterations in bone structure often affect elderly patients, a population for which the risk of radiation is lower because of reduced life expectancy [26]. Moreover, during qualitative assessment of image noise, a slight change in the appearance of noise with AIDR reconstruction can bring a bias during the reading, with the recognition of AIDR compared to FBP sets.

Additionally, we did not study the performances in terms of image quality improvement depending on the body habitus of patients, and in particular the body mass index, given the small number of patients included. Such a correlation would be of interest, though, to determine

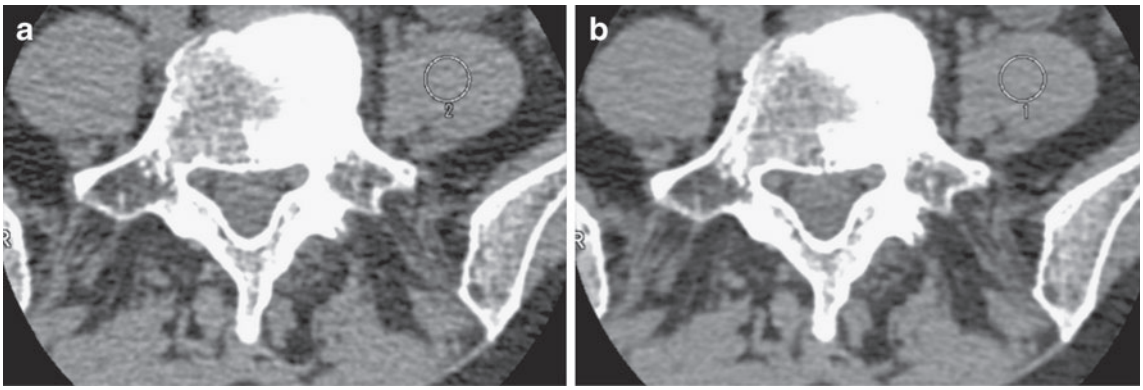

Fig. 5 Transverse lumbar spine CT image reconstructed with traditional 3D-filtered back projection (FBP) (**a**) and adaptive iterative dose reduction (AIDR) (**b**) in a 56-year-old woman. Note the noise reduction with AIDR compared to FBP, without any significant change in image pattern (standard deviation values of the ROIs placed in left psoas are 21.1 HU with FBP and 14.5 HU with AIDR, which corresponds to a noise reduction of 31%)

whether AIDR iterative reconstruction is as effective in patients who are overweight, where image quality is typically worse. Moreover, in our protocol, we did not adapt the kVp according to the body habitus of patients in order to keep the acquisition parameters constant.

Finally, we did not analyse the time needed to reconstruct images with AIDR. It does require more time than a standard FBP reconstruction, but according to the vendor, AIDR reconstruction time per image is only 0.006 s longer than for FBP reconstruction. In practice, when testing for a lumbar examination of 464 images, we effectively noticed a difference of approximately 2 s during the reconstruction process between FBP and AIDR (respectively 33 s vs. 35).

In conclusion, our pilot study shows that compared to the traditional FBP reconstruction technique, AIDR significantly improves image quality in phantom and patient volumetric and wide-volume CT. Further clinical evaluation is required to confirm the radiation dose decreasing potential with AIDR.

References

1. 2007 CT market summary report (2007) Des Plaines, IL: IMV Medical Information Division
2. Brenner DJ, Hall EJ (2007) Computed tomography an increasing source of radiation exposure. N Engl J Med 357:2277–2284
3. Sodickson A, Baeyens PF, Andriole KP et al (2009) Recurrent CT, cumulative radiation exposure and associated radiation-induced cancer risks from CT of adults. Radiology 252:175–184
4. Smith-Bindman R, Lipson J, Marcus R et al (2009) Radiation dose associated with common computed tomography examinations and the associated lifetime attributable risk of cancer. Arch Intern Med 169:2078–2086
5. Berrington de González A, Mahesh M, Kim KP et al (2009) Projected cancer risks from computed tomography scans performed in the United States in 2007. Arch Intern Med 169:2071–2077
6. Mulkens TH, Bellinck P, Baeyaert M et al (2005) Use of an automatic exposure control mechanism for dose optimization in multi-detector row CT examinations: clinical evaluation. Radiology 237:213–223
7. Kalender WA, Buchenau S, Deak P et al (2008) Technical approaches to the optimisation of CT. Phys Med 24:71–79
8. Alkadhi H, Leschka S (2011) Radiation dose of cardiac computed tomography—what has been achieved and what needs to be done. Eur Radiol 21:505–509
9. Christner JA, Zavaletta VA, Eusemann CD, Walz-Flannigan AI, McCollough CH (2010) Dose reduction in helical CT: dynamically adjustable z-axis X-ray beam collimation. AJR Am J Roentgenol 194:W49–W55
10. Gervaise A, Louis M, Batch T et al (2010) Dose reduction at CT of the lumbar spine using a 320-detector scanner: initial results. J Radiol 91:779–785
11. Xu J, Mahesh M, Tsui BM (2009) Is iterative reconstruction ready for MDCT? J Am Coll Radiol 6:274–276
12. Hara AK, Paden RG, Silva AC, Kujak JL, Lawder HJ, Pavlicek W (2009) Iterative reconstruction technique for reducing body radiation dose at CT: feasibility study. AJR Am J Roentgenol 193:764–771
13. Thibault JB, Sauer KD, Bouman CA, Hsieh J (2007) A three-dimensional statistical approach to improved image quality for multislice helical CT. Med Phys 34:4526–4544
14. Gupta AK, Nelson RC, Johnson GA, Paulson EK, Delong DM, Yoshizumi TT (2003) Optimization of eight-element multi-detector row helical CT technology for evaluation of the abdomen. Radiology 227:739–745
15. Pontana F, Duhamel A, Pagniez J et al (2011) Chest computed tomography using iterative reconstruction vs. filtered back projection (part 2): image quality of low-dose CT examinations in 80 patients. Eur Radiol 21:636–643
16. Boedeker KL, McNitt-Gray MF (2007) Application of the noise power spectrum in modern diagnostic MDCT: part II. Noise power spectra and signal to noise. Phys Med Biol 52:4047–4061
17. von Falck C, Galanski M, Shin HO (2010) Informatics in radiology: sliding-thin-slab averaging for improved depiction of low-contrast lesions with radiation dose savings at thin-section CT. Radiographics 30:317–326
18. Prakash P, Kalra MK, Ackman JB et al (2010) Diffuse lung disease: CT of the chest with adaptive statistical iterative reconstruction technique. Radiology 256:261–269
19. Ghetti C, Ortenzia O, Serreli G (2011) CT iterative reconstruction in image space: a phantom study. Phys Med [Epub ahead of print]
20. Spangfort EV (1972) The lumbar disc herniation: a computer-aided analysis of 2,504 operations. Acta Orthop Scand Suppl 142:1–95
21. Silva A, Lawder H, Hara A, Kujak J, Pavlicek W (2010) Innovations in CT dose reduction strategy: application of the adaptive statistical iterative reconstruction algorithm. AJR Am J Roentgenol 194:191–199
22. Pontana F, Pagniez J, Flohr T et al (2011) Chest computed tomography using iterative reconstruction vs. filtered back projection (part 1): evaluation of image noise reduction in 32 patients. Eur Radiol 21:627–635
23. Mitsumori LM, Shuman WP, Busey JM, Kolokythas O, Koprowicz KM (2011) Adaptive statistical iterative reconstruction versus filtered back projection in the same patient: 64 channel liver CT image quality and patient radiation dose. Eur Radiol [Epub ahead of print]
24. Fazel R, Krumholz HM, Wang Y et al (2009) Exposure to low-dose ionizing radiation from medical imaging procedures. N Engl J Med 361:849–857
25. Tins B (2010) Technical aspects of CT imaging of the spine. Insights Imaging 1:349–359
26. Bohy P, de Maertelaer V, Roquigny A, Keyzer C, Tack D, Genevois PA (2007) Multidetector CT in patients suspected of having lumbar disk herniation: comparison of standard-dose and simulated low-dose techniques. Radiology 244:231–524

Chapitre 3

Article 3 : *Réduction de la dose des scanners abdominopelviens grâce aux reconstructions itératives AIDR 3D.*

Gervaise A, Osemont B, Louis M, Lecocq S, Teixeira P, Blum A. Standard dose versus low-dose abdominal and pelvic CT: comparison between filtered back projection versus adaptive iterative dose reduction 3D. *Diagn Interv Imaging* 2014; 95: 47-53.

Diagnostic and Interventional Imaging (2014) **95**, 47—53

ORIGINAL ARTICLE / *Gastrointestinal imaging*

Standard dose versus low-dose abdominal and pelvic CT: Comparison between filtered back projection versus adaptive iterative dose reduction 3D

A. Gervaise[a,b,*], B. Osemont[a], M. Louis[a], S. Lecocq[a], P. Teixeira[a], A. Blum[a]

[a] *Service d'Imagerie Guilloz, Hôpital Central, CHU de Nancy, 29, avenue du Maréchal-de-Lattre-de-Tassigny, 54035 Nancy cedex, France*
[b] *Service d'Imagerie Médicale, Hôpital d'Instruction des Armées Legouest, 27, avenue de Plantières, BP 90001, 57077 Metz cedex 3, France*

KEYWORDS
Multidetector CT;
Dose reduction;
Image quality;
Iterative reconstruction;
Abdominal and pelvic CT

Abstract
Purpose: To compare the dose and image quality of a standard dose abdominal and pelvic CT with Filtered Back Projection (FBP) to low-dose CT with Adaptive Iterative Dose Reduction 3D (AIDR 3D).
Materials and methods: We retrospectively examined the images of 21 patients in the portal phase of an abdominal and pelvic CT scan before and after implementation of AIDR 3D iterative reconstruction. The acquisition length, dose and evaluations of the image quality were compared between standard dose FBP images and low-dose images reconstructed with AIDR 3D and FBP using the Wilcoxon test.
Results: The mean acquisition length was similar for both CT scans. There was a significant dose reduction of 49.5% with low-dose CT compared to standard dose CT (mean DLP of 451 mGy.cm versus 892 mGy.cm, $P < 0.001$). There were no differences in image quality scores between standard dose FBP and low-dose AIDR 3D images (4.6 ± 0.6 versus 4.4 ± 0.6 respectively, $P = 0.147$).
Conclusion: AIDR 3D iterative reconstruction enables a significant reduction in dose of 49.5% to be achieved with abdominal CT scan compared to FBP, whilst maintaining equivalent image quality.

* Corresponding author. Service d'Imagerie Guilloz, Hôpital Central, CHU de Nancy, C29, avenue du Maréchal-de-Lattre-de-Tassigny, 54035 Nancy cedex, France.
E-mail address: alban.gervaise@hotmail.fr (A. Gervaise).

2211-5684/$ — see front matter
http://dx.doi.org/10.1016/j.diii.2013.05.005

The number of CT scans performed has increased relentlessly over the last decade, to more than 68.7 million investigations in the United States in 2007 [1]. Although this increase is associated with a large improvement in diagnostic performance, it is also a source of increased personal and population exposure to radiation [2,3] as well as being the source of a potential risk of radiation-induced cancer from low doses of X-rays [4,5]. Reducing the radiation dose delivered by CT scans has therefore become a major concern, particularly in abdominal imaging where the acquisition protocol may include three or four acquisition phases [6].

The widespread use of several new technologies such as automatic millamperage modulation [7—9] and active collimation [10] has already reduced doses delivered in abdominal and pelvic CT scans. This reduction, however, is limited by the use of standard Filtered Back Projections (or FBP) as these cause a significant increase in image noise if the dose is reduced too much [11]. The recent emergence of iterative reconstructions solves this problem by greatly reducing image noise and therefore allowing the dose to be significantly reduced in comparison with standard FBP reconstructions [12,13].

A first version of the iterative reconstructions was marketed on the 320-detector CT scanner (Aquilion ONE, Toshiba, Japan) in 2010 (Adaptive Iterative Dose Reduction, Toshiba, Japan). This model showed considerable potential to improve image quality of the scanners and reduce their dose, although it had the disadvantage of only being available retrospectively and only for volume and not helicoidal-mode acquisitions [14,15]. A new, more sophisticated version of these iterative reconstructions has now been marketed (Adaptive Iterative Dose Reduction 3D [AIDR 3D], Toshiba, Japan) and is available in our institution. This can be used prospectively and for helicoidal acquisitions. It has a more complicated algorithm than the first version of the AIDR iterative reconstructions and contains iteration loops in the image and raw data fields. To create the AIDR 3D image, the final iterative image and the original image are combined and weighted in order to ensure a reduction in noise, at the same time preserving normal textures and anatomical outlines. Initial tests on model systems on our scanner showed that AIDR 3D iterative reconstructions could potentially reduce the radiation dose by nearly 50%. AIDR 3D is now, therefore, the reconstruction mode used in routine clinical practice. We are not aware, however, of any patient studies which have assessed the utility of this new reconstruction algorithm in order to reduce the radiation dose for abdominal and pelvic CT scans in clinical practice.

The aim of our study was to compare the dose and image quality of an abdominal and pelvic CT scan using standard dose FBP compared to an abdominal and pelvic CT scan with low-dose and AIDR 3D iterative reconstructions and standard FBP reconstructions in the same patient.

Materials and methods

This single-centre study was approved by our regional ethics committee. In view of the retrospective nature of the study, written consent from patients was not required.

Study population

This was a single-centre retrospective study which included 21 patients who had had contrast-enhanced abdominal and pelvic CT in the portal phase within our institution. Both investigations were performed on the same machine (Aquilion ONE), the first using standard dose with standard FBP reconstructions (FBP standard dose group) and the second using low-dose with AIDR 3D iterative reconstructions (AIDR 3D low-dose group). The images obtained with low-dose were also reconstructed by FBP (FBP low-dose group). Patients were identified and selected from our institution's PACS system (Picture Archiving and Communication System) (Impax V5, ES; AGFA Technical Imaging Systems, Ridgefield, NJ, USA) by searching, during the 3 months after the introduction of AIDR 3D iterative reconstructions (from September to November 2011), for all patients who had a portal phase abdominal and pelvic CT scan and who had already had the same scan before the iterative reconstructions were introduced. The exclusion criteria were patients who were minors, pregnant women and those who had an interval of more than 18 months between the two scans. Patients' weights were recorded at the time of the low-dose scan.

Acquisition protocol

All of the abdominal and pelvic scans were obtained using a 320-detector CT scan instrument (Aquilion ONE, Toshiba, Japan) with acquisition covering the abdomen and pelvis from the bases of the lungs to the pubic symphysis. All of the patients had at least one portal phase acquisition after intravenous administration of 150 mL of contrast medium (OMNIPAQUE 350, GE Healthcare, Chalfont St. Giles, UK) via peripheral infusion over a period of 70 seconds with flow rate of 4 mL/s. The acquisition parameters were identical (Table 1) except for the automatic milliamperage modulation noise index in the three planes (^{SURE}Exposure 3D, Toshiba) which were set at 9 for a 5 mm section of the ''soft tissues'' window for the standard dose scan and 10 for the low-dose scan. With the introduction of the AIDR 3D, the automatic milliamperage modulation automatically and prospectively reduces the exposure parameters.

Image reconstruction

For the standard dose scans, the images were reconstructed with FBP reconstructions (standard dose FBP group). Images for the low-dose scans were reconstructed using AIDR 3D iterative reconstructions in ''standard'' mode (AIDR 3D low-dose group) and using FBP reconstructions (FBP low-dose group). The three series of images were reconstructed in 2 mm transverse sections every 1.6 mm with an FC 07 reconstruction filter. All of the images were sent to and archived in our PACS system.

Assessment of image quality

Image noise was assessed quantitatively by measuring the standard deviation of the regions of interest (ROI) located in the liver and aorta (Fig. 1). These regions were positioned in a standardised manner by the same radiologist

Table 1 Scan acquisition and reconstruction settings.

	Standard dose scan	Low-dose scan	
	FBP	AIDR 3D	FBP
Acquisition mode	Helicoidal	Helicoidal	Helicoidal
Detector collimation	64 × 0.5 mm	64 × 0.5 mm	64 × 0.5 mm
Kilovoltage	120	120	120
Milliamperage modulation	SureExposure 3D	SureExposure 3D	SureExposure 3D
Noise index	9	10	10
mA minimum/maximum	50/500	50/500	50/500
Section thickness/interval	2/1.6 mm	2/1.6 mm	2/1.6 mm
Reconstruction algorithm	FBP	AIDR 3D	FBP

FBP: Filtered Back Projection; AIDR 3D: Adaptive Iterative Dose Reduction 3D; SureExposure3D: three dimensional automatic milliamperage (mA) modulation (Toshiba, Japan).

(A.G.) on a 2 mm thick transverse section of the abdomen at the level of the portal vein bifurcation, from an Aquilion ONE post-treatment console (Display console, version 4.74, Toshiba, Japan). For the aorta, noise was defined as having a standard deviation of a $100 \pm 20\,mm^2$ region of interest placed in the centre of the vessel in a homogenous region distant to the walls. For the liver, three circular $200 \pm 50\,mm^2$ regions of interest were positioned in

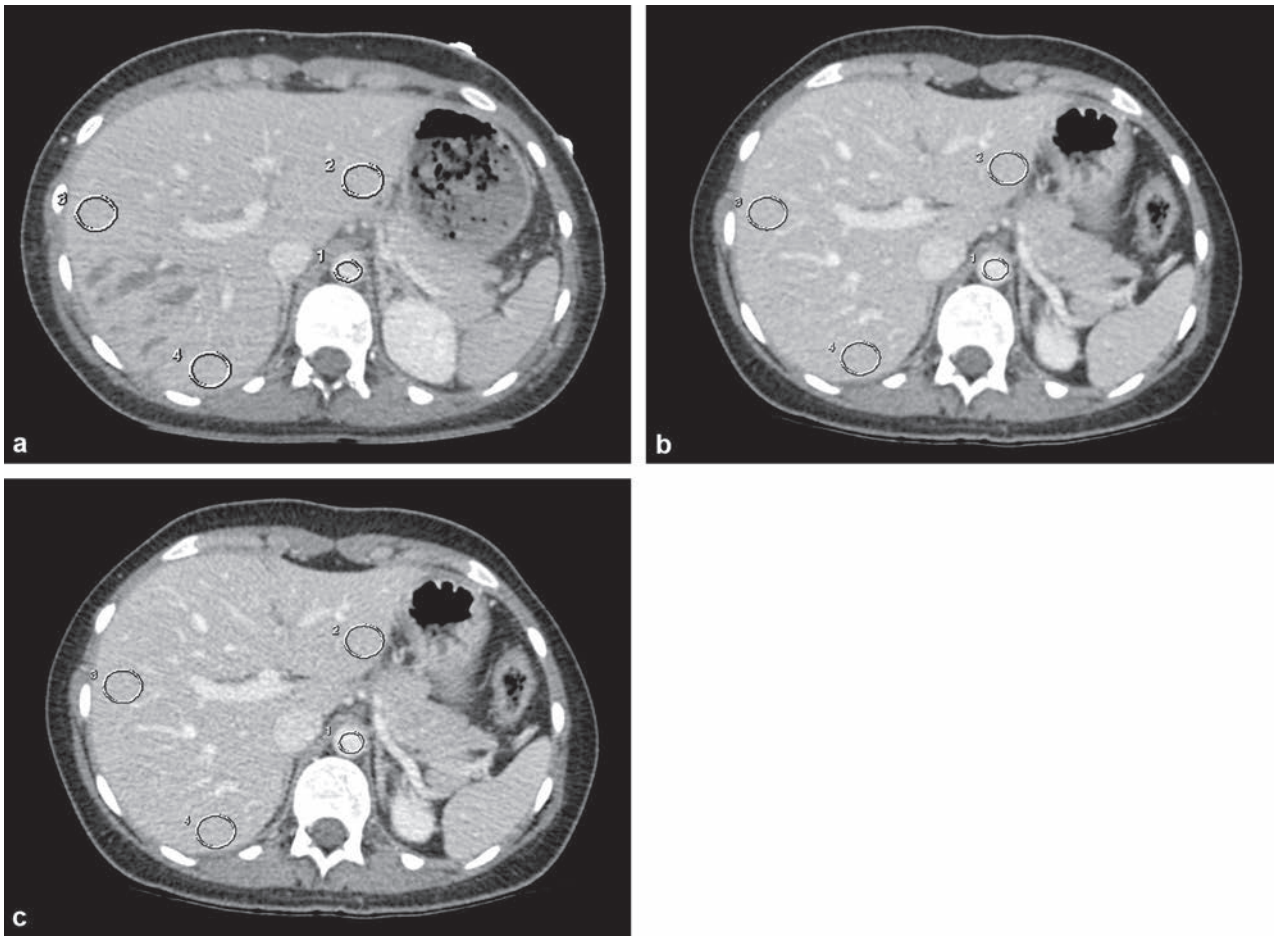

Figure 1. Abdominal CT images in a 26-year-old female patient being followed up for post-traumatic liver fracture. Two-millimetre transverse CT sections of the abdomen at standard dose with FBP reconstructions (a) and low-dose CT with AIDR 3D iterative reconstructions (b) and with FBP reconstructions (c). The position and size of the ROIs in the aorta (ROI #1) and in the liver (ROI #2–4) were maintained between the three image series. Note the large reduction in image noise between the AIDR 3D low-dose (b) and FBP low-dose (c) groups. Also note the similar image noise between the FBP standard dose (a) and AIDR 3D low-dose (b) groups, despite the large reduction in dose with the second scan (529 mGy.cm vs. 267 mGy.cm respectively, i.e. a dose reduction of 50.5%).

the left and right lobes of the liver, carefully avoiding the intra-hepatic vessels, focal lesions and artefacts, as described by Marin et al. [16]. Liver noise was defined as the mean of the standard deviations of the three liver ROIs.

In order to establish the independent relationship between image noise and dose for each of the three series of images, a figure of merit (FOM) was calculated for the aorta and for the liver using the equation described by Marin et al. [16] where B^2 is the square of the noise and ED is the effective dose: $FOM = 1/(B^2 \cdot ED)$.

Three senior radiologists (B.O., M.L. and A.B.) then performed a qualitative assessment of image quality. These radiologists have 6, 9 and 25 years of experience respectively in interpreting abdominal CT scans. They were not involved in patient selection or in positioning the ROIs for the quantitative image analysis. The images were read independently by the three radiologists on randomised, anonymised investigations which did not show the dates that the scans were performed. The assessment was scored on a visual scale from 1 to 5 (1 = unacceptable image quality, unable to interpret; 2 = poor image quality, interfering with interpretation; 3 = average image quality, interpretation possible; 4 = good image quality; 5 = excellent image quality) on PACS consoles after a joint reading session. Image quality scores 1 and 2 were deemed to be unacceptable for interpretation in clinical practice.

Measurement of doses delivered

The doses delivered were provided directly from the investigation report which could be accessed in the PACS system. They correspond to the $CTDI_{vol}$ (volume CT dose index) expressed in mGy and the Product Dose and Length expressed in mGy.cm. The effective dose (ED) expressed in milliSievert (mSv) was calculated using the tissue conversion coefficient (k) for the abdomen of 0.015 [17] by the equation $ED = k \times PDL$ [18].

Evaluation of acquisition lengths

Acquisition length was expressed in centimetres and was measured as the difference in position between the first and last acquisition sections.

Evaluation of transverse and anteroposterior abdominal diameters

Transverse and anteroposterior abdominal diameters (in cm) were measured for each patient on the standard dose and low-dose scans in order to ensure that there had been no significant change in patient body morphology between the two investigations. These measurements were performed by the same radiologist (A.G.), on a PACS console, on the same transverse sections passing through the portal vein bifurcation used to position the ROIs for the quantitative measurement of image noise.

Statistical analyses

Findings were analysed on R for Windows software (R Foundation for Statistical Computing, Vienna, Austria). Mean values were calculated for the image quality from the quantitative analysis by each radiologist to produce an overall image quality score for each group. The Wilcoxon signed rank test was used to compare acquisition lengths, doses delivered and abdominal diameters between the two types of scan. The same test was used to compare the qualitative and quantitative assessments of image quality between the AIDR 3D low-dose, FBP low-dose and FBP standard dose groups. A P value of less than 0.05 was deemed to be a statistically significant difference.

Results

Twenty-one patients were included in the study (10 men and 11 women). The average age of the patients at the time of the low-dose scan was 43 ± 18 years (range: 21 to 86 years) and mean weight was 71 ± 8 kg (range: 45 to 88 kg). The average interval between the two scans was 177 days (range: 92 to 380 days). There were no significant differences in acquisition lengths or abdominal diameters between the low-dose and standard dose scans (Table 2).

Mean $CTDI_{vol}$, DLP and effective doses of the low-dose scans were significantly lower than with the standard dose scans (effective doses of 6.8 ± 2.5 mSv compared to 13.4 ± 4.3 mSv respectively, $P < 0.001$). The average reduction in dose was 49.5% (Table 2).

For the quantitative assessment of image quality, we found that mean image noise in the liver and aorta was

Table 2 Scan acquisition lengths, abdominal diameters and doses delivered.

	Standard dose scan	Low-dose scan	*P* value
Acquisition length (cm)	45.6 ± 4	43.6 ± 2.6	0.07
Abdominal diameters (cm)			
Anteroposterior	23.3 ± 2.7	23.6 ± 3.1	0.304
Transverse	31.7 ± 3.3	31.8 ± 3.2	0.667
CT radiation dose			
$CTDI_{vol}$ (mGy)	19.5 ± 5.6	10.3 ± 3.6	< 0.001
DLP (mGy.cm)	892 ± 284	451 ± 170	< 0.001
Effective dose (mSv)	13.4 ± 4.3	6.8 ± 2.5	< 0.001

Apart from the *P* values, the results are expressed as mean ± standard deviation.

Table 3 Quantitative and qualitative image quality assessment.

	Standard dose scan	Low-dose scan		*P* value		
	FBP	AIDR 3D	FBP	AIDR 3D vs. FBP low-dose	AIDR 3D vs. FBP standard dose	FBP low-dose vs. FBP standard dose
Noise (UH)						
Liver	15.86 ± 2.7	16.47 ± 1.4	27.21 ± 4.2	< 0.001	0.257	< 0.001
Aorta	17.62 ± 3.3	17.70 ± 2.5	31.84 ± 6.8	< 0.001	0.733	< 0.001
FOM ($\times 10^{-4}$)						
Liver	3.47 ± 1.0	6.27 ± 2.0	2.19 ± 1.0	< 0.001	< 0.001	< 0.001
Aorta	2.89 ± 1.0	5.71 ± 2.4	2.0 ± 1.0	< 0.001	< 0.001	0.003
Image quality score	4.6 ± 0.6	4.4 ± 0.6	3.3 ± 0.6	< 0.001	0.147	< 0.001

FBP: Filtered Back Projection; AIDR 3D: Adaptive Iterative Dose Reduction 3D. Apart from the *P* values, the results are expressed as mean ± standard deviation.

significantly lower in the AIDR 3D low-dose group than in the FBP low-dose group with noise reductions of 39 and 44% respectively. However, there was no significant difference between mean liver or aortic image noise between the FBP standard dose and AIDR 3D low-dose groups (Table 3). The mean of the FOMs in the liver and aorta were significantly higher for the AIDR 3D low-dose images compared to the FBP standard dose images (6.27 ± 2.0 compared to 3.47 ± 1.0, $P < 0.001$ for the liver and 5.71 ± 2.4 compared to 2.89 ± 1.0, $P < 0.001$ for the aorta, respectively) and FBP low-dose (Table 3).

The qualitative assessment of the image quality showed this to be significantly higher in the FBP low-dose and AIDR 3D low-dose groups (3.3 ± 0.6 compared to 4.4 ± 0.6 respectively, $P < 0.001$). There was no statistically significant difference in mean image quality score between the FBP standard dose and AIDR 3D low-dose groups (4.6 ± 0.6 compared to 4.4 ± 0.6 respectively, $P = 0.147$) (Table 3).

Discussion

Our study confirms that the use of AIDR 3D iterative reconstructions greatly reduces image noise as compared to standard FBP reconstructions. Our comparison between the FBP low-dose and AIDR 3D low-dose series images shows a significant improvement in subjective image quality and in the quantitative assessment of image noise. Two of the patients in the FBP low-dose group scored 2 out of 5 for quality, thus the quality of the image interfered with interpretation, no patients in the AIDR 3D low-dose group scored 2 and only one of the 21 patients scored 3 in this group.

As a result of this reduction in image noise, it has become possible to reduce acquisition parameters and therefore the dose. Our comparison between the AIDR 3D low-dose and FBP standard dose groups confirms that it is possible to halve the radiation dose delivered in abdominal CT scans by using AIDR 3D iterative reconstructions. This reduction in dose has enabled us to reduce the average PDL in our abdominal scans from 892 mGy.cm to 451 mGy.cm, or a mean dose beneath the diagnostic reference level defined in the 2012 legislation (800 mGy.cm) [19].

The results of our study are similar to those of an initial study on the effectiveness of AIDR iterative reconstructions (Toshiba's first version of iterative reconstructions) on lumbar spine CT scans which showed the potential to reduce the dose by 52% [14]. This dose reduction, however, was only based on indirect calculation by extrapolating the reduction in noise from FBP to AIDR images on the same acquisition.

Our results are also similar to other types of iterative reconstructions which have already been marketed and which are currently available in clinical practice [20–23]. Sagara et al. [20] and Prakash et al. [21] showed that it was possible to reduce abdominal CT scan doses by 33% and 25% respectively, using ASIR, whilst improving image quality in comparison with FBP reconstructed scans in patient studies using Adaptive Statistical Iterative Reconstruction (ASIR). Mitsumori et al. [22] showed that the abdominal scan dose could be reduced by 41% with ASIR in comparison with FBP reconstructions. In addition, as in our own study, May et al. [23] demonstrated a 50% reduction in abdominal scan dose using Iterative Reconstruction in Image Space (IRIS) iterative reconstructions compared to standard FBP reconstructions, with equivalent image quality.

It is difficult, however, to compare our results with other types of iterative reconstructions as their implantation is different for each manufacturer. The ASIR and IRIS iterative reconstructions, for example, respectively require a percentage mixing of FBP and ASIR images and a number of iterations to be selected during the IRIS reconstruction process. The dose reduction and quality of the final image both depend on these parameters [20–24]. If an ASIR percentage that is too high is chosen, or if too many iterations are used for IRIS, changes may occur in the usual appearance of the images with an ''over-smoothing'' effect due to a change in the image noise spectra [11,12].

AIDR 3D also allows us to choose from four predetermined modes: ''weak'', ''mild'', ''standard'' and ''strong''. These different modes allow a greater or lesser number of iterations to be performed and the mixing percentage of AIDR

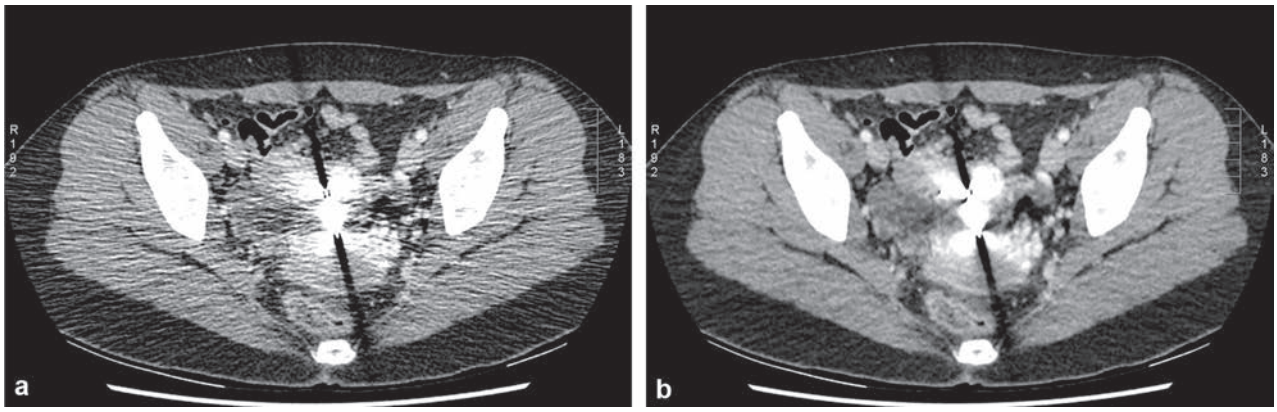

Figure 2. Low-dose abdominal CT in a 22-year-old female patient being followed up for post-traumatic splenic fracture (DLP = 383 mGy.cm). Two-millimetre transverse sections centred on the pelvis using FBP reconstruction (a) and AIDR 3D iterative reconstruction (b). Note the large reduction in image noise from the AIDR 3D iterative reconstructions (b) but also the reduction in metallic artefacts from the intra-uterine device.

3D and FBP to be changed in the iterative reconstruction process. The ''standard'' setting is the one recommended by the manufacturer for abdominal imaging and is a compromise between dose reduction and maintaining usual image quality. In practice, we have not noticed any difference in image texture on the AIDR 3D images and it was difficult for the readers to distinguish the FBP standard dose and AIRD 3D low-dose images (Fig. 1). The ''strong'' setting may cause a slight change in usual image texture, although this setting can further reduce the radiation dose delivered. Yamada et al. showed that by using the ''strong'' setting with AIDR 3D iterative reconstructions, the dose could be reduced by 64% whilst maintaining equivalent image quality compared to standard FBP reconstructions in a study on chest CT scans [25]. Further studies are therefore needed to establish whether it is possible to use the ''strong'' setting in abdominal imaging in order to further decrease the dose without reducing the diagnostic performance of the investigations.

Another advantage of some types of iterative reconstruction algorithms is that they reduce beam intensification artefacts and metallic artefacts. AIDR 3D iterative reconstructions can partially correct these artefacts by using a reconstruction algorithm with a double loop in the raw data fields and in the image field. This partly explains the improvement in subjective image quality between FBP low-dose and AIDR low-dose images (Fig. 2).

There are several limitations to our study. Firstly, it is a retrospective study which included a small number of patients. A larger-scale prospective study is needed in order to confirm these results. Secondly, we only assessed image quality and not the diagnostic performance of the scans in our study. This would have been a more appropriate style of assessment but it is difficult to implement. Thirdly, we did not study the effect of patient body morphology on the effectiveness of iterative reconstructions because of the small numbers of patients included and as body mass index was not available for all patients. It would, however, be useful to carry out such a study with AIDR 3D as several publications have shown that iterative reconstructions produce variable and contradictory results depending on patient morphology [20,22]. Similarly, as this was a retrospective study, we did not have a record of the patient's weight at their first scan and so we were not able to compare their weights between the two investigations to ensure that this had not changed significantly. Menke [26], however, has shown that measurements of anteroposterior and transverse abdominal diameters correlate with patient body morphology and particularly with body mass index. The fact that these abdominal diameters did not change between the two scans in our study argues against a change in body morphology in our patients. Finally, the dose reduction found in our study only applies to abdominal CT scans performed on our scanner and using our protocol. Other studies are needed to assess the dose reduction for other reconstruction parameters, particularly with the ''strong'' setting, and also for other types of CT scan investigations, particularly chest and brain.

Conclusion

AIDR 3D iterative reconstructions can halve the radiation dose from an abdominal CT scan compared to standard FBP reconstructions whilst maintaining equivalent image quality. Further studies are needed to confirm the utility of iterative reconstructions in other types of CT scan investigations, particularly chest and brain.

Disclosure of interest

The authors declare that they have no conflicts of interest concerning this article.

References

[1] 2007 CT market summary report. Des Plaines, IL: IMV Medical Information Division.
[2] Brenner DJ, Hall E. Computed tomography: an increasing source of radiation exposure. N Engl J Med 2007;357:2277—84.
[3] Sodickson A, Baeyens PF, Andriole KP, Prevedello LM, Nawfel RD, Hanson R, et al. Recurrent CT, cumulative radiation

exposure and associated radiation-induced cancer risks from CT of adults. Radiology 2009;252:175—84.
[4] Smith-Bindman R, Lipson J, Marcus R, Kim KP, Mahesh M, Gould R, et al. Radiation dose associated with common computed tomography examinations and the associated lifetime attributable risk of cancer. Arch Intern Med 2009;169:2078—86.
[5] Berrington de González A, Mahesh M, Kim KP, Bhargavan M, Lewis R, Mettler F, et al. Projected cancer risks from computed tomography scans performed in the United States in 2007. Arch Intern Med 2009;169:2071—7.
[6] Guite KM, Hinshaw JL, Ranallo FN, Lindstrom MJ, Lee FT. Ionizing radiation in abdominal CT: unindicated multiphase scans are an important source of medically unnecessary exposure. J Am Coll Radiol 2011;8:756—61.
[7] Cordoliani YS, Boyer B, Le Marec E, Jouan E, Hélie O, Beauvais H. Vade-mecum du scanner hélicoïdal : estimation des doses, choix des paramètres. J Radiol 2002;83:685—92.
[8] Rizzo S, Kalra M, Schmidt B, Dalal T, Suess C, Flohr T, et al. Comparison of angular and combined automatic tube current modulation techniques with constant tube current CT of the abdomen and pelvis. AJR Am J Roentgenol 2006;186:673—9.
[9] Lee S, Yoon SW, Yoo SM. Comparison of image quality and radiation dose between combined automatic tube current modulation and fixed tube current technique in CT of the abdomen and pelvis. Acta Radiol 2011;52:1101—6.
[10] Christner JA, Zavaletta VA, Eusemann CD, Walz-Flannigan AI, McCollough CH. Dose reduction in helical CT: dynamically adjustable z-axis X-ray beam collimation. AJR Am J Roentgenol 2010;194:W49—55.
[11] Xu J, Mahesh M, Tsui BM. Is iterative reconstruction ready for MDCT? J Am Coll Radiol 2009;6:274—6.
[12] Thibault JB, Sauer KD, Bouman CA, Hsieh J. A three-dimensional statistical approach to improved image quality for multislice helical CT. Med Phys 2007;34:4526—44.
[13] Hara AK, Paden RG, Silva AC, Kujak JL, Lawder HJ, Pavlicek W. Iterative reconstruction technique for reducing body radiation dose at CT: feasibility study. AJR Am J Roentgenol 2009;193:764—71.
[14] Gervaise A, Osemont B, Lecocq S, Noel A, Micard E, Felblinger J, et al. CT image quality improvement using adaptive iterative dose reduction with wide-volume acquisition on 320-detector CT. Eur Radiol 2012;22:295—301.
[15] Tatsugami F, Matsuki M, Nakai G, Inada Y, Kanazawa S, Takeda Y, et al. The effect of adaptive iterative dose reduction on image quality in 320-detector row CT coronary angiography. Br J Radiol 2012;85:e378—82.
[16] Marin D, Nelson RC, Schindera ST, Richard S, Youngblood RS, Yoshizumi TT, et al. Low-tube-voltage, high-tube-current multidetector abdominal CT: improved image quality and decreased radiation dose with adaptive statistical iterative reconstruction algorithm–initial clinical experience. Radiology 2010;254:145—53.
[17] Deak PD, Smal Y, Kalender WA. Multisection CT protocols: sex- and age-specific conversion factor used to determine effective dose from Dose-Length-Product. Radiology 2010;257:158—66.
[18] International Commission on Radiological Protection. 2007 recommendations of the International Commission on Radiological Protection (ICRP Publication 103). Ann ICRP 2007;37:1—332.
[19] Arrêté du 24 octobre 2011 relatif aux niveaux de références diagnostiques en radiologie et en médecine nucléaire. Journal Officiel de la République Française, 14 January 2012.
[20] Sagara Y, Hara AK, Pavlicek W, Silva AC, Paden RG, Wu Q. Abdominal CT comparison of low-dose CT with adaptive statistical iterative reconstruction and routine-dose CT with filtered back projection in 53 patients. AJR Am J Roentgenol 2010;195:713—9.
[21] Prakash P, Kalra MK, Kambadakone AK, Pien H, Hsieh J, Blake MA, et al. Reducing abdominal CT radiation dose with adaptive statistical iterative reconstruction technique. Invest Radiol 2010;45:202—10.
[22] Mitsumori LM, Shuman WP, Busey JM, Kolokythas O, Koprowicz KM. Adaptive statistical iterative reconstruction versus filtered back projection in the same patient: 64 channel liver CT image quality and patient radiation dose. Eur Radiol 2012;22:138—43.
[23] May M, Wust W, Brand M, Stahl C, Allmendinger T. Dose reduction in abdominal computed tomography: intra individual comparison of image quality of standard dose and half-dose iterative reconstructions with dual-source computed tomography. Invest Radiol 2011;46:465—70.
[24] Silva A, Lawder H, Hara A, Kujak J, Pavlicek W. Innovations in CT dose reduction strategy: application of the Adaptive Statistical Iterative Reconstruction algorithm. AJR Am J Roentgenol 2010;194:191—9.
[25] Yamada Y, Jinzaki M, Hosokawa T, Tanami Y, Sugiura H, Abe T, et al. Dose reduction in chest CT: Comparison of the adaptive iterative dose reduction 3D, adaptive iterative dose reduction, and filtered back projection reconstruction techniques. Eur J Radiol 2012, http://dx.doi.org/10.1016/j.erad.2012.07.013.
[26] Menke J. Comparison of different body size parameters for individual dose adaptation in body CT of adults. Radiology 2005;236:565—71.

Chapitre 3

Article 4 : *Scanner basse dose avec la modulation automatique du milliampérage, les reconstructions Adaptive Statistical Iterative Reduction et un faible kilovoltage pour le diagnostic des coliques néphrétiques : impact de l'indice de masse corporelle.*

Gervaise A, Naulet P, Beuret F, Henry C, Pernin M, Portron Y, Lapierre-Combes M. Low-dose CT with automatic tube current modulation, adaptive statistical iterative reconstruction, and low tube voltage for the diagnosis of renal colic: impact of body mass index. *Am J Roentgenol* 2014; 202: 553-60.

Low-Dose CT With Automatic Tube Current Modulation, Adaptive Statistical Iterative Reconstruction, and Low Tube Voltage for the Diagnosis of Renal Colic: Impact of Body Mass Index

Alban Gervaise[1]
Pierre Naulet[1]
Florence Beuret[1]
Christelle Henry[2]
Matthieu Pernin[1]
Yann Portron[1]
Marie Lapierre-Combes[1]

OBJECTIVE. The objective of our study was to evaluate the impact of body mass index (BMI) on dose, diagnostic performance, and image quality of a low-dose CT examination for renal colic.

MATERIALS AND METHODS. This retrospective study included all patients who underwent a low-dose CT examination for renal colic performed during the year 2012 with automatic tube current modulation, adaptive statistical iterative reconstruction, and a low tube voltage (kV). Three readers independently reviewed all images for the presence of renal colic and evaluated diagnostic confidence and image quality. The results and doses were compared among patients grouped by body mass index (BMI) and between patients with a BMI < 25 and those with a BMI ≥ 25.

RESULTS. Eighty-six patients were included in the study: 39 patients had a BMI < 25 and 47 had a BMI ≥ 25. No statistically significant difference was found between the accuracy rates for the diagnosis of renal colic when the rates of the three independent readers were averaged for both BMI groups (95.7% vs 96.4%, respectively; $p = 0.83$). Image quality and diagnostic confidence scores were significantly better for patients with a BMI ≥ 25 than for patients with a BMI < 25 (mean image quality score, 3.7 vs 3.4, $p < 0.001$; mean diagnostic confidence score, 2.8 vs 2.5, $p < 0.001$). The mean radiation dose for patients with a BMI < 25 was 2.4 mGy compared with 3.7 mGy for patients with a BMI ≥ 25 ($p < 0.001$).

CONCLUSION. The diagnostic performance of our low-dose CT protocol for renal colic was excellent for all patients, and image quality and diagnostic confidence were significantly better for patients with a BMI ≥ 25. However, our protocol also required exposure to a greater dose of radiation for these overweight and obese patients.

Keywords: body mass index, CT, iterative reconstruction, MDCT, radiation dose, renal colic

DOI:10.2214/AJR.13.11350

Received June 5, 2013; accepted after revision July 15, 2013.

[1]Department of Medical Imaging, Military Hospital Legouest, 27 Avenue de Plantières, BP 90001, Metz 57077, Cedex 3, France. Address correspondence to A. Gervaise (alban.gervaise@hotmail.fr).

[2]Biochemistry Laboratory, University Hospital, Nancy, France.

AJR 2014; 202:553–560

0361–803X/14/2023–553

Over the past years, CT has become a reference technique in medical imaging for the diagnosis of renal colic [1, 2]. It is a fast examination that does not require the IV administration of contrast material. It also has excellent performance for the diagnosis of renal colic and enables the diagnosis of other diseases and abnormalities clinically mimicking renal colic. The main limitation of CT is that it involves an absorption of radiation dose, which is especially limiting in this setting because urinary stone disease mainly affects young people and tends to relapse. Leusmann et al. [3] evaluated the relapse rate of renal colic to be 35% at 10 years after diagnosis, and Katz et al. [4] reported that 4% of patients undergoing CT for suspected renal colic had already undergone at least three CT examinations for the same indication, yielding cumulative doses ranging from 20 to 154 mSv.

Taking into account the potential risks of radiation-induced cancer due to low x-ray doses [5, 6] and the ALARA (as low as reasonably achievable) precautionary principle, dose reduction of CT examinations performed for suspected renal colic is essential.

Thanks to high contrast between most urinary stones and the surrounding soft tissues, several authors have proposed low-dose CT protocols for patients with suspected renal colic using either a higher pitch or a substantially reduced tube current (mA) [7–13]. Many studies have shown that excellent diagnostic performance can be achieved with low-dose CT and that diagnostic performance is equivalent to standard-dose CT. However, Hamm et al. [9] and Poletti et al. [12] found that the diagnostic performance of low-dose CT was decreased in obese patients with a BMI > 30. That decrease in diagnostic performance resulted from the use of a

constant tube current for all patients, leading to a significant decrease in image quality for the studies of obese patients. Thus, some authors have proposed that low-dose CT not be used for studies of obese patients [9, 10, 12], whereas others have recommended the use of an adapted tube current for patients with a BMI > 30 [13].

Since these studies, the introduction of automatic tube current modulation during acquisitions has enabled tube current and image quality to be adapted to the patient's body habitus. Mulkens et al. [14] showed that it was possible to get excellent diagnostic performance for CT studies of all patients with suspected renal colic—including overweight patients and obese patients—by performing low-dose CT examinations using automatic tube current modulation.

The reduction of tube current remains limited by the use of the standard filtered back projection (FBP) reconstruction because the FBP technique significantly increases the image noise when the dose reduction is too important [15]. Recently, the development of iterative reconstructions allowed a significant noise reduction in CT images compared with standard FBP reconstructions [16–18]. While maintaining the same image quality, iterative reconstructions reduce noise so that tube current and tube voltage can be reduced, thus reducing the dose. In their pilot study, Kulkarni et al. [18] confirmed that it was possible to perform an acquisition with automatic tube current modulation, an iterative reconstruction such as adaptive statistical iterative reconstruction (ASIR), and a low tube voltage while guaranteeing an excellent diagnostic performance of low-dose CT compared with standard-dose CT. However, that initial study did not evaluate the impact of patient morphology on image quality, diagnostic performance, and dose.

Our study aimed at assessing the impact of patient morphology on the dose, image quality, and diagnostic performance of our unenhanced low-dose CT protocol, which is performed with a low tube voltage, automatic tube current modulation, and ASIR, in patients with suspected renal colic.

Materials and Methods

This single-center study was approved by our local ethics committee. This study is retrospective, so the patients' written informed consent was not necessary.

Studied Population

This retrospective single-center study included all patients who were referred to our imaging department for evaluation of suspected renal colic and underwent unenhanced abdominopelvic CT performed with our routine low-dose protocol between January 1, 2012, and December 31, 2012. Patients were referred by our emergency department or by a physician from an outside institution. Patient selection was performed retrospectively by retrieving from our PACS (Impax ES, version 6, Agfa Technical Imaging Systems) all the abdominopelvic CT examinations performed in 2012 and by choosing only the unenhanced low-dose CT examinations of patients with suspected renal colic. CT examinations performed with other imaging settings and of patients referred for other indications (e.g., hematuria, follow-up CT for urolithiasis) were not included in our study. One patient was also excluded because of a technical issue during the low-dose CT acquisition.

For all patients, the following parameters were systematically recorded before the examination: sex, age (in years), weight (in kilograms), and height (in meters). For each patient, body mass index (BMI) was calculated as weight in kilograms divided by height in meters squared (weight / height^2 [kg/m^2]). Patients were classified according to their BMI as follows [19]: BMI < 18.5, thin; BMI ≥ 18.5 and < 25, normal weight; BMI ≥ 25 and < 30, overweight; and BMI ≥ 30, obese. Then patients were divided in two groups according to their BMI: patients with a BMI < 25 and those with a BMI ≥ 25.

CT Acquisition and Reconstruction Techniques

All examinations were performed with the patient in a supine position using a 64-MDCT unit (Optima 660, GE Healthcare). Every examination started with an acquisition of two scout views, a lateral view and an anteroposterior view, using 120 kV and 10 mA. The low-dose CT protocol consisted of an unenhanced helical craniocaudal acquisition that was centered on the urinary tract and ranged from the upper pole of the kidneys (spotted on the anteroposterior scout view) to the symphysis pubis. The tube voltage was set at 100 kV, but it remained possible to perform an acquisition using 120 kV for patients who weighed more than 80 kg and using 80 kV for patients who weighed less than 60 kg. Other acquisition settings were constant for all patients: automatic tube current modulation in the *x*-axis, *y*-axis, and *z*-axis (Smart mA, GE Healthcare) with a noise index setting of 50 for a slice thickness of 1.25 mm and a soft-tissue window; tube current minimum and maximum settings of 10 and 300 mA, respectively; a rotation time of 0.7 second; and a pitch of 1.375.

The noise index was set at 50 in consensus with all the radiologists of our department. After a 2-month experience (from November through December 2011) using different noise index levels, we chose the level that seemed to lead to the best trade-off between dose reduction and sufficient image quality for the diagnosis of renal colic.

Images were reconstructed with ASIR (ASiR, GE Healthcare) with a percentage setting of 50, a soft kernel, a slice thickness of 1.25 mm, and a slice interval of 1.25 mm. The ASIR percentage

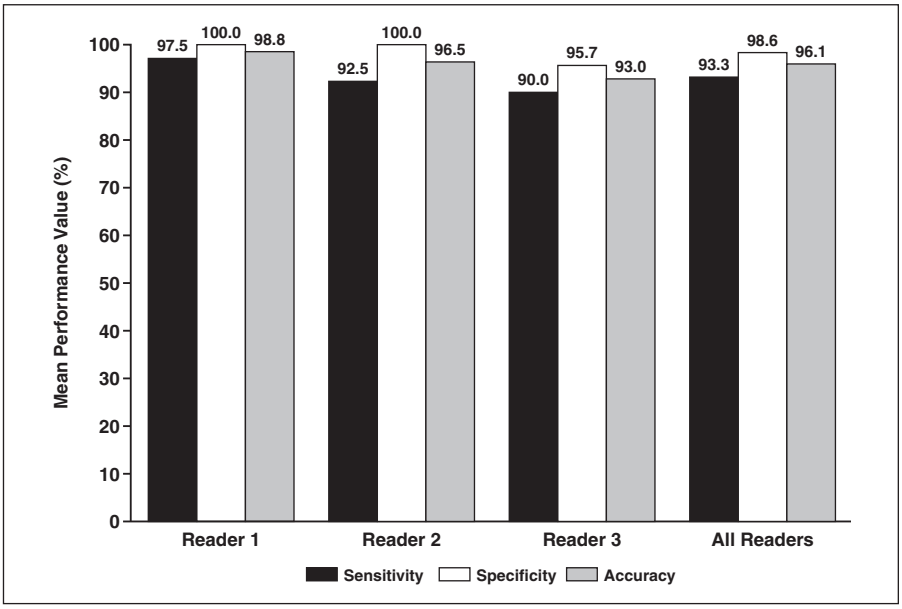

Fig. 1—Bar chart depicts mean sensitivity, specificity, and diagnostic accuracy of our low-dose CT protocol for diagnosis of renal colic for each reader and all three readers combined.

was the proportion of ASIR imaged within a mix of standard FBP images and ASIR images. This percentage was set according to the recommendations of the manufacturer.

When the radiologist had any doubt about the presence of a stone after the unenhanced low-dose acquisition, the radiologist could perform another unenhanced acquisition with a standard dose. The standard-dose study used automatic tube current modulation, a noise index setting of 21.5, and 120 kV, and the other acquisition and reconstruction settings were the same as those for the low-dose study.

Similarly, if no renal colic was visible on the first acquisition and another diagnosis was suspected, the radiologist could perform an additional abdominopelvic acquisition during the portal venous phase with a standard dose to complete the examination. The standard-dose study used a noise index setting of 21.5 and 120 kV, and the other acquisition settings were the same as those for the low-dose study.

All images from the examination and the report including the dosimetric data were sent directly to our PACS and were archived in the database of our PACS.

Images Analysis

Unenhanced low-dose CT images were analyzed by two senior radiologists who had 8 and 5 years of experience, respectively, in abdominopelvic CT reading at the time of the study (readers 1 and 2) and by a third-year resident in radiology (reader 3). The readers were not involved in patient selection and had no information about clinical data or the final diagnosis.

The readers did not have access to the potential additional acquisitions performed at a standard dose with or without contrast material. The CT interpretations were performed independently by the three readers on randomized examinations that had no patient-identifying information. Before interpreting the CT examinations, the readers completed a common training session consisting of 10 unenhanced low-dose abdominopelvic CT studies performed in November or December 2011 that were not included in the study. Images were visualized on a postprocessing workstation (ADW, version 4.6, GE Healthcare). The readers were allowed to use all the available visualization tools. They could increase the slice thickness, select display multiplanar reformations or maximum intensity projections, and use zoom.

During the reading session, the readers assessed the examinations for the presence or absence of renal colic. If the diagnosis was positive for renal colic, the readers recorded the size and localization of the responsible stone. For all examinations, they graded diagnostic confidence on a 3-point Likert scale (1 = no diagnostic confidence, 2 = confidence with reservations, or 3 = total diagnostic confidence) and graded subjective image quality for the diagnosis of renal colic on a 5-point Likert scale (1 = unacceptable image quality, 2 = suboptimal image quality, 3 = acceptable image quality, 4 = good image quality, or 5 = excellent image quality).

Final Diagnosis

For each examination, the final diagnosis was established by another study investigator who had 7 years of experience in abdominopelvic CT reading at the time of the study. He had access to the patient database, which included the unenhanced low-dose CT study and potential additional acquisitions with or without contrast material performed at a standard dose, and to the medical database, which included clinical, biologic, and follow-up information such as follow-up CT, complementary ultrasound or MRI, reports of medical appointments, and surgery reports.

Objective Evaluation of Image Noise

Image noise in unenhanced low-dose CT was objectively evaluated by measuring the SD of the attenuation (in Hounsfield units) in a region of interest (ROI) with an area of 100 mm^2. The ROIs were placed in the left psoas muscle, at the level of the fifth lumbar vertebra, in a standardized way by the same investigator (investigator who established the final diagnosis) on a 1.25-mm-thick slice in soft-tissue window settings on a postprocessing workstation (ADW 4.6).

Evaluation of Radiation Dose

Radiation dose data were directly provided in the examination report, which was accessible from the PACS. The data consisted of the volume CT dose index ($CTDI_{vol}$), in mGy, and the dose-length product (*DLP*), in mGy × cm, of the unenhanced low-dose CT examination. The effective dose (*ED*), in mSv, was calculated using a tissue conversion coefficient (k) for the abdomen of 0.015 [20] according to the following formula [21]:

$$ED = k \times DLP.$$

To compare the average doses of our low-dose CT protocol and the standard-dose CT protocol, we compared the average DLP of the additional contrast acquisition with the average DLP of the unenhanced low-dose acquisition for the patients who underwent an additional contrast-enhanced examination at the standard dose.

Statistical Analysis

Data were analyzed using statistics software (R Foundation for Statistical Computing version 2.15.3) for Microsoft Windows. The sensitivity, specificity, and diagnostic accuracy of the unenhanced low-dose protocol were calculated for each reader on the basis of the presence or absence of renal colic compared with the final diagnosis given by the study investigator as a reference. Interobserver variability was calculated using Cohen's kappa test. Interobserver variability was considered excellent for a kappa value of greater than 0.80. For the patients who underwent an additional standard-dose contrast acquisition, the average DLP of the low-dose CT study and the average DLP of the standard-dose CT study were compared using the Wilcoxon signed rank test. A correlation coefficient was calculated between the CTDI and BMI using a linear correlation Pearson test. The CTDIs, averages of objective image noise measurements, and average scores of image quality and diagnostic confidence (average of the three readers' scores) were compared for the two patient groups (BMI < 25 vs BMI ≥ 25) using a Mann-Whitney *U* test. The average diagnos-

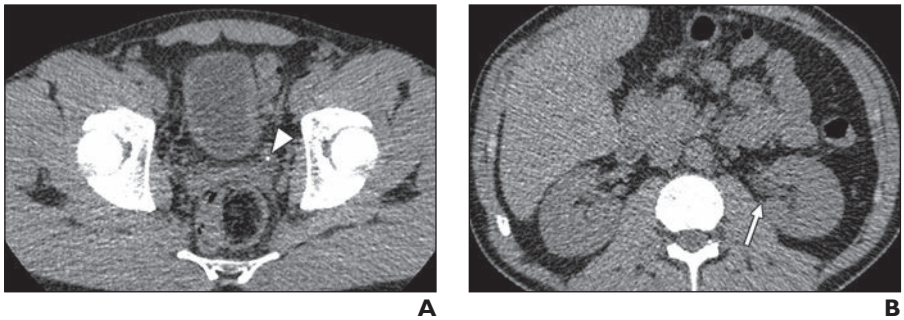

Fig. 2—41-year-old man (height, 1.78 m; weight, 78 kg; body mass index, 25.5) who presented with acute left-sided lumbar pain. Unenhanced low-dose CT examination (100 kV; noise index, 50) with dose-length product of 105 mGy × cm and effective dose of 1.6 mSv was performed.
A, Axial image obtained with 1.25-mm slice thickness shows 2.5-mm urinary stone in pelvic ureter (*arrowhead*) that led to false-negative finding of "small phlebolith" by all three readers.
B, Axial image obtained with 1.25-mm slice thickness shows small obstructive dilatation (*arrow*) without perirenal fat stranding.

tic accuracy, number of false-positives, and number false-negatives were compared using a Fisher test. A p value < 0.05 was considered to indicate a significant statistical difference.

Results

Patient and Acquisition Characteristics

Eighty-six CT examinations of 86 patients were included in this study. There were 49 men and 37 women. The average age of the study group was 43.8 ± 14.7 (SD) years (range, 21–82 years), and the average BMI was 25.3 ± 4.2 (SD) (range, 15.6–42.9; median, 25.3). Based on BMI, four patients (5%) were thin, 35 (41%) had a normal body weight, 39 (45%) were overweight, and eight (9%) were obese. Thirty-nine patients (45%) had a BMI < 25 and 47 (55%) had a BMI ≥ 25.

Among the 86 low-dose CT examinations performed, the tube voltage was modified for six examinations: It was set at 80 kV for one CT study (patient weight, 58 kg; BMI, 22.7) and at 120 kV for five studies (two patients weighing 81 kg with a BMI of 27.7 and 28; three patients weighing 84, 100, and 107 kg with a BMI of 29.5, 31.6, and 42.8, respectively).

For 33 of the 86 patients (38.4%), a complementary contrast acquisition was performed during the portal venous phase using the standard-dose protocol. There were 13 men and 20 women with an average BMI of 24.1 ± 3.1 (SD) (range, 17.6–31.9). For two of the 86 (2.3%) patients, an additional unenhanced acquisition was performed at the standard dose. There were two men with a BMI of 25.9 and 32.

Final Diagnosis

Of the 86 patients, 40 (46.5%) had a final diagnosis of renal colic. The average size of the stones was 4.4 ±2 (SD) mm (range, 2–10 mm). Eight stones were located in the lumbar ureter, two at the cross of the lumbar ureter with the iliac vessels, four in the pelvic ureter, and 26 at the ureterovesical meatus. Among the 46 patients who did not have renal colic, a diagnosis was made in 28 (32.5%): discoradicular abnormalities in 10 patients, urinary tract infections in seven patients, gynecological infections in two patients, pyeloureteral junction syndrome in one patient, renal infarction in one patient, renal colic cured at the time of CT in one patient, acute appendicitis in two patients, ileitis in one patient, diverticulitis in one patient, colitis in one patient, and stomach ulcer in one patient. Finally, for the remaining 18 patients (21%) who did not have renal colic, the causes of the painful symptoms could not be explained.

Diagnostic Performance

The sensitivity, specificity, and diagnostic accuracy of the unenhanced low-dose protocol for each of the three readers and the average of these values are displayed in Figure 1. The interobserver variability for the diagnosis of renal colic between the readers was excellent: Kappa was 0.88 between readers 1 and 3 and between readers 2 and 3 and was 0.95 between readers 1 and 2.

For the most experienced reader (reader 1), the unenhanced low-dose protocol had a high sensitivity and a high specificity, 97.5% and 100%, respectively, and a diagnostic accuracy of 98.8%. Reader 1 made one interpretation mistake (a false-negative), reader 2 made three mistakes (three false-negatives), and reader 3 made six mistakes (four false-negatives and two false-positives). In total, the three readers made 10 mistakes when interpreting seven CT examinations (seven patients). One false-negative interpretation of the same examination was made by all three readers (Fig. 2); for another examination, the interpretations of both readers 2 and 3 were false-negative (Fig. 3). Of the five patients who had at least one false-negative interpretation by one of the readers, three had a stone enclosed in the ureterovesical meatus and two had a stone in the pelvic ureter located just upstream from the ureterovesical meatus. These five stones had a diameter of less than 3 mm.

In terms of diagnostic accuracy, false-negatives, and false-positives, there was no significant difference between the patients with a BMI < 25 and those with a BMI ≥ 25 (Table 1). Of the 10 mistakes, five (three false-negatives and two false-positives) were made interpreting studies of patients with a BMI < 25 and five (five false-negatives) of patients with a BMI ≥ 25. No mistake was made interpreting the studies of the eight patients with a BMI ≥ 30.

Image Quality and Diagnostic Confidence Scores

The mean diagnostic confidence and image quality scores for all patients are recorded in Figure 4; these scores are also sorted according to patient BMI and show that the higher the BMI, the higher the scores. The scores of diagnostic confidence and of image quality were significantly better for patients with a BMI ≥ 25 than for those with a BMI < 25 (Table 1).

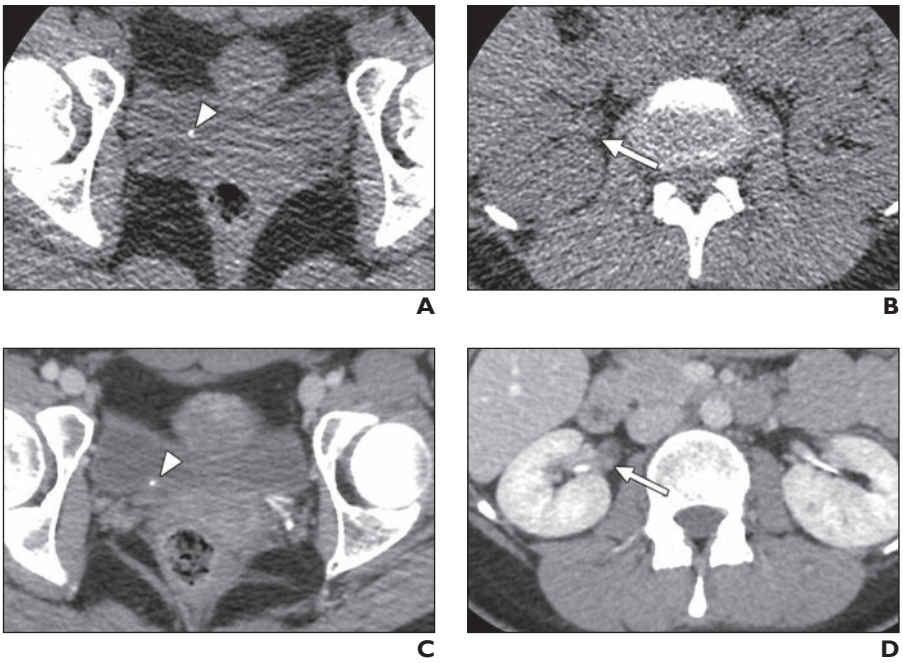

Fig. 3—22-year-old woman (height, 1.72 m; weight, 62 kg; body mass index, 21) who presented with acute right-sided flank pain.
A and **B,** Axial unenhanced low-dose CT images obtained with 1.25-mm slice thickness (100 kV; noise index, 50; dose-length product [DLP], 72 mGy × cm; effective dose [ED], 1.1 mSv) show 2-mm stone at junction of ureter with bladder (*arrowhead*, **A**) with minimal obstructive dilatation (*arrow*, **B**). Stone was misinterpreted as "small phlebolith" by two of three readers.
C and **D,** Axial portal phase enhanced standard-dose CT images obtained with 1.25-mm slice thickness (120 kV; noise index, 21.5; DLP, 333 mGy × cm; ED, 5 mSv) show stone (*arrowhead*, **C**) depicted in **A** and allow better visualization of obstructive dilatation (*arrow*, **D**) in comparison with unenhanced low-dose CT image shown in **B**.

Objective Evaluation of Image Noise

The average of the objective image noise measurements for all patients was 33.6 ± 7.2 (SD) HU. The distribution of noise values according to patient BMI is given in Table 2. Concerning image noise measurements, there was no significant difference between the patients with a BMI < 25 and those with a BMI ≥ 25 (Table 1).

Dose Evaluation

Average CTDIs, DLPs, and EDs for all patients were 3.1 ±1.2 mGy (range, 1.4–8.1 mGy), 140.6 ±59.4 mGy × cm (range, 52.4–383.2 mGy × cm), and 2.1 ±0.9 mSv (range, 0.8–5.7 mSv), respectively. The distribution of CTDIs according to patient BMI is given in Table 2. There was an excellent correlation between patient BMI and the CTDI of the low-dose CT examination: The Pearson linear correlation coefficient was 0.81 (Fig. 5). There was a significant difference between the radiation dose of patients with a BMI < 25 and that of patients with a BMI ≥ 25 (mean, 2.4 vs 3.7 mGy, respectively; $p < 0.001$) (Table 1).

Concerning the 33 examinations with an additional standard-dose contrast-enhanced CT study during the venous portal phase, the average DLP of the contrast acquisitions was 583.2 ± 215.2 mGy × cm (range, 324.0–899.2 mGy × cm). There was a significant difference between the dose of the unenhanced low-dose CT examinations and that of the contrast-enhanced standard-dose CT examinations (140.6 vs 583.2 mGy × cm, respectively; $p < 0.001$), with a 76% reduction in dose for the low-dose CT protocol.

TABLE 1: Dose, Objective Image Noise Measurement, Image Quality and Diagnostic Confidence Scores, Diagnostic Accuracy, and False-Positive and False-Negative Results for All Patients and Patient Groups Classified by Body Mass Index[a] (BMI)

Patient or Study Characteristic	All Patients	BMI < 25	BMI ≥ 25	*p*
No. (%) of patients	86 (100)	39 (45)	47 (55)	
$CTDI_{vol}$ (mGy)				< 0.001
Mean ±SD	3.1 ±1.2	2.4 ±0.8	3.7 ±1.2	
Range	1.4–8.1	1.4–4.3	2.0–8.1	
Objective image noise (HU)				0.56
Mean ±SD	33.6 ±7.2	34.1 ±6.2	33.1 ±6.2	
Image quality score[b]				< 0.001
Mean ±SD	3.6 ±0.7	3.4 ±0.6	3.7 ±0.6	
Diagnostic confidence score[c]				< 0.001
Mean ±SD	2.6 ±0.6	2.5 ±0.6	2.8 ±0.4	
Diagnostic accuracy (%)	96.1	95.7	96.4	0.83
False-negative (no. of examinations)[d]	8	3	5	0.48
False-positive (no. of examinations)[d]	2	2	0	0.14

Note—$CTDI_{vol}$ = Volume CT dose index.
[a]Calculated as weight in kilograms divided by height in meters squared.
[b]Readers graded subjective image quality for the diagnosis of renal colic on the following 5-point Likert scale: 1 = unacceptable image quality, 2 = suboptimal image quality, 3 = acceptable image quality, 4 = good image quality, or 5 = excellent image quality.
[c]Readers graded diagnostic confidence on the following 3-point Likert scale: 1 = no diagnostic confidence, 2 = confidence with reservations, or 3 = total diagnostic confidence.
[d]Average for all three readers.

Discussion

The results of our study confirm that the use of our low-dose CT protocol for the diagnosis of renal colic leads to a 76% dose reduction compared with our standard-dose contrast acquisition (140.6 vs 583.2 mGy × cm, respectively). The average dose of the low-dose CT protocol (2.1 mSv) was less than the average dose of an excretory urography examination (2.6 mSv [22]). This dose value of 2.1 mSv is also in accordance with the doses of low-dose CT examinations performed for the detection of renal colic described in other studies, which ranged from 0.7 to 2.7 mSv [23]. Even the average dose for overweight patients and obese patients (2.5 mSv) was less than the average dose of an excretory urography examination (2.6 mSv [22]).

Despite this dose reduction, the diagnostic performance of our low-dose CT protocol for the detection of renal colic was excellent. The most experienced reader (reader 1) had a diagnostic accuracy of 98.8%, and the average diagnostic accuracy for all three readers was 96.1%, which matches the data described in other studies [23]. Our results also showed excellent interobserver concordance.

As we expected, when comparing the dose results of the two groups of patients with a BMI < 25 and BMI ≥ 25, the dose for the CT examinations of the overweight and obese patients was significantly greater. This difference in dose by patient BMI is because of the use of automatic tube current modulation, which adapts the tube current to the patient's body habitus. A higher tube current value is used for overweight patients and obese patients to maintain image quality; this higher tube current setting, therefore, leads to a significant increase in the dose delivered to these patients. In our study, there was an excellent correlation between the $CTDI_{vol}$ and BMI (Pearson linear correlation coefficient = 0.81), which is equivalent to those reported by Mulkens et al. [14] (range of Pearson correlation coefficients, 0.85–0.88) who also used automatic tube current modulation on a scanner made by another manufacturer. Concerning the diagnostic performance of our low-dose protocol, there is no significant difference for patients with a BMI < 25 and those with a BMI ≥ 25, with diagnostic accuracies of 95.7% and 96.4%, respectively. Our study shows that, thanks to the use of automatic tube current modulation, it is possible to perform a low-dose CT protocol for suspected renal colic in overweight patients and obese patients, which is consistent with the results reported by Mulkens et al. [14]. However, the use of automatic tube current modulation requires an increase in dose when imaging overweight patients and obese patients.

It is interesting to note that, although the quantitative measurements of image noise remained stable regardless of patient BMI, the scores of image quality and of diagnostic confidence increased progressively with BMI. Thus, the image quality and diagnostic confidence scores were significantly better for the patients with a BMI ≥ 25 than for the patients with a BMI < 25. These results could seem paradoxical, but we think that they can be explained by the fact that, at the same noise level, it is easier to diagnose renal colic when the patient has a greater amount of intraabdominal and intrapelvic fat [24]. Indeed, it is easier to delimit the pathway of the ureters when fat is present even if there is greater image noise.

We also think that it is easier to see the indirect signs of renal colic, such as perirenal infiltration or a rim sign, on images of obese patients. In our study, despite the fact that we found the same number of reader interpretation errors for patients with a BMI < 25 as for patients with a BMI ≥ 25, none of the reader interpretation errors was made on examinations of obese patients. Seven of the eight false-negatives were because of the presence of a pelvic phlebolith in patients with a BMI ≤ 25.9. The two false-positive reader interpretation errors were also caused by difficulties differentiating a phlebolith from a urinary stone in two patients of normal weight (BMI of 22.5 and 23.0). These results are in accordance with the study of Mulkens et al. [14] in which two false-positives were two pelvic phleboliths in two thin patients (BMI of 19.8 and 20.1).

In the first studies that used a reduced but constant tube current, diagnostic difficulties mainly involved interpreting examinations of obese patients [9, 12]. Our study shows that the use of automatic tube current modulation seems to lead to the opposite results: Diagnostic difficulties mainly occurred when interpreting examinations of thin patients. We used automatic tube current modulation, which requires a configuration of a noise index and maximal and minimal tube current thresholds. For our low-dose CT protocol, the maximal threshold was set to 300 mA (i.e., 152 mAs). Given the better image quality for patients with a BMI ≥ 25, we think that it would be possible to reduce this maximal threshold to reduce the dose for obese and overweight patients while preserving image quality that is good enough for the diagnosis of renal colic. In a pilot study in which they analyzed the use of automatic tube current modulation with ASIR and a low tube voltage, Kulkarni et al. [18] had indeed set the maximal tube current–exposure time threshold at 55 mAs with a noise index similar to ours. Other studies are necessary to evaluate the optimal maximal tube current threshold.

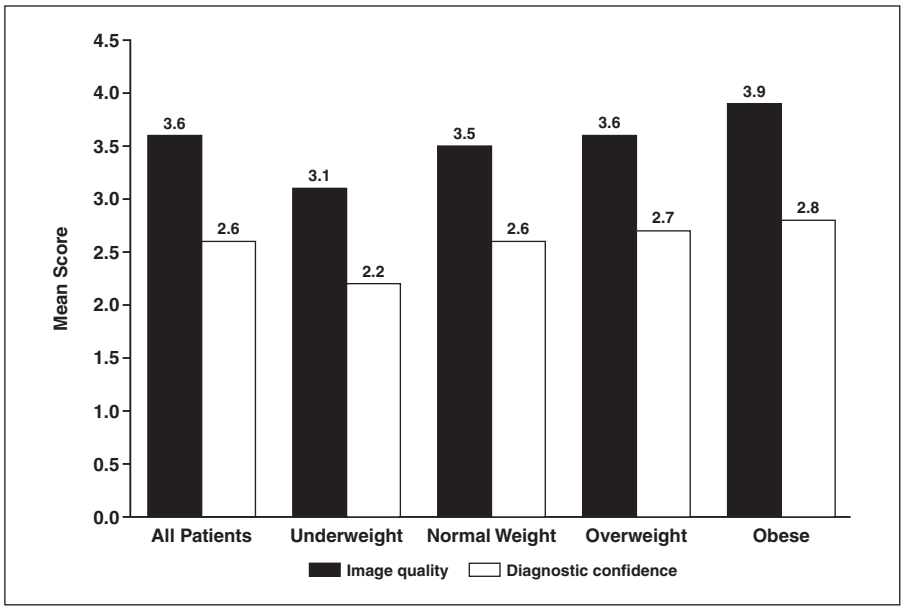

Fig. 4—Bar chart depicts mean scores of image quality and diagnostic confidence of unenhanced low-dose CT protocol for diagnosis of renal colic for all patients and for different categories of patients by body mass index (BMI) (calculated as weight in kilograms divided by height in meters squared). For all examinations, readers graded subjective image quality for diagnosis of renal colic on 5-point Likert scale (1 = unacceptable image quality, 2 = suboptimal image quality, 3 = acceptable image quality, 4 = good image quality, 5 = excellent image quality) and graded diagnostic confidence on 3-point Likert scale (1 = no diagnostic confidence, 2 = confidence with reservations, 3 = total diagnostic confidence).

Our study also confirms that it is possible to perform an acquisition with 100 kV for most patients including overweight patients and obese patients. Reducing the tube voltage from 120 to 100 kV leads to a dose reduction of almost 35%, but it also leads to an increase in the noise of approximately 30% [25]. Thanks to an important reduction in image noise while keeping an equiv-

TABLE 2: Dose Data and Objective Image Noise Measurements for Unenhanced Low-Dose CT Examinations of Patients Classified by Body Mass Index[a] (BMI)

Patient or Study Characteristic	BMI < 18.5 (Thin)	18.5 ≤ BMI < 25 (Normal Weight)	25 ≤ BMI < 30 (Overweight)	BMI ≥ 30 (Obese)
No. (%) of patients	4 (5)	35 (41)	39 (45)	8 (9)
$CTDI_{vol}$ (mGy)				
Mean ±SD	2.0 ±0.6	2.4 ±0.8	3.4 ±0.8	5.1 ±1.9
Range	1.4–2.7	1.5–4.3	2.1–5.1	3–8.1
Dose-length product (mGy × cm)				
Mean ±SD	79.2 ±22.8	109.7 ±35.3	155.0 ±41.3	236.2 ±93.6
Range	52.4–106.6	58.6–209.3	92.5–263.1	124.7–383.2
Effective dose (mSv)				
Mean ±SD	1.2 ±0.3	1.6 ±0.5	2.3 ±0.6	3.5 ±1.4
Range	0.8–1.6	0.9–3.1	1.4–3.9	1.9–5.7
Objective image noise (HU)				
Mean ±SD	34.1 ±7.2	34.1 ±6.2	33.3 ±4.7	32.1 ±6.4

Note—$CTDI_{vol}$ = Volume CT dose index.
[a]Calculated as weight in kilograms divided by height in meters squared.

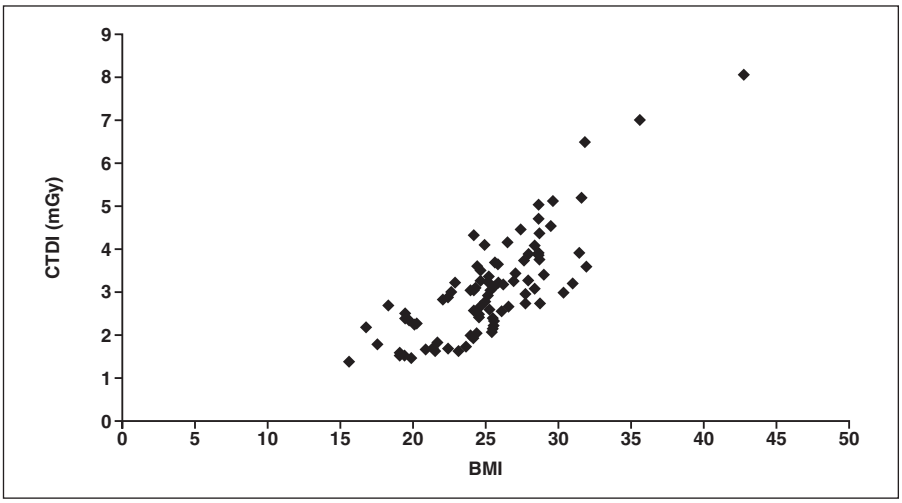

Fig. 5—Graph shows excellent correlation between body mass index (BMI), calculated as weight in kilograms divided by height in meters squared, and CT dose index ($CTDI_{vol}$) of unenhanced low-dose CT: Pearson linear correlation coefficient was 0.81.

alent dose [17], the iterative reconstructions make acquisitions at 100 kV feasible without any important increase in image noise. Only five of the 13 patients weighing more than 80 kg in our study underwent low-dose CT with 120 kV. These cases show that at 100 kV the image quality and the diagnostic performance remain acceptable even for studies of most obese and overweight patients. An even greater tube voltage reduction can be contemplated: Kulkarni et al. [18] reported good image quality using a low tube voltage set at 80 kV in patients who weighed less than 90 kg and at 100 kV in patients who weighed more than 90 kg. However, the possibility of using 80 kV for some categories of patients must be confirmed by other studies based on BMI and not on weight.

There are several limitations to our study that need to be mentioned. First, this study was retrospective and included a relatively low number of patients, especially obese patients. A prospective study of a larger number of patients must be performed to confirm our results. Second, there was no reference imaging technique that could give a final diagnosis for all of our patients, like could have been done thanks to a standard-dose acquisition. This method does not seem ethically acceptable to us because it would have required additional irradiation of a population that includes a large proportion of young or healthy patients. However, the reference method to make the final diagnosis that was chosen, one that relies on all the imaging and patient-tracking data, has been used in several studies [7, 13, 14, 26]. Third, we did not try to assess the performance of our low-dose CT protocol for the detection of a diagnosis because that was not the aim of our study. Moreover, when no abnormality was detected on the low-dose CT study, most of our patients underwent a complementary standard-dose contrast-enhanced CT study. We think that contrast administration in this setting is necessary because even an unenhanced standard-dose CT study with normal findings does not allow pathologic entities such as renal infarcts to be eliminated from the differential diagnosis; most pathologic entities that are diagnosed thanks to unenhanced CT require a complementary contrast acquisition. Finally, our results are valid for only an acquisition performed on the CT unit used for our study with our specific automatic tube current modulation software. Other studies are necessary to generalize these results to CT examinations performed on units made by other manufacturers and also to analyze the effect of some settings, especially the maximal tube current threshold suggested, on dose and on diagnostic performance of low-dose CT.

In conclusion, our unenhanced low-dose CT protocol performed with automatic tube current modulation, a low tube voltage setting, and the ASIR iterative reconstruction for patients with suspected renal colic has an excellent diagnostic performance for all patients. However, better image quality and better diagnostic confidence were achieved for patients with a BMI ≥ 25, despite a greater radiation dose, compared with patients with a BMI < 25.

References

1. Smith RC, Rosenfield AT, Choe KA, et al. Acute flank pain: comparison of non-contrast-enhanced CT and intravenous urography. *Radiology* 1995; 194:789–794
2. Sung MK, Singh S, Kalra MK. Current status of low dose multi-detector CT in the urinary tract. *World J Radiol* 2011; 3:256–265
3. Leusmann DB, Niggemann H, Roth S, von Ahlen H. Recurrence rates and severity of urinary calculi. *Scand J Urol Nephrol* 1995; 29:279–283
4. Katz SI, Saluja S, Brink JA, Forman HP. Radiation dose associated with unenhanced CT for suspected renal colic: impact of repetitive studies. *AJR* 2006; 186:1120–1124
5. Smith-Bindman R, Lipson J, Marcus R, et al. Radiation dose associated with common computed tomography examinations and the associated lifetime attributable risk of cancer. *Arch Intern Med* 2009; 169:2078–2086
6. Berrington de González A, Mahesh M, Kim KP, et al. Projected cancer risks from computed tomography scans performed in the United States in 2007. *Arch Intern Med* 2009; 169:2071–2077
7. Diel J, Perlmutter S, Venkataramanan N, Mueller R, Lane MJ, Katz DS. Unenhanced helical CT using increased pitch for suspected renal colic: an effective technique for radiation dose reduction? *J Comput Assist Tomogr* 2000; 24:795–801
8. Liu W, Esler SJ, Kenny BJ, Goh RH, Rainbow AJ, Stevenson GW. Low dose nonenhanced helical CT of renal colic: assessment of ureteric stone detection and measurement of effective dose equivalent. *Radiology* 2000; 215:51–54
9. Hamm M, Knopfle E, Wartenberg S, Wawroschek F, Weckermann D, Harzmann R. Low dose unenhanced helical computed tomography for the evaluation of acute flank pain. *J Urol* 2002; 167:1687–1691
10. Heneghan JP, McGuire KA, Leder RA, Delong DM, Yoshizumi T, Nelson RC. Helical CT for nephrolithiasis and ureterolithiasis: comparison of conventional and reduced radiation dose techniques. *Radiology* 2003; 229:575–580
11. Kim BS, Hwang IK, Choi YW, et al. Low-dose and standard-dose unenhanced helical computed tomography for the assessment of acute renal colic: prospective comparative study. *Acta Radiol* 2005; 46:756–763
12. Poletti PA, Platon A, Rutschmann OT, Schmidlin FR, Iselin CE, Becker CD. Low-dose versus standard-dose CT protocol in patients with clinically suspected renal colic. *AJR* 2007; 188:927–933
13. Tack D, Sourtzis S, Delpierre I, de Maertelaer V, Gevenois PA. Low-dose unenhanced multidetector CT of patients with suspected renal colic. *AJR* 2003; 180:305–311
14. Mulkens TH, Daineffe S, De Wijngaert R, et al. Urinary stone disease: comparison of standard-

dose and low-dose with 4D MDCT tube current modulation. *AJR* 2007; 188:553–562

15. Xu J, Mahesh M, Tsui BM. Is iterative reconstruction ready for MDCT? *J Am Coll Radiol* 2009; 6:274–276
16. Thibault JB, Sauer KD, Bouman CA, Hsieh J. A three-dimensional statistical approach to improved image quality for multislice helical CT. *Med Phys* 2007; 34:4526–4544
17. Hara AK, Paden RG, Silva AC, Kujak JL, Lawder HJ, Pavlicek W. Iterative reconstruction technique for reducing body radiation dose at CT: feasibility study. *AJR* 2009; 193:764–771
18. Kulkarni NM, Uppot RN, Eisner BH, Sahani DV. Radiation dose reduction at multidetector CT with adaptive statistical iterative reconstruction for evaluation of urolithiasis: how low can we go? *Radiology* 2012; 265:158–166
19. Garrow JS, Webster J. Quetelet's index (W/H2) as a measure of fatness. *Int J Obes* 1985; 9:147–153
20. Deak PD, Smal Y, Kalender WA. Multisection CT protocols: sex- and age-specific conversion factor used to determine effective dose from dose-length product. *Radiology* 2010; 257:158–166
21. International Commission on Radiological Protection. The 2007 recommendations of the International Commission on Radiological Protection: ICRP Publication 103. *Ann ICRP* 2007; 37:1–332
22. Yakoumakis E, Tsalafoutas IA, Nikolaou D, Nazos I, Koulentianos E, Proukakis C. Differences in effective dose estimation from dose-area product and entrance surface dose measurements in intra-venous urography. *Br J Radiol* 2001; 74:727–734
23. Niemann T, Kollmann T, Bongartz G. Diagnostic performance of low-dose CT for detection of urolithiasis: a meta-analysis. *AJR* 2008; 191:396–401
24. Katz DS, Venkataramanan N, Napel S, Sommer FG. Can low dose unenhanced multidetector CT be used for routine evaluation of suspected renal colic? *AJR* 2003; 180:313–315
25. McNitt-Gray MF. AAPM/RSNA physics tutorial for residents: topics in CT—radiation dose in CT. *RadioGraphics* 2002; 22:1541–1553
26. Kluner C, Hein PA, Gralla O, et al. Does ultra-low-dose CT with a radiation dose equivalent to that of KUB suffice to detect renal and ureteral calculi? *J Comput Assist Tomogr* 2006; 30:44–50

FOR YOUR INFORMATION

See the *AJR's* monthly Journal Club article in this issue on page 493.

Discussion et conclusion du chapitre 3 :

Les résultats présentés dans ce chapitre montrent comment il est possible de réduire la dose des scanners en optimisant certains paramètres d'acquisition et de reconstruction des images.

Article 1 : Réduction de dose dans l'exploration du rachis lombaire grâce au scanner 320-détecteurs : étude initiale.

Notre étude montre que le mode d'acquisition peut avoir un impact non négligeable sur la dose des scanners. Lors de l'acquisition de scanners lombaires, nous avons retrouvé une réduction de la dose de 35 % en faveur du mode d'acquisition volumique par rapport au mode d'acquisition hélicoïdal classique, à qualité d'image constante. Ce résultat est principalement dû à la suppression de l'irradiation pré et post-hélice liée au phénomène d'*overranging* en mode hélicoïdal. Par contre, compte-tenu de la longueur d'acquisition importante des scanners lombaires (26 cm), il était nécessaire de réaliser une acquisition de deux volumes successifs. Cette juxtaposition de deux volumes engendre une irradiation supplémentaire à la zone de chevauchement des deux volumes et peut aussi être à l'origine d'un artéfact de décalage sur les images du scanner à la zone de jonction des deux volumes. Ainsi, l'acquisition volumique sera surtout préférée en cas d'acquisition pour des volumes avec une couverture d'acquisition inférieure à 16 cm. Cette étude était une étude initiale. Nous avons essayé de confirmer ces résultats par une nouvelle étude prospective de plus grande envergure mais cette dernière n'a malheureusement pas aboutit. Les résultats intermédiaires ne retrouvaient pas un niveau de réduction de la dose aussi important que dans notre étude initiale. Cette différence peut être liée à plusieurs facteurs. Tout d'abord, dans notre étude initiale, l'indice de bruit de la modulation automatique du mA était légèrement supérieur pour l'acquisition volumique par rapport à l'acquisition hélicoïdale (7,5 versus 6). Cette différence peut expliquer une partie de l'écart de dose entre les deux protocoles. De plus, lors de notre nouvelle étude, un changement de version du logiciel de reconstruction des images a pu également influencer la dose et la qualité des images des scanners. Enfin, l'évaluation de la qualité d'image de notre étude initiale n'était peut-être pas assez pertinente et compte-tenu d'un faible nombre de patients inclus, l'étude initiale n'a peut-être pas permis de montrer une différence significative de qualité d'image alors que celle-ci existait peut-être. Même si l'étude complémentaire n'a

pas permis de retrouver des résultats aussi positifs que dans l'étude initiale, nos résultats ont toutefois été confirmés par une étude portant sur la comparaison des modes d'acquisition volumique et hélicoïdal avec le scanner 320-détecteurs dans une population pédiatrique. Kroft LJ *et al.* ont effectivement montré une réduction de la dose au profit du mode volumique [48]. Cette réduction était d'autant plus importante que la longueur d'acquisition était petite. Ainsi, pour une longueur d'acquisition de 16 cm, il retrouvait une réduction de 18 % de la dose en faveur du mode volumique par rapport au mode hélicoïdal et pour une acquisition de 80 mm, une réduction de 40 % de la dose, à qualité d'image équivalente. Un autre avantage de l'acquisition volumique était la rapidité d'acquisition du volume (0,35 s pour l'acquisition d'un volume de 16 cm), ce qui permettait de réduire de manière importante les artéfacts de mouvement des enfants en comparaison avec le mode hélicoïdal. Au final, le mode d'acquisition volumique sera choisi pour les scanners avec une faible couverture d'acquisition. A l'inverse, pour les scanners ayant une grande couverture d'acquisition, le mode hélicoïdal sera préféré.

Article 2 : Amélioration de la qualité d'image scanographique en utilisant les reconstructions itératives Adaptive Iterative Dose Reduction avec une acquisition wide-volume sur un scanner 320-détecteurs.

Notre étude confirme que les reconstructions itératives AIDR permettent de réduire de manière significative le bruit de l'image par rapport aux reconstructions standard FBP. La réduction du bruit de l'image était calculée à 31 % sur les scanners lombaires des patients. Etant donné qu'il existe une relation directe entre le bruit de l'image et la dose (le bruit de l'image est inversement proportionnel à la racine carrée du mA et le mA est directement proportionnel à la dose [38]), notre étude nous a permis d'estimer qu'il était possible de réduire d'environ 52 % la dose de nos scanners lombaires avec les reconstructions itératives AIDR par rapport aux reconstructions standard en FBP. Par ailleurs, notre étude sur fantôme a montré qu'avec l'utilisation des reconstructions itératives la réduction du bruit de l'image ne s'accompagne pas d'une altération de la résolution spatiale. Ce point est crucial car en pratique clinique d'autres méthodes permettent de réduire le bruit de l'image. En particulier, l'utilisation d'un filtre plus « mou » permet de lisser l'image, de même que l'épaississement des coupes. Toutefois, ces deux méthodes permettant de réduire le bruit de l'image sont aussi à l'origine d'une dégradation de la résolution spatiale, à l'inverse des reconstructions

itératives. Par contre, l'utilisation des reconstructions itératives est à l'origine d'une modification de l'aspect des images qui apparaissent « lissées » ou « informatisées ». Cette modification de l'aspect des images est principalement liée à la modification de la distribution des spectres de fréquence spatiale du bruit entre les images FBP et AIDR [41]. Malheureusement, lors de cette étude, il ne nous a pas été techniquement possible de calculer ces spectres afin de confirmer ces modifications. De même, lors de l'étude sur patient, nous n'avons pu calculer directement la réduction de la dose car il n'était pas éthique de faire deux acquisitions (une à dose normale avec les reconstructions FBP et une à dose réduite de moitié avec les reconstructions AIDR) pour un même patient. Enfin, nous n'avons pu évaluer les reconstructions AIDR qu'en mode volumique car celles-ci n'étaient pas disponibles pour les acquisitions hélicoïdales.

Article 3 : Réduction de la dose des scanners abdominopelviens grâce aux reconstructions itératives AIDR 3D.

Notre étude sur patient évaluant l'impact des reconstructions itératives AIDR 3D a montré qu'il était possible de réduire de moitié la dose d'un scanner abdominopelvien avec les reconstructions itératives AIDR 3D par rapport aux reconstructions standard en FBP. Ces résultats ont été obtenus grâce à l'utilisation de deux scanners d'un même patient réalisés sans et après implantation des reconstructions itératives. Sous réserve de l'évaluation de l'absence de modification du morphotype des patients entre les deux scanners, nous avons ainsi pu montrer directement la réduction de la dose à qualité d'image équivalente grâce aux reconstructions itératives AIDR 3D. A partir d'une même acquisition, nous avons aussi montré que l'utilisation des reconstructions itératives par rapport aux reconstructions en FBP était à l'origine d'une amélioration significative de la qualité d'image objective et subjective. Cette étude montre bien les différentes manières d'utiliser les reconstructions itératives en pratique clinique : soit elles permettent de réduire la dose à qualité d'image constante, soit elles améliorent la qualité d'image à dose constante. Il est aussi possible de réduire un peu la dose tout en améliorant la qualité d'image. Ces différentes options seront choisies notamment en fonction du contexte clinique. Par exemple, chez un patient jeune la réduction de la dose sera favorisée alors que pour une personne âgée pour laquelle le risque de cancer radio-induit devient négligeable, l'amélioration de la qualité d'image sera plus intéressante. Dans notre étude, nous avons aussi retrouvé une patiente porteuse d'un dispositif intra-utérin métallique

pour laquelle les reconstructions itératives AIDR 3D permettaient de réduire les artéfacts métalliques et de renforcement du faisceau par rapport aux images FBP. Il semble donc que ces reconstructions AIDR 3D permettent également de réduire ces artéfacts. Une autre étude portant sur des scanners de patient avec des prothèses métalliques serait intéressante pour vérifier cette hypothèse.

Article 4 : Scanner basse dose avec la modulation automatique du milliampérage, les reconstructions Adaptive Statistical Iterative Reduction et un faible kilovoltage pour le diagnostic des coliques néphrétiques : impact de l'indice de masse corporelle.

Notre étude a permis de montrer que malgré l'utilisation de la modulation automatique du mA durant l'acquisition d'un scanner basse dose pour le bilan d'une colique néphrétique, les scores de qualité d'image subjective et de confiance dans le diagnostic étaient significativement meilleurs chez les patients avec un IMC > 25 kg/m² par rapport aux patients avec un IMC < 25 kg/m². Pourtant, la mesure objective du bruit de l'image confirme le bon fonctionnement de la modulation automatique du mA avec un niveau de bruit de l'image constant quel que soit le morphotype du patient. Ces résultats peuvent sembler paradoxaux, mais ils sont liés au fait qu'à un niveau de bruit de l'image équivalent, il est plus facile de diagnostiquer une colique néphrétique lorsque le patient a beaucoup de graisse intra-abdominale et intra-pelvienne. En effet, la présence de graisse permet de délimiter plus facilement le trajet des uretères, même avec un bruit important de l'image. Cet exemple met en avant la difficulté de trouver des critères pertinents de mesure de la qualité d'image et l'absence de corrélation entre certains paramètres de mesure de la qualité de l'image et la performance diagnostique. Au final, dans une démarche de réduction de la dose au scanner, l'évaluation de la performance diagnostique doit être privilégiée par rapport à l'évaluation de la qualité d'image. Au cours de cette étude, nous avions aussi trouvé de nombreux scanners réalisés dans le cadre du bilan d'une colique néphrétique mais pour lesquels le protocole avait été modifié. En effet, sur 146 scanners réalisés en 2012 pour suspicion de colique néphrétique, seulement 86 scanners avaient été réalisés selon le protocole basse dose et inclus dans notre étude. Soixante scanners avaient un indice de bruit diminué, c'est-à-dire que la qualité d'image avait été améliorée mais aussi que la dose était plus importante. Suite à cette découverte et après information auprès du personnel du service d'imagerie de l'HIA Legouest, il s'est avéré que certains manipulateurs et certains radiologues amélioraient volontairement la

qualité d'image des scanners qu'ils trouvaient trop dégradée. Pourtant, l'analyse des données de notre étude a confirmé l'excellente performance diagnostique de notre protocole basse dose, malgré la dégradation importante de la qualité d'image. Cela montre bien la difficulté de mettre au point un protocole basse dose avec une qualité d'image dégradée et l'importance de la sensibilisation des équipes médicales et paramédicales dans une démarche d'optimisation de la dose.

CHAPITRE 4 : APPLICATIONS CLINIQUES

Ce chapitre est composé de trois articles :

1- Gervaise A, Gervaise-Henry C, Pernin M, Naulet P, Junca-Laplace C, Lapierre-Combes M. Low dose CT for renal colic: how to do in clinical practice? *Diagn Interv Imaging* 2016; 97: 393-400.

2- Gervaise A, Teixeira P, Villani N, Lecocq S, Louis M, Blum A. Dose optimization and reduction in musculoskeletal CT. *Diagn Interv Imaging* 2013; 94: 371-88.

3- Teixeira P, Gervaise A, Louis M, Lecocq S, Raymond A, Aptel S, Blum A. Musculoskeletal Wide detector CT : Principles, Techniques and Applications in Clinical Practice and Research. *Eur J Radiol* 2015; 84: 892-900.

La mise en œuvre pratique des différents facteurs comportementaux et techniques permettant d'optimiser et de réduire la dose d'irradiation au scanner a déjà été décrite dans de nombreuses publications [35, 49-55]. Nous proposons de mettre en avant ces modalités de réduction de la dose dans deux domaines d'imagerie particuliers : l'imagerie des coliques néphrétiques et l'imagerie ostéo-articulaire.

Article 1 : Scanner basse dose pour la recherche d'une colique néphrétique : comment faire en pratique clinique ?

Le scanner est devenu l'examen de référence pour l'étude des coliques néphrétiques [56-57]. Il permet d'en faire le diagnostic, de définir la prise en charge et de rechercher des diagnostics différentiels. Sa principale limite est liée à son caractère irradiant, d'autant plus que la maladie lithiasique urinaire touche principalement des sujets jeunes avec une tendance à la récidive [58-59]. La réduction de la dose des scanners réalisés pour suspicion de colique néphrétique est donc primordiale.

Le but de cette mise au point était de montrer comment il est possible de réaliser en pratique clinique courante un scanner basse dose dans le cadre d'une suspicion de colique néphrétique.

Dans cette mise au point, nous illustrons les différentes modalités de réduction de la dose de ces scanners en distinguant les facteurs comportementaux et les facteurs techniques. Parmi les facteurs comportementaux, la réduction de la couverture d'acquisition est un moyen simple et efficace pour réduire la dose. Les facteurs techniques s'appuient principalement sur l'utilisation de la modulation automatique du mA, la baisse du kV et du mA et l'implantation des reconstructions itératives. Grâce à ces mesures d'optimisation de la dose, il est possible de réaliser des scanners basses doses avec une excellente performance diagnostique et une dose réduite de l'ordre de 75 % par rapport à un scanner abdominopelvien standard.

Article 2 : Optimisation et réduction de la dose en scanner ostéo-articulaire.

Grâce à ses bonnes résolutions temporelle et spatiale, le scanner reste indiqué dans l'évaluation de nombreuses pathologies ostéo-articulaires. De nouvelles techniques

d'exploration telles que le scanner dynamique 4D des articulations et le scanner de perfusion tumorale apportent aussi de nouvelles indications. Le scanner reste toutefois une technique d'imagerie irradiante pour laquelle l'optimisation et la réduction de la dose sont primordiales.

Le but de cette mise au point était de présenter les doses typiques délivrées au cours des scanners en pathologie ostéo-articulaire et d'illustrer les différentes modalités permettant d'optimiser et de réduire ces doses en distinguant les facteurs comportementaux et les facteurs techniques.

L'optimisation du mA et du kV reste indispensable. Ils doivent être adaptés au type d'exploration et au morphotype de chaque individu. L'apparition récente des algorithmes de reconstruction itérative a aussi permis de réduire de manière importante les doses délivrées. Avec l'ensemble de ces techniques d'optimisation et de réduction de la dose, il est dorénavant possible de faire des acquisitions basses-doses voire très-basses-doses permettant d'atteindre un niveau de dose parfois proche d'un bilan radiographique standard. Toutefois, même si ces facteurs techniques permettent de réduire de façon importante les doses délivrées, les facteurs comportementaux, comme le respect des indications ou la limitation de la couverture d'acquisition, restent fondamentaux.

Article 3 : Scanner ostéo-articulaire à large système de détection : principes, techniques et applications en pratique clinique et en recherche.

Le développement des scanners à large système de détection a permis la mise au point de nouvelles applications avancées en scanner ostéo-articulaire : scanner dynamique 4D des articulations et scanner de perfusion tumorale. Bien que ces techniques semblent jouer un rôle important dans le diagnostic de nombreuses pathologies ostéo-articulaires, elles nécessitent la répétition de multiples volumes d'acquisition, ce qui est à l'origine d'une augmentation importante des doses délivrées. La maitrise des protocoles d'acquisition et des doses délivrées est un facteur important pour permettre l'utilisation en pratique clinique de ces nouvelles applications avancées.

Le but de cette mise au point était de fournir un guide pratique permettant d'utiliser ces nouveaux outils en routine clinique.

Dans cette mise au point, nous montrons que l'utilisation d'un scanner à large système de détection permet de réaliser des acquisitions volumiques qui ont pour avantage de supprimer l'effet d'*overranging* par rapport à une acquisition hélicoïdale classique et donc de réduire les doses délivrées. Par ailleurs, l'implantation des reconstructions itératives permet de réduire de moitié les doses délivrées. En parallèle de ces évolutions technologiques, c'est aussi l'optimisation des facteurs comportementaux qui reste indispensable. La limitation de la couverture d'acquisition, la réduction du nombre de phases d'acquisition et l'utilisation d'une acquisition intermittente plutôt que continue sont les principaux moyens comportementaux qui permettent de limiter la dose d'irradiation et l'utilisation en pratique clinique courante de ce type d'applications avancées.

Chapitre 4

Article 1 : *Scanner basse dose pour la recherche d'une colique néphrétique : comment faire en pratique clinique ?*

Gervaise A, Gervaise-Henry C, Pernin M, Naulet P, Junca-Laplace C, Lapierre-Combes M. Low dose CT for renal colic: how to do in clinical practice? *Diagn Interv Imaging* 2016; 97:393-400.

Diagnostic and Interventional Imaging (2016) **97**, 393—400

REVIEW /*Genito-urinary imaging*

How to perform low-dose computed tomography for renal colic in clinical practice

A. Gervaise[a,*], **C. Gervaise-Henry**[b], **M. Pernin**[a], **P. Naulet**[a], **C. Junca-Laplace**[a], **M. Lapierre-Combes**[a]

[a] *Department of medical imaging, HIA Legouest, 57077 Metz, France*
[b] *Department of biochemistry, hôpital Central, CHU de Nancy, 54000 Nancy, France*

KEYWORDS
Computed tomography (CT);
Dose;
Optimization;
Reduction;
Renal colic

Abstract Computed tomography (CT) has become the reference technique in medical imaging for renal colic, to diagnose, plan treatment and explore differential diagnosis. Its main limitation is the radiation dose, especially as urinary stone disease tends to relapse and mainly affects young people. It is therefore essential to reduce the CT radiation dose when renal colic is suspected. The goal of this review was twofold. First, we wanted to show how to use low-dose CT in patients with suspected renal colic in current clinical practice. Second, we wished to discuss the different ways of reducing CT radiation dose by considering both behavioral and technological factors. Among the behavioral factors, limiting the scan coverage area is a straightforward and effective way to reduce the dose. Improvement of technological factors relies mainly on using automatic tube current modulation, lowering the tube voltage and current as well using iterative reconstruction.

Since unenhanced (or plain) computed tomography (CT) was introduced in the 1990s, it has become the reference tool for the diagnosis of renal colic [1—3]. This is because CT has many advantages. It is fast, does not require intravenous administration of iodinated contrast material, has high diagnostic capabilities [2,4], helps exclude other conditions that are clinically similar to renal colic [5—8], provides direct information relative to the size and attenuation value of urinary stones [9] and helps predict spontaneous stone passage [10].

* Corresponding author at: Department of medical imaging, HIA Legouest, 27, avenue de Plantières, BP 90001, 57077 Metz cedex 3, France.
E-mail address: alban.gervaise@hotmail.fr (A. Gervaise).

http://dx.doi.org/10.1016/j.diii.2015.05.013

Its main limitation, however, is the radiation dose given to the patient, especially because urinary stone disease tends to relapse and mainly to affect young people. Katz et al. report that 4% of the patients that undergo CT for suspected renal colic have had at least three CT examinations for the same indication, with cumulated doses ranging from 20 to 154 mSv [11]. Considering the ALARA principle (As Low As Reasonably Achievable) and the potential risks of radiation-induced cancer caused even using low doses of X-rays [12,13], dose reduction in CT for suspected renal colic is hence essential. In this context, many studies have shown that it is possible to detect renal colic with low-dose CT. Doses may be reduced by 75 to 90% compared to standard acquisition doses, without modifying the diagnostic performance [4,14—18]. However, a recent study showed that in most imaging centers low-dose CT protocols were not used to diagnose renal colic [19].

The goal of this review was twofold. First, we wanted to show how to use low-dose CT in patient with suspected renal colic in current clinical practice. Second we wished to discuss the different ways of reducing the CT radiation dose by considering both behavioral and technological factors.

What is low-dose CT?

The definition of low dose is controversial. The term refers to CT scans where, compared to a ''normal'' or ''standard'' dose scan, the image quality has been deliberately modified to reduce the exposure dose while preserving the diagnostic performance [20]. Renal colic is particularly appropriate for low-dose CT because of the excellent spontaneous contrast between most urinary stones that are spontaneously hyperattenuating (between 200 and 2800 HU) [2] and the soft tissues that surround them. Thus, even if the dose reduction is substantial, the naturally high contrast between urinary stones and the surrounding soft tissues prevents too much deterioration of the contrast-to-noise ratio while preserving good diagnostic performance [9].

Data from the literature reveal that the effective ''low dose'' to detect renal colic, is between 1 and 3 mSv [4,19]. The threshold of 3 mSv (i.e. a dose length product [DLP] of 200 mGy.cm) is arbitrary but has become the standard threshold for low-dose CT when investigating renal colic [19] because it corresponds more or less to the average radiation of intravenous urography that used to be the reference modality in the past [21]. If we consider that the average dose of a standard abdomen and pelvic CT is between 10 and 12 mSv [22,23], a low-dose scan of less than 3 mSv corresponds to a dose reduction of more than 75%.

Despite this significant dose reduction, various studies have shown that the diagnostic performance of low-dose CT remains excellent compared to normal-dose CT. A meta-analysis published in 2008 showed an average sensitivity of 96.6% and an average specificity of 94.9% [4]. At the same time, it was shown that low-dose CT could explore differential diagnosis, just like normal-dose unenhanced CT [24] (Fig. 1) and also that there was no significant difference when determining the size and density of the stones [17,25].

Recently, experts have suggested using ''ultra-low-dose'' CT, below the level of 1 mSv and close to the dose used to perform a plain abdominal radiography, i.e. 0.7 mSv [21]. Despite the recent technological advances and the use of new very powerful iterative algorithms for reconstructions, these ultra-low-dose protocols perform less well than low-dose protocols for detecting small urinary stones below 3 mm [18,21].

How to perform low-dose CT to detect renal colic?

The modalities to reduce dose in CT are based on the radioprotection principles of CT dose justification and optimization [26]. These modalities have already been extensively described [27—33]. In this review, we discuss them and concentrate on how to reduce the dose of abdominal and pelvic CT when looking for renal colic. The different modalities depend both on behavioral factors, independent of the CT equipment, and technological factors, some of which depend on how recent the CT equipment is. The behavioral factors are the level of awareness of the medical and paramedical teams, the principles of substitution and justification, as well as limiting the scan coverage area. The technological factors include reduction of the tube current and voltage, automatic tube current modulation and iterative reconstructions, as well as optimization of the pitch and slice thickness.

Compliance with the indications and substitution with a non-radiating imaging technique

Due to its excellent diagnostic performance, CT has become the reference investigation to diagnose renal colic. In 2014 the European Association of Urology has recommended low-dose CT as the first-line imaging modality in case of suspected renal colic (grade A recommendation) [34]. In 2008, the French-speaking Society of medical Emergencies (Société Francophone d'Urgences Médicales) [35] recommended radiologists to perform plain abdomen radiography together with an ultrasound or an unenhanced CT as a first-line examination for suspected non-complicated renal colic. However, CT should be favored if a complicated case is suspected or in special situations (pregnancy, single kidney, transplanted kidney, known uropathy or renal failure) or if there are signs of complications (signs of infection; oliguria, anuria or algesia) and in case of doubtful diagnosis. In pregnant women, ultrasound must be used as first-line modality and, in case of doubtful ultrasound, magnetic resonance imaging should be used as a second-line imaging modality before CT [36].

Raising the awareness and training the medical teams

Raising the awareness and training the radiologists and clinicians is also essential [37]. Clinicians must be able to detect renal colic and ask explicitly the radiologist to look for it. The radiologist must use a low-dose CT protocol with pre-adjusted parameters. It is also essential that clinicians and radiologists agree to seek, not the best possible image quality, but one that is sufficient for diagnosis. For radiologists

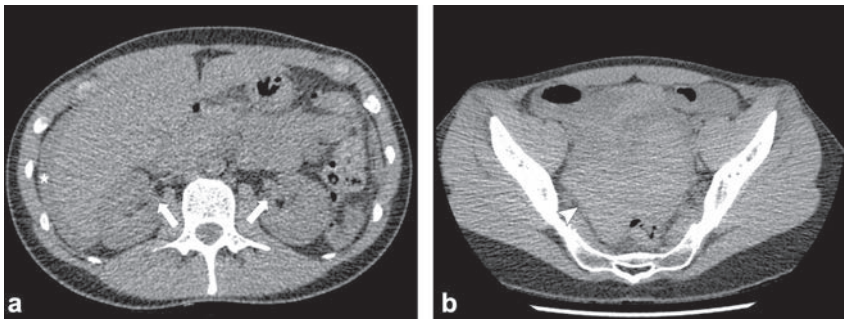

Figure 1. A 28-year-old woman was admitted to the emergency department for pelvic pain irradiating towards the left lumbar fossa. Unenhanced abdominal and pelvic CT (100 kVp, noise index at 50, DLP of 74 mGy.cm and effective dose of 1.1 mSv). Axial views, 1.25 mm centered on the kidneys (a) and the pelvis (b). Low-dose unenhanced CT does not show any dilatation of the pelvicalyceal system (arrows) and no wedged urinary stone, thereby excluding the presence of renal colic. However, even if the dose reduction has been significant, it is possible to evidence intraperitoneal perihepatic effusion (asterisk) as well as a hyperattenuating spontaneous effusion in the Douglas pouch (arrowhead) suggesting hemoperitoneum. Further enhanced CT confirmed hemoperitoneum caused by left ovarian cyst rupture.

and operators to be properly aware of low-dose CT, they must know the delivered doses. Therefore, it is essential that the dose (DLP) be displayed on the CT workstation before any acquisition. Currently all manufacturers systematically provide this display. Awareness is also raised by the software's dose-recording system that allows radiologists to monitor the doses absorbed by the patients and to detect cumulated doses, sometimes substantial [38,39]. More generally, national and international dose registers are available. For instance, the CT Dose Index Registry [40] in the United States has made it possible to evidence that low-dose CT protocols were not sufficiently used to detect renal colic [19].

Limiting the scan coverage area

A straightforward and effective way to reduce doses is to reduce the acquisition length. Unenhanced image acquisition must be restricted to the urinary tract, from the upper pole of the kidneys to the base of the urinary bladder. Besides reducing the CT overall dose by limiting the scan coverage area, this centering prevents radiosensitive organs such as gonads in men and breasts in women to be exposed to X-rays (Fig. 2) [41].

Reducing the tube current (mA) and tube voltage (kV)

Effects of mA and kV

Lowering the tube current lowers the dose proportionally but also causes an increase in image noise proportionally to the reciprocal value of the square root of the mA [42]. In practice, reducing the tube current by half reduces the dose by 50% but increases the image noise by 41%.

Lowering the kV may also reduce the dose. However, this will also increase the image noise [42].

Effect of patient's body mass

Because of the high natural contrast between most urinary stones and surrounding soft tissues, several experts have recommended low-dose CT protocols with significantly lowered tube current, by 10 to 100 milliamperes per second (Fig. 3) [5,24,43—46]. Many studies have shown excellent diagnostic performance for low-dose CT, equivalent to the one of a standard-dose CT [4]. Hamm et al. [44] and Poletti et al. [24] have, however, observed that low-dose CT performed less well in obese patients who had a Body Mass Index (BMI) > 30 kg/m^2. This was associated to the constant mA used for all the patients, resulting in a significant loss of image quality in obese patients. Based on this, some experts have suggested not using low-dose CT for obese patients (> 30 kg/m) [24,44,45] while others have recommended tailoring the mA to these patients [5]. After these studies were published, automatic tube current modulation during acquisition was introduced. This has allowed radiologists to adapt the mA and the image quality to the patient's body mass while reducing the dose by about 43 to 66% [47,48]. Mulkens et al. confirmed that low-dose CT with automatic tube current modulation provides excellent diagnostic performance in all patients with suspected renal colic, including overweight and obese patients [49]. However, in order to preserve an acceptable image quality in overweight patients, the automatic tube current modulation increases the CT dose. Moreover, it has been shown that automatic tube current modulation provides better scores of image quality and diagnostic performance for overweight patients with a BMI $\geq$ 25 kg/m^2 than for patients with a BMI < 25 kg/m^2 [16]. These results may seem inconsistent, but they can be explained by the fact that, with an equivalent level of image noise, it is easier to diagnose renal colic in a patient who has a lot of intra-abdominal and intra-pelvic fat [50]. Indeed, fat may help delineate the ureters from surrounding structures, even if the image noise is high. It also seems easier to detect secondary signs of renal colic such as perirenal stranding and the ''rim sign'' in overweight patients. This is why diagnosis errors are more often observed in thin patients who have a BMI < 25 kg/m^2, in whom it is difficult to distinguish small stones in the lower ureter from pelvic phleboliths, even with normal-dose CT [16,49].

As far as the kV is concerned, beam-hardening artifacts have been observed in overweight patients if the kV has been too much reduced. So, while it is possible to reduce the tube voltage to 80 kVp in a patient with standard morphotype, it

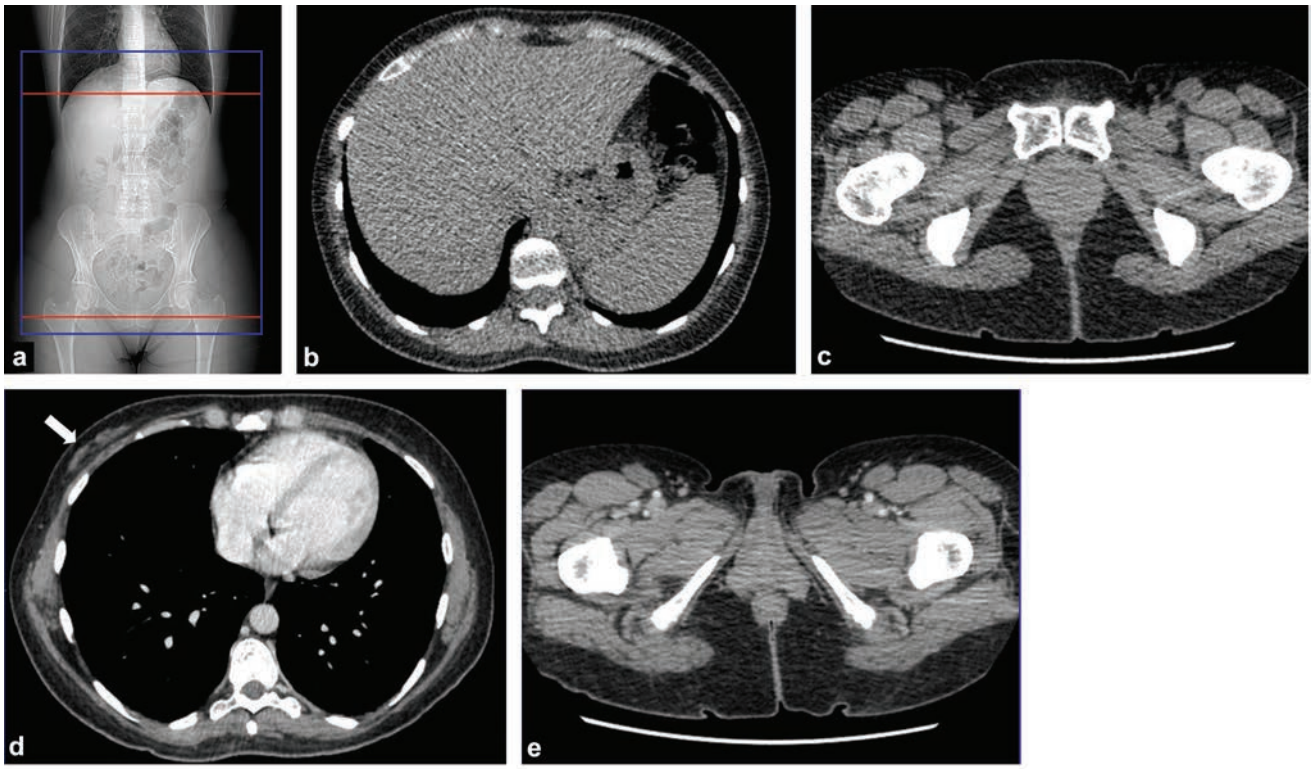

Figure 2. 41-year-old woman with suspected left renal colic. Low-dose unenhanced CT followed by standard-dose abdominal and pelvic enhanced CT (since renal colic was excluded). Scout view (a) shows the borders of the unenhanced (red lines) and enhanced (blue lines) acquisitions and first and last images in axial view without (b and c) and after injection (d and e). Note the low-dose CT centered from the upper pole of the kidneys to the mid pubic symphysis making it possible to reduce by 20% the scan coverage area compared to the standard abdominal and pelvic images (35.1 cm versus 43.7 cm). Also note the presence of mammary tissue (arrow) on the first section of the standard acquisition, absent in the low-dose series of images.

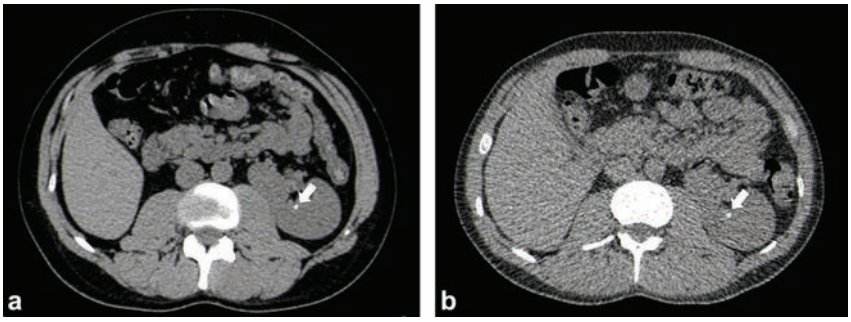

Figure 3. 30-year-old man monitored for a 4-mm urinary stone in the left kidney (arrow). Normal-dose unenhanced abdominal and pelvic CT (120 kVp, noise index at 21.4, DLP at 1189 mGy.cm and effective dose of 17.8 mSv) and (b) follow-up CT with our low-dose protocol (100 kVp, noise index of 50, DLP of 80 mGy.cm and effective dose of 1.2 mSv). Even with a 93.5% reduction of the dose, low-dose CT perfectly shows the left renal stone (arrow).

must be kept to 100 kVp in overweight patients (Figs. 4 and 5) [14,16].

Iterative reconstructions

Reducing mA and kV is limited by the use of conventional Filtered Back Projection (FBP) reconstructions because of the significant increase in image noise when doses have been too reduced [51]. The recent introduction of iterative reconstruction algorithms has significantly reduced image noise compared to standard FBP reconstructions [14—18,52—56]. So, when doses are lowered by mA and kV reductions, iterative reconstructions compensate for the decreased image quality. On standard abdominal and pelvic CT, iterative reconstructions have allowed radiologists to reduce doses by at least 50% [57]. Kulkarni et al. have shown that, for suspected renal colic, it was possible to maintain excellent diagnostic performance equivalent to the one of standard-dose CT by using automatic mA modulation, adaptive statistical iterative reconstruction (ASIR) and a kV fixed at 80 kVp for patients weighing less than 90 kg [14]. Iterative reconstruction also maintains adequate quality of image in

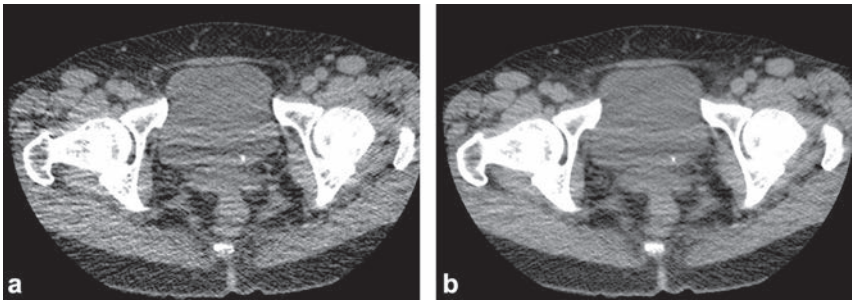

Figure 4. 58-year-old woman (weight, 64 kg; BMI, 22.7 kg/m^2) with left renal colic caused by a 3.5-mm urinary stone wedged in the ureterovesical meatus. Unenhanced low-dose CT with tube voltage at 80 kVp and noise index at 50 for a DLP of 105 mGy.cm. Axial plane, 1.25 mm section (a) and 3-mm (b). Despite the significant reduction of tube voltage, the urinary stone is perfectly visible. However, we observe beam-hardening artifacts (a) partially reduced by the thickening of the sections (b).

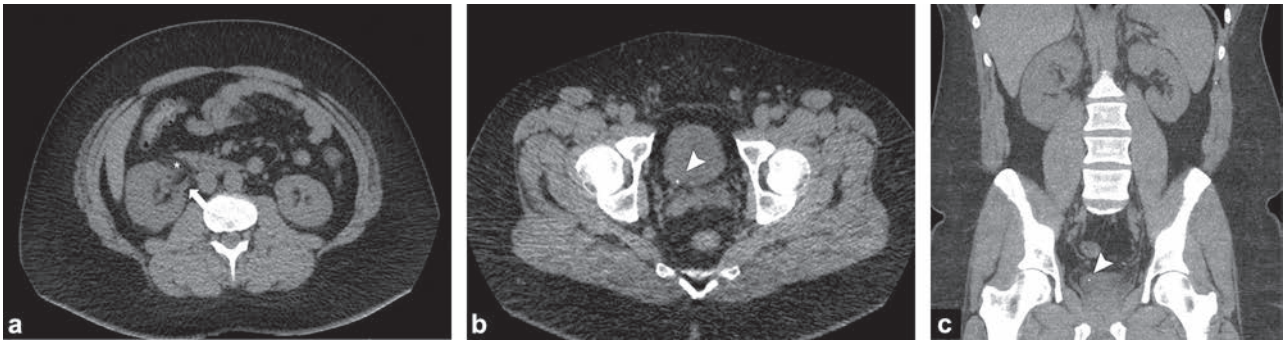

Figure 5. 32-year-old man, obese (BMI, 35.7 kg/m^2), with suspected right renal colic. Low-dose unenhanced CT (100 kVp, noise index at 50, DLP of 325 mGy.cm, effective dose of 4.8 mSv) axial view, 1.25-mm sections centered on the kidney (a) and the urinary bladder (b) and 5-mm coronal MIP reformation (c). For this obese patient, automatic tube current modulation makes it possible to maintain a good quality of image without the need to increase the CT dose. Note how well it is possible to visualize the infiltration around the right kidney (asterisk) and the small dilatation on the right side of the pelvicalyceal system (arrow) proximal to a 2-mm urinary stone wedged in the right ureterovesical meatus (arrow head). The stone is well detected by the 5-mm coronal MIP (c).

overweight patients [16] while using low kV (Fig. 5) and, in addition, has the advantage of reducing beam-hardening artifacts, including at the pelvis [57].

Pitch effect

Some experts have recommended increasing the pitch in low-dose CT protocols for patients with suspected renal colic [58]. Nowadays, pitch does not affect dose anymore, since most CT have automatic tube current modulation software [59]. However, a high pitch, about 1 to 1.5, is better, because it reduces acquisition time and, thereby, movement artifacts by the patient.

Adapting the slice thickness

To obtain high spatial resolution, images should always be acquired using thin sections (1 to 1.25 mm). Thin sections with isotropic voxels enhance the quality of three-dimensional multiplanar reformations and volume rendering [60]. However, thin sections also cause significant increase in image noise, especially if the mA and kV have been considerably reduced, as happens in low-dose CT. So, after using thin sections for image acquisition, it is possible to reconstruct thicker sections during image review at the CT workstation [61]. With thickened 3-mm sections it is possible to reduce image noise while preserving good detectability and characterization of all radiodense urinary stones, including those below 3 mm (Fig. 4) [62,63]. Other abdominal structures are also better visualized. However, 5-mm thickened sections may cause partial-volume artifacts and reduce the detectability of small stones below 3 mm [64]. Small stones and spontaneously dense stones are also more readily detected with thickened sections in maximum intensity projection (MIP) and lower image noise. In their study, Corwin et al. have confirmed that urinary stones and their density are more accurately measured on 5-mm coronal MIP images (Fig. 5) [65].

In routine practice

Acquisition must be centered from the upper pole of the kidneys to the middle of the pubic symphysis. The kV may be reduced to 100 kVp, even 80 kVp in patients that are not overweight, and the level of noise of the automatic tube current modulation may be increased in order to obtain a 75% reduction of dose compared to a standard abdominal and pelvic scan protocol. Iterative reconstructions should be used whenever possible (Table 1). Finally, CT images are visualized on millimetric native axial sections, thick sections (average 3 mm) and 5-mm coronal MIP reformations.

Table 1 Example of a low-dose CT protocol, used in our institution in routine practice to diagnose renal colic with a 64-slice MDCT (OPTIMA CT660, General Electric Healthcare, USA) and iterative reconstructions (Adaptive Statistical Iterative Reconstruction [ASIR]). Comparison between acquisition and reconstruction parameters of this low-dose protocol and those of a standard abdominal and pelvic CT. The differences between the two protocols lie with the limited acquisition duration, the lowering of the tube voltage and the increase of the noise level of the automatic tube current modulation.

Acquisition and reconstruction parameters	Low-dose CT Protocol to detect renal colic	Standard abdominal and pelvic CT Protocol
Acquisition mode/detectors	Helical/64 × 0.5 mm	Helical/64 × 0.5 mm
Start of acquisition	Upper pole of the kidneys	Upper border of the diaphragmatic domes
End of acquisition	Middle of the pubic symphysis	Lower border of the pubic symphysis
Tube voltage	80 kVp for a patient with average BMI 100 kVp for an overweight patient	120 kVp
Tube current (mA)	Automatic tube current modulation	Automatic tube current modulation
Noise index	50	21.5
Min (mA)/Max (mA)	10/300	120/500
Pitch	1.375	1.375
Rotation time	0.7	0.7
Reconstruction algorithm	ASIR 50%	ASIR 50%
Slice thickness (mm)/interval (mm)	1.25/1.25	1.25/1.25

Conclusion

CT has become the reference technique to diagnose renal colic. Because of its ionizing radiation, it is necessary to reduce doses. In order to perform low-dose CT in patients with suspected renal colic, the most important measures to implement are: to increase the awareness of the medical and paramedical teams, to limit the scan coverage area, to use automatic tube current modulation and to reduce mA and kV. Iterative reconstruction algorithms have also made it possible to significantly reduce doses (Boxed text 1). Technological advances and the introduction of new algorithms for even better iterative reconstructions allow us to expect ultra-low CT with excellent diagnostic performance.

Boxed text 1: The 5 golden rules of low-dose CT for suspected renal colic are:

1. Comply with the indications.
2. Center and restrict the acquisition coverage area.
3. Use automatic tube current modulation.
4. Lower tube current and tube voltage.
5. Use iterative reconstructions.

Disclosure of interest

The authors declare that they have no competing interest.

References

[1] Coursey CA, Casalino DD, Remer EM, et al. ACR Appropriateness Criteria® acute onset flank pain: suspicion of stone disease. Ultrasound Q 2012;28:227—33.

[2] Kambadakone AR, Eisner BH, Catalano OA, Sahani DV. New and evolving concepts in the imaging and management of urolithiasis: urologists' perspective. Radiographics 2010;30:603—23.

[3] Roy C, Tuchman C, Guth S, Lang H, Saussine C, Jacqmin D. Scanner hélicoïdal de l'appareil urinaire : principales applications. J Radiol 2000;81:1071—81.

[4] Niemann T, Kollmann T, Bongartz G. Diagnostic performance of low-dose CT for detection of urolithiasis: a meta-analysis. AJR Am J Roentgenol 2008;191:396—401.

[5] Tack D, Sourtzis S, Delpierre I, de Maertelaer V, Gevenois PA. Low-dose unenhanced multidetector CT of patients with suspected renal colic. AJR Am J Roentgenol 2003;180:305—11.

[6] Kluner C, Hein PA, Gralla O, et al. Does ultra-low-dose CT with a radiation dose equivalent to that of KUB suffice to detect renal and ureteral calculi? J Comput Assist Tomogr 2006;30:44—50.

[7] Ather MA, Faizullah K, Achakzai I, Siwani R, Irani F. Alternate and incidental diagnoses on noncontrast-enhanced spiral computed tomography for acute flank pain. Urol J 2009;6:14—8.

[8] Samim M, Goss S, Luty S, Weinreb J, Moore C. Incidental findings on CT for suspected renal colic in emergency department patients: prevalence and types in 5383 consecutive examinations. J Am Coll Radiol 2015;12:63—9.

[9] Sung MK, Singh S, Kalra MK. Current status of low dose multidetector CT in the urinary tract. World J Radiol 2011;3:256—65.

[10] Coll DM, Varanelli MJ, Smith RC. Relationship of spontaneous passage of ureteral calculi to stone size and location as revealed by unenhanced helical CT. AJR Am J Roentgenol 2002;178:101—3.

[11] Katz SI, Saluja S, Brink JA, Forman HP. Radiation dose associated with unenhanced CT for suspected renal colic: impact of repetitive studies. AJR Am J Roentgenol 2006;186:1120—4.

[12] Smith-Bindman R, Lipson J, Marcus R, et al. Radiation dose associated with common computed tomography examinations and the associated lifetime attributable risk of cancer. Arch Intern Med 2009;169:2078—86.

[13] Berrington de González A, Mahesh M, Kim KP, et al. Projected cancer risks from computed tomography scans performed in the United States in 2007. Arch Intern Med 2009;169:2071—7.

[14] Kulkarni NM, Uppot RN, Eisner BH, Sahani DV. Radiation dose reduction at multidetector CT with Adaptive Statistical Iterative Reconstruction for evaluation of urolithiasis: how low can we go? Radiology 2012;265:158—66.
[15] Winklehner A, Lume I, Winklhofer S, et al. Iterative reconstructions versus filtered back-projection for urinary stone detection in low-dose CT. Acad Radiol 2013;20:1429—35.
[16] Gervaise A, Naulet P, Beuret F, et al. Low-dose CT with automatic tube current modulation, adaptive statistical iterative reconstruction and low tube voltage for the diagnosis of renal colic: impact of body mass index. AJR Am J Roentgenol 2014;202:553—60.
[17] Wang J, Kang T, Arepalli C, et al. Half-dose non-contrast CT in the investigation of urolithiasis: image quality improvement with third-generation integrated circuit CT detectors. Abdom Imaging 2015;40:1255—62.
[18] Glazer DI, Maturen KE, Cohan RH, et al. Assessment of 1 mSv urinary tract stone CT with Model-Based Iterative Reconstruction. AJR Am J Roentgenol 2014;203:1230—5.
[19] Lukasiewicz A, Bhargavan-Chatfield M, Coombs L, Ghita M, Weinreb J, Gunabushanam G, et al. Radiation dose index of renal colic protocol CT studies in the United States: a report from the American College of Radiology National Radiology Data Registry. Radiology 2014;271:445—51.
[20] Keyzer C, Tack D. Dose optimization and reduction in MDCT of the abdomen. In: Tack D, Genevois PA, Kalra M, editors. Radiation dose from multidetector CT. Berlin Heidelberg: Springer-Verlag; 2012. p. 369—87.
[21] McLaughlin PD, Murphy KP, Hayes SA, et al. Non-contrast CT at comparable dose to an abdominal radiograph in patients with acute renal colic; impact of iterative reconstruction on image quality and diagnostic performance. Insights Imaging 2014;5:217—30.
[22] McCollough CH, Chen GH, Kalender W, et al. Achieving routine submillisievert CT scanning: report from the summit on management of radiation dose in CT. Radiology 2012;264:567—80.
[23] Gervaise A, Esperabe-Vignau F, Naulet P, Pernin M, Portron Y, Lapierre-Combes M. Évaluation des connaissances des prescripteurs de scanner en matière de radioprotection des patients. J Radiol 2011;92:681—7.
[24] Poletti PA, Platon A, Rutschmann OT, Schmidlin FR, Iselin CE, Becker CD. Low-dose versus standard-dose CT protocol in patients with clinically suspected renal colic. AJR Am J Roentgenol 2007;188:927—33.
[25] Sohn W, Clayman RV, Lee JY, Cohen A, Mucksavage P. Low-dose and standard computed tomography scans yield equivalent stone measurements. Urology 2013;81:231—4.
[26] International Commission on Radiological Protection. Recommendations of the International Commission on Radiological Protection. ICRP Publication 26. Oxford: Pergamon; 1977.
[27] Semelka RC, Armao DM, Elias J, Huda W. Imaging strategies to reduce the risk of radiation in CT studies, including selective substitution with MRI. J Magn Reson Imaging 2007;25:900—9.
[28] Kalra MK, Maher MM, Toth TL, et al. Strategies for CT radiation dose optimization. Radiology 2004;230:619—28.
[29] McCollough CH, Primak AN, Braun N, Kofler J, Yu L, Christner J. Strategies for reducing radiation dose in CT. Radiol Clin North Am 2009;47:27—40.
[30] Lee TY, Chhem RK. Impact of new technologies on dose reduction in CT. Eur J Radiol 2010;76:28—35.
[31] Singh S, Kalra MK, Thrall JH, Mahesh M. CT radiation dose reduction by modifying primary factors. J Am Coll Radiol 2011;8:369—72.
[32] Dougeni E, Faulkner K, Panayiotakis G. A review of patient dose and optimization methods in adult and paediatric CT scanning. Eur J Radiol 2012;81:e665—83.
[33] Gervaise A, Teixeira P, Villani N, Lecocq S, Louis M, Blum A. CT dose optimization and reduction in osteoarticular disease. Diagn Interv Imaging 2014;95:47—53.
[34] Turk C, Knoll T, Petrik A, et al. Guidelines on urolithiasis. Arnhem (The Netherlands): European Association of Urology (EAU); 2014 [100 p] http://www.uroweb.org/wp-content/uploads/22-Urolithiasis_LR.pdf.
[35] El Khlebir M, Fougeras O, Le Gall C, et al. Actualisation 2008 de la 8e conférence de consensus de la Société Francophone d'Urgences Médicales de 1999. Prise en charge des coliques néphrétiques de l'adulte dans les services d'accueil et d'urgences. Prog Urol 2009;19:462—73.
[36] Masselli G, Derme M, Bernieri MG, et al. Stone disease in pregnancy: imaging-guided therapy. Insights Imaging 2014;5:691—6.
[37] Mayo-Smith WW, Hara AK, Mahesh M, Sahani DV, Pavlicek W. How I do it: managing radiation dose in CT. Radiology 2014;273:657—72.
[38] Tamm EP, Szklaruk J, Puthooran L, Stone D, Stevens BL, Modaro C. Quality initiatives: planning, setting up, and carrying out radiology process improvement projects. Radiographics 2012;32:1529—42.
[39] Burckel LA, Defez D, Chaillot PF, Douek P, Boussel L. Use of an automatic recording system for CT doses: evaluation of the impact of iterative reconstruction on radiation exposure in clinical pratice. Diagn Interv Imaging 2015;96:265—72.
[40] Amis ES. CT radiation dose: trending in the right direction. Radiology 2011;261:5—8.
[41] Corwin MT, Bekele W, Lamba R. Bony landmarks on computed tomography localizer radiographs to prescribe a reduced scan range in patients undergoing multidetector computed tomography for suspected urolithiasis. J Comput Assist Tomogr 2014;38:404—7.
[42] Mahesh M. Scan parameters and image quality in MDCT. In: Mahesh M, editor. MDCT physics: The basics—Technology, image quality and radiation dose. Philadelphia: Lippincott Williams & Wilkins; 2009. p. 47—78.
[43] Liu W, Esler SJ, Kenny BJ, Goh RH, Rainbow AJ, Stevenson GW. Low dose nonenhanced helical CT of renal colic: assessment of ureteric stone detection and measurement of effective dose equivalent. Radiology 2000;215:51—4.
[44] Hamm M, Knopfle E, Wartenberg S, Wawroschek F, Weckermann D, Harzmann R. Low dose unenhanced helical computed tomography for the evaluation of acute flank pain. J Urol 2002;167:1687—91.
[45] Heneghan JP, McGuire KA, Leder RA, Delong DM, Yoshizumi T, Nelson RC. Helical CT for nephrolithiasis and ureterolithiasis: comparison of conventional and reduced radiation dose techniques. Radiology 2003;229:575—80.
[46] Kim BS, Hwang IK, Choi YW, et al. Low-dose and standard-dose unenhanced helical computed tomography for the assessment of acute renal colic: prospective comparative study. Acta Radiol 2005;46:756—63.
[47] Kalra MK, Maher MM, D'Souza RV, et al. Detection of urinary tract stones at low-radiation-dose CT with z-axis automatic tube current modulation: phantom and clinical studies. Radiology 2005;235:523—9.
[48] McCollough CH, Bruesewitz MR, Kofler Jr JM. CT dose reduction and dose management tools: overview of available options. Radiographics 2006;25:503—12.
[49] Mulkens TH, Daineffe S, De Wijngaert R, et al. Urinary stone disease: comparison of standard-dose and low-dose with 4D MDCT tube current modulation. AJR Am J Roentgenol 2007;188:553—62.
[50] Katz DS, Venkataramanan N, Napel S, Sommer FG. Can low dose unenhanced MultiDetector CT be used for routine evaluation of suspected renal colic? AJR Am J Roentgenol 2003;180:313—5.

[51] Xu J, Mahesh M, Tsui BM. Is iterative reconstruction ready for MDCT? J Am Coll Radiol 2009;6:274—6.
[52] Thibault JB, Sauer KD, Bouman CA, Hsieh J. A three-dimensional statistical approach to improved image quality for multislice helical CT. Med Phys 2007;34:4526—44.
[53] Hara AK, Paden RG, Silva AC, Kujak JL, Lawder HJ, Pavlicek W. Iterative reconstruction technique for reducing body radiation dose at CT: feasibility study. AJR Am J Roentgenol 2009;193:764—71.
[54] Botsikas D, Stefanelli S, Boudabbous S, Toso S, Becker CD, Montet X. Model-based iterative reconstruction versus adaptive statistical iterative reconstruction in low-dose abdominal CT for urolithiasis. AJR Am J Roentgenol 2014;203:336—40.
[55] Greffier J, Fernandez A, Macri F, Freitag C, Metge L, Beregi JP. Which dose for what image? Iterative reconstruction for CT scan. Diagn Interv Imaging 2013;94:1117—21.
[56] Greffier J, Macri F, Larbi A, Fernandez A, Khasanova E, Pereira F, et al. Dose reduction with iterative reconstruction: optimization of CT protocols in clinical practice. Diagn Interv Imaging 2015;96:477—86.
[57] Gervaise A, Osemont B, Louis M, Lecocq S, Teixeira P, Blum A. Standard dose versus low-dose abdominal and pelvic CT: comparison between filtered back projection versus adaptive iterative dose reduction 3D. Diagn Interv Imaging 2014;95:47—53.
[58] Diel J, Perlmutter S, Venkataramanan N, Mueller R, Lane MJ, Katz DS. Unenhanced helical CT using increased pitch for suspected renal colic: an effective technique for radiation dose reduction? J Comput Assist Tomogr 2000;24:795—801.
[59] Nagel HD. CT parameters that influence the radiation dose. In: Tack D, Genevois PA, editors. Radiation dose from adult and pediatric multidetector computed tomography. Berlin: Springer; 2007. p. 51—79.
[60] McNitt-Gray MF. AAPM/RSNA Physics tutorial for residents: topics in CT. Radiation dose in CT. Radiographics 2002;22:1541—53.
[61] von Falck C, Galanski M, Shin H. Sliding-thin-slab averaging for improved depiction of low-contrast lesions with radiation dose savings at thin-section CT. Radiographics 2010;30:317—26.
[62] Saw KC, McAteer JA, Monga AG, Chua GT, Lingeman JE, Williams Jr JC. Helical CT of urinary calculi: effect of stone composition, stone size, and scan collimation. AJR Am J Roentgenol 2000;175:329—32.
[63] Ketelslegers E, Van Beers BE. Urinary calculi: improved detection and characterization with thin-slice multidetector CT. Eur Radiol 2006;16:161—5.
[64] Memarsadeghi M, Heinz-Peer G, Helbich TH, et al. Unenhanced multi-detector row CT in patients suspected of having urinary stones disease: effect of section width on diagnosis. Radiology 2005;235:530—6.
[65] Corwin MT, Hsu M, McGahan JP, Lamba WM. Unenhanced MDCT in suspected urolithiasis: improved stone detection and density measurements using coronal Maximum-Intensity-Projection images. AJR Am J Roentgenol 2013;201:1036—40.

Chapitre 4

Article 2 : *Optimisation et réduction de la dose en scanner ostéo-articulaire.*

Gervaise A, Teixeira P, Villani N, Lecocq S, Louis M, Blum A. Dose optimization and reduction in musculoskeletal CT. *Diagn Interv Imaging* 2013 ; 94 :371-88.

Diagnostic and Interventional Imaging (2013) **94**, 371—388

REVIEW / *Musculoskeletal imaging*

CT dose optimisation and reduction in osteoarticular disease

A. Gervaise[a,b,*], **P. Teixeira**[a], **N. Villani**[c], **S. Lecocq**[a], **M. Louis**[a], **A. Blum**[a]

[a] *Service d'imagerie Guilloz, hôpital central, CHU de Nancy, 29, avenue du Maréchal-de-Lattre-de-Tassigny, 54035 Nancy cedex, France*
[b] *Service d'imagerie médicale, hôpital d'instruction des armées Legouest, 27, avenue de Plantières, BP 90001, 57077 Metz cedex 3, France*
[c] *Unité de radiophysique médicale, centre Alexis-Vautrin, avenue de Bourgogne, 54511 Vandœuvre-lès-Nancy, France*

KEYWORDS
Dose;
Osteoarticular imaging;
Optimisation;
Reduction;
CT

Abstract With an improvement in the temporal and spatial resolution, computed tomography (CT) is indicated in the evaluation of a great many osteoarticular diseases. New exploration techniques such as the dynamic CT and CT bone perfusion also provide new indications. However, CT is still an irradiating imaging technique and dose optimisation and reduction remains primordial. In this paper, the authors first present the typical doses delivered during CT in osteoarticular disease. They then discuss the different ways to optimise and reduce these doses by distinguishing the behavioural factors from the technical factors. Among the latter, the optimisation of the milliamps and kilovoltage is indispensable and should be adapted to the type of exploration and the morphotype of each individual. These technical factors also benefit from recent technological evolutions with the distribution of iterative reconstructions. In this way, the dose may be divided by two and provide an image of equal quality. With these dose optimisation and reduction techniques, it is now possible, while maintaining an excellent quality of the image, to obtain low-dose or even very low-dose acquisitions with a dose sometimes similar that of a standard X-ray assessment. Nevertheless, although these technical factors provide a major reduction in the dose delivered, behavioural factors, such as compliance with the indications, remain fundamental. Finally, the authors describe how to optimise and reduce the dose with specific applications in musculoskeletal imaging such as the dynamic CT, CT bone perfusion and dual energy CT.

* Corresponding author.
E-mail address: alban.gervaise@hotmail.fr (A. Gervaise).

2211-5684/$ — see front matter
http://dx.doi.org/10.1016/j.diii.2012.05.017

Since its introduction in the 1970s, computer tomography (CT) has played a major role in the diagnosis of a great many osteoarticular diseases. It has quickly become the choice examination in the diagnosis of traumatic, degenerative or even malformative lesions. Even though image quality is altered by metallic artefacts, CT also found indications in postsurgical imaging [1—3]. It is now also used in interventional imaging (injection guidance, bone and soft tissue biopsies, vertebroplasty, etc.) [4]. However, the performance of CT is limited by the inferior analysis of the soft tissue compared with Magnetic Resonance Imaging (MRI). The CT analysis of intra-articular lesions is also very difficult due to the absence of administration of intra-articular contrast product. CT is also a technique of irradiating imaging. For all of these reasons, the MRI has taken a preponderant role in musculoskeletal imaging.

Nevertheless, the scanner plays an important role in osteoarticular disease with the development of multislice CT, the development of multidetector CT and recent technological evolutions that reduce the dose the patient is exposed to. Over the last years, the speed of acquisition and the temporal and spatial resolution of CT have also considerably improved. Sub-millimetric isotropic acquisitions are the rule and multidetector row and three-dimensional (3D) Volume Rendering (VR) reformations improve the evaluation of bone and soft tissue lesions [5]. The improvement in the speed of acquisition reduces movement artefacts and thereby makes the exploration of large volumes possible. This is, for example, especially adapted for the musculoskeletal assessment of multiple trauma patients (Fig. 1).

Other technological advances in osteoarticular imaging are represented by the development of the dual energy CT and the perfusion CT. The dual energy CT is based on double acquisition with two X-ray beams of different kilovoltage. This better characterises the tissue and also reduces metallic artefacts or even provides access to bone subtraction and iodine contrast product [6]. In addition, the tumour perfusion CT, with the acquisition of successive multiple phases, provides functional information to better analyse bone and soft tissue tumours. In addition the functional analysis is more reproducible than that of the MRI [7,8].

As opposed to the MRI, the other advantages of CT are represented by its lower cost, improved availability, the possibility of use on postsurgical or unstable patients and the absence of contra-indications related to prosthetic materials or pacemakers [4,9].

Finally, CT has benefited from a great many technological innovations over the last few years, thereby considerably reducing the dose delivered. The best example is the recent appearance of iterative reconstructions that reduce the dose by half with an equivalent image quality [10]. With these technological innovations and better control of the optimisation of the acquisition parameters, it is now possible to obtain CT imaging with a dose almost equal that of the standard X-ray assessment while the diagnostic performance of Ct is much higher than that of X-rays. With the continued reduction in the dose delivered, the replacement of the X-ray assessment by CT seems to be possible in an increasing number of clinical situations.

After a review of the typical doses delivered during osteoarticular CT, we will in turn discuss the different methods to reduce the dose by emphasising both the behavioural factors and the technical factors.

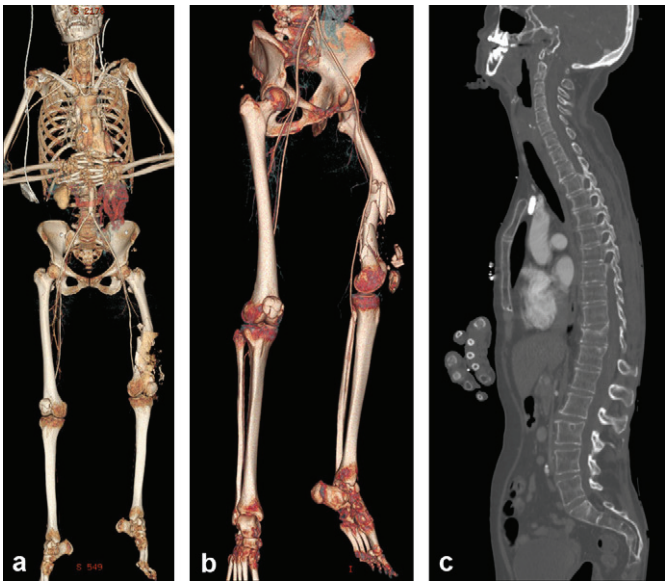

Figure 1. Whole-body computed tomography (CT) in a 55-year-old woman for an assessment after falling out of a window. Acquisition with 64-slice CT covering the whole-body at arterial time, that is, an acquisition of 163 cm in 31 s, with 120 kV, automatic modulation of the dose with mAs between 50 and 134, rotation time of 0.5 s, 64 × 0.5 mm, pitch at 0.868, for a DLP of 1428 mGy cm. Reformation 3D volume rendering (VR) of the whole-body (a) then centred on the left femoral fracture (b) and sagittal reformation on the whole vertebral column (c). This acquisition is obtained in thin slices, providing reformations in 3D VR in order to obtain a global view of the complex fracture of the left femur and its relationship to the superficial femoral artery and help the surgeon with the presurgical assessment. The fractures of both patellas should be noted. The multidetector row reformations with bone filter help better analyse the whole vertebral column and reveal a fracture of the upper vertebral body T11 without recession of the vertebral body.

Typical doses delivered with osteoarticular computer tomography (CT)

The International Commission on Radiological Protection and the European Commission recommend the establishment of diagnostic reference levels (DRL) [11,12]. The European Commission recommended doses defined by the Weighted-Dose-CT-Index (CTDI[w]) and by the Dose-Length Product (DLP) for several types of CT [12]. For the lumbar vertebrae, the recommended reference levels are a CTDI(w) of 35 mGy and a DLP of 800 mGy cm. For the bony pelvis, (hips, sacroiliacs), the recommended reference levels are a CTDI(w) at 25 mGy and a DLP at 520 mGy cm. For the traumatic spine, the recommended values are a CTDI(w) at 70 mGy and a DLP at 460 mGy cm [12]. However, these doses are based on reports dating from the end of the 1980s and the beginning of the 1990s, before the introduction of spiral and multislice CT [13,14]. Since then, the multislice CT radically changed practices. In 2004, The European Commission published new recommendations taking multislice CT into account. However, they did not recommend new dosimetry references in terms of DLP in the osteoarticular realm [15]. In France, the DRL have recently been up-dated [16]. Among those involving adult computed tomography, only one osteoarticular examination is included and only for the lumbar vertebrae with a DLP of 700 mGy cm. These reference levels are partial and only involve very few explorations in osteoarticular imaging. This is all the more so since, with the improvement in the speed of acquisition of multislice CT, it is now possible to obtain whole spinal imaging, leading to new indications such as the possibility of obtaining a whole-body CT in a myeloma assessment [17,18] or even the acquisition of a whole spinal column in osteoporosis [19]. In addition, there is no reference dose for acquisitions of the peripheral joints or for the new perfusion CT or dynamic CT applications.

In the literature, few publications have been devoted to CT doses in the realm of osteoarticular imaging and the results vary greatly. In a review of the literature dating 2008, Mettler et al. [20] find a mean effective dose of 6 mSv for the spine CT with values ranging from 1.5 to 10 mSv. In another review of the literature dating 2011 on 19 studies, Pantos et al. [21] find even greater differences in doses, ranging from 0.8 to 15.7 mSv for a lumbar CT, with a median dose of 5.2 mSv (Table 1). In a 2009 study on the analysis of osteoarticular CT doses in their institution, Biswas et al. [22] report of mean dose of 19.15 mSv for the acquisition of a lumbar CT (Table 2). The great variability in doses is mainly due to the difference in the length of acquisition between the studies. For example, based on a single-slice CT, Galanski et al. [23] found a mean dose of 2.7 mSv for a mean length of acquisition of only 5.8 cm. However, with a 16-slice CT, Biswas et al. [22] found a mean dose of 19.15 mSv but for a mean length of acquisition of 25.5 cm. Therefore, more than the difference in terms of number of CT slices, the dose difference is above all now related to their use. In fact, while the passage from the single-slice CT to the multislice CT was accompanied by an increase in the dose delivered to the patient [24], the passage from 4-slice CT to 16 or 64-slice CT is accompanied by technical improvements resulting in a relatively stable dose [25–27]. Therefore, more than the number of slices, the overall increase in the number of CT carried out [28] and the increase in the length of acquisition now result in an increase in the individual and collective exposure [20,29]. Within the same institution, significant variations in terms of ISDP and DLP are also observed (Tables 2–4) [30,31]. This may be accounted for by the adjustment of the acquisition parameters according to the patient morphotype and the indications. The acquisition parameters may be reduced in the exploration of the bone structures, while the milliamps increase when as assessment of the soft tissue is required. The establishment of new techniques of dose reduction, such as iterative reconstructions, also influences the dose delivered during CT (Table 4).

Very few studies refer to the peripheral joints. As far as we are aware, Biswas et al. [22] reported the only study presenting a full analysis of all of the doses delivered in osteoarticular imaging, including the peripheral joints. These results show that the farther the anatomic zone is from the trunk, the more the effective dose is minimal or even negligible, as for example for the wrist (Table 2). This is because the peripheral joints are smaller, thereby allowing for a reduction in the acquisition parameters and providing shorter lengths of acquisition. However, this is mainly due to the fact that the tissue-weighting factor used in calculating the effective dose is very small in view of the absence of a radiosensitive organ nearby. Table 5 sums up the values of the tissue-weighting factors used by Biswas et al. [22] in the estimate of the effective dose as a function of the different anatomic locations of osteoarticular CT (the effective dose (E) in mSv is calculated from the Dose-Length Product (DLP) in mGy cm multiplied by a tissue-weighting factor (k) according to the formula: $E = DLP \times k$).

Table 1 Doses of spinal computed tomography (CT) according to a review of the literature by Pantos et al. [21].

Type of CT	CTDI(w)[a] (mGy)	DLP[a] (mGy cm)	Effective dose[a] (mSv)
Cervical vertebrae	44.3 (5.3–103.2)	324 (56–1275)	2.6 (0.3–7.5)
Dorsal vertebrae	NA	253 (66–515)	4.6 (1.0–9.8)
Lumbar vertebrae	30.3 (10.6–59.7)	302 (49–870)[b]	5.2 (0.8–15.7)

NA: not available; DLP: dose-length product.

[a] The values are indicated as the median and the extreme values in brackets.

[b] Note the difference in the dose of lumbar CT between the review of the literature by Pantos et al. [21] and the values provided by Biswas et al. [22] within their institution (Table 2). This difference is mainly due to an increase in the dose after the passage from the single-slice CT to the multislice CT (Pantos et al. mainly take studies on single-slice CT into account [21] while Biswas et al. use a 16-slice CT [22]) as well as the increase in the acquisition lengths that also accompanied the distribution of multislice CT.

Table 2 Doses of the peripheral joint and spinal computed tomography (CT) according to Biswas et al. [22] (gathered with a 16-slice CT).

Joints	CTDI(w)[a] (mGy)	DLP[a] (mGy cm)	Effective dose[a] (mSv)
Wrist and hand	14.41 ± 15.52	137 ± 134	0.03 ± 0.03
Elbow[b]	21.52 ± 23.83	293 ± 311	0.14 ± 0.22
Shoulder	19.49 ± 13.77	316 ± 211	2.06 ± 1.52
Hip	19.83 ± 7.67	422 ± 174	3.09 ± 1.37
Knee	18.39 ± 14.43	356 ± 289	0.16 ± 0.12
Ankle and foot[c]	17.88 ± 13.39	310 ± 210	0.07 ± 0.05
Cervical vertebrae	64.17 ± 29.04	1414 ± 831	4.36 ± 2.03
Dorsal vertebrae	64.39 ± 22.23	2171 ± 805	17.99 ± 6.12
Lumbar vertebrae	66.53 ± 21.56	1701 ± 689	19.15 ± 5.63

DLP: dose-length product.
[a] The values are indicated as the mean ± standard deviation.
[b] Only elbow (elbow above the head).
[c] Unilateral.

Table 3 Osteoarticular computed tomography (CT) doses within our institution with our previous 16-slice CT (Sensation 16, Siemens) [30].

Type of CT	CTDI(w)[a] (mGy)	DLP[a] (mGy cm)	Effective dose [a] (mSv)
Cervical vertebrae	21 (18.5–45.2)	411 (321–766)	1.3 (1–2.4)
Lumbar vertebrae	32 (23.4–56.4)	782 (399–1527)	8.8 (4.5–17.2)
Pelvic bone	21 (15.6–33.4)	602 (366–1359)	4.4 (2.7–9.9)
Shoulders	25 (23.4–35.0)	332 (253–688)	2.2 (1.6–4.5)
Knee	18 (10.9–31.2)	425 (195–757)	0.2 (0.1–0.3)

DLP: dose-length product.
[a] The values are indicated as the median and the extreme values in brackets.

Ways to reduce the dose in osteoarticular computer tomography (CT)

The ways to reduce the CT dose are based on the three main principles of radioprotection: justification, optimisation and substitution [32]. They have been adopted by the Euratom 97/43 European Community Directive [33] and by the ALARA (As Low As Reasonably Achievable) principle of precaution. All of these ways have been extensively detailed in the literature [9,34–38]. We will discuss them, in turn distinguishing the behavioural from the technical factors and focusing on their applications in the realm of osteoarticular CT.

Table 4 Doses with the lumber vertebrae computed tomography (CT) and shoulder arthro-CT within our institution. Gathered with a 320-slice CT (Aquilion One, Toshiba) before and after implant of AIDR 3D iterative reconstructions (Adaptive Iterative Dose Reduction 3D, second version of the Toshiba iterative reconstructions).

	CTDI(w)[a] (mGy)	DLP[a] (mGy cm)	Effective dose[a] (mSv)
Lumber vertebrae CT			
Before implant of iterative reconstructions[b]	40.2 ± 11.4	1094 ± 309	12.32 ± 3.5
With AIDR 3D	25.5 ± 11.9	695 ± 338	7.83 ± 3.8
Shoulder artho-CT			
Before implant of iterative reconstructions[b]	43.9 ± 15.9	611 ± 259	3.98 ± 1.7
With AIDR 3D	16.1 ± 4.3	205 ± 82	1.34 ± 0.5

DLP: dose-length product.
[a] The values are indicated as the mean ± standard deviation.
[b] CT imaging acquired by filtered back projection with QDS (Quantum Denoising System, Toshiba).

Table 5 Tissue-weighting factors used to calculate the effective dose for different anatomic locations in osteoarticular disease, calculated according to Biswas et al. [22].

Computed tomography (CT)	Tissue-weighting factor[a] (μSv/mGy cm)
Shoulder	6.52
Elbow[b]	0.48
Wrist and hand	0.22
Hip	7.31
Knee	0.44
Ankle and foot[c]	0.23
Cervical vertebrae	3.08
Dorsal vertebrae	8.29
Lumbar vertebrae	11.26

[a] These factors were calculated from the relationship between the effective dose and the dose-length product by Biswas et al. [22]. Note that Biswas et al. calculated these factors using IMPACT dosimetry software based on the ICRP 60 data [11]. New factors have to be re-calculated to take into account the new ICRP 103 data.
[b] Only elbow (elbow above the head).
[c] Unilateral.

Behavioural factors

Awareness and education

First, like in other domains, the education and awareness of radiologists and radiology technicians is an important element in the reduction of the dose in osteoarticular disease. Wallace et al. [39] have shown that, after doctor education, it was possible to obtain a 29% reduction in the dose of lumbar CT at several institutions. This education also emphasises the situations in which the reduction in the dose is especially important. For example, the patient's age is a major factor since the potential risk of radio-induced cancer due to low-doses of X-rays decreases with age [40]. Special care is the rule for young subjects. In addition, the anatomic location of the CT is important. The effective dose of an acquisition at a distance from radiosensitive organs, as is the case for the peripheral joints, will be negligible (with effective doses sometimes lower than those of a chest X-ray!) as opposed to lumbar CT imaging or proximal joint CT imaging (however, it should be noted that the calculation of the effective dose does not take into account the radiosensitivity of tissue related to age). However, the awareness of radiologists and operators requires knowledge of the doses delivered. From this point of view, the display of the DLP on the CT console before the acquisition is indispensable and currently systematically available for all manufacturers. This awareness is also increasingly guaranteed by the software used in the gathering and analysis of the doses delivered. This software allows for dosimetric monitoring per patient and detects the cumulate dose, which is sometimes high. The software also includes dosimetric warnings that help optimise the protocols and help monitor the overall reduction in the doses during optimisation [41]. More globally, national or international dose registers are also being created, such as, for example, the CT Dose Index Registry [42]. Under the initiative of the American College of Radiology, this dose register aims at obtaining the CT radiation doses from a great many American and foreign radiology departments in order to compare the doses and harmonise practices.

Justification and substitution

Justification and substitution are also two important elements in osteoarticular imaging where substitution by non-irradiating imaging techniques such as sonography or MRI is often possible [4,9,43]. For example, Oikarinen et al. [44], in their study on 30 lumbar CT carried out in patients under the age of 35 years, demonstrated that only seven of them (23%) were indicated. Of the 23 lumbar CT not indicated, 20 of them would have been able to benefit from an MRI whereas imaging was not indicated for the other three patients. Clarke et al. [45] also demonstrated that 90% of the lumbar CT could be replaced by an MRI. However, the MRI is not always possible due to problems of claustrophobia, non-compatible implants, pacemakers or even precarious medical conditions [9]. In addition, in certain diseases, the performance of CT is superior that of MRI [4]. For example, in the study on the spine, the CT has proven to be more sensitive in the detection of bone changes following an infection [46]. CT is also better than MRI in the characterisation of certain structures such as gas and calcifications. With its good spatial resolution, CT also provides a better visualisation of scaphoid fractures [47] or even the detection of certain osteoid ostomas that remain invisible in MRI [48]. The angio-CT is sometimes more efficient than the angio-MRI in the assessment of vascular invasion of musculoskeletal tumours [49,50]. In our institution, CT imaging is indicated in the following situations: complex fractures, fractures with suspicion of vascular impairment, fractures-dislocations, initial assessment of musculoskeletal tumours, postsurgical monitoring, bone dysplasia and congenital malformations, disco-radicular spinal disease and assessment of joint impairment. In addition, arthro-CT may be carried out for almost all joints. It provides a better visualisation of superficial cartilaginous lesions than the MRI. It is also possible to carry our useful multislice reformations with the CT in a postsurgical assessment [51,52]. CT arthrography of the wrist also enables a better analysis of ligament lesions than the MRI or MR arthrography [53] while CT arthrography of the shoulder is a very efficient imaging technique for the detection of SLAP lesions [54].

Length of exploration and number of acquisitions

During CT imaging, the dose can be controlled by reducing the number of acquisitions (that is, the number of phases) and the length of the zone explored [55]. The length should be restricted to the zone of interest, previously detected by the CT topogram(s). As indicated above, this is one of the main reasons in the differences in doses between the different examinations. As regards the number of acquisition phases, CT often only includes one phase without injection in osteoarticular disease. However, with the development of interventional CT imaging and dynamic and perfusion CT, the limitation in the number of phases is of prime importance.

Position and centering

Exact centering of the anatomic zone for the CT imaging at the centre of the ring provides optimum image quality and dose delivered. The spatial resolution is actually better at the centre of the ring since more data is obtained there than at the periphery [56]. Moreover, good centring is especially required with the use of milliamper automatic modulation since this modulation considers that the patient is at the centre of the ring [57]. In case of poor centring, the automatic modulation significantly increases the dose [58]. The patient's position also has an effect on the dose and quality of the image. The volume explored should be as thin as possible to limit the artefacts of beam hardening and reconstruction. This is why the shoulders are placed at a different height during exploration of the pectoral girdle (Fig. 2). During the imaging of a leg joint (foot, ankle, knee), the volume explored should be reduced by raising the opposite leg. Similarly, the peripheral joints should be acquired as far as possible from the patient's trunk in order to reduce the dose received by radiosensitive organs. Biswas et al. [22] demonstrated that the acquisition of an elbow along the body compared with a position above the head was responsible for a considerable increase in the effective dose (8.35 versus 0.14 mSv).

Technical factors

Type of computer tomography (CT) acquisition

With the development of multislice CT, the spiral mode has extensively replaced sequential axial acquisition. However, the appearance of wide-area detector CT has enabled its return. The 320-slice CT has, with a single rotation, helped acquire a volume of up to 16 cm in length, thereby covering most joints (shoulder, wrist, hand, hip, sacroiliac, knee, ankle and foot). The advantage of this type of volume acquisition is that it considerably reduces the time of acquisition (up to 0.175 s for the acquisition of a volume of 16 cm, without shift between the first and last slice) and therefore patient movement artefacts. In addition, this type of volume acquisition reduces the irradiation compared with the spiral mode. In fact, with wide-area detector CT, the shadow phenomenon (or overbeaming) is proportionally smaller than that with 16 or 64-slice CT [59,60]. It should be noted that this shadow phenomenon is independent of the collimation and is therefore relatively greater in case of narrower collimation. Therefore, the use of a reduced number of slices should be avoided with a multislice CT. The use of the volume mode also eliminates pre and postspiral irradiation (or overranging), characteristic of the spiral mode [61]. The dose of additional irradiation due to pre and postspiral irradiation is higher with an increase in the number of detectors and is also proportionally higher for acquisitions of smaller length [62] as is the case for acquisitions of the peripheral joints. With the acquisition of shorter anatomic zones with a 16 or 64-slice CT, certain authors recommend the use of the axial and non-spiral mode to eliminate the dose due to overranging [34,63].

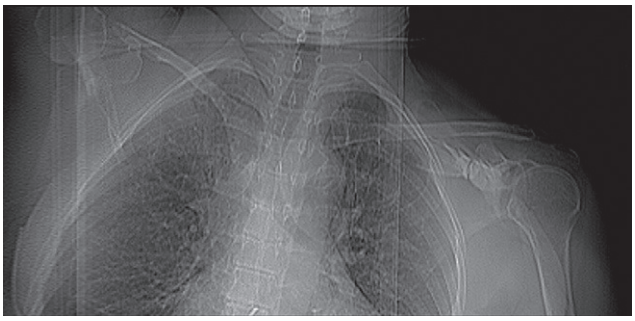

Figure 2. Front topogram before arthro-computed tomography (CT) of the left shoulder. Note the patient's position with ascension of the contralateral shoulder, allowing for a reduction in the thickness of the zone to scan as well as a reduction in the hardening artefacts of the beam.

Kilovoltage

The reduction in kilovoltage is the source of a major reduction in the dose. However, it is also the cause of an increase in noise (for example, by maintaining the other parameters constant, a reduction in kilovoltage from 120 to 80 kV reduces the dose delivered by a factor of 2.2 [58] but also increases the noise by a factor of 2 [58,64]). In practice, the increase in noise results in a deterioration in the quality of the image that becomes grained. This appearance is harmful during the analysis of structure with small differences in density (as is the case for the analysis of soft tissue) in view of an alteration in the contrast to noise ratio. However, it is not harmful for the analysis of bone structures due to a high natural contrast. It is therefore possible to acquire peripheral joints (wrist, knee, ankle, foot) at 100 or even 80 kV (Fig. 3). For example, for a CT of the wrist with a centred acquisition of 6 cm, with 80 kV and 50 mAs, the quality of the image is satisfactory for the bone analysis, including a cast immobilisation (Fig. 4). This acquisition provides a total DLP total of 20.9 mGy cm, corresponding to an effective dose of 0.0046 mSv (with a tissue conversion factor of 0.22 μSv/mGy cm according to Biswas et al. [22]). By comparison, this effective dose is only 3.3 times as high as that of an X-ray assessment comprising five wrist incidences (4.6 versus 1.38 μSv) [65] and is less irradiating than a front chest X-ray (about 0.07 mSv) [66]. For thicker proximal joints (shoulder, hip, sacroiliac, spine), the kilovoltage should be adapted to the patient's morphotype: 120 kV in a patient with a standard morphotype, 100 kV in thin patients while in overweight patients, a kilovoltage at 135—140 kV is sometimes required in order to maintain a satisfactory quality of image. Given that the iodine attenuation value increases with a decrease in kilovoltage [67], during arthro-CT of the proximal joints, it is preferable to use a maximum kilovoltage at 120 in order to improve the contrast to noise ratio. For the same reasons, peripheral arthro-CT (wrist, knee, ankle) may be carried out at 80 kV (Fig. 5). During vascular or perfusion exploration, a reduction in the kV is also possible at 100 or even 80 kV according to the thickness of the anatomic zone to cover [68]. Certain teams have also proposed low-dose acquisition protocols at 100 kV for the assessment of spinal trauma [69], myeloma [70] or even at 80 kV for the assessment of scoliosis [71] or even osteoporosis [72].

Milliamps

A milliamp reduction induces a proportional reduction in the dose delivered as well as an increase in image noise (the

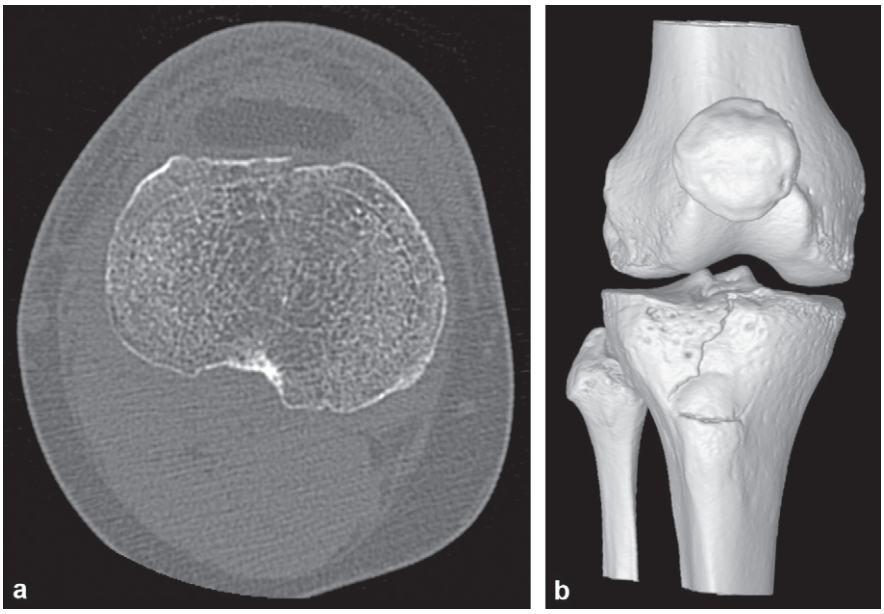

Figure 3. Computed tomography (CT) of the right knee in a 41-year-old woman for a knee trauma. Acquisition with a 320-slice CT and volume rendering (VR) with 100 kV, 100 mAs, rotation time of 0.5 s, slice thickness 0.5 mm and 16 cm coverage for a total DLP of 93.5 mGy cm, corresponding to an effective dose of about 0.04 mSv. Axial plane of 0.5 mm passing through the anterior tibial tubercle (ATT) (a) and Reformation 3D VR (b): non-displaced fracture of the ATT with irradiating secondary articular fracture between the tibial spine and the medial tibial plateau.

noise value in inversely proportional to the square root of the milliamps). This may be harmful for the interpretation of the examinations requiring a good contrast to noise ratio, such as for the analysis of disco-radicular disease. In their study on lumbar CT, Bohy et al. [73] demonstrated that not more than a 35% reduction in milliamps was possible in the standard protocol since the diagnostic performance deteriorated beyond this point. In this study, Bohy et al. [73] used constant milliamps but adapted the body mass index for each patient. The development of the automatic modulation in the milliamps in the three planes allowed for the automation of the adaption of the milliamps to the patient's morphotype [74]. Van Straten et al. [75] demonstrated that this modulation was especially useful in the shoulder and pelvic regions where it reduced the effective dose by 11 and 17% respectively. Its use is also of interest in adapting the milliamps to the patient's morphology during the acquisition of lumbar CT imaging, while maintaining the same

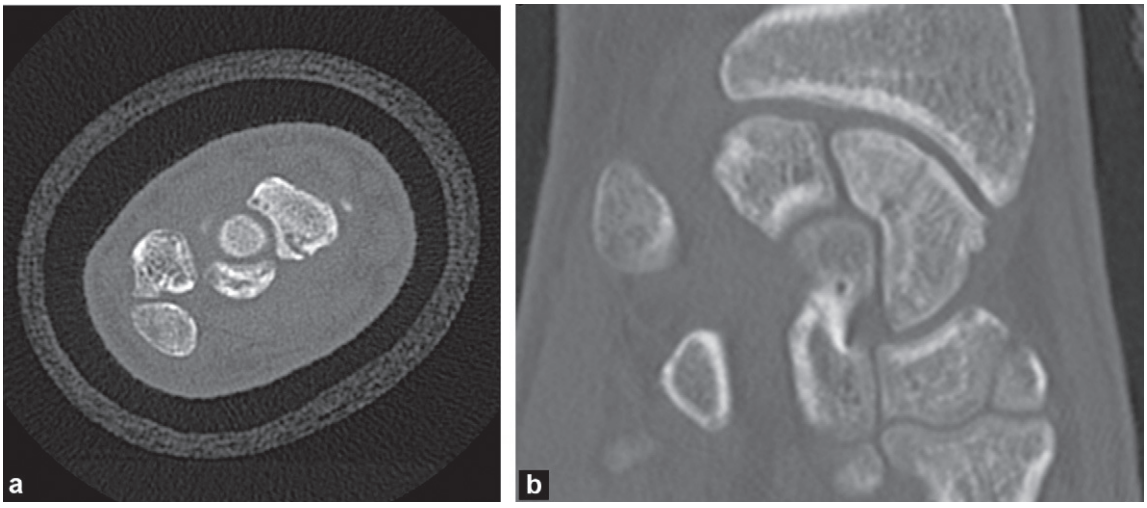

Figure 4. Computed tomography (CT) with cast immobilisation of the right wrist in a 19-year-old man for an assessment after 4 months of a Schernberg type III scaphoid burst fracture. Acquisition with a 320-slice CT with volume rendering (VR) and a height of 6 cm with 80 kV, 50 mAs, rotation time of 0.5 s, slice thickness 0.5 mm and AIDR 3D iterative reconstruction for a dose-length product (DLP) of 20.9 mGy cm, corresponding to an effective dose of 0.0046 mSv. Axial plane of 0.5 mm (a) and front reformation of 1.5 mm (b) revealing the persistence of the fracture and absence of signs of consolidation. Note the good quality of the image in spite of the presence of cast immobilisation and the major reduction in the acquisition parameters and the DLP.

Figure 5. Arthro-computed tomography (CT) of the left ankle in a 41-year-old man referred for an assessment of the persistent pain of the ankle after a serious sprain. Acquisition with a 320-slice CT scanner with volume rendering (VR) with 80 kV, 50 mAs, slice thickness of 0.5 mm, rotation time of 0.5 s, adaptive iterative dose reduction (AIDR) 3D iterative reconstruction, with a total dose-length product (DLP) of 23.7 mGy cm, corresponding to an effective dose of 0.005 mSv. Note the excellent analysis of the cartilage in spite of the major rerduction in the acquisition parameters and the dose.

image quality. Mulkens et al. [76] also demonstrated that the use of the automatic milliamp modulation in the three planes reduced the dose of a lumbar CT by 37%. Mastora et al. [77] also demonstrated that, during the exploration of the thoracic outlet syndrome, the use of automatic milliamp modulation allowed for a 35% reduction in the dose without a loss of image quality. Moreover, certain authors proposed carrying out a low-dose protocol with low milliamps. For example, Horger et al. [17] demonstrated that the low-dose acquisition of a whole-body CT was possible in the diagnosis of lytic lesions and the assessment of the fracture risk in patients monitored for multiple myeloma. A collimation of 16×1.5 mm was used with 120 kV and between 40 and 70 mAS milliamps per second. The effective dose of the CT carried out with 40 mAs was only 1.7 times higher than the dose of a standard whole-body X-ray assessment (4.1 mSv versus 2.4 mSv) [17].

Pitch

With certain current multislice CT comprising modern techniques of automatic milliamp modulation, the change in the pitch does not change the dose since it results in an automatic adaption of the milliamps [78]. A high pitch, of about 1.5, is preferable to reduce the time of acquisition and the movement artefacts (for example, during the exploration of a multi trauma patient). Nevertheless, the pitch should remain under two in order to maintain the optimum quality of the multiplane reformations [78] and avoid the appearance of spiral artefacts [34]. On the other hand, a low pitch is preferred for the reduction of metallic artefacts related to osteosynthesis materials [79].

Slice thickness

In general, the acquisitions are carried out in thin slices (0.5 to 1 mm), required for the analysis of bone structures and reconstructed in thicker slices (2 to 5 mm) for the analysis of soft tissue. The sub-millimetric slices improve the spatial resolution, reduce the effects of partial volume and allow for multiplane reformations [80]. However, at constant noise, the acquisition in thin slices is the cause of an increase in the irradiation [81]. If there is an excess reduction in the milliamps, the acquisition in thin slices leads to a major increase in the image noise. Therefore, whereas the acquisition is obtained in sub-millimetric slices, during the interpretation of the images, the thickening of the slices helps increase the signal to noise ratio [80] and improve the analysis of the soft tissue [82,83].

Field collimator

Field collimators are placed at the outlet from the tube and help limit the beam of exposure at the field chosen, thereby allowing for a reduction in the dose. The smallest possible field collimation should be used, in particular with the exploration of the small joints.

Iterative reconstructions

The use of CT iterative reconstructions represents major progress in the reduction of the dose (Table 4). The first results show that they allow for a reduction of up to 50% of the dose, while maintaining the same image quality [84,85]. Until now, few studies have assessed the value of iterative reconstructions in musculoskeletal imaging. In our institution, we carried out a study on 15 lumbar CT acquired with volume mode on a 320-slice CT with Adaptive Iterative Dose Reduction (AIDR), the first version of the iterative reconstruction by Toshiba and by comparing them with standard reconstructions in Filtered Back Projection (FBP). Our results found a mean reduction of 31% in the image noise with AIDR compared with the FBP images [10], without an alteration in the spatial resolution. This noise reduction corresponds to a potential reduction in the dose of 52%. These initial results are promising, especially since the versions of iterative reconstruction are quickly evolving. In our institution, the new version of AIDR 3D iterative reconstructions was recently installed and new studies are required to assess their impact on the reduction in the dose and the improvement of image quality (Fig. 6). While these iterative reconstructions are of particular interest in reducing the dose of CT imaging requiring a good contrast to noise ratio, their performance on examinations where bone analysis is of major importance, such as for example in the search for a fracture, is not as important. In fact, the high natural contrast of the bone structures allows for low-dose noise acquisitions without this affecting the interpretation in a significant manner [86]. Nevertheless, one of the benefits of iterative reconstructions is the possibility of reducing the artefacts related to FBP reconstructions and, in particular, the beam hardening artefacts [87] (Fig. 7). This is of particular interest in the analysis of the soft tissue and bone structures in contact with osteosynthesis material.

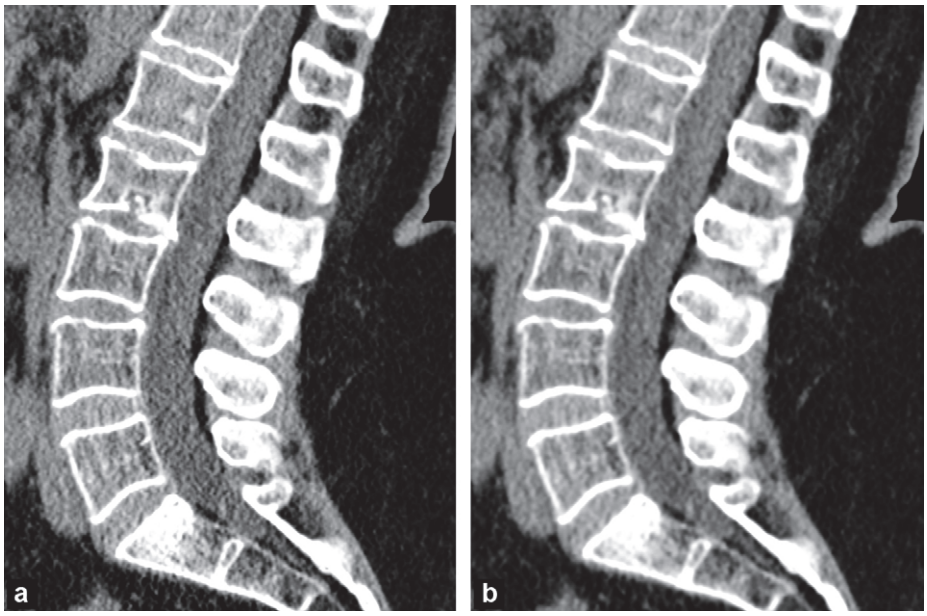

Figure 6. Lumbar computed tomography (CT) in a 67-year-old woman with a body mass index of 31 kg/m^2. Acquisition from T12 to S2 with 135 kV, automatic milliamp modulation with noise index at 8, rotation time of 0.75 s, spiral 64-slice acquisition of 0.5 mm for a dose-length product (DLP) of 804 mGy cm. Sagittal reformations of 2 mm with standard reconstruction in filtered back projection (a) and with adaptive iterative dose reduction (AIDR) 3D iterative reconstructions (b). Note the reduction in image noise with the iterative reconstructions, the origin of improved visualisation of the disc bulge.

Traditionally, the best visualisation of metal materials requires an increase in the acquisition parameters such as the kilovoltage and milliamps as well as a low pitch and a thin collimation. All of these parameters result in an increase in the dose [88]. Iterative reconstructions allow for a reduction in these artefacts while avoiding an increase in the dose by the optimisation of other parameters (Fig. 8).

Noise reduction filter

The improvement in the contrast to noise ratio required for the analysis of the soft tissue, in particular for discoradicular disease, may also be obtained by the use of noise reduction filters by post-treatment software. These filters are applied on already reconstructed images. This allows them to be used with any CT image, including 3D reformations. As opposed to the filters used during the reconstruction of images, some of these noise reduction filters seem able to smooth the image without altering the spatial resolution. However, studies have to be carried out in order to confirm the value of this new post-treatment hardware.

Active collimation

Although not accessible in the choice of parameters, this technology is worth describing. Sheilds help reduce pre- and postspiral irradiation phenomena by using active collimation in the z-axis at the beginning and end of the spiral [89]. These shields are of particular interest when the pre- and postspiral irradiation accounts for a large share of the dose of patient irradiation, that is, during short acquisition with a 16 or 64-slice CT. Christner et al. [90] have shown that with a 64-slice CT, for a pitch of 1, a beam collimation of 38.4 mm and an acquisition length of 15 cm, the shields provide a 16% reduction in the total dose delivered to the patient. However, with an acquisition greater than 300 mm with a 64-slice CT, the pre- and postspiral irradiation accounts for less than 3% of the total dose, irrespective of the pitch [90]. In osteoarticular disease, this active collimation is therefore of great interest in reducing the dose during acquisition with 16 or 64-slice CT of the shoulders and hips considering the low coverage and the proximity of radiosensitive organs (thyroid and gonads).

In practice

The justification and substitution of examinations by CTgraphy remains fundamental: ''a scan that is not carried out is one that irradiates the least''. The limitation of the coverage of CT imaging is also a simple way to reduce the irradiation: ''the smaller the acquisition coverage, the smaller the dose''. The volume acquired should be as thin as possible and a small field collimation should be used for the exploration of small joints. The kilovoltage and milliamps should be adapted to the type of acquisition (reduction of these acquisition parameters for the exploration of a peripheral joint, reduction of the kilovoltage for the acquisition of an arthro-CT), the indication (analysis of the soft tissue requiring higher milliamps than the analysis of bone structure) and the morphotype of each individual. The new techniques to reduce the dose should also be used as soon as possible (automatic modulation of the milliamps and the kilovoltage, iterative reconstructions, active collimation). Finally, with dynamic or perfusion acquisition, the dose should be reduced by limiting the number of acquisition phases (Boxed text 1).

Nevertheless, even if the reduction of the dose is primordial, in particular in young subjects, it should not be carried

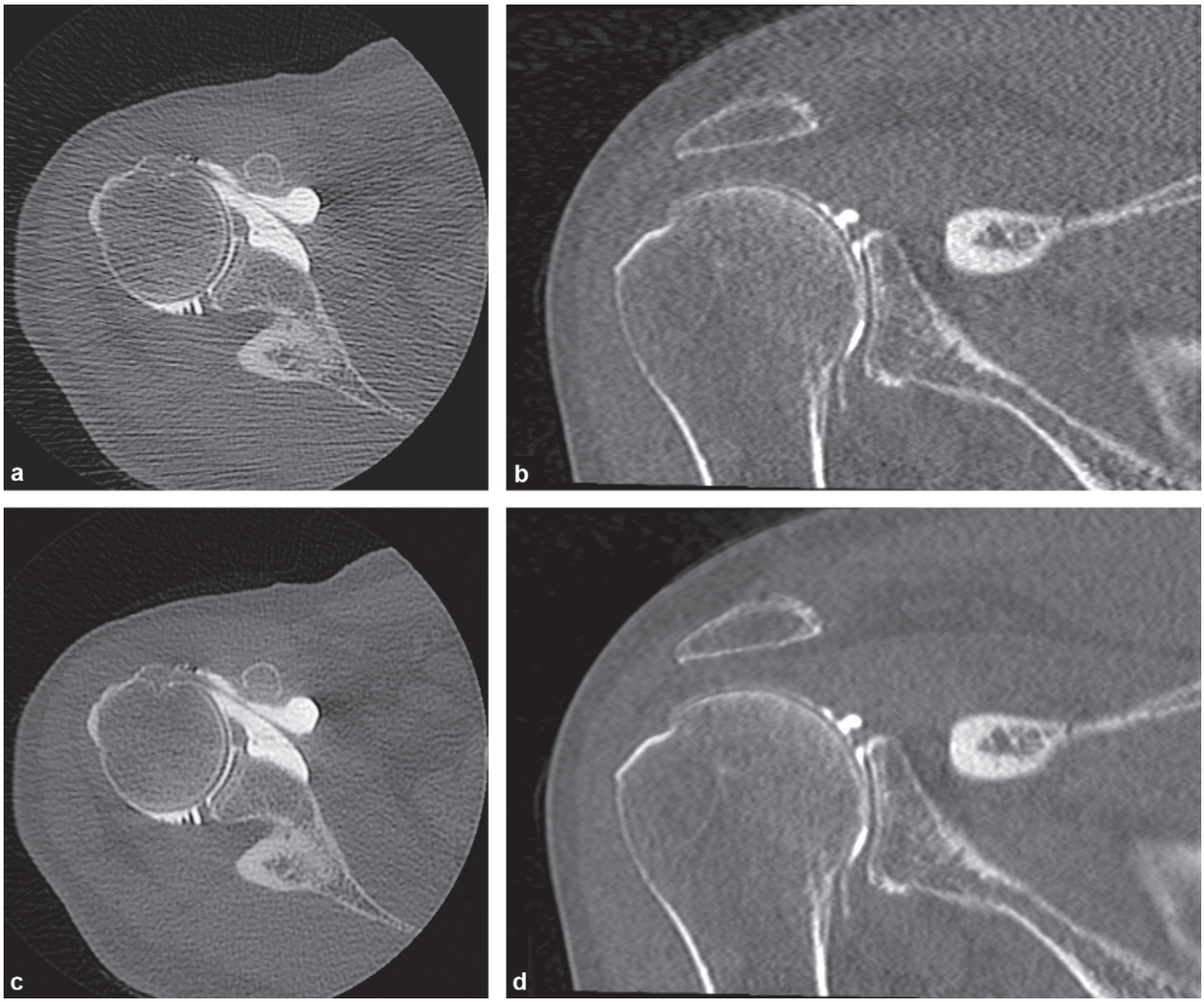

Figure 7. Arthro-computed tomography (CT) of the right shoulder in a 73-year-old man. Acquisition with volume rendering (VR) with a 320-slice CT with 120 kV, 150 mAs, rotation time of 0.75 s, slice thickness of 0.5 mm for a dose-length product (DLP) of 175 mGy cm. Filtered back projection reconstruction in native axial section of 0.5 mm (a) and frontal reformation in 1.5 mm section (b) and adaptive iterative dose reduction (AIDR) 3D iterative reconstructions in native axial section of 0.5 mm (c) and in frontal reformation in 1.5 mm section (d). Note the reduction in image noise as well as the major reduction in hardening artefacts of the beam due to the AIDR 3D iterative reconstructions, resulting in the improved visualisation of the cartilage of the upper edge of the humerus head.

out at the expense of the quality of the image and especially of the diagnostic performance: CT imaging with a reduced dose that provides poor image quality and does not allow for a diagnosis is more harmful than CT imaging with a normal dose that allows for a proper diagnosis.

Dynamic computed tomography (CT) imaging of the joints

Joint kinematics may be examined by a static study in different positions or by a continuous dynamic study. The latter should be privileged during study of the joint kinematics [91—93] since the constraints differ between a system in action and a static system [94,95]. The improvement in the temporal resolution of multislice CT and the development of multidetector CT now allows for dynamic studies to be carried out on the peripheral joints [96,97]. The adaptation of the acquisition parameters as well as the application of recent methods of dose reduction help maintain a low-dose delivered to the patient, often lower than that with traditional acquisition on a conventional CT. Therefore, CT imaging is a tool of functional analysis improving knowledge of the joint kinematics and its dysfunctions.

The dynamic study of joints is possible in spiral mode with a 64-slice CT. Tay et al. [98] have shown, in an experimental study, that it is possible to obtain the dynamic acquisition of a wrist in four phases with a very low pitch (0.1) by using a protocol with retrospective synchronisation of the movement. However, this technique induces a great many movement and ''step'' artefacts and a major increase in irradiation [98] rendering the efficacy much lower than that of volume acquisitions with multidetector CT.

Boxed text 1 The seven gold rules to reduce radiation by osteoarticular computed tomography (CT).

- Comply with the indications.
- Whenever possible, prefer a non-irradiating method of imaging.
- Limit the CT coverage.
- Limit the number of acquisition phases during dynamic and perfusion examinations.
- Adapt the kilovoltage and milliamps to the indications and morphology of each patient.
- Reduce the kilovoltage during the exploration of the peripheral joints and arthro-CT.
- Use modern methods to reduce the dose (iterative reconstructions, automatic modulation of the milliamps...).

In our institution, we study joint kinematics with a 320-slice CT. This allows for the acquisition of a volume up to 16 cm long. A rotation time of 0.35 s combined with a technique of partial data reconstruction (reconstruction of data over 180° by rotation) provides a temporal resolution of 0.175 s per rotation. Volume acquisition also has several advantages: reduction of the dose compared with the spiral mode by elimination of pre- and postspiral irradiation [61] and acquisition of the entire volume at one time, without shift between the first and last slices or shift due to the movement of the table. With this technique, it is possible to study the kinematics of the peripheral joints and provide diagnostic information in several clinical indications: occult instabilities of the wrist, femoro-patellar syndrome, posterior conflict of the ankle, thoracic outlet syndrome. Nevertheless, these indications are new and an assessment of the diagnostic performance of this type of examination is required in order to justify their use, especially in view of their irradiating nature. In fact, these dynamic studies require the repetition of several acquisitions leading to an increase in the irradiation when compared with a single acquisition. Nevertheless, on a peripheral joint, with the possibility of obtaining low-dose acquisitions without disturbing the interpretation of the movement [99], it is possible to obtain dynamic acquisitions with an effective dose under 1 mSv. For example, for the study of the kinematics of radio-ulnar deviation of the wrist with 12-phase volume rendering (80 kV, 11 mAs, rotation time of 0.35 s, acquisition coverage of 6 cm), the DLP is only 91.2 mGy cm, corresponding to an effective dose of 0.02 mSv (Fig. 9). With this low effective dose, it is possible to study several types of movement (for example for the wrist: flexion/extension, tightening, ulnar and radial deviation) while maintaining a total effective dose much lower than 1 mSv. In the same way, for a dynamic exploration of the ankle, the DLP is under 200 mGy cm, corresponding to an effective dose of 0.046 mSv.

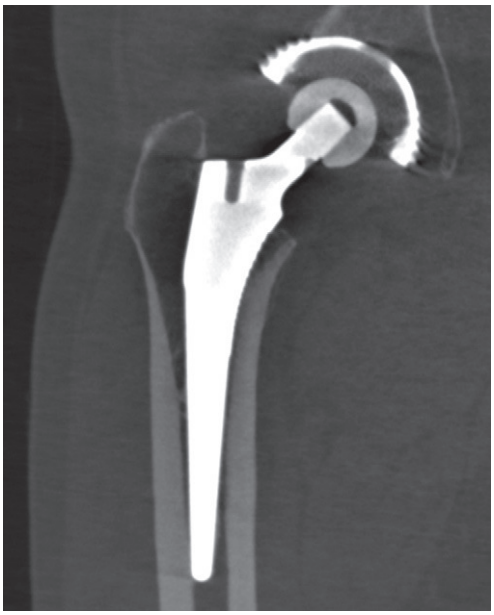

Figure 8. Computed tomography (CT) of the right hip in a 70-year-old man for an assessment of right coxalgia on a total hip replacement. Spiral acquisition with a 320-slice CT with 135 kV, 15 mAs, rotation time at 0.5 s, 64 × 0.5 mm and AIDR 3D iterative reconstruction for a dose-length product (DLP) of 326 mGy cm. Frontal reformation in 2 mm section. Note the excellent quality of the image due to a reduction in the metallic artefacts by iterative reconstructions that also allow for a reduction in the dose.

For dynamic explorations of the hips and shoulders, it is especially important to reduce the dose due to the optimisation of the acquisition parameters. If the dynamic exploration only involves bone segments, the high natural contrast of the bone allows for a considerable reduction in the kilovoltage and milliamps [100]. It is also important to reduce and centre the acquisition coverage of the zone of interest. In addition, even if Hristrova et al. [96] demonstrated that image quality is improved by the continuous acquisition of data, the additional irradiation makes acquisition in intermittent mode preferable, with a number of phases in general limited to 12. On the pelvis, this allows the dose of irradiation to be kept at less than 10 mSv, corresponding to a standard multiphase abdominal and pelvic examination.

Perfusion computed tomography (CT)

Perfusion CT was first described a great many years ago [101]. Like with dynamic examinations, the CT perfusion of musculoskeletal tumours is possible due to an improvement in the temporal resolution of multislice CT imaging and the development of multidetector CT. The study of perfusion by CT combines the advantages of perfusion imaging, providing data similar to that provided by the MRI but with better visualisation of the bone invasion (periosteal reaction, cortical break, osteolysis), the femoral necrosis and the neovascularisation. The quantification of perfusion curves by CT is as easy as with MRI [102]. This tumoral perfusion may be carried out in spiral mode with a multislice CT due to a 2D scanning movement [103] or in ''step-and-shoot'' volume rendering with a multidetector CT. The advantage of tumoral perfusion with volume rendering is that it is obtained without moving the table and therefore there are fewer movement artefacts, helping improve the quality of the reconstructions and perfusion curves. This technique

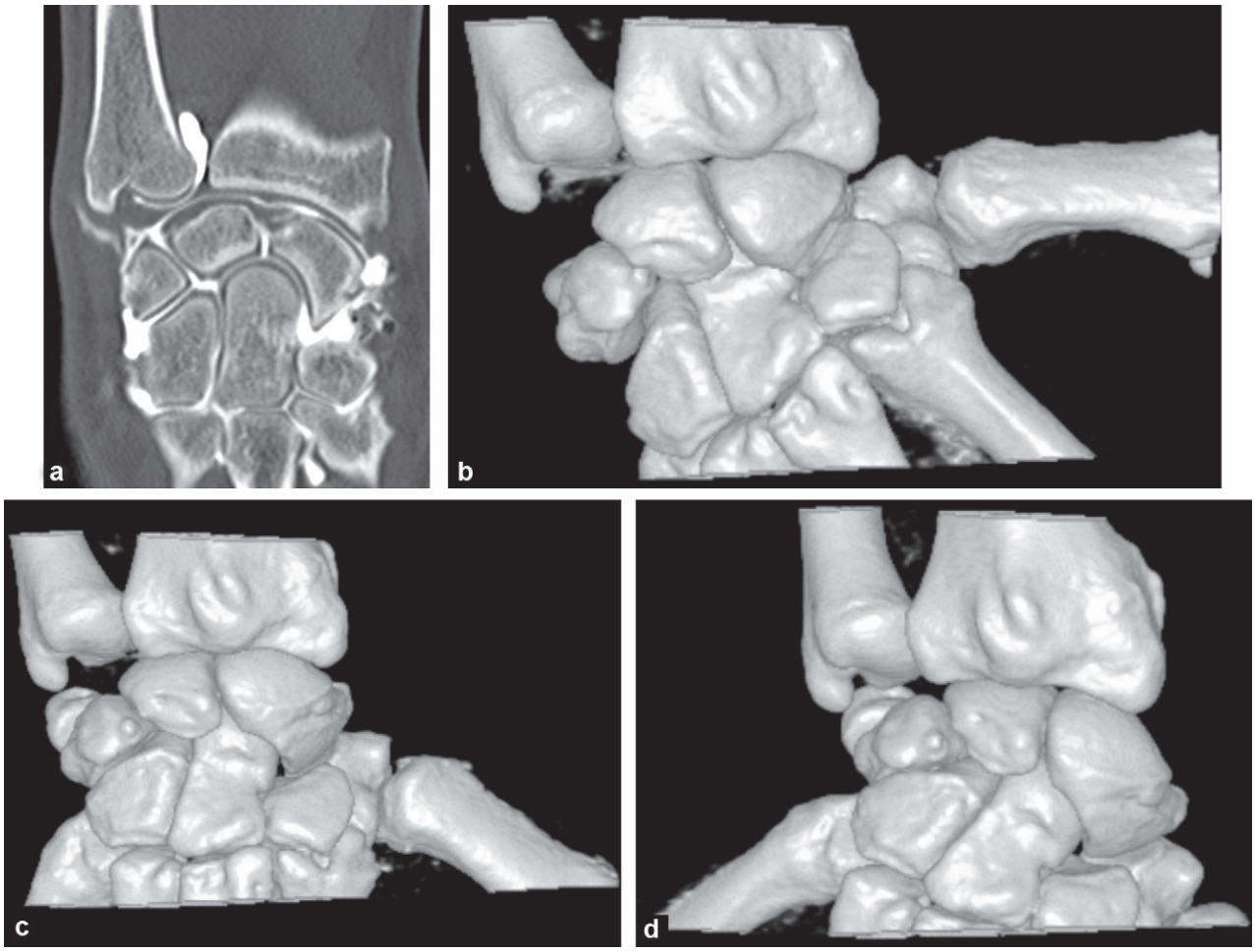

Figure 9. Dynamic arthro-computed tomography (CT) of the left wrist in a 37-year-old man for an assessment of persistent pain at the wrist following a trauma. Acquisition with a 320-slice CT with static acquisition of the arthro-CT with volume rendering (VR) with 80 kV, 50 mAs, rotation time at 0.5 s, thickness of the section 0.5 mm, 8 cm coverage for a dose-length product (DLP) of 25.7 mGy cm, then dynamic acquisition during a movement of radio-ulnar deviation comprising 12 volume acquisitions with 80 kV, 11 mAs, rotation time of 0.35 s, 0.5 mm section thickness and 6 cm coverage for a total DLP of 91.2 mGy cm. Frontal reformation of the arthro-CT in 1.5 mm section (a) revealing a transfixing rupture of the lunotriquetral ligament. The 3D VR reformations of the dynamic CT (a: radial deviation; b: neutral position; c: ulnar deviation) do not reveal instability of the carpus with dynamic movements of the radio-ulnar deviation of the wrist.

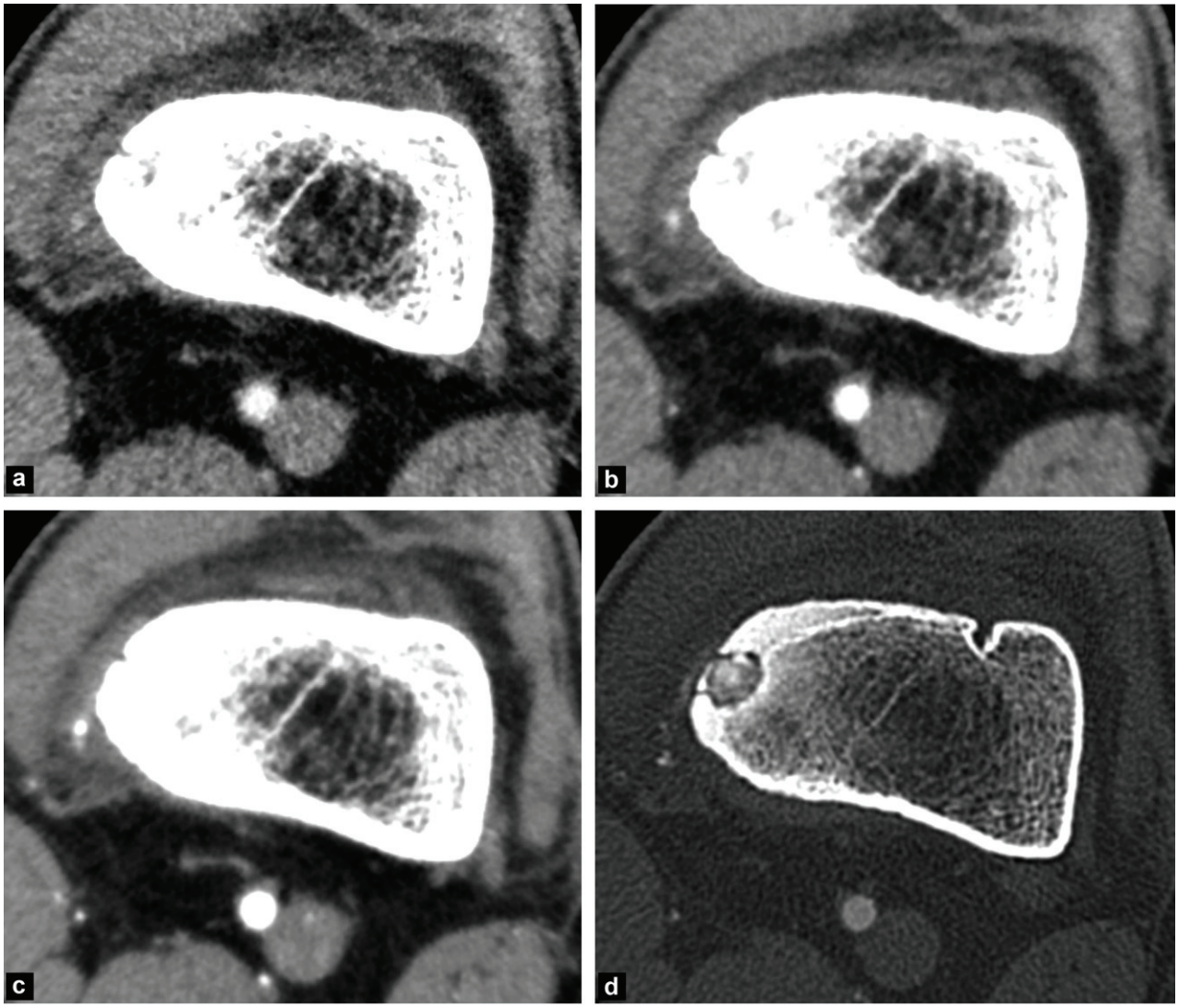

Figure 10. Bone perfusion computed tomography (CT) in an 18-year-old man for an assessment of osteoid osteoma of the distal femoral metaphysis of the left knee. Volume acquisition with a 320-slice CT of 15 phases (acquisition without injection then acquisition after injection with nine phases every 5 s then five phases every 10 s) with 100 kV, 50 mAs, rotation time of 0,5 s, section thickness of 0.5 mm and 4 cm coverage for a total dose-length product (DLP) total of 123 mGy cm. 0.5 mm axial sections in filtered back projection (a), with AIDR iterative reconstruction (b) and after temporal fusion of the different phases (c), 0.5 mm axial sections at arterial time (phase 4) without (d) and with bone subtraction (e) and perfusion curve (f). Note the deterioration in the quality of the native images (a) due to the major reduction in the acquisition parameters and the improvement in image quality due to iterative reconstructions (b) and the temporal fusion technique (c). Also note the hypervascularisation of the nidus of the osteoid osteoma with intense enhancement at arterial time, fully visible due to the reconstructed images with bone subtraction (d). The hypervascular aspect of the enhancement of the nidus is also confirmed by the perfusion curve (f) of the nidus (green curve) when compared with the perfusion curve of a region of interest placed in the popliteal artery (purple curve).

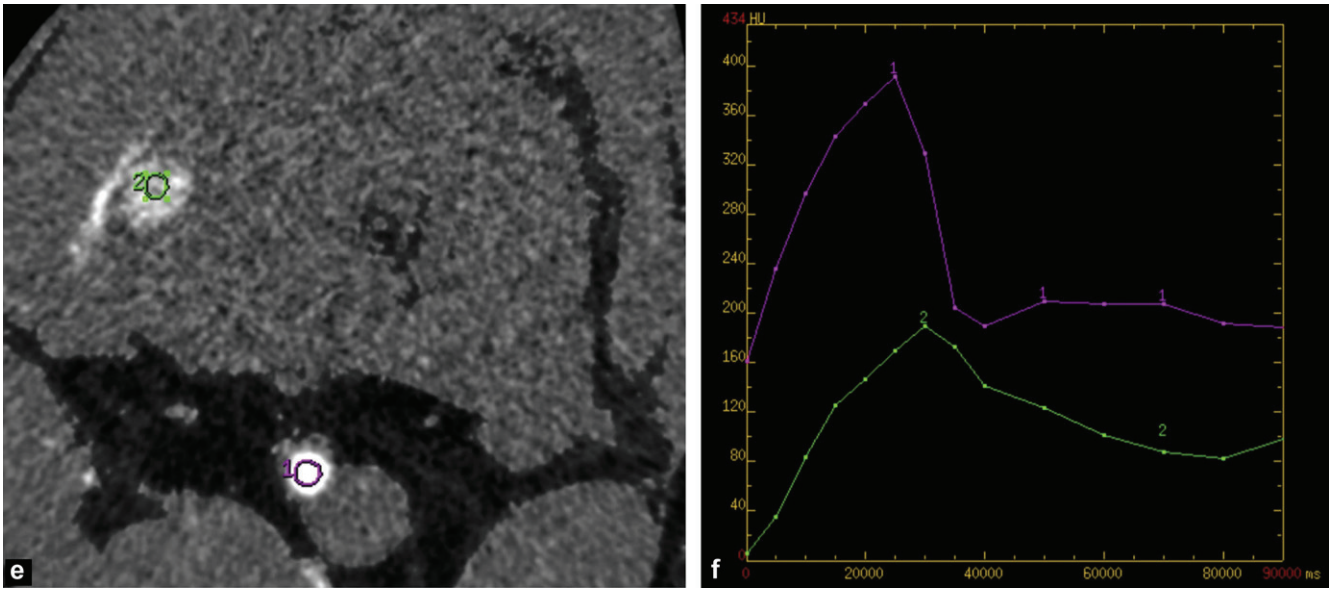

Figure 10. (*continued*).

also allows for use of the fist acquisition as a bone subtraction mask, improving the detection and characterisation of bone anomalies. However, these perfusion studies give rise to a high increase in the dose delivered [103]. The protocol is optimised by reducing the coverage of the CT imaging, by limiting the number of acquisition phases and by adapting the acquisition parameters (reduction in the kilovoltage and milliamps). However, this reduction in the acquisition parameters leads to the deterioration of image quality. This may be compensated by carrying out a temporal fusion of the different phases. This technique allows for a summation of several images derived from different acquisition phases in order to obtain an image with less noise and of better quality (Fig. 10).

In our institution, we have, for example, studied the value of tumoral perfusion in the diagnosis and monitoring of osteoid osteomas [104]. In this disease, the MRI may be faulty [48] and the use of CT imaging more easily indicates the diagnosis by detecting the bone reaction around a small nidus. In addition to this anatomic data, the perfusion CT detects the hypervascularisation of the nidus (Fig. 10). The subtraction of the phases after injection with the first acquisition without injection allows for a sequence of bone subtraction revealing the bone marrow oedema around the nidus. All of this information, usually provided by the MRI, is now accessible with CT imaging. Nevertheless, the value and role as compared with the MRI has to be assessed, since the indications for perfusion CT remain limited to when there is a doubt as to the diagnosis in view of the irradiant nature of this technique and the youth of the patients monitored. To control the dose of irradiation, we target the zone of CT coverage at the zone of interest (only 4 to 8 cm suffices). Moreover, we choose a kV and mAs adapted to the morphotype of the patient and the anatomic zone. The number of phases is also limited to 15 or 16, with an acquisition every 5 s pour for the first nine phases (arterial phases) and then every 10 s. All of these measures allow for a perfusion CT with a total DLP generally between 100 and 500 mGy cm (Figs. 10 and 11).

Dual energy computed tomography (CT)

Dual energy CT is based on the acquisition of two superimposable images with two different kilovoltages. Based on these native images, it is possible to reconstruct a virtual image corresponding to any voltage of the x tube [6]. Each manufacturer proposes dual energy acquisitions on their CT. However, the techniques used often differ. This accounts for the differences in terms of performance and clinical applications between these techniques. For Siemens, dual energy acquisition is obtained from a bi-tube CT. With each rotation, this allows for an image to be obtained with one tube set at 80 kV and the other at 140 kV. For the other manufacturers, only one tube is used to create the dual energy. General Electrics uses a generator that allows for a switch in 0.5 ms between high and low voltage. It is thereby possible, during a single rotation, to switch 500 times and obtain two series of raw data in order to reconstruct two images, one at 80 kV and the other at 140 kV. As for Toshiba, it benefits from the wide coverage of its system of detection (16 cm per revolution) to propose two consecutive revolutions with a change in voltage between both revolutions. Finally, Philips uses a double layer of detector, the first measuring all of the rays transmitted and the second only measuring the hardest beams [105]. Several applications of the dual energy CT in the osteoarticular domain are now clinically available although still in the assessment phase [6]: improvement in tissue characterisation, bone subtraction, differentiation of bone and iodine contrast product or even reduction of metallic artefacts. The improvement in tissue characterisation was first used for the detection and characterisation of urate deposits in gout [106,107]. An initial study by Nicolaou et al. [108] demonstrated that the dual energy acquisition of all peripheral joints (elbows, wrists, hands, knees, ankles and feet) provides good sensitivity and good specificity in the detection of locations of topaceous gout while the total effective dose ranged from only 2 to 3 mSv. Another dual energy application is the possibility of obtaining reconstructions in bone subtraction. It is then

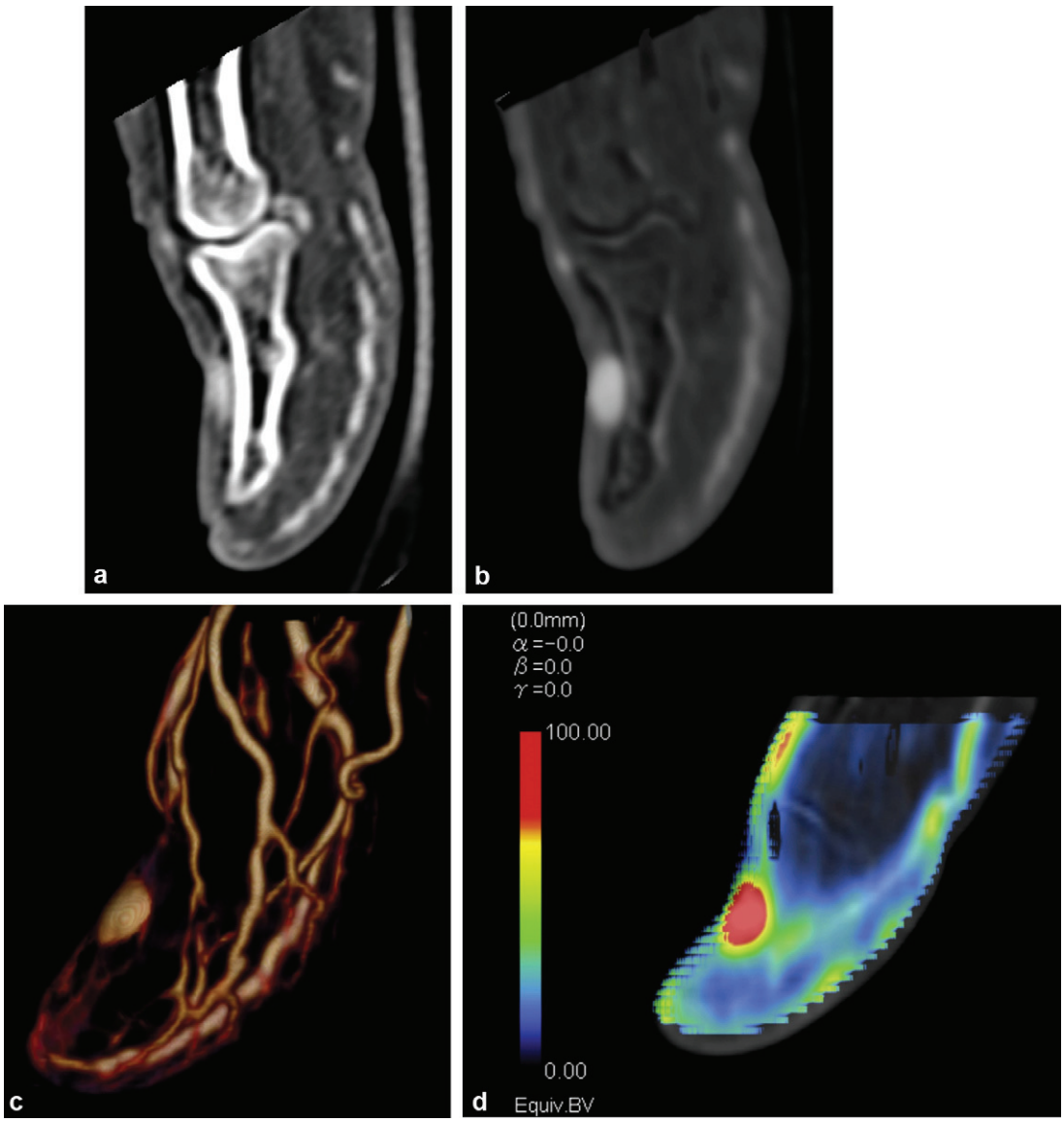

Figure 11. Perfusion computed tomography (CT) of a 68-year-old man presenting a glomic tumour of the left thumb. Volume acquisition with a 320-slice CT and 17 phases (acquisition without injection and then acquisition after injection with 10 phases every 5 s then six phases every 10 s) with 80 kV, 40 mAs, rotation time of 0.5 s, section thickness of 0.5 mm and 4 cm cover for a total dose-length product (DLP) of 274 mGy cm. Sagittal reformations in 1.5 mm section after injection (phase 7) without (a) and with bone subtraction (b), 3D volume rendering (VR) reformation with bone subtraction (c) and map of tumoral perfusion of the blood volume (d). Note the excellent visualisation of the glomic tumour due to the images in bone subtraction (b) as well as the high quality of the 3D VR reformations revealing the distal vascularisation of the thumb (c).

possible to detect the bone marrow oedema. Pache et al. [109] demonstrated that it was possible to detect post-traumatic bone marrow oedema in knee CT imaging, with an increase in irradiation of about 28% compared with a conventional CT. The dual energy bone CT may also become an alternative in case of counter-indication for an MRI or if it is unavailable. However, clinical studies are required to specify the role of this technique compared with the MRI. Subhas et al. [67] demonstrated that the use of dual energy on a shoulder arthro-CT provides a better signal to noise ratio with an equivalent dose. Finally, with a dose equivalent that of a standard single energy acquisition, Bamberg et al. [110] demonstrated that the use of dual energy allowed for a reduction in prosthesis-related metallic artefacts.

Conclusion

Computed tomography is an imaging technique that continues to benefit from a great deal of technological progress. These technological developments, in particular with the development of iterative reconstructions, provide a considerable reduction in the dose delivered to the patient. They also make it possible to access new applications such as perfusion CT or dynamic CT. The modern techniques for dose reduction are of special interest in applications that involve repeated acquisition phases. Nevertheless, the optimisation of the milliamps and kilovoltage, the limitation in the coverage of CT as well as compliance with the indications are still the main ways to limit the doses delivered to patients. These

new indications and the possibility of obtaining low-dose or even very low-dose acquisitions, while maintaining excellent image quality, give CT a major role in musculoskeletal disease. While CT has already replaced the standard X-ray assessment in certain indications, its role with respect to non-irradiating imaging techniques, such as the MRI, still has to be defined.

Disclosure of interest

The authors declare that they have no conflicts of interest concerning this article.

References

[1] Blum A, Walter F, Ludig T, Zhu X, Roland J. Scanners multicoupes : principes et nouvelles applications scanographiques. J Radiol 2000;81:1597—614.

[2] Cotten A, Iochum S, Blum A. 3D imaging in musculoskeletal system. In: Baert AL, Caramella D, Bartolozzi C, editors. 3D image processing. Techniques and clinical applications. Berlin Heidelberg, New York: Springer; 2002. p. 247—55.

[3] Fayad LM, Bluemke DA, Fishman EK. Musculoskeletal imaging with computed tomography and magnetic resonance imaging: when is computed tomography the study of choice? Curr Probl Diagn Radiol 2005;34:220—37.

[4] West ATH, Marshall TJ, Bearcroft PW. CT of the musculoskeletal system: what is left is the days of MRI? Eur Radiol 2009;19:152—64.

[5] Iochum S, Ludig T, Walter F, Fuchs A, Henrot P, Blum A. Intérêt de la technique de rendu volumique en pathologie ostéoarticulaire. J Radiol 2001;82:221—30.

[6] Karcaaltincaba M, Aktas A. Dual energy CT revisited with multidetector CT: review of principles and clinical applications. Diagn Interv Radiol 2011;17:181—94.

[7] Oldrini G, Lombard V, Roch D, Detreille R, Lecocq S, Louis M, et al. Courbes de rehaussement des tumeurs osseuses et des parties molles : comparaison entre scanner et IRM (abstract). J Radiol 2009;90:1578.

[8] Goh V, Padhani AR. Imaging tumor angiogenesis: functional assessment using MDCT or MRI? Abdom Imaging 2006;31:194—9.

[9] Semelka RC, Armao DM, Elias J, Huda W. Imaging strategies to reduce the risk of radiation in CT studies, including selective substitution with MRI. J Magn Reson Imaging 2007;25:900—9.

[10] Gervaise A, Osemont B, Lecocq S, Noel A, Micard E, Felblinger J, et al. CT image quality improvement using adaptive iterative dose reduction with wide-volume acquisition on 320-detector CT. Eur Radiol 2012;22:295—301.

[11] International Commission on Radiological Protection. Recommendations of the International Commission on Radiological Protection. ICRP Publication 60. Oxford: Pergamon; 1991.

[12] European Commission. European guidelines on quality criteria for computed tomography. Report EUR 16262. Luxembourg, 1999.

[13] Shrimpton PC, Edyvean S. CT scanner dosimetry. Br J Radiol 1998;71:1—3.

[14] Hidajat N, Wolf M, Nunnemann A, Liersch P, Gebauer B, Teichgräber U, et al. Survey of conventional and spiral CT doses. Radiology 2001;218:395—401.

[15] Bongartz G, Golding SJ, Jurik AG, Leonardi M, van Persijn van Meerten M, Rodríguez R, et al. European Guidelines for Multislice Computed Tomography. Funded by the European Commission (Contract number FIGMCT2000-20078-CT-TIP). 2004.

[16] Arrêté du 24 octobre 2011 relatif aux niveaux de références diagnostiques en radiologie et en médecine nucléaire. Journal officiel de la république française, 14 janvier 2012.

[17] Horger M, Claussen CD, Bross-Bach U, Vonthein R, Trabold T, Heuschmid M, et al. Whole-body low-dose multidetector row CT in the diagnosis of multiple myeloma: an alternative to conventional radiography. Eur J Radiol 2005;54:289—97.

[18] Gleeson TG, Moriarty J, Shortt CP, Gleeson JP, Fitzpatrick P, Byrne B, et al. Accuracy of whole-body low-dose multidetector CT (WBLDCT) versus skeletal survey in the detection of myelomatous lesions, and correlation of disease distribution with whole-body MRI (WBMRI). Skeletal Radiol 2009;38:225—36.

[19] Damilakis J, Adams JE, Guglielmi G, Link TM. Radiation exposure in X-ray-based imaging techniques used in osteoporosis. Eur Radiol 2001;20:2707—14.

[20] Mettler FA, Huda W, Yoshizumi TT, Mahesh M. Effective doses in radiology and diagnostic nuclear medicine: a catalog. Radiology 2008;248:254—63.

[21] Pantos I, Thalassinou S, Argentos S, Kelekis NL, Panayiotakis G, Efstathopoulos EP. Adult patient radiation doses from non-cardiac CT examinations: a review of published results. Br J Radiol 2011;84:293—303.

[22] Biswas D, Bible JE, Bohan M, Simpson AK, Whang PG, Grauer JN. Radiation exposure from musculoskeletal computerized tomographic scans. J Bone Joint Surg Am 2009;91:1882—9.

[23] Galanski M, Nagel HD, Stamm G. CT radiation exposure risk in Germany. Rofo 2001;173:R1—66.

[24] Thomton FJ, Paulson EK, Yoshizumi TT, Frush DP, Nelson RC. Single versus multidetector row CT: comparison of radiation doses and dose profiles. Acad Radiol 2003;10:379—85.

[25] Mori S, Endo M, Nishizawa K, Murase K, Fujiwara H, Tanada S. Comparison of patient doses in 256-slice CT and 16-slice CT scanners. Br J Radiol 2006;79:56—61.

[26] Jaffe TA, Yoshizumi TT, Toncheva G, Anderson-Evans C, Lowry C, Miller CM, et al. Radiation dose for body CT protocols: variability of scanners at one institution. AJR Am J Roentgenol 2009;193:1141—7.

[27] Fuji K, Aoyama T, Yamauchi-Kawaura C, Koyama S, Yamauchi M, Ko S, et al. Radiation dose evaluation in 64-slice CT examinations with adult and paediatric anthropomorphic phantoms. Br J Radiol 2009;82:1010—8.

[28] Brenner DJ, Hall EJ. Computed tomography an increasing source of radiation exposure. N Engl J Med 2007;357:2277—84.

[29] Richards PJ, George J, Metelko M, Brown M. Spine computed tomography doses and cancer induction. Spine 2010;35:430—3.

[30] Blum A, Noel A, Winninger D, Batch T, Ludig T, Ferquel G, et al. Dose optimization and reduction in CT of the musculoskeletal system including the spine. In: Tack D, Genevois PA, editors. Radiation dose from adult and pediatric multidetector computed tomography. Berlin: Springer; 2007. p. 185—94.

[31] Gervaise A, Teixeira P, Villani N, Lecocq S, Louis M, Blum A. Dose optimization and reduction in musculoskeletal CT including the spine. In: Tack D, Kalra M, Genevois PA, editors. Radiation dose from adult and pediatric multidetector computed tomography. 2nd ed Berlin: Springer; 2012, in press.

[32] International Commission on Radiological Protection. Recommendations of the International Commission on Radiological Protection. ICRP Publication 26. Oxford: Pergamon; 1977.

[33] European Community. Council Directive 97/43/EURATOM, 30 June 1997, on health protection of individuals against the dangers of ionizing radiation in relation to medical exposure (repealing Directive 84/466/Euratom). Off J Eur Commun 1997;L18040:22—7.

[34] Kalra MK, Maher MM, Toth TL, Hamberg LM, Blake MA, Shepard JA, et al. Strategies for CT radiation dose optimization. Radiology 2004;230:619—28.
[35] McCollough CH, Primak AN, Braun N, Kofler J, Yu L, Christner J. Strategies for reducing radiation dose in CT. Radiol Clin North Am 2009;47:27—40.
[36] Lee TY, Chhem RK. Impact of new technologies on dose reduction in CT. Eur J Radiol 2010;76:28—35.
[37] Singh S, Kalra MK, Thrall JH, Mahesh M. CT radiation dose reduction by modifying primary factors. J Am Coll Radiol 2011;8:369—72.
[38] Dougeni E, Faulkner K, Panayiotakis G. A review of patient dose and optimization methods in adult and paediatric CT scanning. Eur J Radiol 2012;81:665—83.
[39] Wallace AB, Goergen SK, Schick D, Soblusky T, Jolley D. Multidetector CT dose: clincal pratice improvement strategies from a successful optimization program. J Am Coll Radiol 2010;7:614—24.
[40] Brenner DJ, Shuryak I, Einstein AJ. Impact of reduced patient life expectancy on potential cancer risks from radiologic imaging. Radiology 2011;261:193—8.
[41] Tamm EP, Rong XJ, Cody DD, Ernst RD, Fitzgerald NE, Kundra V. Quality initiatives: CT radiation dose reduction: how to implement change without sacrificing diagnostic quality. Radiographics 2011;31:1823—32.
[42] Amis ES. CT radiation dose: trending in the right direction. Radiology 2011;261:5—8.
[43] Borgen L, Ostense H, Stranden E, Olerud HM, Gudmundsen TE. Shift in imaging modalities of the spine through 25 years and its impact on patient ionizing radiation doses. Eur J Radiol 2006;60:115—9.
[44] Oikarinen H, Meriläinen S, Pääkkö E, Karttunen A, Nieminen MT, Tervonen O. Unjustified CT examinations in young patients. Eur Radiol 2009;19:1161—5.
[45] Clarke JC, Cranley K, Kelly BE, Bell K, Smith PH. Provision of MRI can significantly reduce CT collective dose. Br J Radiol 2001;74:926—31.
[46] Tins BJ, Cassar-Pullicino VN, Lalam RK. Magnetic resonance imaging of spinal infection. Top Magn Reson Imaging 2007;18:213—22.
[47] Memarsadeghi M, Breitenseher MJ, Schaefer-Prokop C, Weber M, Aldrian S, Gäbler C, et al. Occult scaphoid fractures: CT versus MR imaging. Radiology 2006;240:169—76.
[48] Liu PT, Chivers FS, Roberts CC, Schultz CJ, Beauchamp CP. Imaging of osteoid osteoma with dynamic gadolinium-enhanced MR imaging. Radiology 2003;227:691—700.
[49] Argin M, Isayev H, Kececi B, Arkun R, Sabah D. Multidetector row computed tomographic angiography findings of musculoskeletal tumors: retrospective analysis and correlation with surgical findings. Acta Radiol 2009;50:1150—9.
[50] Thévenin FS, Drapé JL, Biau D, Campagna R, Richarme D, Guerini H, et al. Assessment of vascular invasion by bone and soft tissue tumors of the limbs: usefulness of MDCT angiography. Eur Radiol 2010;20:1524—31.
[51] Omoumi P, Mercier GA, Lecouvet F, Simoni P, Vande Berg BC. CT arthrography, MR arthrography, PET, and scintigraphy in osteoarthritis. Radiol Clin North Am 2009;47: 595—615.
[52] Wyler A, Bousson V, Bergot C, Polivka M, Leveque E, Vicaut E, et al. Comparison of MR arthrography and CT arthrography in hyaline cartilage-thickness measurement in radiographically normal cadaver hips with anatomy as gold standard. Osteoarthritis Cartilage 2009;17:19—25.
[53] Moser T, Dosch JC, Moussaoui A, Dietemann JL. Wrist ligament tears: evaluation of MRI and combined MDCT and MR arthrography. AJR Am J Roentgenol 2007;188:1278—86.
[54] Kim YJ, Choi JA, Oh JH, Hwang SI, Hong SH, Kang HS. Superior labral anteroposterior tears: accuracy and interobserver reliability of multidetector CT arthrography CT for diagnosis. Radiology 2011;260:207—15.
[55] Rehani MM, Bongartz G, Kalender W. Managing X-ray dose in computed tomography: ICRP special task force report. Ann ICRP 2000;30:7—45.
[56] Kalra MK, Toth TL. Patient centering in MDCT: dose effects. In: Tack D, Genevois PA, editors. Radiation dose from adult and pediatric multidetector computed tomography. Berlin: Springer; 2007. p. 129—32.
[57] Li J, Udayasankar UK, Toth TL, Seamans J, Small WC, Kalra MK. Automatic patient centering for MDCT: effect on radiation dose. AJR Am J Roentgenol 2007;188:547—52.
[58] Mahesh M. Scan parameters and image quality in MDCT. In: Mahesh M, editor. MDCT physics: the basics — Technology, image quality and radiation dose. Philadelphia: Lippincott Williams & Wilkins; 2009. p. 47—78.
[59] Perisinakis K, Papadakis AE, Damilakis J. The effect of X-ray beam quality and geometry on radiation utilization efficiency in multidetector CT imaging. Med Phys 2009;36:1258—66.
[60] Mori S, Nishizawa K, Kondo C, Ohno M, Akahane K, Endo M. Effective doses in subjects undergoing computed tomography cardiac imaging with the 256-multislice CT scanner. Eur J Radiol 2008;65:442—8.
[61] Gervaise A, Louis M, Batch T, Lœuille D, Noel A, Guillemin F, et al. Réduction de dose dans l'exploration du rachis lombaire grâce au scanner 320-détecteurs : étude initiale. J Radiol 2010;91:779—85.
[62] van der Molen AJ, Geleijns J. Overranging in multisection CT: quantification and relative contribution to dose - comparison of four 16-section CT scanners. Radiology 2007;242:208—16.
[63] Schilham A, van der Molen AJ, Prokop M, Jong HW. Overranging at multisection CT: an underestimated source of excess radiation exposure. Radiographics 2010;30:1057—67.
[64] Kalender WA, Deak P, Kellermeier M, van Straten M, Vollmar SV. Application and patient size-dependent optimization of X-ray spectra for CT. Med Phys 2009;36:993—1007.
[65] Noël A, Ottenin MA, Germain C, Soler M, Villani N, Grosprêtre O, et al. Comparison of irradiation for tomosynthesis and CT of the wrist. J Radiol 2011;92:32—9.
[66] Gervaise A, Esperabe-Vignau F, Naulet P, Pernin M, Portron Y, Lapierre-Combes M. Évaluation des connaissances des prescripteurs de scanner en matière de radioprotection des patients. J Radiol 2011;92:681—7.
[67] Subhas N, Freire M, Primak AN, Polster JM, Recht MP, Davros WJ, et al. CT arthrography: in vitro evaluation of single and dual energy for optimization of technique. Skeletal Radiol 2010;39:1025—31.
[68] Nakaura T, Awai K, Oda S, Yanaga Y, Namimoto T, Harada K, et al. A low-kilovolt (peak) high tube current technique improves venous enhancement and reduces the radiation dose at indirect multidetector row CT venography: initial experience. J Comput Assist tomogr 2011;35:141—7.
[69] Mulkens TH, Marchal P, Daineffe S, Salgado R, Bellinck P, te Rijdt B, et al. Comparison of low-dose with standard-dose multidetector CT in cervical spine trauma. Am J Neuroradiol 2007;28:1444—50.
[70] Kröpil P, Fenk R, Fritz LB, Blondin D, Kobbe G, Mödder U, et al. Comparison of whole-body 64-slice multidetector computed tomography and conventional radiography in staging of multiple myeloma. Eur Radiol 2008;18:51—8.
[71] Abul-Kasim K, Gunnarsson M, Maly P, Ohlin A, Sundgren PC. Radiation dose optimization in CT planning of corrective scoliosis surgery. A phantom study. Neuroradiol J 2008;21:374—82.
[72] Damilakis J, Adams JE, guglielmi G, Link TM. Radiation exposure in X-ray-based imaging techniques used in osteoporosis. Eur Radiol 2010;20:2707—14.
[73] Bohy P, de Maertelaer V, Roquigny A, Keyzer C, Tack D, Genevois PA, et al. in patients suspected of having lumbar

disk herniation: comparison of standard-dose and simulated low-dose techniques. Radiology 2005;244:524—31.
[74] McCollough CH, Bruesewitz MR, Kofler JM. CT dose reduction and dose management tools: overview of available options. Radiographics 2006;26:503—12.
[75] van Straten M, Deak P, Shrimpton PC, Kalender WA. The effect of angular and longitudinal tube current modulations on the estimation of organ and effective doses in X-ray computed tomography. Med Phys 2009;36:4881—9.
[76] Mulkens TH, Bellinck P, Baeyaert M, Ghysen D, Van Dijck X, Mussen E, et al. Use of an automatic exposure control mechanism for dose optimization in multidetector row CT examinations: clinical evaluation. Radiology 2005;237:213—23.
[77] Mastora I, Rémy-Jardin M, Seuss C, Scherf C, Guillot JP, Rémy J. Dose reduction in spiral CT angiography of thoracic outlet syndrome by anatomically adapted tube current modulation. Eur Radiol 2001;11:590—6.
[78] Nagel HD. CT parameters that influence the radiation dose. In: Tack D, Genevois PA, editors. Radiation dose from adult and pediatric multidetector computed tomography. Berlin: Springer; 2007. p. 51—79.
[79] Stradiotti P, Curti A, Castellazzi G, Zerbi A. Metal-related artifacts in instrumented spine. Techniques for reducing artifacts in CT and MRI: state of the art. Eur Spine J 2009;18: S102—8.
[80] von Falck C, Galanski M, Shin H. Sliding-thin-slab averaging for improved depiction of low-contrast lesions with radiation dose savings at thin-section CT. Radiographics 2010;30:317—26.
[81] McNitt-Gray MF. AAPM/RSNA physics tutorial for residents: topics in CT. Radiation dose in CT. Radiographics 2002;22:1541—53.
[82] Walter F, Ludig T, Iochum S, Blum A. Multidectector CT in musculoskeletal disorders. JBR-BTR 2003;86:6—11.
[83] Blum A. Scanner volumique multicoupe : principes applications et perspectives. JBR-BTR 2002;85:82—99.
[84] Hara AK, Paden RG, Silva AC, Kujak JL, Lawder HJ, Pavlicek W. Iterative reconstruction technique for reducing body radiation dose at CT: feasibility study. AJR Am J Roentgenol 2009;193:764—71.
[85] Silva A, Lawder H, Hara A, Kujak J, Pavlicek W. Innovations in CT dose reduction strategy: application of the adaptive statistical iterative reconstruction algorithm. AJR Am J Roentgenol 2009;194:191—9.
[86] Gervaise A. Impact des algorithmes itératifs de reconstruction sur l'interprétation des images en scanographie. 50e Journées scientifiques de la SFPM. Nantes, 9 juin 2011.
[87] Boas FE, Fleischmann D. Evaluation of two iterative techniques for reducing metal artifacts in computed tomography. Radiology 2011;259:894—902.
[88] Buckwalter KA, Lin C, Ford JM. Managing postoperative artifacts on computed tomography and magnetic resonance imaging. Semin Musculoskelet Radiol 2011;15: 309—19.
[89] Stierstorfer K, Kuhn U, Wolf H, Petersilka M, Suess C, Flohr T. Principle and performance of a dynamic collimation technique for spiral CT. (abstract) In: Radiological Society of North America scientific assembly and annual meeting program. Oak Brook, IL: Radiological Society of North America, 2007, SSA16-04.
[90] Christner JA, Zavaletta VA, Eusemann CD, Walz-FlanniganAI, McCollough CH. Dose reduction in helical CT: dynamically adjustable z-axis X-ray beam collimation. AJR Am J Roentgenol 2010;194:W49—55.
[91] Wolfe SW, Neu C, Crisco JJ. In vivo scaphoid, lunate and capitate kinematics in flexion and in extension. J Hand Surg Am 2000;25:860—9.
[92] Moojen TM, Snel JG, Ritt MJ, Venema HW, Kauer JM, Bos KE. In vivo analysis of carpal kinematics and comparative review of the literature. J Hand Surg Am 2003;28:81—7.
[93] Foumani M, Strackee SD, Jonges R, Blankevoort L, Zwinderman AH, Carelsen B, et al. In vivo three-dimensional carpal bone kinematics during flexion-extension and radioulnar deviation of the wrist: dynamic motion versus step-wise static wrist positions. J Biomech 2009;42:2664—71.
[94] Berdia S, Short WH, Wermer FW, Green JK, Panjabi M. The hysteresis effect in carpal kinematics. J Hand Surg Am 2006;31:594—600.
[95] Short WH, Werner FW, Fortino MD, Mann KA. Analysis of the kinematics of the scaphoid and lunate in the intact wrist joint. Hand Clin 1997;13:93—108.
[96] Hristova L, Batch T, Blum A. Analyse des artefacts de mouvement de l'exploration dynamique et volumique au scanner 320 barrettes (abstract). J Radiol 2009;90:1583.
[97] Blum A, Lecocq S, Roch D, Louis M, Batch T, Dab F, et al. Étude cinématique du poignet en 3D et 4D avec un scanner 320 canaux. In: SIMS Opus XXXVI Poignet et main. Montpellier: Sauramps médical; 2009 [p. 375—89].
[98] Tay SC, Primak AN, Fletcher JG, Schmidt B, Amrami KK, Berger RA, et al. Four-dimensional computed tomographic imaging in the wrist: proof of feasibility in a cadaveric model. Skeletal Radiol 2007;36:1163—9.
[99] Snel JG, Venema HW, Moojen TM, Ritt JP, Grimbergen CA, den Heeten GJ. Quantitative in vivo analysis of the kinematics of carpal bones from three-dimensional CT images using a deformable surface model and a three-dimensional matching technique. Med Phys 2000;27:2037—47.
[100] Gurung J, Khan MF, Maataoui A, Herzog C, Bux R, Bratzke H, et al. Multislice CT of the pelvis: dose reduction with regard to image quality using 16-row CT. Eur Radiol 2005;15:1898—905.
[101] Levine E, Neff JR. Dynamic computed tomography scanning of benign bone lesions: preliminary results. Skeletal Radiol 1983;9:238—45.
[102] Miles KA, Charnsangavej C, Lee F, Fishman E, Horton K, Lee TY. Application of CT in the investigation of angiogenesis in oncology. Acad Radiol 2001;7:840—50.
[103] Ketelsen D, Horger M, Buchgeister M, Fenchel M, Thomas C, Boehringer N, et al. Estimation of radiation exposure of 128-slice 4D-perfusion CT for the assessment of tumor vascularity. Korean J Radiol 2010;11:547—52.
[104] Heck O, Louis M, Wassel J, Lecocq S, Gondim-Teixeira P, Moisei A, et al. Apport du scanner volumique dynamique dans le diagnostic d'ostéome ostéoïde. Paris: Poster journées françaises de radiologie; 2010.
[105] Lefevre JE, Harbourg B. Mieux voir, plus rapidement et avec moins de dose. Rapport de la Société française de radiologie 2010; http://www.sfrnet.org
[106] Flohr TG, McCollough CH, Bruder H, Petersilka M, Gruber K, Süss C, et al. First performance evaluation of a dual-source CT (DSCT) system. Eur Radiol 2006;16:256—68.
[107] Choi HK, Al-Arfaj AM, Eftekhari A, Munk PL, Shojania K, Reid G, et al. Dual energy computed tomography in tophaceous gout. Ann Rheum Dis 2009;68:1609—12.
[108] Nicolaou S, Yong-Hing CJ, Galea-Soler S, Hou DJ, Louis L, Munk P. Dual energy CT as a potential new diagnostic tool in the management of gout in the acute setting. AJR Am J Roentgenol 2010;194:1072—8.
[109] Pache G, Krauss B, Strohm P, Saueressig U, Blanke P, Bulla S, et al. Dual energy CT virtual non-calcium technique: detecting post-traumatic bone marrow lesions-feasibility study. Radiology 2010;256:617—24.
[110] Bamberg F, Dierks A, Nikolaou K, Reiser MF, Becker CR, Johnson TRC. Metal artefact reduction by dual energy computed tomography using monoenergetic extrapolation. Eur Radiol 2011;21:1424—9.

Chapitre 4

Article 3 : *Scanner ostéo-articulaire à large système de détection : principes, techniques et applications en pratique clinique et en recherche.*

Teixeira P, Gervaise A, Louis M, Lecocq S, Raymond A, Aptel S, Blum A. Musculoskeletal Wide detector CT : Principles, Techniques and Applications in Clinical Practice and Research. *Eur J Radiol* 2015; 84:892-900.

European Journal of Radiology 84 (2015) 892–900

Contents lists available at ScienceDirect

European Journal of Radiology

journal homepage: www.elsevier.com/locate/ejrad

Review

Musculoskeletal wide detector CT: Principles, techniques and applications in clinical practice and research

Pedro Augusto Gondim Teixeira[a,*], Alban Gervaise[b], Matthias Louis[a], Sophie Lecocq[a], Ariane Raymond[a], Sabine Aptel[a], Alain Blum[a]

[a] Guilloz Imaging Department, Central Hospital, University Hospital Center of Nancy, 29 avenue du Maréchal de Lattre de Tassigny, 54035 Nancy Cedex, France
[b] Medical Imaging Department, Legouest Military Instruction Hospital, 27 Avenue de Plantières, BP 90001, 57077 Metz Cedex 3, France

ARTICLE INFO

Article history:
Received 28 August 2014
Received in revised form
15 December 2014
Accepted 31 December 2014

Keywords:
Wide area detector CT
Musculoskeletal
CT perfusion
Dynamic CT
Bone subtraction
Dualenergy

ABSTRACT

A progressive increase in the detector width in CT scanners has meant that advanced techniques such as dynamic, perfusion and dual-energy CT are now at the radiologist's disposal. Although these techniques may be important for the diagnosis of various musculoskeletal diseases, data acquisition and interpretation can be challenging. This article offers a practical guide for the use of these tools including acquisition protocol, post-processing options and data interpretation based on 7 years of clinical experience in a tertiary university hospital.

1. Introduction

In the past, the increased availability of MRI and growing awareness of dose-related patient hazards limited the use of musculoskeletal CT in clinical practice. However, more recently multiple advances in CT technology resulted in a "comeback", supported by a considerable decline in radiation exposure and the establishment of clear guidelines and dose limits for clinical use [1–4]. Multi detector CT scanners are now widely available. Musculoskeletal (MSK) CT studies are frequently performed, last only a few seconds and are little more irradiating than conventional radiographs. Furthermore, CT has a better diagnostic performance than radiography for the evaluation of patients with a prosthesis and the number of CT studies performed in this setting is increasing steadily [5].

In the middle of past decade the increase in the number of detector rows led to an increase in detector width (slice wars) [6]. Coverage has increased from 2 mm with 4 detector-rows up to 160 mm with 320 detector-rows. This tendency is apparent in machines from all the major CT manufacturers, with 3 out of 4 selling scanners with a *Z*-axis coverage over 80 mm [6]. Wide area-detector CT (WADCT), herein defined as multi detector CT scanners with more than 80 mm of detector width, allows more frequent use of sequential acquisition, which has three major advantages with respect to helical acquisition: higher temporal resolution, dose-reduction (e.g. no over-ranging and a reduction of the over-beaming contribution to total exposure), and easier data post-processing [7,8]. The latter relates to the absence of slice interpolation and to the fact that every voxel of a given volume is acquired at almost the same time (temporal uniformity).

Dose saving technology implemented by all manufacturers (both software and hardware) has led to a two to four fold decrease in the dose delivered in a CT examination and is in great part responsible for the increase in clinical availability of advanced CT applications [2]. Iterative reconstruction (IR) is probably the most significant of these developments. IR algorithms are now standard for most commercial CT scanners and can reduce roughly by half the dose maintaining the same image quality [7,9–11]. IR is most effective when acquisitions have low contrast to noise ratio, which is particularly interesting for low dose multiphasic protocols [11,12].

WADCT is suited to dynamic study of joints, which can be imaged in wide ranges of motion using sequential acquisition. Dynamic CT is the only clinically available technique that allows volumetric study of bone and intra-articular ligaments during physiologic motion or under stress. This helps overcome

* Corresponding author. Tel.: +33 3 83 85 21 61; fax: +33 3 83 85 97 25.
E-mail address: ped_gt@hotmail.com (P.A. Gondim Teixeira).

http://dx.doi.org/10.1016/j.ejrad.2014.12.033
0720-048X/

some limitations of evaluation of dynamic pathology with static imaging and fluoroscopy. Moreover, WADCT is likely to increase the diagnostic performance of CT perfusion, by the use of associated techniques such as digital subtraction angiography (DSA)-like bone subtraction. WADCT also increases the availability of dual-energy, which can be performed without hardware features dedicated for dual-energy acquisitions (sandwich detectors, dual source, rapid kV switching).

Although the primary role of MRI in identifying and characterizing MSK pathologic processes remains undisputed, new applications of WADCT may provide additional information and increase the diagnostic performance of CT. Against that background, increased knowledge of the indications of advanced WADCT techniques and of data acquisition and post-processing is of relevance. This article offers practical guidelines for the application of dynamic CT, CT perfusion and dual-energy for the evaluation of MSK pathology.

2. Materials and methods

From March 2008 to December 2013 a 320 detector-row CT scanner (Aquilion ONE, Toshiba Medical Systems, Otawara, Japan) has been used for the evaluation of patients with various types of musculoskeletal disorders (traumatic, degenerative, inflammatory and tumoral) at a tertiary university hospital by a team of musculoskeletal radiologists (seven physicians). An average of 30 advanced CT studies (Dynamic CT, perfusion CT and dual-energy CT) are performed weekly in our institution. The team's experience with the used of advanced CT techniques is reported along with a systematic literature review.

3. Dynamic CT

Dynamic CT uses multiple, low-dose, sequential acquisitions of the same anatomic area during motion. This technique requires wide detector systems to be performed for it strongly relies on high temporal resolution, which is possible with wide detector CT using sequential acquisition (all portions of the volume must be imaged at the same time). A single movement or stress maneuver is studied per acquisition. Although this technique is most frequently used for the evaluation of the wrist, it can be used on various joints (shoulder, hip, elbow, knee, and ankle) [13]. Multiple maneuvers have been described in the literature, especially for the wrist [14–16]. With respect to fluoroscopy, dynamic CT allows multiplanar and 3-D study of bone and intra-articular ligaments overcoming contrast and superimposition issues with the former technique at the expense of a lower temporal resolution.

Two scanning modes can be used for the acquisition of dynamic data:

Intermittent acquisition (volumes separated by a variable time interval) is used by default as it limits radiation exposure. The inter-volume interval is usually 1 s and 10–15 volumes are sufficient to image most of the dynamic pathology encountered. This technique is not suitable for the evaluation of fast or jerky movements especially those whose speed cannot be controlled by the patient for it lacks sufficient temporal resolution.

Continuous acquisition (no interval between volumes) offers maximal temporal resolution at the expense of a higher dose. Temporal resolutions of 200 ms or lower can be achieved with this method by using partial volume reconstruction techniques. Continuous acquisitions should not last more than 5 s in order to maintain dose exposure within acceptable limits. This acquisition mode is recommended in cases of joint or ligamentous snapping, in which, the symptoms cannot be reproduced with a slow controlled motion.

Regardless of the acquisition method dynamic CT can be performed in the extremities (ankle, knee, wrist, elbow), with very low effective doses (0.04 ± 0.05 and 0.05 ± 0.06 mSv for intermittent and continuous acquisition respectively). The effective dose is much higher for proximal joints such as hip and shoulder (mean 5.5 ± 1.8 and 6.2 ± 1.2 mSv respectively) where dynamic CT should be performed only in selected patients.

Dynamic CT can be coupled with arthrography for the analysis of intra-articular ligaments.

To be reliable and reproducible, dynamic CT requires proper patient training and direct visual surveillance of the acquisition. Prior to the examination, patients are trained to focus on quality of motion and timing. Stabilization of adjacent body parts is important to allow a single movement in one plane of the space to be performed. Avoiding unwanted motion is critical to the interpretation and post-processing of dynamic data. For optimal quality, the motion has to be controlled and smooth, with each maneuver lasting between 10 and 15 s. Patient guidance and surveillance systems are now available to optimize the quality of dynamic acquisitions [17].

The speed of motion that can be evaluated with dynamic CT is limited. Faster movements can lead to significant degradation of image quality [18]. Excessive motion artifacts appear as ghosting and linear streaks and are frequently located over 5 cm of the fulcrum of motion (where linear speeds are higher), with limited impact on the interpretation of more proximal structures. There are two ways of reducing motion artifacts: slowing patient motion or increasing volume acquisition speed. Tube rotation speed, has a strong impact on image quality and should be kept as high as possible to avoid motion artifacts. Partial scanning and high pitch techniques (e.g. dual source CT) can provide full volume reconstruction with less than 360° of tube rotation with can greatly reduce volume acquisition time [19].

Dynamic CT offers considerable advantage over imaging the extremes of joint range, since dynamic abnormalities can be limited to a particular maneuver or motion path. Punctual motion anomalies can be identified with dynamic CT. In cases of patellar maltracking, abnormal motion is present at some point of the first 30° of knee flexion when the patella engages the trochlea. Similarly, in cases of midcarpal instability there is abrupt, abnormal motion of the whole first carpal row at some point of radio-ulnar deviation or dart throwing maneuver [20]. In the wrist, there are variations in bone position (or angulation) that are specific of a motion path, a phenomenon called hysteresis. The hysteresis of a bone (e.g. lunate) is increased in cases of wrist instability [21].

Analysis of dynamic CT data can be challenging. Image interpretation on a workstation that allows multiplanar and volume rendering (VR) of multiple volumes is recommended. Soft tissue kernels yield better results for VR reconstruction while sharp bone kernels are recommended for multiplanar reconstructions. VR images are used for the initial study of inter-bone relations. The findings have to be confirmed on multiplanar reformats, which are also used for the study of intra-articular ligaments with dynamic CT arthrography. Dedicated analysis software allowing bone locking (e.g. after volume registration, all motion is displayed with respect to a single bone, which remains static or locked) and the automatic propagation of distance and angular measurement throughout the study volumes is currently undergoing clinical testing.

Dynamic CT has three main applications:

1. *Entrapment, impingement and snapping*. Because of the multiple possible etiologies of these syndromes, it may be difficult to ascertain clinically which structure is responsible for patient symptoms. With static imaging, the diagnosis of snapping and impingement syndromes is based solely on secondary findings, which can be insufficient. The advantage of dynamic studies is that the zone of impingement is directly demonstrated, helping confirm the diagnosis and guide surgical therapy (Fig. 1).

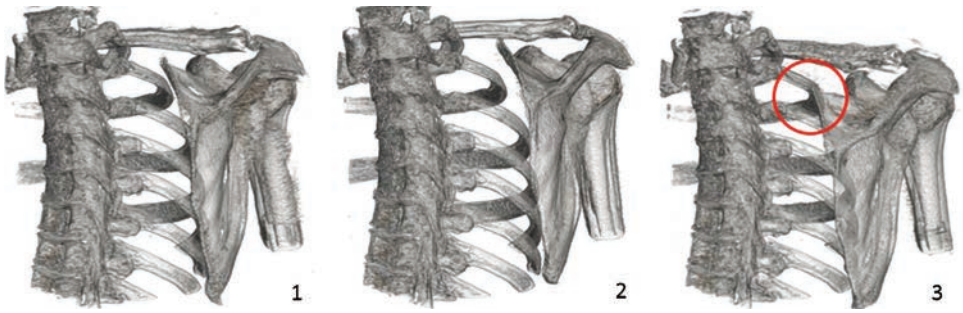

Fig. 1. 39 year-old female with right scapular pain and grinding. No anomalies were identified on conventional imaging studies. Images 1–3 were extracted from a dynamic CT study using continuous acquisition. The superior scapular angle impinges against the second rib at the end of shoulder girdle rotation (red circle). The acquisition lasted 5 s and the temporal resolution after post-processing was 200 ms. Supplementary material – video 1.

In this context, dynamic CT is indicated when the diagnosis is not reached with conventional methods, particularly in the pre-operative evaluation.

Dynamic CT angiography can be performed for the evaluation of neuro-vascular entrapment syndromes, such as thoracic outlet syndrome or popliteal artery entrapment, to detect bony or soft tissue compression. With WADCT, multiple volumes can be acquired during the first pass of a single contrast bolus, which allows multiple maneuvers (e.g. gastrocnemius contraction and hamstring contraction for popliteal artery entrapment) to be performed with a single injection. Additionally, CT angiography can be performed during head rotation or other maneuvers eliciting patient symptoms, for the evaluation of thoracic outlet syndrome, increasing the sensitivity for the detection of impingement. The amount of contrast injected is reduced when compared to conventional CT angiography, which requires one contrast bolus per maneuver or position evaluated (Fig. 2).

2. *Evaluation of the sufficiency of intra-articular ligaments.* A ligament is considered sufficient when it is able to withstand physiological stress without significant elongation. Ligament sufficiency cannot be evaluated with static imaging [22]. With dynamic CT arthrography, some ligaments (e.g. scapho-lunate and luno-triquetral ligaments) can be evaluated under stress. The main application of this technique is the evaluation of dynamic carpal instability (Fig. 3).
3. *Analysis of complex motion.* In some joints, such as the wrist and the subtalar joint, motion is too complex (e.g. multiple moving structures, rotatory motion) and even static evaluation at the extremes of joint amplitude (regardless of the imaging method: radiographs, CT or MRI) is not sufficient to demonstrate dynamic pathologic processes [23]. Dynamic CT is able to identify brief changes in bone relation during the course of a given motion, making it particularly interesting for the evaluation of complex movements.

Table 1 demonstrates the acquisition protocol for the most frequently used maneuvers for various joints and their indications.

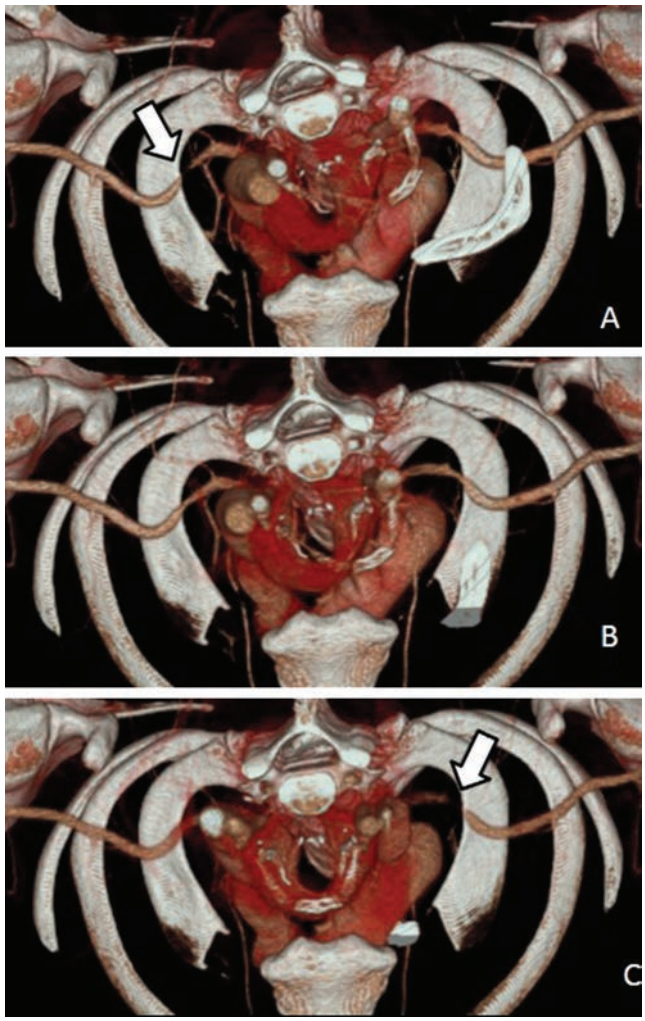

Fig. 2. 35 year-old female with a chronic bilateral paresthesia of the superior limbs. Dynamic CT angiography was performed with the arms above the shoulder line during left to right head motion. Volume rendered upper view of the thoracic outlet with the head turned to the left, front and right (A, B and C respectively). Note the stenosis of the subclavian artery on the extremes of head motion (arrows in A and C), confirming the diagnosis of thoracic outlet syndrome. No compression is seen in neutral position (B).

4. CT perfusion

The aim of CT perfusion, also based on low-dose intermittent acquisition of a target area, is analysis of the first passage of the contrast medium bolus. The use of CT perfusion can be facilitated by a wide detector system, but this technique can be performed with most CT scanner models. Perfusion can provide useful hemodynamic information in cases of vascular tumor or micro-traumatic vascular injury (e.g. hypothenar hammer syndrome) (Fig. 4). Similar to MRI perfusion, CT perfusion can be useful for tumor characterization, differentiation between residual/recurrent tumor and post-operative fibrosis and biopsy targeting [24,25]. In preliminary testing, the effectiveness of CT guided ablation could be confirmed with intraoperative CT perfusion, which demonstrated the absence of nidus enhancement immediately after ablation (Fig. 5).

It is important to keep in mind that MRI remains the method of choice for perfusion studies as it has a higher sensitivity for contrast detection and uses no ionizing radiation. CT perfusion is, however,

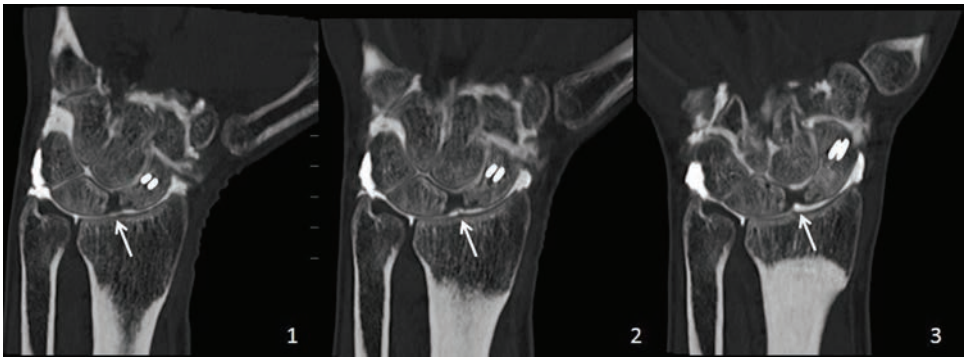

Fig. 3. 34 year-old male with scaphoid fracture and rupture of the scapholunate ligament treated surgically with persistent wrist pain. Figs. 1–3 are a series of three coronal images extracted from a dynamic CT arthrography. In the neutral position (Image 1) there is a normal scapholunate distance and a thickened but continuous scapholunate ligament (arrow). Throughout ulnar deviation (Images 2 and 3) there is thinning and elongation of the scapholunate ligament, that is insufficient, allowing scapholunate diastasis (arrows). Supplementary material – video 2.

Table 1
Protocol recommendations and indications for dynamic CT.

Joint	Maneuver	Indication	Study type	*Z*-axis coverage (mm)	Tube output[a]	Scanning mode
Wrist	Radio-ulnar deviation	Ulno-lunar impingement, carpal instability	Dynamic CT	80	80 kVp, 100 mAs	Intermittent
	Clenching fist examination	Dissociative carpal instability	Dynamic CT arthrography	60	80 kVp, 100 mAs	Continuous
	Dart throwing	Carpal instability	Dynamic CT	80	80 kVp, 100 mAs	Intermittent
	Prono-supination	DRUJ[b] instability	Dynamic CT	60	80 kVp, 100 mAs	Intermittent
Scapulo-thoracic	Shoulder blade rotation (reproduce patient symptoms)	Snapping scapula syndrome	Dynamic CT	140 or higher	100 kVp, 200 mAs	Continuous
Thoracic outlet	Head rotation with arms over shoulders	Thoracic outlet syndrome	Dynamic CT angiography	80–100	100 kVp, 150 mAs	Intermittent
Hip	Flexion-internal rotation	Femoro-acetabular impingement	Dynamic CT	80	100 kVp, 200 mAs	Intermittent
	Flexion-extension	Lateral snapping hip	Dynamic CT	80	100 kVp, 200 mAs	Intermittent
Knee	Flexion-extension (comparative)	Patellar maltracking	Dynamic CT	140 or higher	100 kVp, 150 mAs	Intermittent
	Sural triceps and hamstrings contraction (sequentially)	Popliteal entrapment syndrome	Dynamic CT angiography	140 or higher	100 kVp, 150 mAs	Intermittent

[a] Susceptible to changes according to patient body habitus.
[b] DRUJ = distal radio-ulnar joint.

a valuable option when MRI is contra-indicated or unavailable. Despite these advantages of MRI over CT, in clinical practice, CT and MRI perfusion have a similar diagnostic performance [26,27]. The main advantage of CT over MRI relates to the linear association between iodine concentration and CT number, which is not the case for MRI and gadolinium. This feature makes density-related perfusion parameters easier to calculate and compare [28].

Three types of perfusion parameters are available for analysis: visual, semi-quantitative and quantitative.

Visual analysis is performed by direct comparison of tumor enhancement with nearby arterial enhancement on 4-D series displayed on soft tissue windowing. Tumor enhancement should be evaluated for density and timing using arterial enhancement as a reference. Additionally, the presence of intra-tumoral neovessels can be evaluated with either conventional or VR reconstructions. Neovessels are intimately associated with tumor aggressiveness and are characterized by an erratic variation in caliber that leads to the formation of a non-organized intra-tumoral vascular network (Fig. 6) [29].

Semi-quantitative analysis is based on the construction of a time-to-density graph, which yields various perfusion parameters useful for lesion characterization as demonstrated in Fig. 7 [25]. Although semi-quantitative parameters are easy to obtain, intra- and inter-patient comparisons should be performed with caution even with similar injection protocols. Some time-related parameters (e.g. time-to-peak, delay of enhancement) are dependent on the anatomic location of the tumor. Density-related parameters are dependent on tube output (kVp), scanner calibration, iodine concentration of the contrast media and injection rate. One of the most reliable semi-quantitative parameters is the delay between arterial and tumor peaks, which can be compared directly in most patients.

Quantitative analysis is based on estimation of the tissue concentration of iodine using mathematical pharmacokinetic models – most frequently bicompartmental single arterial input models such as Brix's or Toft's models [30,31]. Parameters related to capillary density, and vessel permeability can be calculated. The most frequently calculated quantitative parameters are plasmatic volume (V_p%), volume transfer constant form the plasma to the extravascular extracellular space (EES) (K^{trans}), rate constant of the backflux

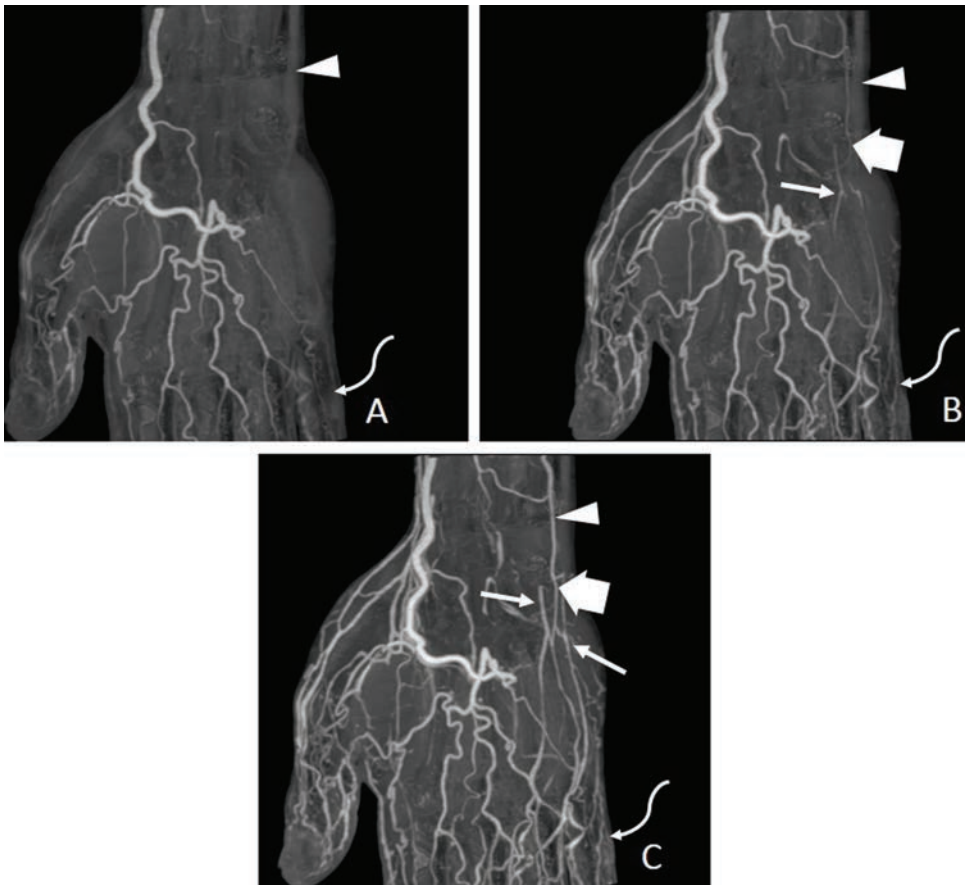

Fig. 4. 58 year-old male smoker with persistent coldness and discoloration of the 4th and 5th fingers. (A–C) CT perfusion sequential MIP images of the hand and wrist. There is a late filling of the ulnar artery (arrowheads) with an obstruction at the level of the pisiform bone (fat arrows). Collateral vessels at the level of Guyon's canal are seen in the latter phases (thin arrows). The proper digital arteries of the fifth finger are not seen (squiggly arrows). Note that the superficial and deep palmar arches are filled through the radial artery.

from the EES to the plasma (k_{ep}) and EES volume (V_e%). Compared to brain, quantitative perfusion parameters in body CT perfusion require more complex (and hence less precise) calculation methods because outside the blood–brain barrier normal capillaries allow the passage of contrast medium molecules. Quantitative parameters are highly dependent on the model used for calculation, but inter-patient comparisons are possible provided the model and acquisition parameters are the same. Quantitative perfusion is a subject of intense research. It requires dedicated software and further studies are still necessary to establish diagnostic criteria for MSK pathology.

There is no consensus on the best acquisition protocol [32,33]. Table 2 demonstrates the parameters of the CT perfusion protocol used in our institution. Timing is crucial for perfusion and the use of bolus tracking is recommended. In our experience, with WADCT and using an adequate protocol, CT perfusion can usually be performed with a DLP under 800 mGy cm. This is a lower level of exposure than abdominal or thoracic MDCT with helical acquisition. CT perfusion is particularly interesting in the extremities, where it can be performed with very low effective doses – usually under 0.5 mSv. In the trunk and pelvic and shoulder girdles effective dose levels are still prohibitive [34].

Table 2
CT perfusion acquisition protocol recommendations.

CT perfusion MSK	
Tube output	Adapted to anatomy and patient body habitus
Z-axis coverage	40–160 mm[a]
Slice thickness	0.5 mm
Injection rate	5 ml/s
Contrast volume	2 ml/kg[b]
Bolus tracking	Yes
Number of phases	18
Inter volume delay – arterial phase	5 s
Inter volume delay – venous phase	10 s

[a] *Z*-axis coverage should be kept as low as possible to avoid unnecessary radiation exposure.
[b] Up to a maximum of 150 ml.

4.1. Digital subtraction angiography-like bone subtraction

Calcification, bone and iodinated contrast medium share a similar density in Hounsfield units. Although intra-osseous enhancement is measurable with conventional CT images, it is very difficult to identify visually. Classic bone subtraction does not allow evaluation of intra-osseous enhancement. Digital subtraction angiography (DSA)-like bone subtraction uses a pre-contrast mask volume that can be registered and subtracted from one or more post-contrast volumes provided the same acquisition parameters are used (Fig. 8). With DSA-like bone subtraction enhancement of densely calcified or non-lytic bone lesions can be seen on CT.

DSA-like bone subtraction offers a significant improvement in the visualization of intra-osseous enhancement. Teixeira et al. reported a sensitivity of over 70% and a specificity of 100% for the identification of bone marrow edema pattern (BMEP) adjacent to bone tumors using MRI as standard of reference [35]. DSA-like bone

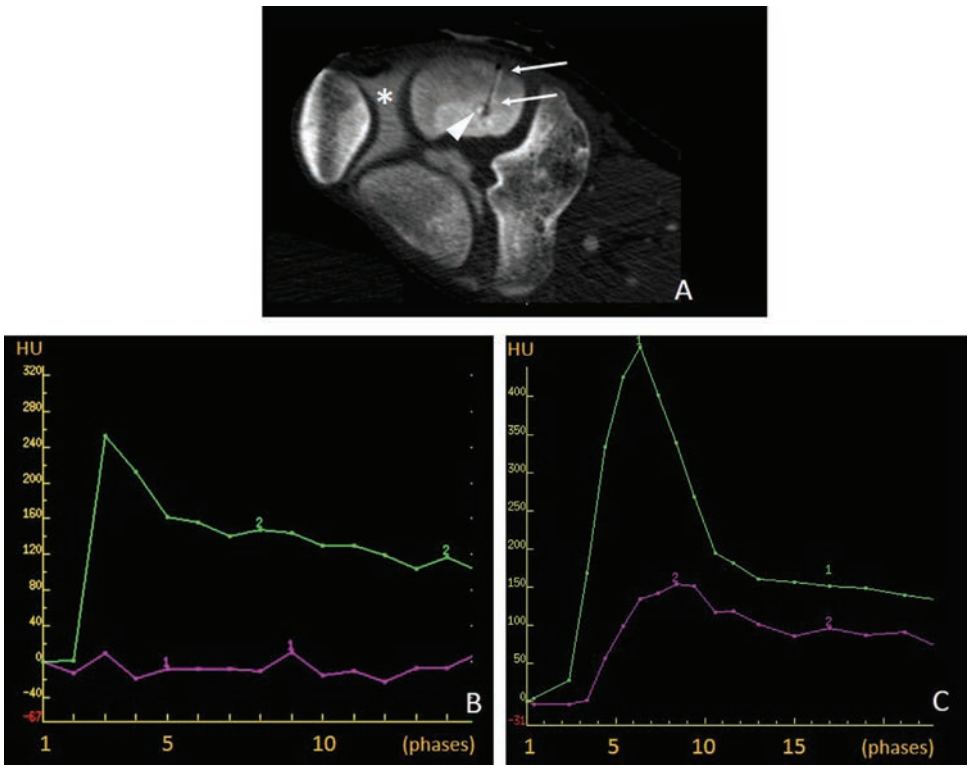

Fig. 5. 16 year-old male with a trabecular osteoid osteoma of the medial femoral condyle of the left knee. (A) Intraoperative axial oblique CT perfusion image performed immediately after percutaneous laser therapy (500 J for 3 min). The needle track (arrows) is seen confirming the adequate needle position with respect to the nidus (arrowhead). Saline–iodine solution was used as a coolant agent for chondral protection (*). (B) Time-to-density graph obtained after laser therapy showing no enhancement in the nidus (purple curve) and popliteal artery enhancement (green curve). (C) CT perfusion time-to-density graph obtained 1 week before treatment showing typical steep and early nidus enhancement (purple curve).

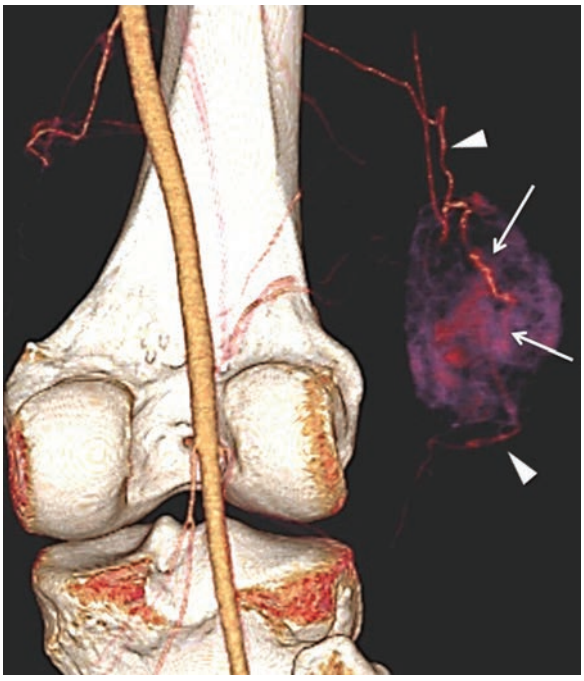

Fig. 6. 51 year-old male with a biopsy-proven fibrosarcoma. 3-D volume rendered image at the late arterial phase demonstrating the feeding vessels at the superior and inferior poles of a soft tissue mass (arrowheads). Neovessels are seen inside the mass (arrows). Note the tortuosity and the erratic variation in caliber of the intra-tumor vessels.

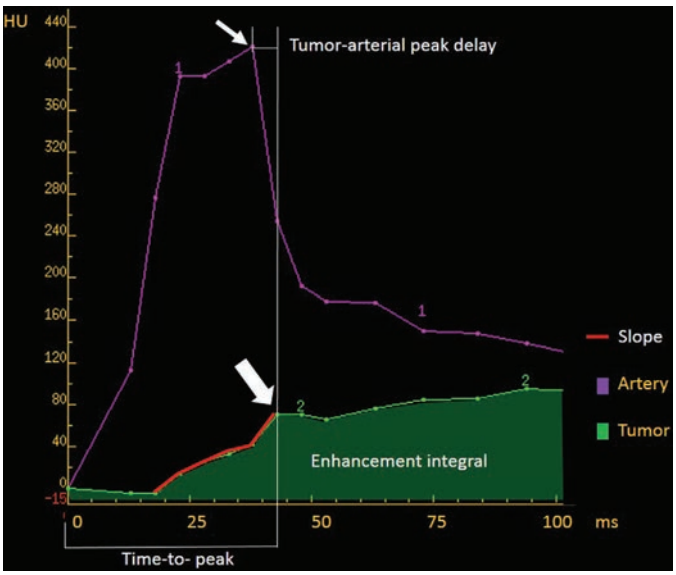

Fig. 7. CT perfusion of a grade III soft tissue sarcoma of the right arm of a 65 year-old male. Time-to-density graph comparing the tumor enhancement (green curve) with that of the brachial artery (purple curve). Tumor and artery enhancement peaks are indicated by the fat and thin arrows, respectively. The thin white lines indicate the most frequently used time-related semi-quantitative parameters (time-to-peak and tumor-arterial peak delay). The enhancement slope is demonstrated by the red line over the tumor enhancement curve. Finally, the area under the tumor curve represents the enhancement integral and is related to tumor capillary density.

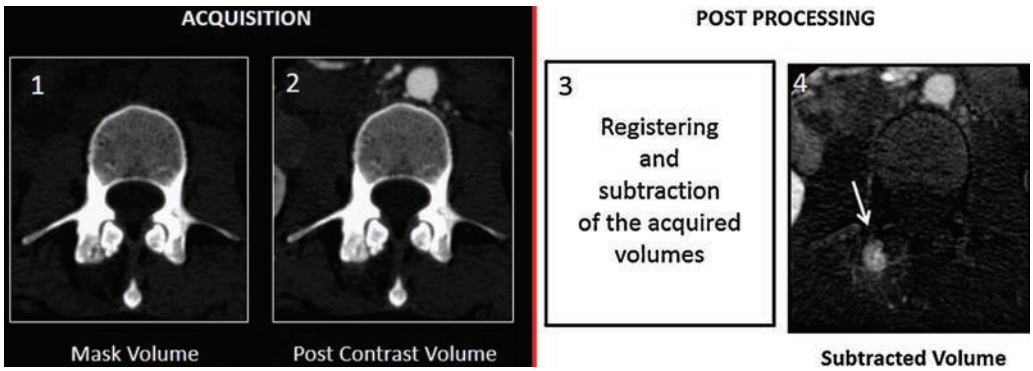

Fig. 8. Schematic representation of the DSA-like bone subtraction procedure. In the first two steps, the mask volume and the post-contrast volume are acquired. Images (1 and 2) Axial CT of the fifth lumbar vertebra. Note osseous enhancement is very faint and easily missed. Step 3 can be performed any time after acquisition with a dedicated workstation. Image (4) Axial bone subtracted CT image showing a focal zone of contrast enhancement at the right superior articular facet (arrow).

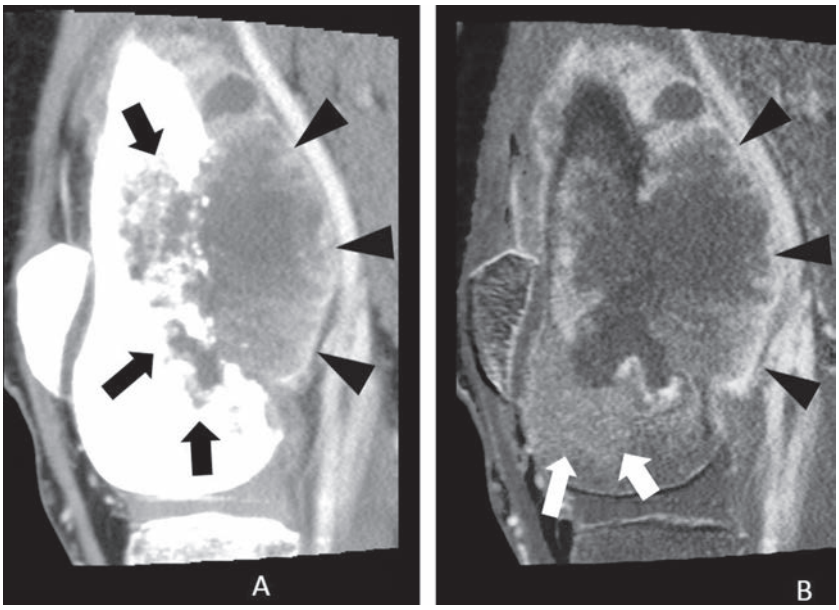

Fig. 9. 64 year-old female with a sarcomatoid carcinoma of the distal femur, pre-operative evaluation. (A) Sagittal post-contrast CT image viewed in a soft tissue window setting in the venous phase demonstrating an aggressive lytic bone tumor with irregular margins (arrows), cortical destruction and a soft tissue mass (arrowheads). (B) Sagittal bone subtracted CT image of the same anatomic region demonstrating enhancement in both the lytic and soft tissue components of this lesion (arrowheads) but also at the non-lytic bone (white arrows).

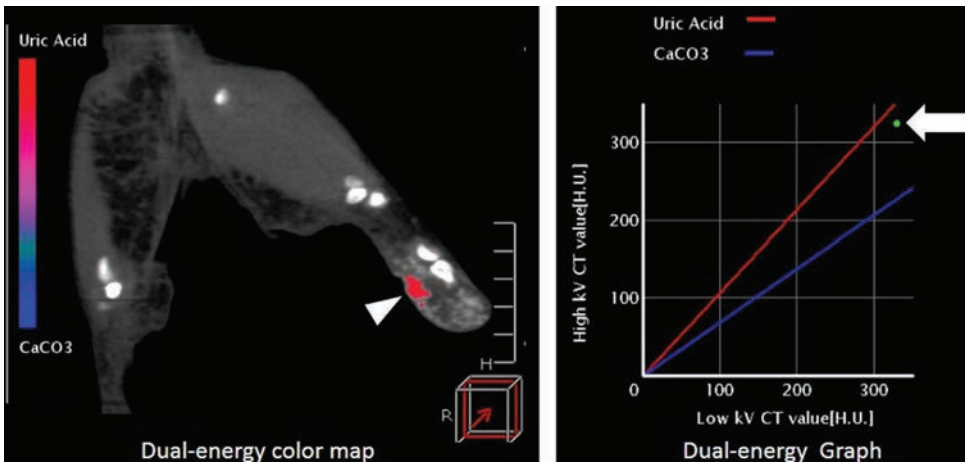

Fig. 10. 66 year-old male in chronic dialysis due to a bilateral nephrectomy secondary to a multifocal tubulo-papilary carcinoma. Dual-energy was performed with 80 and 135 kVp. Dual-energy graph and color map for the differentiation between uric acid and calcium carbonate ($CaCO_3$). The color map demonstrates the presence of uric acid in the soft tissue calcification seen at the distal thumb (arrowhead). The green dot in the graph (arrow) depicts the behavior of a region of interest placed on the soft tissue calcification that is close to that of uric acid (red line).

subtraction is particularly useful for the evaluation of small lytic bone lesions and for the diagnosis of osteomyelitis (Fig. 9).

5. Dual-energy

Dual-energy relies on element-specific attenuation behavior on exposure to X-ray beams with different energies. There are multiple ways of performing dual-energy acquisitions (dual source, sandwich detectors, rapid kVp switching) [36]. With WADCT, dual-energy is performed by the acquisition of two successive volumes of the same anatomic region with different tube kVp settings (usually 80 and 135 kVp). Although this technique offers a limited spectral separation and requires specific software, it does not have specific hardware requirements. Dual-energy is mainly used in MSK for differentiation between intra-articular and peri-articular hyperdense materials, which is useful for the differential diagnosis of gout. Dual-energy can also be used to differentiate between calcification and iodine on CT arthrography [37]. Additionally, virtual non-contrast medium enhanced images can be obtained by selectively subtracting the contrast medium from a contrast-enhanced examination [38].

Dual-energy acquisitions are interpreted based on prior knowledge of the expected behavior of a particular element. Post-processing software can then reconstruct color-coded functional maps that identify a particular element, most frequently iodine, calcium or uric acid. Data can also be presented in the form of graphs comparing the behavior of an ROI with that of known elements (Fig. 10).

6. Conclusion

WADCT offers new diagnostic possibilities for the diagnosis of MSK disorders through the application of dynamic, perfusion and dual-energy CT. These techniques are readily available and can be performed with various CT scanner models on the market. This article offers a practical guide to the clinical application of these tools and to interpretation of the data they yield, which it is to be hoped will increase their use and allow better result comparison in future research.

Funding

This work was not funded.

Conflict of interest

Two authors involved in this work, (P.A.G.T. and A.B.) participate on a non-remunerated research contract with Toshiba Medical systems for the development and clinical testing of post processing tools for MSK CT. The other authors have no potential conflicts of interest to disclose.

References

[1] Lee T-Y, Chhem RK. Impact of new technologies on dose reduction in CT. Eur J Radiol 2010;76(October (1)):28–35.
[2] McCollough CH, Chen GH, Kalender W, Leng S, Samei E, Taguchi K, et al. Achieving routine submillisievert CT scanning: report from the summit on management of radiation dose in CT. Radiology 2012;264(August (2)):567–80.
[3] Berland, Lincoln L, Armstrong, Mark R, Cody Dianna D, Mahadevappa M, Mayo-Simith William W. ACR practice guideline for performing and interpreting diagnostic computed tomography (CT). American College of Radiology; 2011. Available from: http://www.acr.org/~/media/ACR/Documents/PGTS/guidelines/CT_Performing_Interpreting.pdf [Internet].
[4] Bongartz G, Golding SJ, Jurik AG, Leonardi M, van Meerten EvP, Geleijns J, et al. European guidelines on quality criteria for computed tomography. European Commission's Radiation Protection Actions; 1998. Available from: http://w3.tue.nl/fileadmin/sbd/Documenten/Leergang/BSM/European_Guidelines_Quality_Criteria_Computed_Tomography_Eur_16252.pdf [Internet].
[5] Miller TT. Imaging of hip arthroplasty. Eur J Radiol 2012;81(December (12)):3802–12.
[6] Parrish FJ. Volume CT: state-of-the-art reporting. Am J Roentgenol 2007;189(September (3)):528–34.
[7] Gervaise A, Osemont B, Lecocq S, Noel A, Micard E, Felblinger J, et al. CT image quality improvement using adaptive iterative dose reduction with wide-volume acquisition on 320-detector CT. Eur Radiol 2012;22(February (2)):295–301.
[8] Gervaise A, Teixeira P, Villani N, Lecocq S, Louis M, Blum A. CT dose optimisation and reduction in osteoarticular disease. Diagn Interv Imaging 2013;94(April (4)):371–88.
[9] Maxfield MW, Schuster KM, McGillicuddy EA, Young CJ, Ghita M, Bokhari SAJ, et al. Impact of adaptive statistical iterative reconstruction on radiation dose in evaluation of trauma patients. J Trauma Acute Care Surg 2012;73(December (6)):1404–9.
[10] Mitsumori LM, Shuman WP, Busey JM, Kolokythas O, Koprowicz KM. Adaptive statistical iterative reconstruction versus filtered back projection in the same patient: 64 channel liver CT image quality and patient radiation dose. Eur Radiol 2012;22(January (1)):138–43.
[11] Wang R, Schoepf UJ, Wu R, Reddy RP, Zhang C, Yu W, et al. Image quality and radiation dose of low dose coronary CT angiography in obese patients: sinogram affirmed iterative reconstruction versus filtered back projection. Eur J Radiol 2012;81(November (11)):3141–5.
[12] Desai GS, Uppot RN, Yu EW, Kambadakone AR, Sahani DV. Impact of iterative reconstruction on image quality and radiation dose in multidetector CT of large body size adults. Eur Radiol 2012;22(August (8)):1631–40.
[13] Wassilew GI, Janz V, Heller MO, Tohtz S, Rogalla P, Hein P, et al. Real time visualization of femoroacetabular impingement and subluxation using 320-slice computed tomography. J Orthop Res 2013;31(February (2)):275–81.
[14] Shores JT, Demehri S, Chhabra A. Kinematic "4 dimensional" CT imaging in the assessment of wrist biomechanics before and after surgical repair. Eplasty 2013;13:e9.
[15] Halpenny D, Courtney K, Torreggiani WC. Dynamic four-dimensional 320 section CT and carpal bone injury – a description of a novel technique to diagnose scapholunate instability. Clin Radiol 2012;67(February (2)):185–7.
[16] Edirisinghe Y, Troupis JM, Patel M, Smith J, Crossett M. Dynamic motion analysis of dart throwers motion visualized through computerized tomography and calculation of the axis of rotation. J Hand Surg Eur Vol 2014;39(May (4)):364–72.
[17] Labone N, Kammacher W, Blum A. Etude préliminaire d'un outil d'aide à l'acquisition 4D au scanner. Oral presentation. Paris, France: Journées Francaises de Radiologie; 2014.
[18] Fahmi F, Beenen LFM, Streekstra GJ, Janssen NY, de Jong HW, Riordan A, et al. Head movement during CT brain perfusion acquisition of patients with suspected acute ischemic stroke. Eur J Radiol 2013;82(December (12)):2334–41.
[19] Hou DJ, Tso DK, Davison C, Inacio J, Louis LJ, Nicolaou S, et al. Clinical utility of ultra high pitch dual source thoracic CT imaging of acute pulmonary embolism in the emergency department: are we one step closer towards a non-gated triple rule out? Eur J Radiol 2013;82(October (10)):1793–8.
[20] Garcia-Elias M. The non-dissociative clunking wrist: a personal view. J Hand Surg Eur Vol 2008;33(December (6)):698–711.
[21] Berdia S, Short WH, Werner FW, Green JK, Panjabi M. The hysteresis effect in carpal kinematics. J Hand Surg Am 2006;31(April (4)):594–600.
[22] Van Dyck P, Gielen JL, Vanhoenacker FM, Wouters K, Dossche L, Parizel PM. Stable or unstable tear of the anterior cruciate ligament of the knee: an MR diagnosis? Skeletal Radiol 2012;41(March (3)):273–80.
[23] Van de Giessen M, Foumani M, Vos FM, Strackee SD, Maas M, Van Vliet LJ, et al. A 4D statistical model of wrist bone motion patterns. IEEE Trans Med Imaging 2012;31(March (3)):613–25.
[24] Teixeira PAG, Chanson A, Beaumont M, Lecocq S, Louis M, Marie B, et al. Dynamic MR imaging of osteoid osteomas: correlation of semiquantitative and quantitative perfusion parameters with patient symptoms and treatment outcome. Eur Radiol 2013;23(9 (Sep)):2602–11.
[25] Gondim Teixeira PA, Lecocq S, Louis M, Aptel S, Raymond A, Sirveaux F, et al. Wide area detector CT perfusion: can it differentiate osteoid osteomas from other lytic bone lesions? Diagn Interv Imaging 2014;95(6 (Jun)).
[26] Otton J, Morton G, Schuster A, Bigalke B, Marano R, Olivotti L, et al. A direct comparison of the sensitivity of CT and MR cardiac perfusion using a myocardial perfusion phantom. J Cardiovasc Comput Tomogr 2013;7(April (2)):117–24.
[27] De Simone M, Muccio CF, Pagnotta SM, Esposito G, Cianfoni A. Comparison between CT and MR in perfusion imaging assessment of high-grade gliomas. Radiol Med 2013;118(February (1)):140–51.
[28] Goh V, Padhani AR. Imaging tumor angiogenesis: functional assessment using MDCT or MRI? Abdom Imaging 2006;31(April (2)):194–9.
[29] Van Rijswijk CSP, Geirnaerdt MJA, Hogendoorn PCW, Taminiau AHM, van Coevorden F, Zwinderman AH, et al. Soft-tissue tumors: value of static and dynamic gadopentetate dimeglumine-enhanced MR imaging in prediction of malignancy. Radiology 2004;233(November (2)):493–502.
[30] Brix G, Semmler W, Port R, Schad LR, Layer G, Lorenz WJ. Pharmacokinetic parameters in CNS Gd-DTPA enhanced MR imaging. J Comput Assist Tomogr 1991;15(August (4)):621–8.
[31] Tofts PS. Modeling tracer kinetics in dynamic Gd-DTPA MR imaging. J Magn Reson Imaging 1997;7(February (1)):91–101.
[32] Miles KA. Perfusion CT for the assessment of tumour vascularity: which protocol? Br J Radiol 2003;76(1):S36–42.
[33] Kambadakone AR, Sharma A, Catalano OA, Hahn PF, Sahani DV. Protocol modifications for CT perfusion (CTp) examinations of abdomen-pelvic tumors:

impact on radiation dose and data processing time. Eur Radiol 2011;21(June (6)):1293–300.
[34] Biswas D, Bible JE, Bohan M, Simpson AK, Whang PG, Grauer JN. Radiation exposure from musculoskeletal computerized tomographic scans. J Bone Joint Surg Am 2009;91(August (8)):1882–9.
[35] Gondim Teixeira PA, Hossu G, Lecocq S, Razeto M, Louis M, Blum A. Bone marrow edema pattern identification in patients with lytic bone lesions using digital subtraction angiography-like bone subtraction on large-area detector computed tomography. Invest Radiol 2014;49(March (3)):156–64.
[36] Vrtiska TJ, Takahashi N, Fletcher JG, Hartman RP, Yu L, Kawashima A. Genitourinary applications of dual-energy CT. AJR Am J Roentgenol 2010;194(June (6)):1434–42.
[37] Glazebrook KN, Guimarães LS, Murthy NS, Black DF, Bongartz T, Manek NJ, et al. Identification of intraarticular and periarticular uric acid crystals with dual-energy CT: initial evaluation. Radiology 2011;261(November (2)):516–24.
[38] Toepker M, Moritz T, Krauss B, Weber M, Euller G, Mang T, et al. Virtual noncontrast in second-generation, dual-energy computed tomography: reliability of attenuation values. Eur J Radiol 2012;81(March (3)):e398–405.

Discussion et conclusion du chapitre 4 :

Nos articles montrent comment il est possible d'optimiser et de réduire la dose dans plusieurs domaines d'applications cliniques et mettent en avant l'intérêt de combiner l'utilisation des facteurs comportementaux et des facteurs techniques.

Article 1 : Scanner basse dose pour la recherche d'une colique néphrétique : comment faire en pratique clinique ?

Les scanners réalisés dans le cadre d'une suspicion de colique néphrétique représentent un cas particulier en imagerie abdominale. Premièrement, ils sont réalisés la plupart du temps avec une seule acquisition sans injection. Deuxièmement, il est possible de réduire la longueur d'acquisition en centrant le scanner sur les voies urinaires [46]. Enfin, le bruit de l'image peut être augmenté de manière significative sans altérer la performance diagnostique. Cela est lié à l'hyperdensité spontanée de la plupart des calculs urinaires et à l'important RCB entre les calculs urinaires et les parties molles environnantes [57]. Les doses des scanners réalisés pour le bilan d'une colique néphrétique peuvent donc être réduites de manière importante, de l'ordre de 70 à 90 % par rapport à une acquisition abdominopelvienne standard, sans en altérer la performance diagnostique [60-61]. Cet exemple est intéressant car il met en avant la relation qu'il peut exister entre la dose, la qualité d'image et la performance diagnostique. Au final, le but de toute démarche d'optimisation de la dose est de maintenir une excellente performance diagnostique pour la dose d'irradiation la plus faible possible. Pour cela, la qualité d'image peut être plus ou moins volontairement dégradée en fonction des structures qui sont analysées. De plus, cet exemple montre l'intérêt en pratique clinique courante de combiner l'utilisation des facteurs comportementaux et techniques dans une démarche d'optimisation de la dose d'irradiation au scanner. Ainsi, tandis que les reconstructions itératives permettent de réduire environ de moitié la dose à qualité d'image équivalente, la réduction de la longueur d'acquisition avec un centrage du scanner sur les voies urinaires est une manière simple pour réduire de façon significative, de l'ordre de 15 à 20 %, la dose délivrée au patient. Enfin, malgré l'utilisation des algorithmes de reconstructions itératives, les données de la littérature montrent qu'à ce jour il n'est pas encore possible de réduire la dose sous le seuil de 1 mSv sans altérer la visualisation des calculs urinaires de moins de 3 mm [62-63]. Bien que n'ayant pas de traduction médicale directe, le franchissement de ce

seuil « psychologique » sera peut-être bientôt possible grâce aux nouvelles générations de reconstructions itératives en cours de développement.

Article 2 : Optimisation et réduction de la dose en scanner ostéo-articulaire.

Le scanner ostéo-articulaire comporte de nombreuses particularités. Tout d'abord, il est souvent possible de substituer le scanner par un examen d'imagerie non irradiant comme l'IRM ou l'échographie. Par exemple, à l'HIA Legouest, les scanners lombaires ou cervicaux des patients de moins de 60 ans adressés pour la recherche d'un conflit disco-radiculaire sont systématiquement substitués en IRM, en l'absence de contre-indication à celle-ci. Deuxièmement, le scanner en imagerie ostéo-articulaire regroupe de nombreux types d'examens : scanner des articulations périphériques ou proximales, scanner du rachis, arthroscanner, scanner dynamique ou de perfusion, scanner double-énergie. Les doses délivrées au patient en scanner ostéo-articulaire sont donc très variables, d'un facteur 1 à 1000, car elles dépendent principalement des longueurs d'acquisition et des coefficients de conversation tissulaire qui sont très différents d'une localisation anatomique à l'autre [64]. Par exemple, un scanner d'une articulation périphérique comme le poignet a une dose inférieure à la dose d'une radiographie thoracique de face (moins de 0,05 mSv) tandis que la dose d'un scanner lombaire peut aller jusqu'à 5 à 10 mSv. Parallèlement, les modalités d'optimisation et de réduction de la dose doivent être adaptées en fonction des localisations anatomiques et du type d'examen réalisé. Ainsi, il faut différencier les scanners dont l'intérêt est principalement lié à l'analyse de l'os et ceux s'intéressant aux parties molles. Pour les premiers, le bon RCB permet d'augmenter le bruit de l'image sans altérer la performance diagnostique. Il est donc possible de réduire de manière importante les doses. Pour les scanners s'intéressant aux parties molles, comme par exemple les scanners du rachis réalisés pour la recherche d'un conflit disco-radiculaire, le faible RCB nécessite de maintenir une bonne qualité d'image et de ce fait les doses délivrées sont plus importantes. Pour ce type de scanners, l'utilisation des reconstructions itératives et de la modulation automatique du mA sont alors les deux principales mesures qui permettent d'optimiser la dose.

Article 3 : Scanner ostéo-articulaire à large système de détection : principes, techniques et applications en pratique clinique et en recherche.

En scanner ostéo-articulaire, de nouvelles applications avancées ont vu le jour ces dernières années : scanner dynamique 4D des articulations, scanner de perfusion tumorale ou encore scanner double-énergie. Ces techniques semblent jouer un rôle important dans le diagnostic de nombreuses pathologies ostéo-articulaires. Toutefois, les scanners dynamiques et de perfusion nécessitent la répétition de multiples volumes d'acquisition. La maîtrise des doses délivrées est un facteur primordial pour permettre l'utilisation en pratique clinique de ces nouvelles applications avancées. Pour les articulations périphériques, les coefficients de conversion tissulaire pour le calcul des doses efficaces sont très faibles car ces articulations sont éloignées des organes radio-sensibles. De ce fait, même avec la répétition de 10 à 15 volumes d'acquisition, le centrage de la couverture d'acquisition et la réduction des paramètres d'acquisition permettent de maintenir des doses très faibles, inférieures à 1 mSv. A partir de tests que nous avons réalisés sur cadavres, nous pensons qu'il est encore possible de réduire de manière importante les paramètres d'acquisition et donc la dose des scanners dynamiques, tout en conservant une qualité d'image suffisante pour l'analyse des mouvements. Par exemple, pour une acquisition dynamique de la cheville, la dose d'une phase d'acquisition semble pouvoir être divisée par 10 par rapport à un protocole standard de scanner de la cheville, sans que cela n'altère la qualité de l'analyse du mouvement. Ainsi, même si une acquisition dynamique nécessite l'acquisition de 10 volumes, la dose globale d'un scanner dynamique de la cheville pourrait être équivalente à la dose d'un scanner standard de la cheville. Malheureusement, tandis qu'un premier test s'est révélé très concluant, de nouveaux tests réalisés chez quatre autres cadavres n'ont pas permis d'obtenir les mêmes résultats. Cela pourrait être lié à la qualité de l'os des cadavres. En effet, la trame osseuse des quatre autres cadavres était très déminéralisée ce qui pourrait être à l'origine d'un défaut de fonctionnement du logiciel de post-traitement (4D Ortho, Toshiba Medical System, Otawara, Japon) utilisé pour quantifier les mouvements de la cheville. De nouveaux tests sur patients seraient intéressants afin de poursuivre l'optimisation des scanners dynamiques de la cheville.

CONCLUSION GENERALE ET PERSPECTIVES

1- Conclusion générale :

Dans cette thèse, nous avons étudié plusieurs facteurs techniques et comportementaux qui permettent d'optimiser et de réduire la dose d'irradiation au scanner.

Nous avons montré que la sensibilisation des médecins prescripteurs de scanner est encore à poursuivre compte tenu d'un défaut de connaissance de ces praticiens concernant les niveaux de dose délivrée et les risques potentiels de cancer radio-induit lié aux faibles doses de rayons X qui en découlent. Nous avons aussi montré que des mesures simples comme la limitation du nombre de phases d'acquisition ou encore la réduction de la couverture d'acquisition du scanner peuvent permettre chacune de réduire d'environ 20 % la dose délivrée au patient dans certaines situations spécifiques. Souvent mise au second plan derrière les innovations technologiques récentes, la mise en œuvre des facteurs comportementaux dans une démarche d'optimisation et de réduction de la dose reste toutefois fondamentale.

Parallèlement, les évolutions technologiques récentes ont permis une réduction importante de la dose d'irradiation au scanner. En premier lieu, l'implantation des reconstructions itératives a permis de diviser par deux la dose d'irradiation au scanner par rapport aux reconstructions standard en rétroprojection filtrée, à qualité d'image équivalente et sans altération de la résolution spatiale des images. Nous avons aussi montré que pour des scanners avec une faible longueur d'acquisition, l'utilisation du mode d'acquisition volumique à partir d'un scanner à large système de détection permet de réduire la dose par rapport à l'acquisition hélicoïdale classique. Enfin, l'utilisation de la modulation automatique du milliampérage permet aussi d'optimiser la dose en adaptant le milliampérage au morphotype des patients et en permettant d'avoir un bruit constant de l'image d'un patient à l'autre. Toutefois, dans notre étude portant sur un protocole de scanner basse dose réalisé dans le cadre d'une suspicion de colique néphrétique, nous avons montré que même si le bruit de l'image est constant d'un patient à l'autre, la qualité d'image subjective et la performance diagnostique peuvent varier en fonction du morphotype des patients. Ainsi, dans une démarche d'optimisation et de réduction de la dose, la performance diagnostique est un critère d'évaluation plus pertinent que la qualité d'image.

Enfin, nous avons proposé différentes manières de réduire et d'optimiser les doses en pratique clinique courante. L'optimisation conjointe des facteurs techniques et comportementaux permet la réalisation de scanner basse dose pour l'exploration des coliques

néphrétiques. Avec ce type de protocole, la dose peut être réduite de l'ordre de 70 à 90 %, par rapport à une acquisition abdominopelvienne standard, sans altération de la performance diagnostique. De même, la maitrise des doses par l'utilisation du mode d'acquisition intermittent, par la limitation de la couverture d'acquisition et du nombre de phases d'acquisition et par l'implantation des reconstructions itératives a permis l'utilisation en pratique clinique courante des protocoles de scanner dynamique 4D des articulations ou encore de scanner de perfusion tumorale.

2- Perspectives :

Durant la dernière décennie, les niveaux de dose d'irradiation au scanner ont été largement diminués. Par exemple, pour un scanner abdominopelvien, grâce principalement à l'implantation des reconstructions itératives mais aussi à l'amélioration des détecteurs et à l'utilisation de la modulation automatique du milliampérage et de la collimation active, la dose délivrée moyenne est passée de 10 mSv à environ 2,8 mSv [55], soit une réduction de 72 % de la dose, à qualité d'image équivalente.

Cette dynamique de réduction des doses délivrées au scanner ne semble pas s'arrêter. De nouvelles générations de reconstruction itérative sont encore en cours de développement. Les nouveaux algorithmes itératifs récemment commercialisés proposent d'ores-et-déjà des niveaux de réduction de la dose de l'ordre de 70 à 80 % contre 30 à 50 % pour les algorithmes de la première génération [65-66].

De nouvelles innovations technologiques sont aussi en cours de développement. Par exemple, L'apparition récente des détecteurs compteurs de photons ou « *Photon Counting Detector* » pourrait offrir de nouvelles opportunités de réduction de la dose d'irradiation au scanner. Le principe de ce type de détecteur est d'utiliser un semi-conducteur ultra-rapide afin de pouvoir compter directement chaque interaction avec un photon. Le remplacement des détecteurs actuels à base de scintillateurs à cristaux par ces nouveaux détecteurs pourrait offrir de nouveaux avantages comme la réduction de la sensibilité au bruit électronique, l'augmentation du RCB, une amélioration de la résolution spatiale, une meilleure décomposition des matériaux et enfin une réduction de la dose d'irradiation. [67]. Cette nouvelle technologie est encore en cours d'évaluation mais des premiers tests sur des patients ont montrés des résultats prometteurs [68].

Un changement complet de technologie pourrait aussi intervenir et modifier totalement les niveaux de dose d'irradiation délivrée en scanographie. Des chercheurs proposent d'introduire une nouvelle technologie basée sur la détection ultrasonique de l'absorption des rayons X [69]. En effet, lors de l'interaction d'un photon X avec la matière, une onde ultrasonore est émise. La détection de cette onde permet donc de savoir qu'il y a eu absorption d'un photon X. Des résultats expérimentaux montrent que, si un tel système arrive à être développé pour une application humaine, il serait possible d'avoir une vitesse d'acquisition des images cent fois plus rapide tout en ayant une dose délivrée de rayons X cent fois plus faible [69]. Bien que cette technologie ne soit encore qu'au stade de la recherche fondamentale, elle ouvre la porte à de nombreuses perspectives pour les années à venir pour la réduction de la dose d'irradiation au scanner.

Il serait aussi intéressant d'approfondir les recherches concernant l'impact des faibles doses de rayons X sur le risque de cancer radio-induit. En effet, avec des doses de plus en plus faibles, il pourrait s'avérer que leur impact devienne insignifiant voire nul, ce qui pourrait alors changer totalement la manière d'utiliser le scanner en pratique clinique courante. De même, de nos jours, les niveaux des doses délivrées au scanner s'approchent de plus en plus des doses liées à la réalisation d'un bilan radiographique standard. C'est par exemple le cas pour le scanner thoracique où des protocoles de scanner très basse dose ont montré une performance diagnostique supérieure à la radiographie thoracique avec des doses d'irradiation très proches [70]. Grâce à la réduction importante des doses délivrées en scanographie, les indications de scanner pourraient alors être étendues à de nombreuses pathologies pour lesquelles le bilan radiographique standard est de nos jours réalisé en première intention. Au final, la réduction de plus en plus importante des doses délivrées au scanner permet de supprimer son inconvénient majeur et offre au scanner de nouvelles et nombreuses opportunités de développement futur.

REFERENCES BIBLIOGRAPHIQUES

1- Brenner DJ, Hall EJ. Computed tomography: an increasing source of radiation exposure. *N Engl J Med* 2007; 357(22): 2277-84.

2- Etard C, Sinno-Tellier S, Aubert B. Exposition de la population française aux rayonnements ionisants liée aux actes de diagnostic médical en 2007. Rapport InVS/IRSN. Juin 2010.

3- Exposition de la population française aux rayonnements ionisants liée aux actes de diagnostic médical en 2012. Rapport PRP-HOM N°2014-6.

4- Board of Radiation Effects Research Division on Earth and Life Sciences National Research Council of the National Academies. Health risks from exposure to low levels of ionizing radiation: BEIR VII Phase2. Washington, DC: National Academies Press; 2006.

5- Brenner DJ, Doll R, Goodhead DT, Hall EJ, Land CE, Little JB, *et al*. Cancer risks attributable to low doses of ionizing radiation: assessing what we really know. Proc Natl Acad Sci USA 2003; 100(24): 13761-6.

6- Little MP, Wakeford R, Tawn EJ, Bouffler SD, Berrington de Gonzalez A. Risks associated with low doses and low dose rates of ionizing radiation: why linearity may be (almost) the best we can do. *Radiology* 2009; 251(1): 6-12.

7- Smith-Bindman R, Lipson J, Marcus R, Kim KP, Mahseh M, Gould R, *et al*. Radiation dose associated with common computed tomography examinations and the associated lifetime attributable risk of cancer. *Arch Intern Med* 2009; 169(22): 2078-86.

8- Tubiana M, Aurengo A, Averbeck A. La relation dose-effet et l'estimation des effets cancérigènes des faibles doses de rayonnements ionisants. Paris : Académie Nationale de Médecine, Institut de France – Académie des Sciences; 2005.

9- Tubiana M, Feinendegen LE, Yang C, Kaminski JM. The linear no-threshold relationship is inconsistent with radiation biologic and experimental data. *Radiology* 2009; 251(1): 13-22.

10- Doss M. Linear no-threshold model vs radiation hormesis. *Dose Response* 2013; 11: 480-97.

11- Directive 97/43/Euratom du 30 juin 1997 relative à la protection sanitaire des personnes contre les dangers des rayonnements ionisants lors d'expositions à des fins médicales.

12- Directive 2013/59/Euratom du 5 décembre 2013 fixant les normes de base relatives à la protection sanitaire contre les dangers résultant de l'exposition aux rayonnements ionisants.

13- Wallace AB, Goergen SK, Schick D, Soblusky T, Jolley D. Multidetector CT dose: clinical practice improvement strategies from a successful optimization program. *J Am Coll Radiol* 2010; 7(8): 614-24.

14- Tamm EP, Rong XJ, Cody DD, Ernst RD, Fitzgerald NE, Kundra V. Quality initiatives: CT radiation dose reduction: How to implement change without sacrificing diagnostic quality. *Radiographics* 2011; 31(8): 1823-32.

15- Amis ES Jr. CT radiation dose: trending in the right direction. *Radiology* 2011; 261(1): 5-8.

16- Brenner DJ, Shuryak I, Einstein AJ. Impact of reduced patient life expectancy on potential cancer risks from radiologic imaging. *Radiology* 2011; 261(1): 193-8.

17- Oikarinen H, Meriläinen S, Pääkkö E, Karttunen A, Nieminen MT, Tervonen O. Unjustified CT examinations in young patients. *Eur Radiol* 2009; 19(5): 1161-5.

18- Chuong AM, Corno L, Beaussier H, Boulay-Coletta I, Millet I, Hodel J, *et al*. Assessment of bowel wall enhancement for the diagnosis of intestinal ischemia in patients with small bowel obstruction. *Radiology* 2016 Feb 11: 151029 [Epub ahead of print].

19- Kurabayashi M, Okishige K, Ueshima D, Yoshimura K, Shimura T, Suzuki H, *et al*. Diagnostic utility of unenhanced computed tomography for acute aortic syndrome. *Circ J* 2014; 78(8): 1928-34.

20- Esposito AA, Zilocchi M, Fasani P, Giannitto C, Maccagnoni S, Maniglio M, *et al*. The value of precontrast thoraco-abdominopelvic CT in polytrauma patients. *Eur J Radiol* 2015; 84(6): 1212-8.

21- Badawy MK, Galea M, Mong KS, U P. Computed tomography overexposure as a consequence of extended scan length. *J Med Imaging Radiat Oncol* 2015; 59(5): 586-9.

22- Michalakis N, Keyzer C, De Maertelaer V, Tack D, Genevois PA. Reduced z-axis coverage in multidetector-row CT pulmonary angiography decreases radiation dose and diagnostic accuracy of alternative diseases. *Br J Radiol* 2014; 87(1033): 20130546.

23- Atalay MK, Walle NL, Grand DJ, Mayo-Smith WW, Cronan JJ, Egglin TK. Scan length optimization for pulmonary embolism at CT angiography: analysis based on the three-dimensional spatial distribution of 370 emboli in 100 patients. *Clin Radiol* 2011; 66(5): 405-11.

24- Kalra MK, Toth TL. Patient centering in MDCT: dose effects. In: Tack D, Genevois PA (eds) Radiation dose from adult and pediatric multidetector computed tomography. Springer, Berlin, 2007, pp 129-132.

25- Li J, Udayasankar UK, Toth TL, Seamans J, Small WC, Kalra MK. Automatic patient centering for MDCT: effect on radiation dose. *Am J Roentgenol* 2007; 188(2): 547-52.

26- Mahesh M. Scan parameters and image quality in MDCT. In: Mahesh M (eds) MDCT physics: The basics—Technology, image quality and radiation dose. Lippincott Williams & Wilkins, Philadelphia, 2009, pp 47-78.

27- Ciarmatori A, Nocetti L, Mistretta G, Zambelli G, Costi T. Reducing absorbed dose to eye lenses in head CT examinations: the effect of bismuth shielding. *Australas Phys Eng Sci Med* 2016 Apr 20. [Epub ahead of print].

28- van der Molen AJ, Geleijns J. Overranging in multisection CT: quantification and relative contribution to dose- comparison of four 16-section CT scanners. *Radiology* 2007; 242(1): 208-16.

29- Christner JA, Zavaletta VA, Eusemann CD, Walz-Flannigan AI, McCollough CH. Dose reduction in helical CT: dynamically adjustable z-axis X-ray beam collimation. *Am J Roentgenol* 2010; 194(1): W49-55.

30- Boedeker KL, McNitt-Gray MF. Application of the noise power spectrum in modern diagnostic MDCT: part II. Noise power spectra and signal to noise. *Phys Med Biol* 2007; 52(14): 4047-61.

31- Kalra MK. Automatic exposure control in multidetector-row CT. In: Tack D, Genevois PA, Kalra M. (eds). Radiation dose from multidetector CT. Springer-Verlag Berlin Heidelberg, 2012, p369-387.

32- Singh S, Kalra MK, Thrall JH, Mahesh M. Automatic exposure control in CT: applications and limitations. *J Am Coll Radiol* 2011; 8(6): 446-9.

33- Kalender WA, Deak P, Kellermeier M, van Straten M, Vollmar SV. Application and patient size-dependent optimization of x-ray spectra for CT. *Med Phys* 2009; 36(3): 993-1007.

34- Nagel HD. CT parameters that influence the radiation dose. In: Tack D, Genevois PA (eds) Radiation dose from adult and pediatric multidetector computed tomography. Springer, Berlin, 2007, pp 51-79.

35- Kalra MK, Maher MM, Toth TL, Hamberg LM, Blake MA, Shepard JA, *et al*. Strategies for CT radiation dose optimization. *Radiology* 2004; 230(3): 619-28.

36- Stradiotti P, Curti A, Castellazzi G, Zerbi A. Metal-related artifacts in instrumented spine. Techniques for reducing artifacts in CT and MRI: state of the art. *Eur Spine J* 2009; 18 Suppl 1: 102-8.

37- von Falck C, Galanski M, Shin HO. Sliding-thin-slab averaging for improved depiction of low-contrast lesions with radiation dose savings at thin-section CT. *Radiographics* 2010; 30(2): 317-26.

38- McNitt-Gray MF. AAPM/RSNA physics tutorial for residents: topics in CT. Radiation dose in CT. *Radiographics* 2002; 22(6): 1541-53.

39- Walter F, Ludig T, Iochum S, Blum A. Multi-dectector CT in musculo-skeletal disorders. *JBR-BTR* 2003; 86(1): 6-11.

40- Blum A. Scanner volumique multicoupe: principes, applications et perspectives. *JBR-BTR* 2002; 85(2): 82-99.

41- Xu J, Mahesh M, Tsui BM. Is iterative reconstruction ready for MDCT? *J Am Coll Radiol* 2009; 6(4): 274-6.

42- Thibault JB, Sauer KD, Bouman CA, Hsieh J. A three-dimensional statistical approach to improved image quality for multislice helical CT. *Med Phys* 2007*;* 34(11): 4526-44.

43- Hara AK, Paden RG, Silva AC, Kujak JL, Lawder HJ, Pavlicek W. Iterative reconstruction technique for reducing body radiation dose at CT: feasibility study. *Am J Roentgenol* 2009; 193(3): 764-71.

44- Krille L, Hammer GP, Merzenich H, Zeeb H. Systematic review on physician's knowledge about radiation doses and radiation risks of computed tomography. *Eur J Radiol* 2010; 76(1): 36-41.

45- Brown N, Jones L. Knowledge of medical imaging radiation dose and risk among doctors. *J Med Imaging Radiat Oncol* 2013; 57(1): 8-14.

46- Corwin MT, Bekele W, Lamba R. Bony landmarks on computed tomography localizer radiographs to prescribe a reduced scan range in patients undergoing multidetector computed tomography for suspected urolithiasis. *J Comput Assist Tomogr* 2014; 38(3): 404-7.

47- Corwin MT, Chang M, Fananapazir G, Seibert A, Lamba R. Accuracy and radiation dose reduction a limited abdominopelvic CT in the diagnosis of acute appendicitis. *Abdom Imaging* 2015; 40(5): 1177-82.

48- Kroft LJ, Roelofs JJ, Geleijns J. Scan time and patient dose for thoracic imaging in neonates and small children using axial volumetric 320-detector row CT compared to helical 64-, 32-, and 16- detector row CT acquisitions. *Pediatr Radiol* 2010; 40(3): 294-300.

49- Zacharias C, Alessio AM, Otto RK, Iyer RS, Philips GS, Swanson JO, *et al*. Pediatric CT: strategies to lower radiation dose. *Am J Roentgenol* 2013; 200(5); 950-6.

50- Semelka RC, Armao DM, Elias J, Huda W. Imaging strategies to reduce the risk of radiation in CT studies, including selective substitution with MRI. *J Magn Reson Imaging* 2007; 25(5): 900-9.

51- McCollough CH, Primak AN, Braun N, Kofler J, Yu L, Christner J. Strategies for reducing radiation dose in CT. *Radiol Clin North Am* 2009; 47(1): 27-40.

52- Lee TY, Chhem RK. Impact of new technologies on dose reduction in CT. *Eur J Radiol* 2010; 76(1): 28-35.

53- Singh S, Kalra MK, Thrall JH, Mahesh M. CT radiation dose reduction by modifying primary factors. *J Am Coll Radiol* 2011; 8(5): 369-72.

54- Dougeni E, Faulkner K, Panayiotakis G. A review of patient dose and optimisation methods in adult and paediatric CT scanning. *Eur J Radiol* 2012; 81(4): e665-83.

55- McCollough CH, Chen GH, Kalender W, Leng S, Samei E, Taguchi LK, *et al*. Achieving routine submillisievert CT scanning: report from the summit on management of radiation dose in CT. *Radiology* 2012; 264(2): 567-80.

56- Coursey CA, Casalino DD, Remer EM, Arellano RS, Bishoff JT, Dighe M, *et al*. ACR Appropriateness Criteria® acute onset flank pain: suspicion of stone disease. *Ultrasound Q* 2012; 28(3): 227-33.

57- Kambadakone AR, Eisner BH, Catalano OA, Sahani DV. New and evolving concepts in the imaging and management of urolithiasis: urologists' perspective. *Radiographics* 2010; 30(3): 603-23.

58- Broder J, Bowen J, Lohr J, Babcock A, Yoon J. Cumulative CT exposures in emergency department patients evaluated for suspected renal colic. *J Emerg Med* 2007; 33(2): 161-8.

59- Katz SI, Saluja S, Brink JA, Forman HP. Radiation dose associated with unenhanced CT for suspected renal colic: impact of repetitive studies. *Am J Roentgenol 2006*; 186(4): 1120-4.

60- Niemann T, Kollmann T, Bongartz G. Diagnostic performance of low-dose CT for detection of urolithiasis: a meta-analysis. *Am J Roentgenol* 2008; 191(2): 396-401.

61- Sung MK, Singh S, Kalra MK. Current status of low dose multi-detector CT in the urinary tract. *World J Radiol* 2011; 3(11): 256-65.

62- Glazer DI, Maturen KE, Cohan RH, Davenport MS, Ellis JH, Knoepp US, *et al*. Assessment of 1 mSv urinary tract stone CT with model-based iterative reconstruction. *Am J Roentgenol* 2014; 203(6): 1230-5.

63- McLaughlin PD, Murphy KP, Hayes SA, Carey K, Sammon J, Crush L, *et al*. Non-contrast CT at comparable dose to an abdominal radiograph in patients with acute renal colic; impact of iterative reconstruction on image quality and diagnostic performance. *Insights Imaging* 2014; 5(2): 217-30.

64- Biswas D, Bible JE, Bohan M, Simpson AK, Whang PG, Grauer JN. Radiation exposure from musculoskeletal computerized tomographic scans. *J Bone Joint Surg Am* 2009; 91(8): 1882-9.

65- Dodge CT, Tamm EP, Cody DD, Liu X, Jensen CT, Wei W, *et al*. Performance evaluation of iterative reconstruction algorithms for achieving CT radiation dose reduction - a phantom study. *J Appl Clin Med Phys* 2016; 17(2): 5709.

66- Lubner MG, Pickhardt PJ, Tang J, Chen GH. Reduced image noise at low-dose multidetector CT of the abdomen with prior image constrained compressed during sensing algorithm. *Radiology* 2011; 260(1): 248-56.

67- Taguchi K, Iwanczyk JS. Vision 20/20: Single photon counting x-ray detectors in medical imaging. *Med Phys* 2013; 40(10): 100901.

68- Pourmorteza A, Symons R, Sandfort V, Mallek M, Fuld MK, Henderson G, *et al*. Abdominal imaging with contrast-enhanced photon-counting CT: first human experience. *Radiology* 2016; 279(1):239-45.

69- Xiang L, Han B, Carpenter C, Pratx G, Kuang Y, Xing L. X-ray acoustic computed tomography with pulsed x-ray beam from a medical linear accelerator. *Med Phys* 2013; 40(1): 010701.

70- McLaughlin PD, Ouellette HA, Louis LJ, Mallinson PI, O-Connell T, Mayo JR, *et al.* The emergence of ultra-low-dose computed tomography and the impending obsolescence of the plain radiograph? *Can Assoc Radiol J* 2013; 64(4):314-8.

RESUME

Depuis son introduction dans les années 1970, le scanner est devenu une technique d'imagerie médicale incontournable grâce à son excellente performance pour le diagnostic de nombreuses pathologies. Toutefois, le scanner est un examen d'imagerie irradiant. Compte-tenu des risques potentiels de cancer radio-induit liés aux faibles doses de rayons X, la réduction de la dose d'irradiation au scanner est primordiale. Dans ce travail, nous avons étudié plusieurs facteurs techniques et comportementaux qui permettent d'optimiser et de réduire la dose d'irradiation au scanner, tout en préservant une excellente performance diagnostique. Du côté des facteurs comportementaux, la sensibilisation des équipes médicales et paramédicales est fondamentale dans une démarche d'optimisation de la dose d'irradiation au scanner. De même, la limitation du nombre de phases d'acquisition et la réduction de la couverture d'acquisition sont deux manières simples pour réduire les doses délivrées. Du côté des facteurs techniques, nous avons montrés que l'utilisation des reconstructions itératives, par rapport aux reconstructions standards en rétroprojection filtrée, permet de réduire de moitié la dose d'irradiation des scanners, à qualité d'image équivalente. L'acquisition en mode volumique pour les scanners avec une faible couverture d'acquisition et l'utilisation de la modulation automatique du milliampérage permettent aussi de réduire et d'optimiser les doses. Enfin, nous nous sommes intéressés à l'optimisation de protocoles de scanner en pratique clinique courante en se focalisant sur les scanners réalisés pour la recherche d'une colique néphrétique et pour les scanners en imagerie ostéo-articulaire. Dans ce dernier domaine, nous avons aussi proposé des protocoles de scanner pour des applications cliniques avancées comme le scanner dynamique des articulations ou le scanner de perfusion tumorale.

Mots-clés : Dose d'irradiation ; Optimisation ; Rayons X ; Réduction ; Scanner.

ABSTRACT

Since its introduction in the 1970s, computed tomography (CT) has become the technique of reference in medical imaging for many diseases due to its high diagnostic performance. Its main limitation is the radiation dose delivered to the patient. Considering the potential risks of radiation-induced cancer caused even with low dose exposure, dose reduction in CT is essential. In this work, we studied several technical and behavioral factors that allow for CT radiation dose reduction and optimization, without modifying the diagnostic performance. Among the behavioral factors studied, education and awareness of radiologists and radiology technicians are important elements for CT radiation dose reduction. Limiting CT scan coverage and the number of acquisition phases is also a straightforward and effective way to reduce dose exposure. Regarding technical factors, we have shown that iterative reconstruction algorithms can reduce in half the radiation dose in comparison with standard filtered back projection, while maintaining equivalent image quality. The use of wide volume mode for acquisitions with a short coverage and the use of the automatic tube current modulation can also be used to reduce and optimize CT radiation dose. Finally, we provide guidelines to optimize CT radiation dose in some clinical settings such as renal colic and musculoskeletal CT. We also propose practical guidelines for advanced clinical applications of joint dynamic CT and perfusion CT in musculoskeletal disease.

Keywords: Computed Tomography; Optimization; Radiation dose; Reduction; X-Ray.